Aus der Abteilung für Immunbiochemie
der Medizinische Fakultät Mannheim
Direktorin: Prof. Dr. rer. nat. Adelheid Cerwenka

The impact of vitamin A metabolites on natural killer cell functions

Inauguraldissertation
zur Erlangung des akademischen Grades
Doctor scientiarum humanarum (Dr. sc. hum.) der
Medizinischen Fakultät Mannheim
der Ruprecht-Karls-Universität
zu
Heidelberg

vorgelegt von
Mingeum Jeong

aus
Cheongju-si, Republik Korea

2022

Dekan: Prof. Dr. med. Sergij Goerdt
Referentin: Prof. Dr. rer. nat. Adelheid Cerwenka

TABLE OF CONTENTS

Pages

1 INTRODUCTION

1.1 The immune system

The immune system is a defense system evolved to protect the host from foreign invaders (e.g. viruses, bacteria and other pathogens) and abnormal self-cells (e.g. stressed or transformed cells). The balance of immune responses is required to maintain the host's health. Hyperactive or overactive immune responses, such as in autoimmune disease or extreme allergic reactions, can attack normal and healthy tissues. On the other hand, immune deficiencies can cause failure of pathogen eliminations or abnormal self-cell eliminations. The immune system, which comprises various proteins, cells, and organs, is categorized in two major classes: innate immunity and adaptive immunity. Innate immune system provides the first line of protection (e.g. mucus barriers), and the immediate defense via phagocytes, natural killer cells, and complement. The adaptive immune system comprises specialized lymphocytes characterized by memory responses. One important feature of the immune system is to distinguish self- and non-self-molecules. Recognition of non-self-molecules by myeloid cells can trigger their immune responses, and further antigen presentation by myeloid cells to T cells can initiate adaptive immune responses, which are mediated by activated T cells and B cells.

1.1.1 Innate immunity

Innate immunity is the earliest defense mechanism to protect the host from daily exposure to foreign factors, including pathogenic microorganisms and their products. The first lines of defenses against infection are physical barriers between the internal and external territories, e.g. epithelia of the skin, eyes, nose, lung, and gastrointestinal tract. In addition to the physical aspect of defense, epithelia work as chemical barriers. For instance, mucus and mucins produced by goblet cells and enterocytes in the gastrointestinal tract can control bacteria interaction with the host (Pelaseyed et al., 2014). Small intestine epithelial cells produce antibacterial peptides, such as cryptdins and defensins (Eisenhauer, Harwig, & Lehrer, 1992). Furthermore, the commensal bacteria located in intestinal lumen can protect healthy individuals by competing with pathogenic microorganisms (Ivanov & Littman, 2011).

The humoral response of the innate immune system is mediated by the complement system, which is activated by the enzymatic cascades. Thus, a small number of activated complement proteins can lead to the amplified immune responses to opsonize and kill pathogens. Complement activation comprises three pathways: the classic pathway, the lectin pathway and the alternative pathway. The alternative pathway initiates the activation of the complement system. In response to the complement activation, fluid-phase complements form membrane attack

complex (MAC) on the surface of pathogens, which directly leads to osmotic lysis of pathogens. The activation of the alternative pathway can provide amplification loops to the other two pathways. The classical pathway is triggered by indirect pathogen recognition via the antigen-antibody-complex, and the lectin pathway is launched by direct recognition via binding of mannose-binding lectin (MBL) or ficolins with surface sugars or acetylated residues of pathogen. Both the classical and lectin pathways result in the formation of MAC and induce the elimination of pathogens (Taylor, Botto, & Walport, 1998).

The disruption of the physical barrier, such as wounds, can facilitate pathogen-infection of the host. In most cases, the innate immune system recognizes and destroys pathogens. For example, macrophages perform phagocytosis by binding to pathogens and internalize them in a vesicle fused with lysosomes (Aderem & Underhill, 1999). Upon the phagocytosis, macrophages produce toxic nitrogen oxides, antimicrobial peptides and cytokines, and create acidic environment, in order to destroy pathogens (Kinchen & Ravichandran, 2008; Lehrer, Selsted, Szklarek, & Fleischmann, 1983; Nathan & Hibbs, 1991). The cytokines produced by macrophages contribute to inflammation that can further attract other leukocytes, such as neutrophils, eosinophils, and lymphocytes, as well as assist monocyte to differentiate into dendritic cells (DCs) or macrophages (Arango Duque & Descoteaux, 2014).

Phagocytosis is induced by the recognition of pathogens or apoptotic cells. Despite the absence of antigen-specific memory responses, innate immune cells can still recognize the regular patterns of repetitive structure on pathogens, so-called pathogen-associated molecular patterns (PAMPs). In addition to PAMPs, damage-associated molecular patterns (DAMPs) released by damaged or dying self-cells can be recognized as well. As an evolutionary consequence of preserved recognition systems, phagocytes express pattern recognition receptors (PRRs). Recognition of PAMPs and DAMPs via PRRs induces phagocytosis and mediates immune responses. PRR family includes Toll-like receptors (TLRs), nucleotide oligomerization domain (NOD)-like receptors (NLRs), retinoic acid-inducible gene-I (RIG-I)-like receptors (RLRs) and C-type lectin receptors (CLRs) (D. Li & Wu, 2021). TLR family is an important PRR that recognizes repeated structure of carbohydrates or lipids on bacteria (e.g. lipopolysaccharide (LPS) and lipoteichoic acids), glucose units on fungi (e.g. Zymosan), virus-derived nucleic acids (e.g. dsRNA and ssRNA) or heat-shock proteins of the host (Akira & Takeda, 2004).

In addition to pro-inflammatory cytokine production, the activation of PRRs trigger the expression of co-stimulatory molecules on the surface of myeloid cells. For instance, DCs produce IL-12 upon the TLR2-activation, and macrophages upregulate expression of CD80 (B7.1), CD86 (B7.2) and MHC class II in a TLR4-MyD88-dependent manner upon LPS-exposure (Akira, Hoshino, & Kaisho, 2000; Hoshino et al., 1999; Thoma-Uszynski et al., 2000). Using these co-stimulatory molecules together with MHC class II molecules, antigen-presenting cells

(APCs), such as macrophages or DCs, can present digested peptides and activate naïve T cells, which can initiate the adaptive immunity (Janeway, 1989; Kruisbeek et al., 1985; Sharpe & Freeman, 2002).

1.1.2 Adaptive immunity

The adaptive immunity operates when pathogens circumvent the defense of innate immunity. Conventionally, specificity and memory responses were considered two unique features of adaptive immunity, in contrast to innate immunity. However, the recent studies demonstrated that innate immune cells, namely NK cells, are capable to exert antigen-specific memory responses upon the exposure to viral antigens and haptens (Paust et al., 2010; J. C. Sun, Beilke, & Lanier, 2009). Additionally, NK cells exposed to inflammatory cytokines were shown to respond rapidly upon subsequent activation, illustrating memory-like innate immune responses (Cooper et al., 2009).

Similar to the innate immunity, the adaptive immune system comprises cellular and humoral compartments. Cellular immune responses are carried out by T cells. T cell receptors (TCR) are expressed on the surface of T cells and the engagement of TCRs is required for T cell activation. $CD4^+$ T cells recognize antigen presented by APCs via MHC class II molecules, whereas $CD8^+$ T cells recognize antigen presented by APCs via MHC class I molecules (Mondino, Khoruts, & Jenkins, 1996). Additionally, CD28 expressed by T cells receives co-stimulatory signals through the interaction with CD80 (B7-1) or CD86 (B7-2) expressed on APCs. The TCR signal and CD28 activation initiate the activation of $CD4^+$ T cells and $CD8^+$ T cells, and the different cytokines drive the polarization of T cells (L. Zhou, Chong, & Littman, 2009) (Figure 1.1). For example, IL-12, a pro-inflammatory cytokine, drives the differentiation of type 1 helper T cells (T_H1 cells), which express the transcription factor T-bet, and secrete type 1 cytokines, such as IFN-γ. In the presence of IL-4, type 2 helper T cells (T_H2 cells) are developed, expressing the transcription factor GATA3 and secreting type 2 cytokines, including IL-4, IL-5, and IL-13. TGF-β, together with IL-6, drives the differentiation of type 17 helper T cells (T_H17 cells), expressing the transcription factor Rorγt and producing type 3 cytokines e.g. IL-17 and IL-22. TGF-β, together with IL-2, drives the development of regulatory T (Treg) cells, expressing the transcription factor FoxP3 and producing TGF-β. In the presence of type 1 cytokines, TCR and co-stimulatory signals can launch the differentiation of $CD8^+$ T cells to cytotoxic T cells.

In humoral immune responses, the activation of B cells is mediated in a T cell-dependent or a T cell-independent manner (Y. J. Liu, Zhang, Lane, Chan, & MacLennan, 1991; Parker, 1993). The activated B cells differentiate into plasma cells that can produce soluble form of antibodies,

called immunoglobulins (Ig). Immunoglobulins comprise five classes, which are IgM, IgD, IgG, IgA and IgE. In addition to different classes of Ig, activated B cells express B cell receptors (BCR), a membrane-bound immunoglobulin with an intracellular signal transduction module.

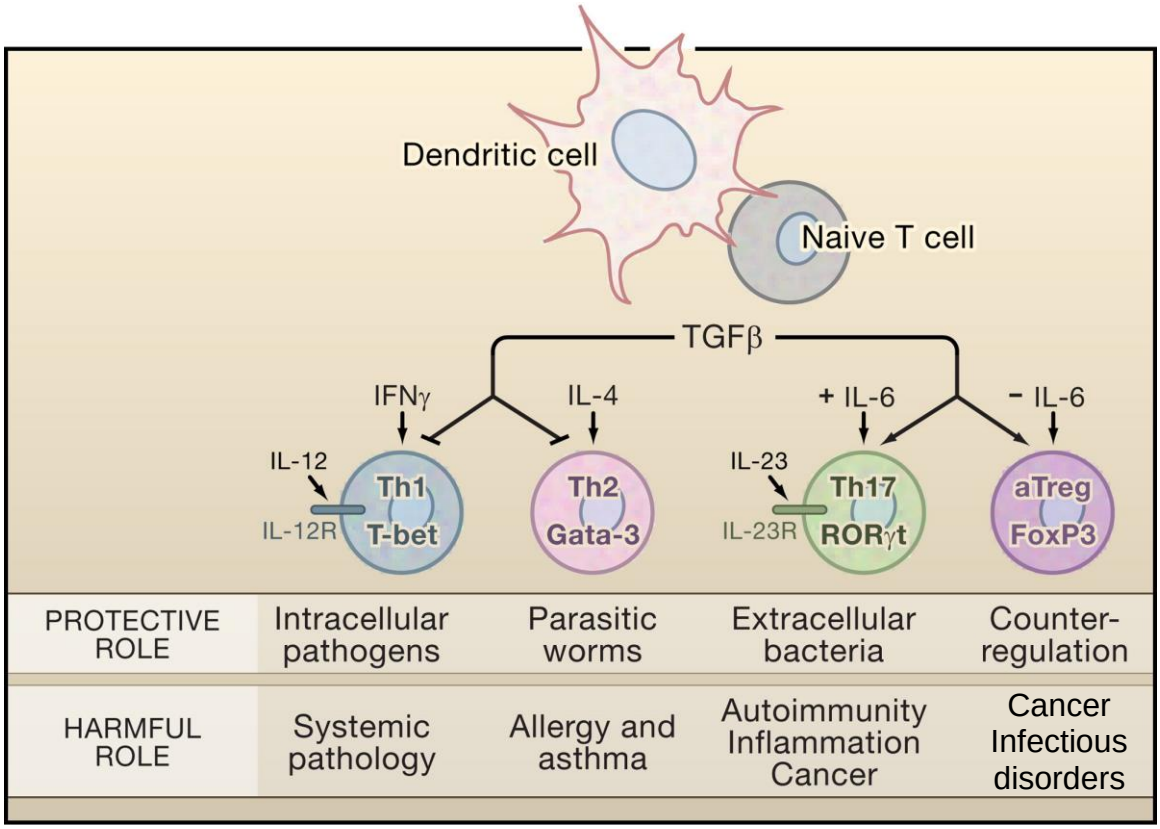

Figure 1.1. Heterogeneity in helper T cell fates. Antigen recognition together with co-stimulatory signals and cytokines on naïve T cells initiates the differentiation to type 1 helper T cells (T_H1 cells), type 2 helper T cells (T_H2 cells), type 17 helper T cells (T_H17 cells) or regulatory T cells (Treg). T_H1 cell require IFN-γ and IL-12 for development, and display a protective role against intracellular pathogens. T_H2 cells, differentiated in the presence of IL-4, can support protection against parasitic infections. T_H17 cells are developed in the presence of transforming growth factor β (TGFβ), IL-6 and IL-23, and provide host defense against extracellular bacteria. In the absence of IL-6, TGFβ induces the differentiation of Treg cells, which regulate protective immune responses (The figure is adopted from (Reiner, 2007)).

TCR or BCR repertoire determines the antigen specificity of T cells or B cells, respectively. The diversity of TCRs and BCRs is generated by somatic recombination of variable (V), diversity (D), and joining (J) gene segments, a process regulated by enzymes, namely recombination-activated genes (RAG1 and RAG2). Thus, the deficiency of RAG results in the absence of T cells and B cells in mice (Mombaerts et al., 1992; Shinkai et al., 1992). The combination of α and β chains or γ and δ chains increases further a variety of TCRs, while B cells form BCRs with two heavy chains and two light chains (κ and λ chains). B cells undergo three processes of Ig diversification, which are somatic hypermutation, class switch recombination, and gene conversion, and these processes maximize the potential antigen-binding specificities of TCRs and BCRs. Subsequently, self-reactive T cells or B cells are deleted upon the exposure

to self-antigens, which contributes to immune tolerance to self-molecules (Goodnow, Crosbie, Jorgensen, Brink, & Basten, 1989; C. A. Smith, Williams, Kingston, Jenkinson, & Owen, 1989).

Upon the first infection, naïve T cells differentiate into effector T cells, which can exert cytotoxicity and produce effector molecules. After the clearance of antigens, a part of effector T cells resides as long-lived memory T cells that comprise effector memory cells, central memory cells, and resident memory cells. Resident memory T cells continue to be situated in the inflamed tissue, whereas effector memory T cells and central memory T cells patrol in the circulation. Central memory T cells are also commonly found in secondary lymphoid organs due to the high expression of homing receptors. Upon the secondary infection, effector memory T cells can be recruited to infected tissues from circulation, and central memory T cells can be activated by antigen presentation of local APCs, followed by cell expansion and re-circulation to the infection site. On the other side, B cells are activated and develop to plasma cells, producing a large amount of antibodies, and memory B cells. Upon the secondary infection, memory B cells respond rapidly by producing high amounts of antibodies with higher affinity compared to naïve B cells. One of the applications of memory immune responses is vaccination, leading to a long-term protection against viruses or bacteria.

1.2 Innate lymphoid cells (ILCs)

Innate lymphoid cells (ILCs) are derived from common lymphoid progenitors (CLP) in fetal livers and adult bone marrow (Chea et al., 2016; Constantinides, McDonald, Verhoef, & Bendelac, 2014; Ishizuka et al., 2016; Klose et al., 2014). The development of ILCs initiates from common innate lymphoid progenitors (CILP), which is a downstream of CLP. CLIP segregates into two main lineages, NK progenitor (NKP) and common helper innate lymphoid precursor (CHILP). The transcription factor GATA3 is required for the development of helper-like ILCs, which are progenies of CHILP, while NK cells, derived from NKP, are independent of the GATA3 expression and require the presence of the transcription factor Eomes (Daussy et al., 2014; Serafini et al., 2014; Yagi et al., 2014) (Figure 1.2).

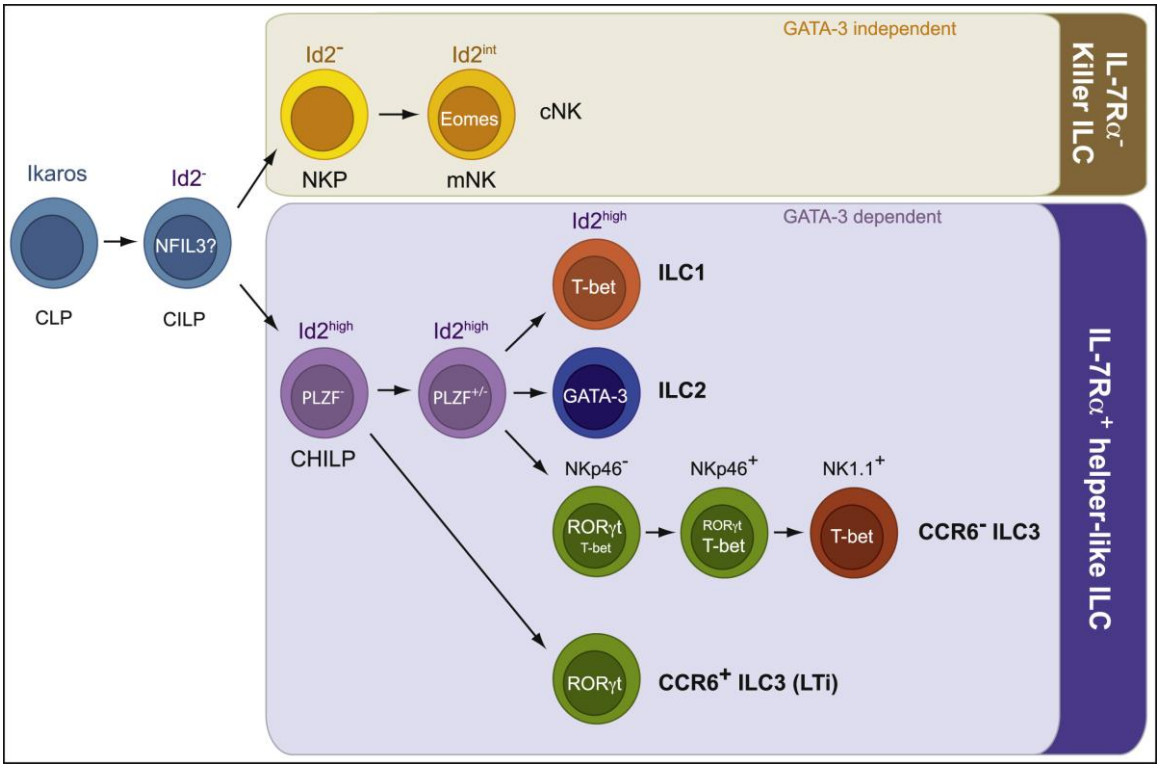

Figure 1.2. The lineage map for killer ILC and helper-like ILC development. CLP, common lymphoid progenitors; CILP, common innate lymphoid progenitor; NKP, NK progenitor; mNK, mature NK cells; cNK, conventional NK cells; CHILP, common helper innate lymphoid precursor; LTi, lymphoid-tissue inducer cells; Id2, inhibitor of DNA binding 2; NFIL3, nuclear Factor, interleukin 3 regulated (The figure is adopted from (Diefenbach, Colonna, & Koyasu, 2014)).

1.2.1 Classification of ILCs

ILCs are the first line defenders in innate immunity and considered innate counterparts of T cells. Similar to T cells, consisting of T helper cells and cytotoxic T cells, ILCs are classified into two groups. The first group comprises helper-like ILCs, including type 1 ILCs (ILC1s), type 2 ILCs (ILC2s), type 3 ILCs (ILC3s) and lymphoid-tissue inducer (LTi) cells, and the second group comprises killer ILCs, namely natural killer (NK) cells (Figure 1.3).

Tissue-resident ILC1s and conventional NK cells belong to group 1 ILCs. Although NK cells and ILC1s are derived from the separate developmental pathways (Figure 1.2), they present common features. For instance, NK cells and ILC1s express the transcription factor T-bet and they can produce inflammatory cytokines, such as IFN-γ and TNF-α, upon activation. T-bet regulates the development and maturation of NK cells and ILC1s, as well as IFN-γ production of NK cells (Daussy et al., 2014; Gordon et al., 2012; Townsend et al., 2004). In addition to the expression of T-bet, NK cells express the transcription factor Eomes, which is essential for NK cell development (Klose et al., 2014). NK cells are similar to killer $CD8^+$ T cells, concerning Eomes expression and IFN-γ secretion (Figure 1.3). Both NK cells and killer $CD8^+$ T cells can be recruited from blood to inflammatory sites and carry out cytotoxic functions. On the other hand, ILC1s are found in organs, e.g. liver, intestine, and adipose tissue, and share similarities with $CD4^+$ T_H1 cells, such as T-bet expression and high IFN-γ production (Figure 1.3).

Comparable to $CD4^+$ T_H2 cells, ILC2s are identified as GATA3-expressing ILCs. ILC2s express IL-33R (ST2), KLRG1 and CRTH2 on the cell surface (Vivier et al., 2018) and upon stimulation, they can produce type 2 cytokines, including IL-4, IL-5 and IL-13 (Figure 1.3). ILC2s are tissue-resident cells, found abundantly in mucosal area of airways and lungs. They play an essential role to support the host's defense and maintain tissue homeostasis in lungs (Bouchery et al., 2015; Gasteiger, Fan, Dikiy, Lee, & Rudensky, 2015; Halim et al., 2014; Y. Huang et al., 2018; Silver et al., 2016).

As a counterpart of $CD4^+$ T_H17 and T_H22 cells, group 3 ILCs are characterized by the expression of Rorγt, a transcription factor. Despite the common expression of Rorγt, ILC3s display heterogeneous population, including NKp46-expressing cells, NKp46-non-expressing cells, and CCR6-expressing LTi cells. Upon activation, group 3 ILCs can produce IL-17A, IL-17F, IL-22 or lymphotoxins (Figure 1.3). The major source of IL-22 in guts is group 3 ILCs, together with γδT cells. The signaling of IL-22 in the small intestine sustains tissue homeostasis and immune responses by regulating epithelial cells and supporting resistance of colonization (Aparicio-Domingo et al., 2015; Goto et al., 2014; Gronke et al., 2019; Huber et al., 2012; Pham et al., 2014; Satoh-Takayama et al., 2008; Sonnenberg, Fouser, & Artis, 2011). Moreover,

intestinal group 3 ILCs are involved in T cell-mediated intestinal immune tolerance. As examples, group 3 ILCs could induce selective death of activated T cells and support Treg cells in the intestine, by producing IL-2 (Hepworth et al., 2015; L. Zhou et al., 2019).

In summary, helper-like ILCs are tissue-resident, thus, they are early innate responders against viruses, bacteria, fungi or parasites at the host barrier surfaces as well as important contributors for tissue repairing; meanwhile, NK cells are circulating innate lymphocytes, which can be recruited to infected tissues or tumors. They can mediate immune protection and tissue homeostasis by performing cytoxicity.

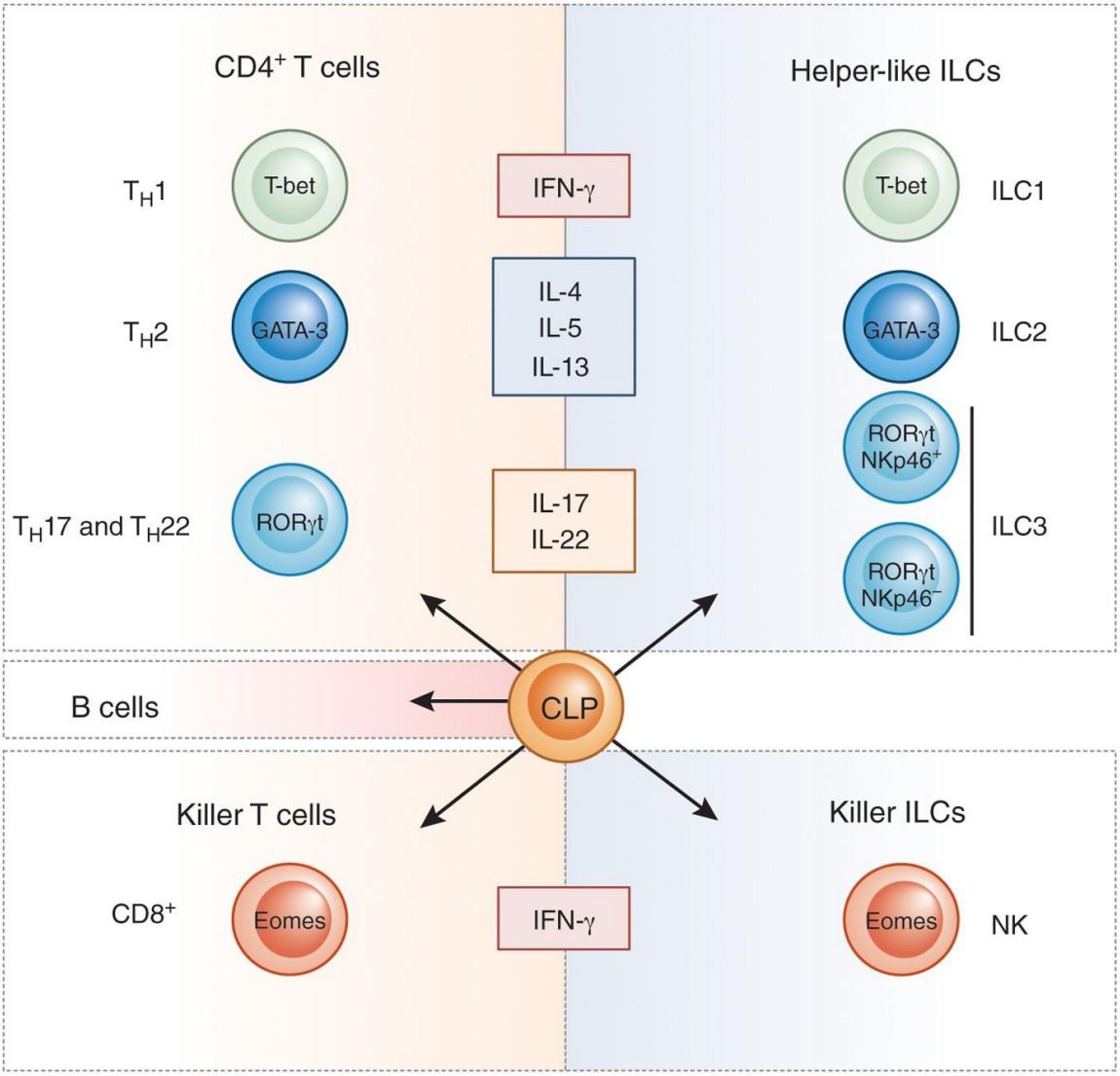

Figure 1.3. The diversity of innate lymphoid cells (ILCs) as a counterpart of T cells. ILC1, ILC2, ILC3, and NK cells share similarities with $CD4^+$ T_H1 cells, $CD4^+$ T_H2 cells, $CD4^+$ T_H17 and T_H22 cells, and $CD8^+$ T cells. Cytokines and transcription factors expressed by each cell type are displayed. (The figure is adopted from (Eberl, Di Santo, & Vivier, 2015)).

1.2.2 Group 1 ILC population in different organs

In murine livers, group 1 ILCs, defined as $CD3^-$ $NK1.1^+$ $NKp46^+$ cells, comprise approximately 10-20% of intrahepatic lymphocytes (Tian, Chen, & Gao, 2013). Conventional NK cells express CD49b (DX5), a type of integrin, on the cell surface, whereas hepatic ILC1s (tissue-resident NK cells) express CD49a on the cell surface. Initially, CD49a-expressing ILC1s were considered immature NK cells due to the low expression of CD11b and high expression of CD27 (Abel, Yang, Thakar, & Malarkannan, 2018). Later, it was discovered that ILC1s and NK cells are originated from the different progenitors. Hepatic ILC1s can be further characterized with the high expression of TRAIL, CD200R, and CXCR6 on the cell surface; whereas CD49b-expressing NK cells do not express those molecules, but instead express Eomes, CD62L and Ly49 receptors (Jiao, Huntington, Belz, & Seillet, 2016; Robinette et al., 2015). In addition to livers, $CD49b^-$ $CD49a^+$ ILC1s are found in other tissues, such as skin and uterus (Sojka et al., 2014).

In adipose tissues, group 1 ILCs consist of heterogeneous subpopulations, including $CD49a^+$ $CD49b^-$ cells, $CD49a^-$ $CD49b^+$ cells, and $CD49a^-$ $CD49b^-$ cells (Liou et al., 2014; O'Sullivan et al., 2016). Each subpopulation shows diverse surface expression of the inhibitory receptors KLRG1, and NK cell maturation markers, such as CD27 and CD11b, as well as differential effector functions (O'Sullivan et al., 2016).

Group 1 ILCs comprise $NK1.1^+$ $NKp46^+$ $CD127^-$ NK cells and $NK1.1^+$ $NKp46^+$ $CD127^+$ ILC1s in murine spleen. $NK1.1^+$ $NKp46^+$ $CD127^-$ NK cells are the major population of group 1ILCs in spleens, comprising more than 90% of group 1 ILCs (Robinette et al., 2015; Sojka et al., 2014). Through the comparison of gene expression analyzed by Principal component analysis (PCA), splenic NK cells and hepatic NK cell clustered closely, among various types of ILC1s obtained from different organs (Robinette et al., 2015). This indicates that a large number of genes were commonly expressed in splenic and hepatic NK cells. Besides, NK cells in spleens and livers express Eomes and Ly49D at protein level (Sojka et al., 2014; H. Sun, Sun, Tian, & Xiao, 2013). Similar to spleens, group 1 ILCs are mainly composed of NK cells in lungs. Lung NK cells present similarities with hepatic NK cells and splenic NK cells, e.g. the expression of Eomes and Ly49 receptor family (H. Sun et al., 2013).

1.2.3 Group 1 ILC activation

In contrast to T cells or B cells, where antigen-specific receptors play important roles for the activation, the balance between signals from activating receptors and signals from inhibitory receptors is crucial for NK cells (Table 1.1). For instance, murine NK cells express activating receptors, such as NKp46 and NKG2D, and the cross-linking of these receptors can promote

activation, proliferation and IFN-γ release by NK cells (Jamieson et al., 2002; Reichlin & Yokoyama, 1998; Smyth et al., 2004). Inhibitory receptors, such as Ly49 receptors on mouse NK cells and killer cell immunoglobulin-like receptors (KIRs) or CD94/NKG2A on human NK cells, are expressed on the surface (Table.1.1). When these receptors encounter MHC class I molecules on normal and healthy cells, NK cells do not conduct lysis of target cells due to inhibitory signals (Figure 1.4). Target cells, which downregulated or lack MHC class I expression, can be detected and eliminated by NK cells, proposed as “missing-self” recognition (Karlhofer, Ribaudo, & Yokoyama, 1992; Ljunggren & Karre, 1990). The balance of numerous signals transmitted from activating and inhibitory receptors regulate the activation and effector functions of NK cells (Guia, Fenis, Vivier, & Narni-Mancinelli, 2018). Similar to NK cells, ILC1s express a lectin-like receptor NK1.1, and activating receptors, such as NKp46 and DNAM-1, and the engagement of these receptors initiates the activation and IFN-γ secretion. However, inhibitory receptors, such as Ly49 receptors, are not expressed on ILC1s, suggesting that ILC1s do not perform “missing-self” recognition (Klose & Artis, 2020).

Table 1.1. Receptors and ligands on NK cells (The table is adopted from (Paul & Lal, 2017)).

Type	Receptors	Ligands	Species
Activating receptors	NKG2D	Rae-1a-e, MULT-1, H60 MIC-A/B, ULBP1-4	Mouse Human
	CD94-NKG2C	Qa1b HLA-E	Mouse Human
	Ly49D	H-2D^{d}	Mouse
	Ly49H	m157 of MCMV	Mouse
	NKp30	B7H6, BAT3, pp65 of HCMV	Human
	NKp46	Heparin, viral hemagglutinin (HA) and hemagglutinin-neuraminidase (HN)	Mouse/Human
	NKp44	Viral HA and HN, proliferating cell nuclear antigen (PCNA), proteoglycans	Mouse/Human
	DNAM-1	CD112, CD155	Mouse/Human
Inhibitory receptors	Ly49A	H-2D^{b,d,k,p}, H-2M3	Mouse
	Ly49C	H-2D^{b,d,k}, H-2K^{b,d,k}, m157 of MCMV	Mouse
	KIR2DL1-3	HLA-C1,2	Human
	KIR3DL1-2	HLA-Bw4, HLA-A3, -A11	Human
	CD94-NKG2A	Qa1b HLA-E	Mouse Human
	CD244 (2B4)	CD48	Mouse/Human

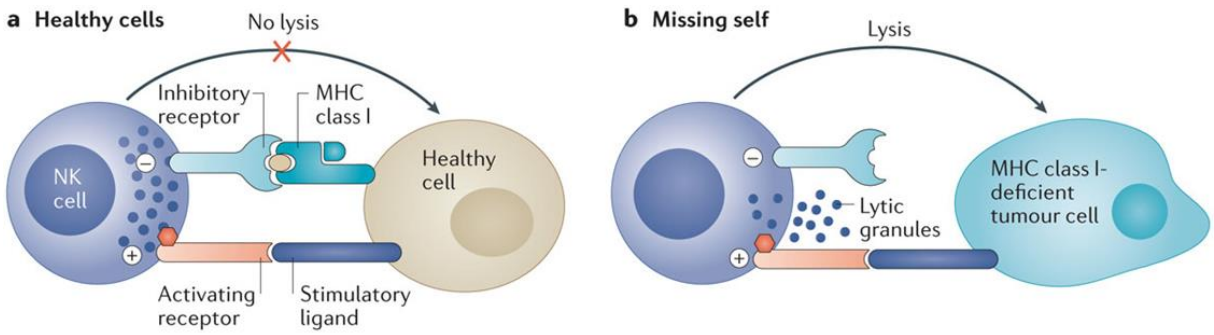

Figure 1.4. Activating and inhibitory signals on NK cells. (a) NK cell recognition of healthy cells. (b) "Missing-self" recognition (The figure is adopted from (Morvan & Lanier, 2016)).

Additionally, various cytokines can induce the activation of NK cells and ILC1s. Both NK cells and ILC1s express surface receptors of pro-inflammatory cytokines, such as IL-12, IL-15 and IL-18 (Robinette et al., 2015). The stimulation through these receptors triggers early immune responses of NK cells, e.g. production of IFN-γ, TNF-α, or IL-2, during tumor growth/metastasis or parasite/viral infection (Ferlazzo et al., 2004; Gazzinelli et al., 1994; Hashimoto et al., 1999; Hyodo et al., 1999; Kodama et al., 1999; B. Liu et al., 2004; K. S. Wang, Frank, & Ritz, 2000). The secretion of IFN-γ, TNF-α, and GM-CSF by ILC1s were mediated by the engagement of pro-inflammatory cytokines and their receptors (Mortha & Burrows, 2018; Vivier et al., 2018). Type I IFNs, such as IFN-α and IFN-β, which are abundantly produced by myeloid cells in viral infections, was reported to regulate NK cell expansion and responses (Kwaa, Talana, & Blankson, 2019; Madera et al., 2016; Nguyen et al., 2002; Orange & Biron, 1996; Swann et al., 2007). IL-10, a pleiotropic molecule, was reported to enhance NK cell cytotoxicity against tumor cells (Mocellin et al., 2004; J. Y. Park et al., 2011) and effector functions via metabolic reprogramming of NK cells (Z. Wang et al., 2021). Furthermore, cytokine production and cytotoxicity of NK cells were effectively supported by IL-10, in the presence of inflammatory cytokine, such as IL-15 or IL-18 (Cai, Kastelein, & Hunter, 1999; J. Y. Park et al., 2011). However, other studies described the opposite impact of IL-10 on NK cells. IL-10 and TGFβ were demonstrated to support limited functionalities of NK cells, such as cytolytic activity and IFN-γ production, upon stimulation with cytokine and in diseases (D'Andrea et al., 1993; Lassen, Lukens, Dolina, Brown, & Hahn, 2010; Rook et al., 1986; Stacey, Marsden, Wang, Wilkinson, & Humphreys, 2011; Viel et al., 2016).

NK cells can be activated in response to stimulation with receptors and/or cytokines, and the activated NK cells perform cytotoxicity using several distinct mechanisms. For example, mechanisms include the lysis of target cells-mediated by perforin and granzymes, and the apoptosis of target cells induced via death receptor-ligand engagement (Prager & Watzl, 2019).

1.2.4 NK cell cytotoxicity

The chemokines released from inflamed tissue or tumor attract circulatory NK cells to the sites (Bernardini, Gismondi, & Santoni, 2012; Maghazachi, 2010; Vitale, Cantoni, Pietra, Mingari, & Moretta, 2014). In contact with target cells, recruited NK cells can destroy susceptible target cells via perforin/granzyme-mediated lysis or death receptor-initiated apoptosis (Figure 1.5). Perforin and granzyme are stored in lytic granules that translocate to the contact site with target cells, and secrete their content toward target cells upon the fusion of granules to target cell membrane. This process is called “degranulation”. Upon degranulation, NK cells express lysosomal-associated membrane protein 1 (LAMP1, CD107a) and lysosomal-associated membrane protein 2 (LAMP2, CD107b) on the surface (Aktas, Kucuksezer, Bilgic, Erten, & Deniz, 2009); thus, CD107a and CD107b can be used as functional markers of NK cell activity (Alter, Malenfant, & Altfeld, 2004; Kannan et al., 1996). Perforin and granzymes play an important role in NK cell-mediated tumor killing to decrease susceptibility to virus (Andoniou et al., 2014; Mullbacher et al., 1999; Smyth et al., 1999; van den Broek, Kagi, Zinkernagel, & Hengartner, 1995). Perforin is a membrane-disrupting protein, which can form pores on target cell membrane and enable passive diffusion of granzymes into target cells (Lieberman, 2003). Granzymes are a family of 10 granule serine protease, including granzyme A, B, C, D, E, F, G, H, K, and M. Granzyme B is the most abundant type in mice and human, and it initiates mitochondrial damage-induced cell death via caspase-dependent and -independent pathways (Alimonti, Shi, Baijal, & Greenberg, 2001; V. K. Chiu, Walsh, Liu, Reed, & Clark, 1995; Metkar et al., 2003; Trapani et al., 1998; G. Q. Wang et al., 2001) (Figure 1.5A).

NK cells express ligands of tumor necrosis factor (TNF) family, such as Fas ligand (FasL) and TNF-related apoptosis inducing ligand (TRAIL) (Dostert, Grusdat, Letellier, & Brenner, 2019) . FasL or TRAIL can bind to Fas or TRAIL receptor (TRAIL-R) on target cells respectively, resulting in apoptotic signal transduction via caspase pathway (Figure 1.5B). Several studies revealed that pro-inflammatory cytokines, such as IL-2 and IL-15, enhanced surface expression of TRAIL and FasL on murine NK cells, and both murine and human NK cells performed TRAIL- or FasL-induced cytotoxicity against tumor cells (Kashii, Giorda, Herberman, Whiteside, & Vujanovic, 1999; Kayagaki et al., 1999; Screpanti, Wallin, Grandien, & Ljunggren, 2005; Zamai et al., 1998). Compared to NK cells, ILC1s preferentially express death-receptor ligand TRAIL in both human and mice (Stegmann et al., 2016; Takeda et al., 2005), and execute TRAIL-mediated cytotoxicity against target cells (Sag, Ayyildiz, Gunalp, & Wingender, 2019). Furthermore, human ILC1s from healthy donors showed death receptor Fas (CD95) expression on the cell surface (Zhao et al., 2018). However, the role of Fas on ILC1s remains to be further investigated.

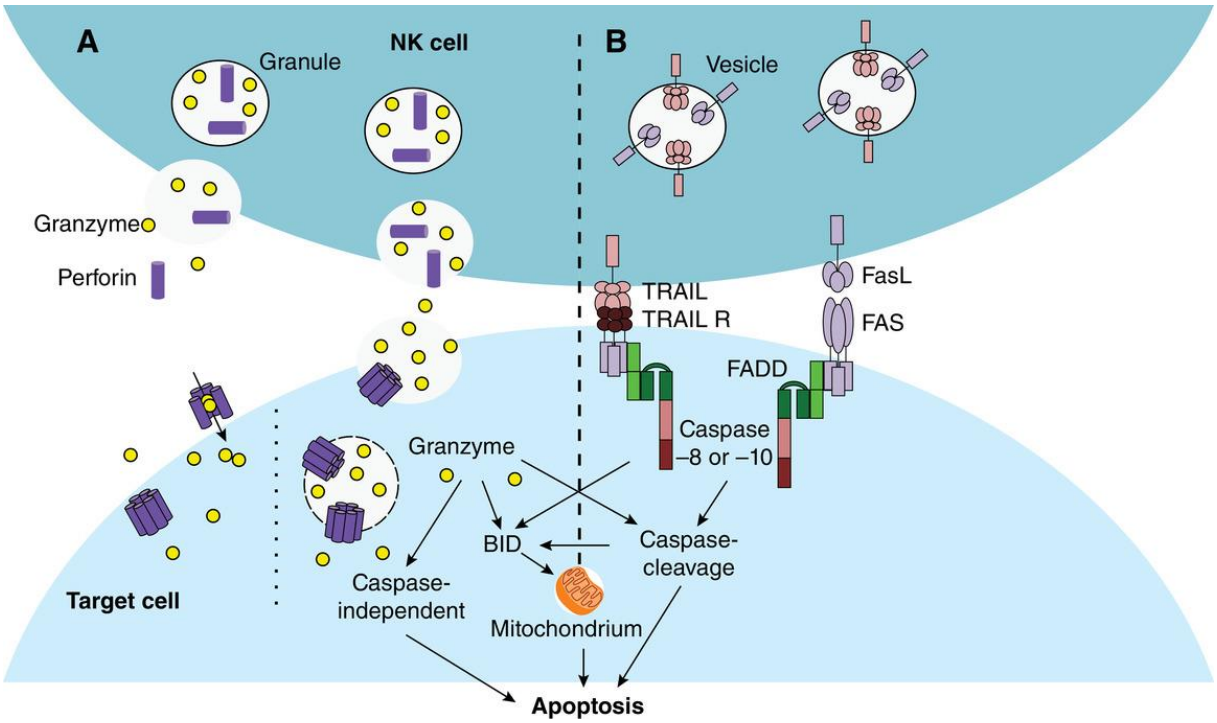

Figure 1.5. Two mechanisms of NK cell-induced target cell killing. (A) Perforin/granzyme-mediated cytotoxicity. (B) Death receptor-mediated cytotoxicity via TRAIL/TRAIL-R or FasL/Fas axis (The figure is adopted from (Prager & Watzl, 2019)).

Additionally, NK cells implement antibody-dependent cellular cytotoxicity (ADCC), a cytolysis mediated by immune cells with FcRIIIA (CD16A) (Leibson, 1997). IgG antibodies bind to antigens on the surface of target cells, and FcRIIIA recognizes Fc fragment of cell-bound antibodies. The engagement of FcRIIIA induces tyrosine kinase activities and transcriptional changes, resulting in lytic granule-induced cytotoxicity against target cells (Einspahr, Abraham, Binstadt, Uehara, & Leibson, 1991; Vivier et al., 1991). NK cell-mediated ADCC plays a crucial role in anti-tumor or anti-viral therapies. As examples, monoclonal antibodies binding to tumor-associated antigens (TAA), e.g. Rituximab (anti-CD20), trastuzumab (anti-HER2), Cetuximab (anti-EGFR), and Daratumumab (anti-CD38), are exploited as treatment of different types of cancers (Ochoa et al., 2017).

1.2.5 NK cell cytokine production

NK cells can produce a set of soluble molecules, including IFN-γ, TNF-α, GM-CSF and IL-10 (Perussia, 1996). IFN-γ was initially detected in human NK cells and $CD3^+$ T cells upon stimulation with IL-2 (Ortaldo et al., 1984; Trinchieri et al., 1984). IFN-γ belongs to the type II interferon (IFN) family, and is a pleiotropic pro-inflammatory cytokine, exerting antiviral and anti-tumor functions (Jorgovanovic, Song, Wang, & Zhang, 2020). The absence of IFN-γ signaling enhanced a susceptibility of host to infection (S. Huang et al., 1993; B. Lu et al., 1998). In the tumor microenvironment (TME), IFN-γ was shown to trigger the apoptosis of tumor cells (Poggi, Massaro, Negrini, Contini, & Zocchi, 2005; Ross & Caligiuri, 1997; R. Wang, Jaw, Stutzman, Zou, & Sun, 2012). Along with the direct effect of IFN-γ on target cells, IFN-γ can shape immune responses through the education of immune cells. IFN-γ supports transition of naïve T cells to T_H1 cells via the upregulation of the transcription factor T bet (Muller et al., 2017; Szabo et al., 2000). Furthermore, IFN-γ was reported to increase the expression of MHC molecules on myeloid cells, which could promote pathogen-derived antigen recognition (Pan et al., 2004; Russell, Dudani, Krishnan, & Sad, 2009; Weidinger, Henning, ter Meulen, & Niewiesk, 2001). In combination with IFN-γ, TNF-α was displayed to play a protective role upon different bacterial infections (Doherty et al., 1992; Nakane, Okamoto, Asano, Kohanawa, & Minagawa, 1995; Nakano, Onozuka, Terada, Shinomiya, & Nakano, 1990), and to induce maturation of myeloid cells, such as DCs (Ferlazzo et al., 2002; Gerosa et al., 2002).

GM-CSF is a member of the colony-stimulating factor (CSF) family, along with M-CSF and G-CSF. The main sources of GM-CSF are epithelial cells, endothelial cells and fibroblasts (Becher, Tugues, & Greter, 2016). Upon stimulation of the receptors CD16 and NKp30, uterine decidual NK cells upregulated the expression of Csf2 (encoding GM-CSF), and NK cells isolated from peripheral blood release GM-CSF (Aste-Amezaga, D'Andrea, Kubin, & Trinchieri, 1994; Cuturi et al., 1989; El Costa et al., 2008; Jokhi, King, Sharkey, Smith, & Loke, 1994). Stimulatory cytokines, such as IL-12 and IL-18, were reported to induce GM-CSF production by NK cells (Aste-Amezaga et al., 1994; Brady et al., 2010). GM-CSF is considered an important cytokine that supports the homeostasis and differentiation of DCs upon inflammation or in *in vitro* culture (Caux et al., 1996; Greter et al., 2012; Inaba, Inaba, et al., 1992; Inaba, Steinman, et al., 1992). Furthermore, GM-CSF is reported to boost the progression of diseases, such as arthritis and multiple sclerosis (Campbell et al., 1998; Cook et al., 2012; McQualter et al., 2001). Louis et al. showed that GM-CSF released by synovial NK cells contributed to arthritis progression through the promotion of inflammatory cell infiltration (Louis et al., 2020). However, the roles of GM-CSF derived from NK cells in different diseases are not fully uncovered.

In the early stage of infection, NK cells were reported to produce pro-inflammatory cytokines, while, in the late phase, they produce immunosuppressive cytokine, such as IL-10 (Rojas, Avia, Martin, & Sevilla, 2017). Clark et al. showed the switch of cytokine production of NK cells, from IFN-γ to IL-10, after infection with *Listeria monocytogenes* (Clark et al., 2016). Other studies reported the ability of NK cells to secret IL-10 in several bacterial and viral infections (Ali, Komal, Almutairi, & Lee, 2019; Clark, Schmidt, Aguilera, & Lenz, 2020; Jensen et al., 2021; Perona-Wright et al., 2009; Wagage et al., 2014). As an anti-inflammatory molecule, IL-10 can regulate immune responses and protect the host from tissue damage. Jensen et al. demonstrated IL-10 produced by NK cells was beneficial to enhance host survival in sepsis models (Jensen et al., 2021). However, the regulatory mechanism mediated by IL-10 can increase the host susceptibility to infection through enabling pathogens to evade immunity. Research showed that NK cell-derived IL-10 restricted the activation of virus specific-T cells, resulting in a high risk of infection (Brockman et al., 2009; H. Li et al., 2018). The production of IL-10 by NK cells could be regulated by several mechanism, e.g. by aryl hydrocarbon receptor (AHR), Signal transducer and activator of transcription 3 (STAT3) or STAT4 (Clark, Burrack, Jameson, Hamilton, & Lenz, 2019; Grant et al., 2008; Wagage et al., 2014).

1.2.6 NK cell metabolism

To provide energy for the relevant effector functions, NK cells regulate their metabolism in steady-state and upon activation. Quiescent NK cells show a low rate of glycolysis combined with a low activity of mitochondrial oxidative phosphorylation (OXPHOS) (Loftus et al., 2018; Slattery et al., 2021), whereas activated NK cells increase glucose uptake, and enhance glycolysis and OXPHOS, in order to generate adenosine triphosphates (ATP) as energy sources (Gardiner & Finlay, 2017).

Upon cytokine-stimulation, several papers reported that the mTOR pathway is a key regulator of NK cell metabolism and cytotoxic functions (Donnelly et al., 2014; Mao et al., 2016; Marcais et al., 2014). For instance, mouse and human NK cells, which presented a low rate of metabolism *ex vivo*, were reported to increase glycolysis and glucose uptake in a mTOR-dependent manner, during the short-term stimulation (18 hours) with IL-2/IL-12 (mouse) or IL-2/IL-15 (human) (Donnelly et al., 2014; Keating et al., 2016). This metabolic transition to glycolysis from OXPHOS was crucial for the secretion of IFN-γ and Granzyme B by NK cells (Donnelly et al., 2014). In contrast, Marçais et al. showed that NK cell metabolism was maintained upon short-term exposure to IL-15, while the stimulation with IL-15 for 5 days enhanced both glycolysis and OXPHOS of NK cells via the mTOR pathway (Marcais et al., 2014). In addition to glycolysis and OXPHOS, L-amino acid transport and de novo polyamine synthesis are required to maintain metabolic and functional responses in cytokine-activated NK cells (Loftus et al., 2018;

O'Brien et al., 2021). Activated NK cells displayed higher expression of CD71 (transferrin receptor) and CD98 (amino acid transporter), and enhanced glucose uptake, shown as a higher amount of 2-NBDG (an analog of glucose), compared to resting NK cells. In accordance to Marçais et al., Keppel et al. showed that the short-term stimulation with IL-12/IL-18 or via activating receptors (4 hours and 6 hours respectively) did not change metabolic activities of NK cells (Keppel, Saucier, Mah, Vogel, & Cooper, 2015). IFN-γ production upon receptor triggering was regulated by mitochondrial respiration, but IFN-γ production triggered by IL-12/IL-18 was shown to be independent of glycolysis and mitochondrial respiration. On the contrary, two studies illustrated that restricted glycolysis and mitochondrial respiration negatively regulated effector functions of NK cells that were previously exposed to cytokines (Assmann et al., 2017; Kedia-Mehta et al., 2021).

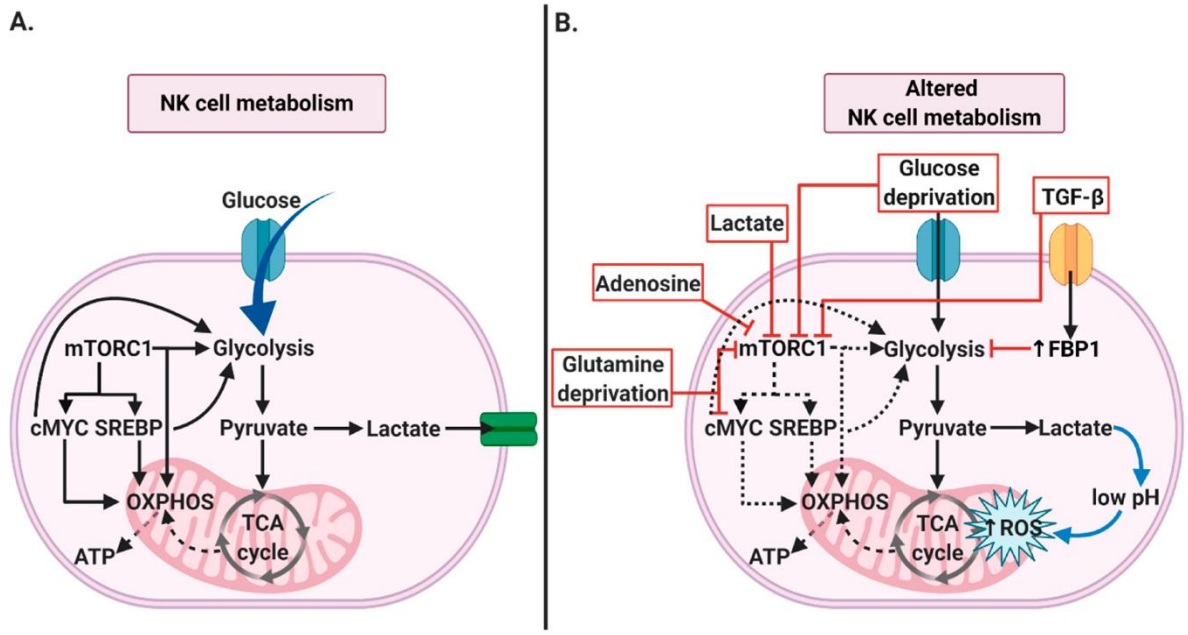

Figure 1.6. NK cell metabolism upon activation and in disease. (A) Upon activation, NK cells utilize glucose for glycolysis and oxidative phosphorylation (OXPHOS). Key regulators of glycolysis and OXPHOS, such as mTORC1, cMYC, and SREBP, are displayed. (B) NK cell metabolism is altered in disease, including cancer. Signaling via TGFβ, lactate, or adenosine, and deprivation of glucose or glutamine induce alteration in NK cell metabolism (The figure is adopted from (Domagala et al., 2020)).

NK cell metabolism is influenced by the microenvironment, which can be determined by the health status of individuals (Figure 1.6). For instance, tumor cells can cause glucose deprivation and lactate abundancy, along with a low extracellular pH (Kato et al., 2013). Tumor cells engineered to produce less amount of lactates progressed slowly, and in this tumor microenvironment (TME), NK cells and T cells displayed enhanced IFN-γ secretion (Brand et al., 2016). Additionally, NK cells obtained from breast cancer patients displayed a lower glycolytic capacity and respiration, as well as dysfunctional mitochondria, compared to NK cells obtained from

healthy individuals (Slattery et al., 2021). The blockade of TGFβ, a cytokine abundantly found in the TME, could restore the malfunction of cancer patient-derived NK cells (Slattery et al., 2021; Zaiatz-Bittencourt, Finlay, & Gardiner, 2018). Viral infections, where NK cells can perform cytotoxicity to restrict the spread of virus rapidly, create an environment that modulates mitochondrial morphology and metabolism of NK cells. For instance, after 7 days of viral infections, Ly49H-expressing NK cells showed a reduced membrane potential and increased production of reactive oxygen species (ROS), indicating potential metabolic changes in NK cells (O'Sullivan, Johnson, Kang, & Sun, 2015). Upon acute viral infection, activated NK cells, which could produce inflammatory cytokines, showed upregulated glycolysis and OXPHOS, along with increased CD98 and CD71 expression, and they required amino acid and iron availability for cytotoxicity and cytokine production (Littwitz-Salomon et al., 2021).

In obese individuals, NK cells are constantly exposed to a low-level inflammation, and high amounts of adipokines and fatty acids. It has been reported that individuals with obesity displayed impaired NK cell functions, such as reduced secretion of lytic molecules and cytotoxicity against tumor cell (Tobin et al., 2017). Michelet et al. showed that NK cells obtained from obese subjects accumulated lipid via a PPARα- and PPARδ-axis, resulting in a loss of effector functions (Michelet et al., 2018).

1.2.7 NK cells as regulators of adaptive immunity

NK cells can be recruited to inflamed tissue and exert cytotoxicity, as well as they can interact with other types of innate immune cells. Literature demonstrated that interaction between NK cells and dendritic cells (DCs) mediates innate immune responses and is important to develop T cell-mediated immune responses (Walzer, Dalod, Robbins, Zitvogel, & Vivier, 2005). *In vitro* and *in vivo* studies observed that the interaction between NK cells and DCs could empower activation and proliferation of NK cells, cytokine production from both DCs and NK cells, and maturation of DCs (Ferlazzo et al., 2002; Gerosa et al., 2002; Osada et al., 2001; Piccioli, Sbrana, Melandri, & Valiante, 2002; Yu et al., 2001). In detail, the engagement of NK cells and DCs induced the production of pro-inflammatory cytokines, such as IL-12 and IL-18 by DCs, and these cytokines were regulators of IFN-γ production and lytic activity of NK cells (Borg et al., 2004; Gerosa et al., 2002; Yu et al., 2001). IFN-γ or TNF-α produced by NK cells triggered maturation of immature DCs, resulting in the upregulation of CD83, CD86 and MHC I molecule (Piccioli et al., 2002; Vitale et al., 2005).

In contrast to supporting DC maturation, NK cells could restrict DC functions by killing immature dendritic cells (iDCs), when the ratio of NK cells to DCs is high (Carbone et al., 1999; Ferlazzo

et al., 2002; Piccioli et al., 2002; Wilson et al., 1999). Several pathways were reported to participate in NK cell-mediated DC elimination. For example, DC elimination could be triggered by NK cell activation via NKp30 engagement in human (Ferlazzo et al., 2002), and via DNAM-1/CD155 interaction (Seth et al., 2009), TRAIL-induced apoptosis (Hayakawa et al., 2004), and NK recognition of DCs expressing reduced MHC class I molecules (Carbone et al., 1999; Della Chiesa et al., 2003). On the other hand, TGFβ1 downregulated activating receptor expression, such as NKp30 and NKG2D, resulting in the inefficient DC killing by NK cells (Castriconi et al., 2003).

Researches showed the importance of crosstalk between NK cells and DCs in a reciprocal manner to activate both cells upon viral infections, bacterial infection and tumors. As examples, NK cells expressing Ly49 receptors were required to maintain $CD8\alpha^+$ DCs, and reciprocally these NK cells required the presence of $CD8\alpha^+$ DCs for expansion (Andrews, Scalzo, Yokoyama, Smyth, & Degli-Esposti, 2003). Contact between NK cells and virus-infected DCs via activating receptors NKp46 and NKG2D was essential for increased CD69 expression and IFN-γ production by NK cells (Draghi et al., 2007). NK cell interaction with bacteria-infected DCs could improve NK cell activation and the ability to remove immature DCs (Ferlazzo et al., 2003), implying improved immune responses against bacterial infection. In tumor-bearing mice, DCs triggered NK cell-mediated anti-tumor immunity, and *in vitro*, the contact between DCs and NK cells enhanced the cytotoxicity and IFN-γ production of NK cells (Fernandez et al., 1999). Furthermore, Buentke et al. and Parolini et al. reported the close contact of NK cells and DCs in atopic dermatitis-like skin lesion and in inflamed dermal endothelium (Buentke et al., 2002; Parolini et al., 2007). In addition, NK cell-mediated killing was enhanced against DCs cultured with *Malassezia*, a yeast-allergen inducing atopic eczema and dermatitis (Buentke et al., 2002). Yet, NK cells obtained from hepatitis C virus-infected patients negatively regulated DC maturation via engagement of the inhibitory receptor CD94/NKG2A (Jinushi et al., 2004).

Maturation of DCs can be induced by interaction with NK cells, and mature DCs were reported to migrate to lymph nodes in a CCR7-dependent manner (Jang et al., 2006; Ohl et al., 2004). In lymph nodes, mature DCs can potentiate the development of naïve T cells (Lanzavecchia & Sallusto, 2001). Several researches examined that DCs conditioned by the interaction with NK cells could modulate T cell priming. NK cells activated with tumor cells could induce DC maturation and IL-12 release by DCs (Mailliard et al., 2003; Mocikat et al., 2003). IL-12 produced by DCs differentiated naïve T cells to T_H1 cytokine-producing cells (Mailliard et al., 2003), and enhanced $CD8^+$ T cell memory responses upon tumor challenges (Mocikat et al., 2003). In uveitis, IFN-γ-producing NK cells were recruited to draining lymph nodes by DCs in a CXCR3-dependent manner (Chong et al., 2015). This interaction between NK cells and DCs

induced IL-27 production by DCs, and IL-27 triggered IL-10 release by T-bet-expressing $CD4^+$ T cells, which could alleviate disease.

In addition to the indirect effect of NK cells on T cell priming via the crosstalk with DCs, it is demonstrated that NK cells can directly regulate T cell responses. First, studies showed that IFN-γ produced by NK cells was essential for T_H1 polarization and type 1 cytokine production *in vitro* (Martin-Fontecha et al., 2004; Morandi, Bougras, Muller, Ferlazzo, & Munz, 2006) and during *L. major* infection (Laouar, Sutterwala, Gorelik, & Flavell, 2005). In contrast, it was reported that NK cells could negatively regulate T cell responses. As an example, in MCMV-infected animals, IL-10 released by NK cells limited $CD8^+$ T cell responses, leading to the protective effect against MCMV infection (S. H. Lee, Kim, Fodil-Cornu, Vidal, & Biron, 2009). NK cells eliminated $CD4^+$ T cells and $CD8^+$ T cells *in vitro* via NKG2D-NKG2D-L axis, resulting in the inhibition of T cell responses (Cerboni et al., 2007; Rabinovich et al., 2003). Additionally, NK cell-mediated T cell killing was observed in the virus-infected animals (Crouse et al., 2014; Lang et al., 2012; Peppa et al., 2013; Waggoner, Cornberg, Selin, & Welsh, 2011; Waggoner, Taniguchi, Mathew, Kumar, & Welsh, 2010; Xu et al., 2014). In detail, T cell killing was facilitated by the absence of receptor 2B4 on NK cells, the increased TRAIL-R expression on T cells, and the upregulated expression of NCR1 (NKp46) ligand (Crouse et al., 2014; Peppa et al., 2013; Waggoner et al., 2010). Furthermore, the interaction of Qa-1-NKG2A prohibited the lysis of activated T cells by NK cells, and the absence of Qa-1 on $CD4^+$ T cells could lead to T cell elimination in a NK cell-dependent manner (L. Lu et al., 2007; Xu et al., 2017). On the other hand, type I IFN signaling could protect T cells from lysis by NK cells (Crouse et al., 2014; Xu et al., 2014).

1.3 Vitamins

Vitamins are micronutrients found in plant-derived food and animal products in small amounts. They are not main sources of energy production, but still essential for well-being. Vitamins comprise water-soluble and lipid-soluble molecules. Water-soluble vitamins include the vitamin B family and vitamin C (ascorbic acid). Vitamins B are crucial cofactors for carbohydrate and protein metabolism, mitochondrial electron transport, and nucleic acid formation. Vitamin C is a potent antioxidant and needed for synthesis of carnitine. Vitamin A, D, E, and K are lipid-soluble and stored in adipose tissue. The main role of vitamin A and E is performing antioxidant activities. Vitamin D, which can be synthesized in skin during sunlight exposure, is responsible for calcium absorption and bone metabolism. Vitamin K regulates protein synthesis and is involved in blood clotting.

1.3.1 Vitamin A metabolism

Vitamin A is a lipid-soluble micronutrient, found in diets containing carotenoids and retinyl esters. In intestinal lumen, retinyl esters and carotenoids are hydrolyzed to retinol and absorbed by intestinal epithelium cells, called enterocytes (Blomhoff, Green, Berg, & Norum, 1990). Absorbed retinol is partially oxidized to retinal by alcohol dehydrogenase (ADH), and retinal is further oxidized to retinoic acid (RA) by retinal dehydrogenase (RALDH) in $CD103^{+}$ DCs. Rest of retinol is esterified to retinyl esters by lecithin retinol acyltransferase (LRAT) or acyl-CoA retinol acyltransferase (ARAT). Retinlyl esters are loaded to chylomicrons in order to enter blood circulation, and transported mainly to liver, but as well to bone marrow, lung and heart (Blomhoff, Helgerud, Rasmussen, Berg, & Norum, 1982; Hussain et al., 1989).

In liver, hepatocytes uptake and hydrolyze retinyl esters from chylomicrons to retinol. Retinol binding protein 4 (RBP4), produced by hepatocytes, binds to retinol (Muenzner et al., 2013). Retinol bound to RBP4 can be secreted back to the circulation, depending on the extracellular retinol concentration, and after the secretion, retinol is absorbed via the stimulated by retinoic acid 6 (STRA6) receptor, expressed on stromal cells and myeloid cells. The remaining retinol is transported and stored in hepatic stellate cells (HSCs), as retinyl esters, or converted to retinoic acid (RA) by ADH and RALDH (Blomhoff et al., 1990). Converted RA engages with retinoic acid receptor (RAR), retinoid X receptor (RXR) or peroxisome proliferator activated receptor (PPAR), and activates ligand-dependent transcription. Two RA-binding proteins, cellular retinoic acid binding protein II (CRABP II) and fatty acid-binding protein 5 (FABP5), direct this engagement (Saeed, Dullaart, Schreuder, Blokzijl, & Faber, 2017). A high ratio of CRABP II to FABP5 induces RA binding to RARs; meanwhile a high ratio of FABP5 to CRABP II induces RA binding to PPARs (Figure 1.7).

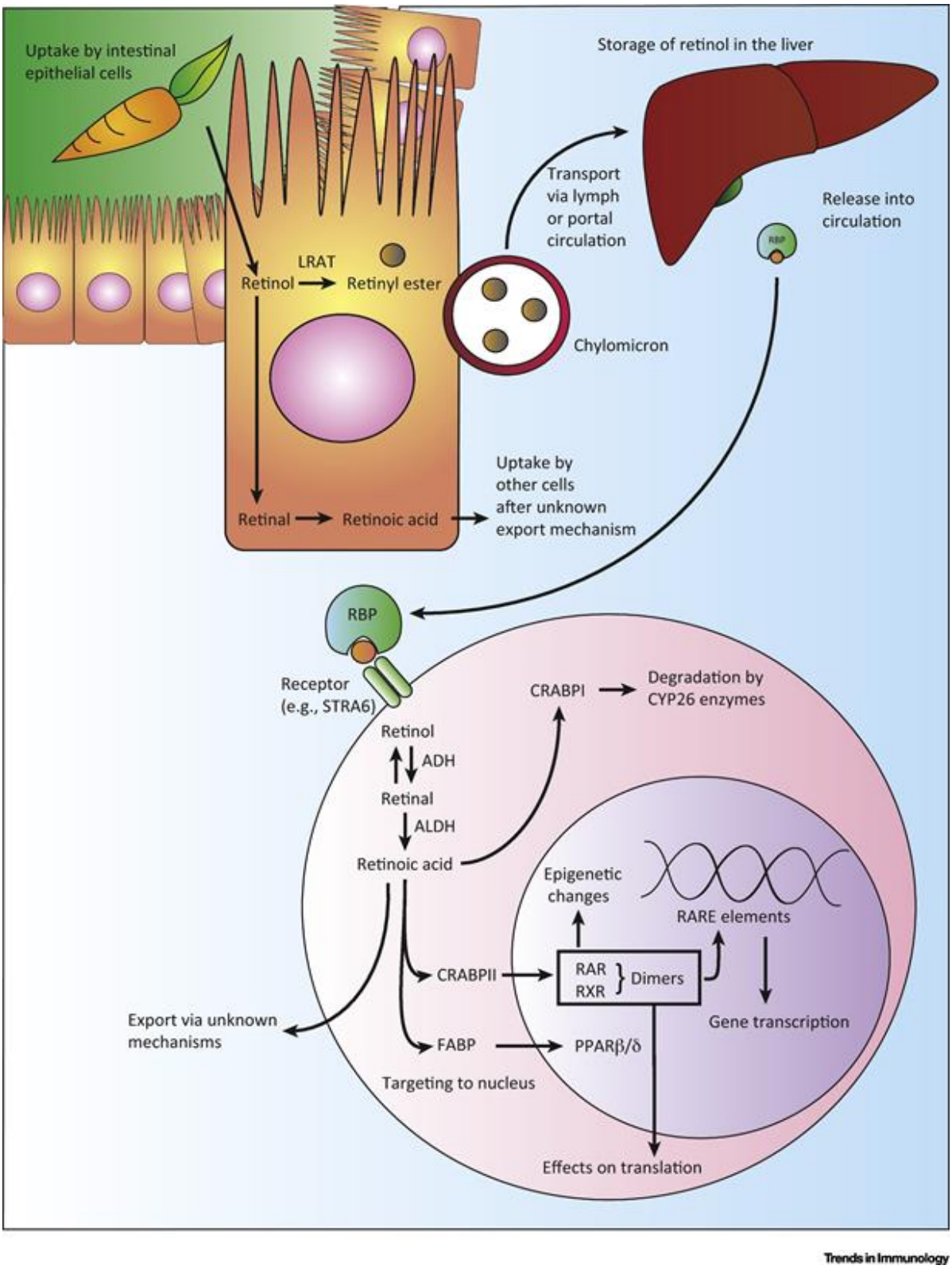

Figure 1.7. Vitamin A metabolism and signaling. Vitamin A precursors are metabolized by enterocytes and esterified in retinyl esters by the enzyme lecithin retinol acyltransferase (LRAT). Retinyl esters packed in chylomicron are transported to liver for storage. Retinol complexed with retinol-binding protein (RBP) in the liver is released to circulation. Stimulated by retinoic acid 6 (STRA6), expressed on the cell surface, binds to the retinol-RBP complex. After uptake, retinol is oxidized to retinal by the enzyme alcohol dehydrogenase (ADH), and to retinoic acid (RA) by the enzyme retinal dehydrogenase (RALDH). RA bound to cellular retinoic acid-binding protein II (CRABP II) or fatty acid-binding protein (FABP) translocates to the nucleus and regulates gene transcription. The remaining RA can bind to CRABP I and is degraded by cytochrome P450 family 26 (CYP26) (The figure is adopted from (Erkelens & Mebius, 2017)).

Table 1.2. Retinoid-binding proteins and receptors (The table is adopted from (Blomhoff et al., 1990; Bushue & Wan, 2009)).

Protein	Ligands	Suggested function
RBP	Retinol	Blood plasma transport of retinol
IRBP	Retinol, retinal	Intercellular transport of retinol or retinal in visual cycle
CRABP I **CRABP II** **FABP5**	all-trans RA, 9-cis RA	Intracellular transport of retinol Regulate free retinoic acid concentration
RARα **RARβ** **RARγ**	all-trans RA, 9-cis RA	Ligand-dependent transcription factor
RXRα **RXRβ** **RXRγ**	9-cis RA	Ligand-dependent transcription factor
PPARβ/δ	all-trans RA, 9-cis RA	Ligand-dependent transcription factor

1.3.2 Impact of vitamin A on immune cells

Researchers reported that vitamin A metabolites, such as retinol and RA, were present in lymphoid and non-lymphoid organs and circulation (Kane, Folias, & Napoli, 2008). Vitamin A metabolites play an important role in immune cell development and responses. In the intestine, where vitamin A precursor and retinyl esters are metabolized to RA, $CD103^+$ DCs expressing RALDH are the main source synthesizing RA in lamina propria, together with epithelial cells and stromal cells. RA produced by $CD103^+$ DCs was reported to induce the expression of gut-homing receptors, such as CCR9 and α4β7 on intestinal DCs, T cells and ILC1, resulting in cell migration to the intestine (T. Feng, Cong, Qin, Benveniste, & Elson, 2010; Iwata et al., 2004; Kim, Taparowsky, & Kim, 2015). $CD103^+$ DCs promote tolerogenic immune responses in the intestine via the generation of Treg cells (Coombes et al., 2007; Ruane & Lavelle, 2011; C. M. Sun et al., 2007). Upon inflammation, $CD103^+$ DCs migrate to draining mesenteric lymph nodes (mLN), and display efficient T cell stimulation, compared to $CD103^-$ DCs in lamina propria (Jaensson et al., 2008; Schulz et al., 2009). RA signals regulate homeostasis of intestinal DCs, differentiation of splenic DCs (Beijer et al., 2013; Duriancik & Hoag, 2010; Klebanoff et al., 2013), and phenotype of intestinal cDC1 and cDC2 (Zeng, Bscheider, Lahl, Lee, & Butcher, 2016). *at*RA supports anti-inflammatory characteristics of DCs by inducing FoxP3-expressing Treg cells (Coombes et al., 2007; C. M. Sun et al., 2007). Besides, vitamin A is required for the proper development of $CD169^+$ macrophages, found in the intestine and involved in antigen presentation to B cells (Hiemstra et al., 2014).

Vitamin A metabolites also influence tissue-resident lymphocytes, innate lymphoid cells (ILCs). Maternal retinoid intake and fetal RA signals control LTi cell maturation (van de Pavert et al., 2014). Spencer et al. described that vitamin A deficiency drove the reduction in ILC3 numbers, resulting in increased susceptibility to bacterial infection in the gut. On the other hand, vitamin A deficiency improved ILC2-mediated host survival (Spencer et al., 2014). RA enhanced IL-22 production by γδ T cells and ILCs in the gut during bacterial infection (Mielke et al., 2013). Altogether, RA regulates intestinal immune responses by promoting IL-22 production.

In addition to VA-induced T cell migration to intestine, vitamin A metabolites contribute to regulatory T cell responses. *at*RA inhibited IL-6-induced T_H17 cells and promoted differentiation of Treg cells (Mucida et al., 2007). In the presence of TGFβ, *at*RA promoted FoxP3 expression and differentiation towards Treg cells (J. Ma et al., 2014; Schambach, Schupp, Lazar, & Reiner, 2007). Apart from the differentiation, *at*RA was reported to maintain the stability of Treg cells and their regulatory functions upon inflammation (Kwok et al., 2012; X. Zhou et al., 2010). Accordingly, the inhibition of RAR signal by pan-RAR antagonist LE540, reduced the number of FoxP3-expressing Treg cells in mucosa upon challenge with *Listeria monocytogenes* (Mucida et al., 2007). Likewise, mice fed with vitamin A-deficient (VAD) diet failed to suppress T cell responses upon LCMV infection (Liang et al., 2020). Additional treatment with *at*RA promoted the protective effect against LCMV infection and type I diabetes, via shaping the functionality of T cells in VAD diet-fed mice (Liang et al., 2020; Van et al., 2009).

1.3.3 Vitamin A in disease

During the early phase of infections, protein synthesis of RBP is noted to be downregulated (Birch & Schreiber, 1986), which results in increased RA turnover in the intestine, and decreased transport of retinol via the RBP complex. Animals challenged with LPS displayed hyporetinolema due to reduced liver RBP synthesis (Iyer & Vaishnava, 2019). In comparison to downregulated RBP synthesis, serum amyloid A (SAA1), a protein that retinol can alternatively bind to with high affinity, is upregulated in the intestine and livers during bacterial infection (Derebe et al., 2014) (Figure 1.8).

Several studies demonstrated the high susceptibility against intestinal infection in VAD diet-fed mice. As examples, *Citrobacter rodentium*-infected animals showed exacerbated inflammation and epithelial hyperplasia upon feeding with VAD diet (McDaniel et al., 2015), mainly due to altered ILC3 and T_H17 response. Another study showed that infection to *C. rodentium* itself decreased the amount of retinol in lung, but not in intestine and serum, as well as reduced retinyl ester amount in lung and liver (Restori, McDaniel, Wray, Cantorna, & Ross, 2014). After the bacterial clearance, downregulated retinol concentration in lung could not be rescued. In

contrast, when intestinal epithelial cells were genetically modified to block RA production, they exerted a protective role against *Salmonella Typhimurium* challenge, along with decreased IL-22 production in intestine (Grizotte-Lake et al., 2018). Infection with *Streptococcus pneumoniae* increased retinol amount in lung, and did not affect it in the liver (Restori et al., 2014). Similarly, epidemiological researches discovered that children with respiratory infection, gastroenteritis or worm-infection, displayed low capacity of vitamin A absorption and storage compared to healthy children (Sivakumar & Reddy, 1972, 1975), and tuberculosis patients had significantly lower concentrations of vitamin A in serum than healthy individuals (Mugusi, Rusizoka, Habib, & Fawzi, 2003; Qrafli et al., 2017; Ramachandran et al., 2004).

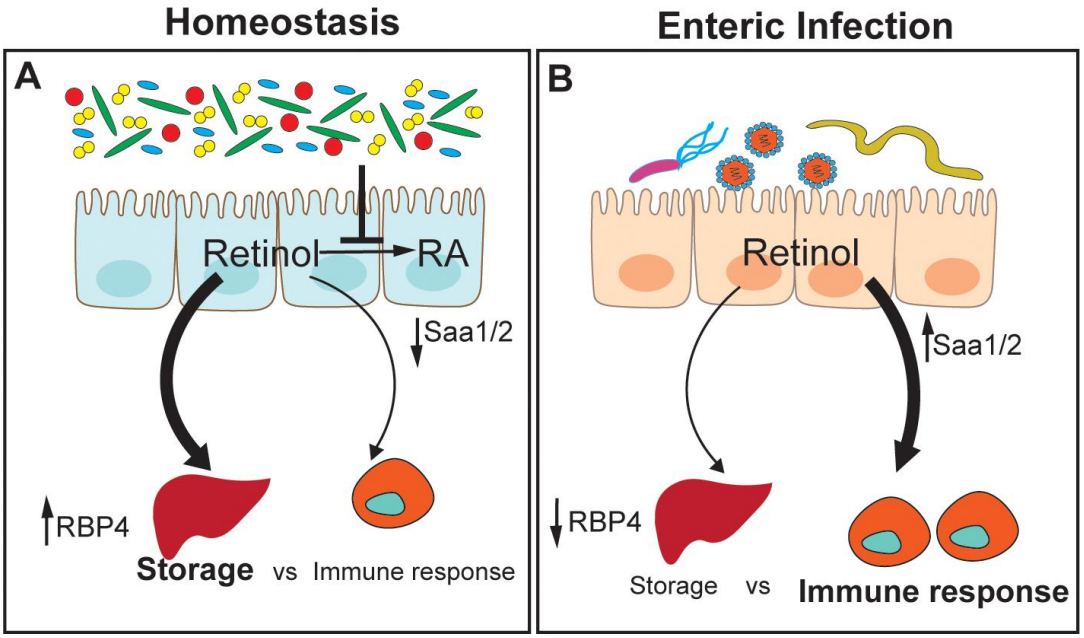

Figure 1.8. Retinol conversion and transport during health and disease. (A) During homeostasis, gut bacteria suppress the conversion of dietary retinol into RA and promote its storage. Retinol transporter RBP4 is the main transporter of retinol to and from the liver. (B) During infection, RBP4 amounts drop, reducing retinol transport and storage in the liver. Acute-phase RBPs, such as SAAs, increase in the intestinal tissue and upregulate the local immune response to infection. RA, retinoic acid; RBP, retinol-binding protein; SAA, serum amyloid A (The figure is adopted from (Iyer & Vaishnava, 2019)).

In liver diseases, such as inflammation, steatosis, fibrosis and hepatocellular carcinoma, hepatic stellate cells (HSCs) play a regulatory role. As an example, HSCs promoted regeneration of hepatocytes via hepatocyte growth factor (HGF), TGF-α and IL-6 (Friedman, 2008). HSCs in rat liver mitigated the capacity to store vitamin A after the partial hepatoectomy (PHx) and upon the induction of cholangiofibrosis (Higashi et al., 2005; Imai et al., 2000). The absence of RA signal in hepatocytes induced hepatic steatosis, defined as excessive accumulation of triglyceride in liver and high-RA diet could alleviate the progress of steatosis (Yanagitani et al., 2004). In accordance, previous study showed that RA treatment activated genes involved in fatty acid oxidation, and inhibited lipid synthesis in livers (Amengual, Ribot, Bonet, & Palou, 2010). Furthermore, *in vitro* culture, HSCs promoted FoxP3 expression and abolished IL-17

production by OT-II TCR transgenic T cells primed by DCs in RA-dependent manner (Ichikawa, Mucida, Tyznik, Kronenberg, & Cheroutre, 2011). During hepatic fibrosis, quiescent HSCs experience morphological and functional changes, including loss of retinol, and become activated HSCs (Friedman, 2008). Despite retinol release from activated HSCs, additional *at*RA-treatment and vitamin A-coupled liposomes suppressed CCl_4-induced hepatic fibrosis (Hisamori et al., 2008; Murakami et al., 2011; Y. Sato et al., 2008; Senoo & Wake, 1985). In accordance, upon *at*RA-treatment, activated HSCs reduced the production of TGFβ, IL-6, and collagen, which contributed to worsening of liver function (Hisamori et al., 2008). Cirrhotic and hepatocellular carcinoma patients displayed low amount of retinol compared to healthy individuals (Clemente et al., 2002).

Vitamin A metabolites are conventionally considered as anti-cancer agents due to their inhibitory effect on tumor cell growth and evasion (M. C. Chen, Hsu, Lin, & Yang, 2014). Many researches demonstrated the inhibitory effects of vitamin A metabolites on melanoma tumor cells. For example, cell growth of murine melanoma cells and colony formation of human melanoma were curbed by retinoids *in vitro* (Lotan, Giotta, Nork, & Nicolson, 1978; Meyskens & Salmon, 1979). This inhibition was mediated by the activation of cyclic AMP-dependent protein kinase and the modified basement membrane components in melanoma cells (Ludwig, Lowey, & Niles, 1980; Sengupta, Ray, Chattopadhyay, Biswas, & Chatterjee, 2000; Z. Wang, Cao, D'Urso, & Ferrone, 1992). Similar effects of RA were observed in human-originated prostatic cancer cells *in vitro* (Halgunset, Sunde, & Lundmo, 1987; Jutley, Reaney, Kelleher, & Whelan, 1990). Furthermore, anti-cancer effects of *at*RA via cell cycle inhibition and apoptosis induction were identified on gastric cancer cells (Naka et al., 1997; Patrad, Niapour, Farassati, & Amani, 2018; Ye et al., 2004). In animal studies, encapsulated *at*RA treatment suppressed colony formation of B16F10 melanoma cells in lung, and reduced tumor volume (Siddikuzzaman & Grace, 2012, 2014; Yao, Zhang, Zhou, Liu, & Zhang, 2013). *at*RA loaded in lipid nanoparticles displayed anti-cancer efficacy in gastric cancers (T. Li, Zhang, Meng, Bo, & Ke, 2017). Furthermore, *at*RA-treatment combined with a lipid immune activator, alpha-galactosylceramide (αGalCer), reduced breast tumor growth and lung metastasis. These studies postulate the therapeutic impact of retinoids for cancer treatment.

In contrast to anti-cancer effects shown by retinoid-treatment, a recent study illustrated immunosuppressive influence of *at*RA metabolized by sarcoma cells (Devalaraja et al., 2020). It was reported that the different types of murine sarcoma cells could shape the *at*RA-enriched TME in *in vivo* studies, and tumor-derived *at*RA supported monocyte differentiation to tumor-associated macrophages (TAMs), resulting in immune suppressive effect against tumor cells.

2 THE AIM OF STUDY

The improved understanding of how nutrients affect the immune system has resulted in the prevention of diseases, the promotion of immunity, and the development of immunotherapy. In accordance, vitamin A, one of the essential micronutrients, is responsible for the homeostasis of barrier tissues and the host protection from infectious pathogens. NK cells, a group of innate lymphocytes, are reported to be recruited to inflamed tissues to perform cytotoxicity against abnormal cells, as well as to tune immune responses in the liver and adipose tissue, where vitamin A is abundant. Vitamin A was reported to induce regulatory phenotypes in lymphocytes, such as T cells and ILC3s. However, the comprehension of vitamin A impact on NK cells remains unclear. In this regards, we hypothesized that vitamin A could regulate the NK cell-mediated immune responses. Our aim is to investigate the effect of vitamin A on the phenotype and effector functions of NK cells

Here, we elucidated the following aspects:

1. Identification of the transcriptome, metabolomics, and functionality of NK cells exposed to vitamin A-enriched microenvironment
2. Investigation on the interaction of vitamin A-conditioned NK cells with other immune cells
3. Dissection of the molecular mechanism of vitamin A-mediated NK cell responses

To address these aspects, we used *in vitro* culture system and mouse disease models, and generated specific conditional gene-knockout mice. Together, we believe that the findings obtained in the project will broaden the knowledge of the essential micronutrient's effect on the immune system.

3 MATERIALS AND METHODS

3.1 Materials

3.1.1 Laboratory equipment

Table 2.1. Laboratory equipment.

Product	Company
200 Gel Imaging Workstation	Azure biosystem
C1000 Touch™ Thermal Cycler	Bio-Rad
FACS Aria™ Fusion Cell Sorter	BD Biosciences
GentleMACS™ Octo Dissociator	Miltenyi Biotec
LSR Fortessa™ Cell Analyzer	BD Biosciences
Plate reader Infinite 200 pro	Tecan
pH Meter Seven Compact	Zeiss
QuantStudio™ 5 Real-Time PCR System, 384-well	Applied Biosystems
Seahorse™ XF HS Mini Analyzer	Agilent
Incubator BD056	BINDER

3.1.2 Chemicals

Table 2.2. Chemicals and biological reagents.

Product	Company	Catalog no.
7-AAD	BD Bioscience	15868458
Aqua Zombie™	Biolegend	423102
BODIPY™ FL C16	Invitrogen	10654623
CellROX™ Deep Red Reagent	Thermo Fischer	C10422
Collagenase IV	Worthington (Pan Biotech)	LS0004188
1α,25-Dihydroxyvitamin D3	Sigma-Aldrich	D1530-10UG
Deoxyribonuclease I Crude	Sigma-Aldrich	DN25_1G
GolgiPlug™ Protein Transport Inhibitor (containing Brefeldin A)	BD Bioscience	555029
GolgiStop™ Protein Transport Inhibitor (containing Monensin)	BD Bioscience	554724
Hyaluronidase Type V	Sigma-Aldrich	H6254-1G
Lipopolysaccharide E.coli O26:B6	Sigma-Alrich	L2654
Lympholyte®-M	Cedarlene	CL5035
Nuclease-free Water (not DEPC treated)	Ambion	AM9937

β-mercaptoethanol	VWR chemicals	0482-100ML
MitoTracker™ Green FM	Thermo Fischer	M7514
MitoProbe™ TMRM Assay Kit	Thermo Fischer	M20036
MM 11253	Sigma-Aldrich	SML2015
Percoll®	GE Health	17-0891-01
Poly-D-Lysine	Sigma	P6407
Recombinant Human IL-2	Hoffmann-La Roche	1104-0890
Recombinant Mouse IFN-γ	Peprotech	315-05
Recombinant Mouse IL-12	Peprotech	210-12
Recombinant Mouse IL-15	Peprotech	210-15
Recombinant Mouse IL-18	MBL	B002-5
Recombinant Mouse IL-1b	Peprotech	211-11b
Recombinant Mouse IL-23	Biolegend	589002
Recombinant Mouse TGF-β1	Biolegend	763102
Recombinant Mouse IL-6	Peprotech	216-16
Recombinant Mouse IL-4	Peprotech	214-14
Retinoic Acid	Sigma-Aldrich	R2625
Ro-415253	Sigma-Aldrich	SML0573
SCH 58261	Sigma-Aldrich	S4568
T 0070907	Tocris (R&D)	2301
Tween 20	Sigma-Aldrich	P9416
UltraPure™ 0,5M EDTA, pH 8	Invitrogen	15575020
ZM 241385	Sigma-Aldrich	Z0153

3.1.3 Cell culture media and solutions

Table 2.3. Cell culture media and solutions.

Product	Company	Catalog no.
β-mercaptoethanol	GIBCO-Invitrogen	31350010
Cell Dissociation Solution, non-enzymatic (1x)	Sigma-Aldrich	C5914
Dimethylsulphoxide Hybri Max™ (DMSO)	Sigma-Aldrich	D2650
Dulbecco's Modified Eagle's Medium (DMEM) with Glucose, L-glutamine, Sodium pyruvate, and Sodium bicarbonate	Sigma-Aldrich	D6459
Dulbecco's Phosphate Buffered Saline (PBS)	GIBCO-Invitrogen	14190
Fetal Bovine Serum, Origin: EU Approved 10270	GIBCO-Invitrogen	10270
GBSS	Pancoll-biotech	P04-48500

Gibco™ RPMI 1640 Medium	Fisher Scientific	11530586
L-Glutamine 200 mM (100x)	GIBCO-Invitrogen	25030
Non-essential Amino Acids (100x)	GIBCO-Invitrogen	11140035
Penicillin/Streptomycin Solution	GIBCO-Invitrogen	15140
Seahorse™ XF RPMI media & Calibrant	Agilent	103576-100
Seahorse™ XF 100 mM Pyruvate Solution	Agilent	103578-100
Seahorse™ XF 1.0 M Glucose Solution	Agilent	103577-100
Sodium Pyruvate MEM 100mM	GIBCO-Invitrogen	11360088
Trypsin-EDTA (1x) HBSS, without Ca^{2+}/Mg^{2+} with EDTA	GIBCO-Invitrogen	25300
GM-CSF produced by cell line X6310-GMCSF (DMEM-G)		

3.1.4 Cell isolation and culture products

Table 2.4. Cell isolation and culture products.

Product	Company	Catalogue no.
6.5 mm Transwell®, 0.4 µm Polyester Membrane Insert, Sterile	Corning	3470
Cell Lifter	Corning	3008
Cryovial, 2 mL sterile	Greiner Bio-one	122263
Falcon® 40 µm Cell Strainer, Blue, Sterile	Corning	352340
Falcon® 70 µm Cell Strainer, White, Sterile	Corning	352350
Falcon® 100µm Cell Strainer, Yellow, Sterile	Corning	352360
Falcon® 6-well Clear Flat Bottom, not Treated Cell Culture Plate, Sterile	Corning	351146
Falcon® 24-well Polystyrene Clear Flat Bottom, not Treated Cell Culture Plate, Sterile	Corning	351147
GentleMACS™ C Tubes	Miltenyi Biotec	130-093-237
MACS™ LS Columns	Miltenyi Biotec	130-042-401
RNase-free Microfuge Tubes (1.5 mL)	Thermofisher Ambion	AM12400
Serological pipette 5 ml, padded	Sarstedt AG & Co.	861253001
Serological pipette 10 ml, padded	Sarstedt AG & Co.	861254001
Serological pipette 25 ml, padded	Sarstedt AG & Co.	861685001
Seahorse™ XF HS Miniplate Kit	Agilent	103725-100
Tissue Culture Plate, Round Bottom	Sarstedt AG & Co.	83.3924.300
Tissue Culture Flask with Filter Screw Caps	Sarstedt AG & Co.	83.3912.302
TPP® tissue culture plates, 96 well plate, Round bottom, Polystyrene, Sterile	TPP	Z707899-162EA

3.1.5 Kits

Table 2.5. Kits.

Product	Company	Catalog no.
Adenosine Assay Kit	BioCat	MET-5090-CB
Annexin V staining kit	Biolegend	640912
Annexin V Binding buffer	Biolegend	422201
BD Horizon™ Brilliant Stain buffer	BD	566349
CellTrace™ Violet Cell Proliferation Kit	Invitrogen	C34557
Cytofix/Cytoperm™ buffer	BD	554714
FITC BrdU Flow Kit	BD	557891
Fixation/Permeabilization Solution Kit	BD	554714
FoxP3 Transcription factor staining buffer	eBioscience	00-5523-00
GeneChip™ Mouse Genome 430 2.0 Array	Applied Biosystem	900499
Liver Dissociation Kit, mouse	Miltenyi Biotec	130-105-807
Mouse NK Cell Isolation Kit	Miltenyi Biotec	130-115-818
Mouse naïve $CD4^+$ T Cell isolation kit	Miltenyi Biotec	130-104-453
Mouse IFN-γ ELISA MAX™ Standard set	Biolegend	430801
MyTaq™ Extract-PCR Kit	Meridian Bioscience	BIO-21127
ProtoScript® II First Strand cDNA Synthesis Kit	New England Biotechnology	E6560S
PowerUp™ SYBR™ Green Master Mix	Applied Biosystem	A25918
RNeasy® Mini Kit	Qiagen	74104
RNA Clean and Concentrator - 5	Zymo Research	R1013
RT^2 First Strand Kit	Qiagen	330404
RT^2 SYBR Green qPCR Mastermix	Qiagen	330501
RT^2 Profiler™ PCR Array Mouse Cytokines & Chemokines	Qiagen	PAMM-150Z
RT^2 Profiler™ PCR Array Mouse Retinoic Acid Signaling	Qiagen	PAMM-180Z
Seahorse™ XF Cell Mito Stress Test Kit	Agilent	103010-100
TURBO DNA-free™ kit	Ambion	AM1907

3.1.6 Buffers and solutions

Table 2.6. Buffers and solutions.

Solution	Ingredients
1.5M Sodium Chloride (NaCl) solution	87.66g of sodium chloride in 1L water
40% Percoll®, freshly prepared	4mL isotonic Percoll® solution 6mL PBS
70% Percoll®, freshly prepared	7mL isotonic Percoll® solution 3mL PBS
ACK lysis buffer	0.605 g Tris base 4.01g Ammoniochloride Fill up to 500 mL with ddH_2O Adjust pH to 7.2
BM-DC media	DMEM with high glucose 10% FCS 10% GM-CSF 1% L-glutamine 1% Non-essential amino acid 1% Sodium Pyruvate 1% Penicillin/Streptomycin 0.1% β-mercaptoethanol (for cell culture)
Cell Lysis buffer for RNA Isolation	RLT buffer from Qiagen 1% β-mercaptoethanol
Cell-Freezing media	FCS 10% DMSO
Complete DMEM	DMEM with high glucose 10% FCS 1% Penicillin/Streptomycin
Complete RPMI	RPMI 1640 with high glucose 10% FCS 1% Penicillin/Streptomycin
ELISA wash buffer	1x PBS 0.05% Tween-20
ELISA stop solution	2N H_2SO_4
FACS buffer	PBS 1% FCS 0.02% NaN_3 2 mM EDTA
Isotonic Percoll® solution	9 parts stock Percoll® 1 part 1.5M NaCl solution

Liver and lung digestion media for gentleMACS™ dissociation	DMEM 1% L-glutamine
MACS buffer	PBS 0.1% BSA 2 mM EDTA
Perm buffer	1 part 10x Permeabilization buffer concentrate 9 parts distilled water
Primary cell culture media (PCCM)	RPMI 1640 with high glucose 10% FCS 1% L-glutamine 1% Non-essential amino acid 1% Sodium Pyruvate 1% Penicillin/Streptomycin 0.1% β-mercaptoethanol (for cell culture use)
Sort buffer	PBS 1% FCS 2 mM EDTA

3.1.7 Primary antibodies for flow cytometry

Table 2.7. Primary antibodies for flow cytometry.

Specificity	Fluorochromes	Clone	Company	Catalog no.
IL-17A	FITC	TC11-18H10.1	Biolegend	506907
KLRG1	FITC	2F1	Southern Biotech	1807-02
CD38	FITC	T10	Biolegend	102705
CD200R	FITC	OX-2R	Biolegend	123910
DNAM-1	FITC	10E5	Biolegend	128803
Ly6C	FITC	RB6-8C5	BD Pharmingen	553126
CD71	FITC	RI7217	Biolegend	113086
CD8	FITC	Ly-2	BD Bioscience	553031
CD86	FITC	GL-1	Biolegend	105006
CD107a	FITC	1D4B	Biolegend	121606
Ki67	FITC	16A8	Biolegend	652409
CD11c	PerCP-Cy5.5	N418	Biolegend	117328
CD49a	PerCP-Cy5.5	HA31/8	BD Bioscience	564862
CD11c	PerCP-Cy5.5	NF18	Biolegend	117327
T-bet	PerCP-Cy5.5	4B10	Biolegend	644806
CD44	PerCP-Cy5.5	IM7	Biolegend	103031
NK1.1	PerCP/Cy5.5	PK136	Biolegend	108728

CD45.1	PerCP-Cy5.5	A20	Biolegend	110728
IκBζ	PerCP-eFluor 710	LK2NAP	Invitrogen	46-6801-82
CD73	PE	TY/11.	Biolegend	127205
TRAIL	PE	N2B2	Biolegend	109305
CD254 (RANKL)	PE	IK22/5	Biolegend	510005
IRF8	PE	V3GYWCH	Invitrogen	12-9852-82
CD80	PE	16-10A1	Biolegend	104708
CCL5 (RANTES)	PE	2E9/CCL5	Biolegend	149103
CD62L	PE	MEL-14	Biolegend	104407
CD200R	PE	OX-110	Biolegend	123908
TNFα	PE	MP6-XT22	Biolegend	506305
Eomes	PE Texas Red	X4-83	BD Bioscience	567167
FoxP3	PE-CF-594	FJK-16s	eBiosciences	61-5773-80
CD38	PE-Dazzle	90	Biolegend	102729
CD11b	PE-Dazzle	M1/70	Biolegend	101255
CXCR3	PE-Cy7	S18001A	Biolegend	155909
CD127	PE-Cy7	A7R34	Biolegend	135014
TIGIT	PE-Cy7	1G9	Biolegend	142107
CD69	PE-Cy7	H1.2F3	BD Pharmingen	552879
CD49d	PE-Cy7	A7R34	Biolegend	103705
NKp46	PE-Cy7	29A1.4	Biolegend	137618
CD62L	PE-Cy7	MEL-14	Biolegend	104453
CD19	PE-Cy7	6D5	Biolegend	115520
Eomes	PE-Cy7	Dan-11mag	eBioscience	25-4875-82
CD36	APC	HM36	Biolegend	102610
IFN-γ	APC	XMG1.2	Biolegend	505810
GM-CSF	APC	MP1-22E9	Biolegend	505413
RANK	APC	REA961	Miltenyi	130-116-068
IL-18Rα	APC	BG/IL18Ra	Biolegend	132903
CD39	APC	Duha59	Biolegend	143809
CD96	APC	3.3	Biolegend	131712
CCR9	Alexa Fluor 647	9B1	Biolegend	129709
CXCR6	Alexa Fluor 647	SA051D1	Biolegend	151115
NKG2D	APC	CX5	Biolegend	130212
PD-1	APC	29F.1A12	Biolegend	135209
I-A/I-E	Alexa Fluor 647	M5/114.15.2	Biolegend	107618

CD44	APC	IM7	eBioscience	17-0441-82
NK1.1	APC	PK136	Biolegend	108710
NKp46	APC	29A1.4	Biolegend	137608
GATA-3	APC	16E10A23	Biolegend	653809
Rogt	APC	Q31-378	BD Bioscience	562682
CD155	APC	TX56	Biolegend	131510
Ly6G	APC Cy7	1A8	Biolegend	127624
F4/80	APC Cy7	BM8	Biolegend	123118
SiglecF	APC Cy7	E50-2440	BD Bioscience	565527
FcεRI	APC Cy7	MAR-1	Biolegend	134325
Ter119	APC Cy7	TER-119	Biolegend	116223
TCRγδ	APC Cy7	H57-597	Biolegend	109219
CD19	APC Cy7	6D5	Biolegend	115530
CD4	APC-Cy7	GK1.5	Biolegend	100414
CD45.2	APC-Cy7	104	Biolegend	109824
CD3ε	APC-Cy7	145-2C11	Biolegend	100329
DNAM-1	APC-Cy7	10E5	Biolegend	128816
CD3ε	BV421	145-2C11	Biolegend	100335
NKp46	BV421	29A1.4	Biolegend	137612
TCRβ	BV421	H57-597	Biolegend	109230
NK1.1	BV650	PK136	Biolegend	108735
IFN-γ	BV650	XMG1.2	Biolegend	563854
CD62L	BV650	MEL-14	Biolegend	104453
CD160	BV650	CNX46-3	BD Bioscience	740637
CD11b	BV650	M1/70	Biolegend	101259
CD4	BV650	RM4-5	Biolegend	100555
TCRγδ	BV711	GL3	Biolegend	563994
CD45.1	BV711	A20	Biolegend	110739
NK1.1	BV711	PK136	Biolegend	108745
CD3ε	BV711	145-2C11	Biolegend	100349
IL-10	BV711	JES5-16E3	BD Bioscience	564081
Tbet	BV785	4B10	Biolegend	644835
NK1.1	BV785	PK136	Biolegend	108749
CD4	BV785	GK1.5	Biolegend	100453
CD45	BV785	30-F11	Biolegend	103149
CD3ε	BV785	145-2C11	Biolegend	100355
CD3ε	BUV395	145-2C11	BD Bioscience	563565
CD45.2	BUV395	104	BD Bioscience	564616

KLRG1	BUV563	2F1	BD Bioscience	741343
CD4	BUV563	GK1.5	BD Bioscience	612923
CD45	BUV737	30-F11	BD Bioscience	748371
CD3ε	BUV805	500A2	BD Bioscience	741928
TCRβ	BUV805	H57-597	BD Bioscience	748405
CD45.2	BUV805	104	BD Bioscience	741957
Phospho-Stat4	PE	D2E4	Cell signaling	13223
Phospho-NF-κB p65 (Ser536)	PE	93H1	Cell signaling	5733
Phospho-IKKα/β (Ser176/180)	PE	16A6	Cell signaling	14938

3.1.8 Antibodies for functional assays

Table 2.8. Antibodies for functional assays.

Antibody	Clone	Company	Catalog no.
Ultra-LEAF™ Purified anti-mouse CD16/CD32	93	Biolegend	101329
LEAF™ Purified anti-mouse NK-1.1	PK136	Biozol	108712
anti-mouse NKp46/NCR1	polyclonal	R&D	AF2225
anti-mouse NKG2D/CD314	A10	Biolegend	115602
Ultra-LEAF™ Purified anti-mouse IL-4	11B11	Biolegend	504122
Ultra-LEAF™ Purified anti-mouse IFN-γ	R4-6A2	Biolegend	505709
Ultra-LEAF™ Purified anti-mouse IL-2	JES6-1A12	Biolegend	503706
Ultra-LEAF™ Purified anti-mouse CD3ε	145-2C11	Biolegend	100340
Ultra-LEAF™ Purified anti-mouse CD28	37.51	Biolegend	102116
anti-mouse IL-10	JES5-2A5	Bio X Cell	BE0049
anti-mouse CCL1/I-309/TCA-3	148113	R&D	MAB845
anti-mouse CCL5/RANTES	53405	R&D	MAB478
anti-mouse TGFβ	1D11	R&D	MAB1835

3.1.9 Purified fusion-proteins for functional assays

Table 2.9. Purified fusion-proteins for functional assays.

Recombinant protein	Linker	C-terminus	Company	Catalog no.
Recombinant mouse Ephrin-A2 Fc Chimera	IEGRMDP	Mouse IgG 2a	R&D	8415-A2-200
Recombinant mouse CD155/PVR Fc Chimera	IEGRMDP	Mouse IgG 2a	R&D	9670-CD-050

3.1.10 Isotype controls

Table 2.10. Isotype controls.

Specificity	Fluorochrome	Clone	Company	Catalog no.
Rat IgG2b	Alexa Fluor 647	RTK4530	Biolegend	400626
Rat IgG1	APC	RTK2071	Biolegend	400412
Rat IgG2a	APC	54447	R&D	IC006A
Rat IgG2b	APC	RTK4530	Biolegend	400612
Rat IgG2b	APC/Fire	RTK4530	Biolegend	400670
Rat IgG2a	BV421	RTK2758	Biolegend	400549
Rat IgG1	FITC	RTK2071	Biolegend	400406
Rat IgG2a	FITC	RTK2758	Biolegend	400506
Rat IgG2b	FITC	RTK4530	Biolegend	400606
Arm Hamster	PE	A19-3	BD	553972
Mouse IgG2a	PE	MOPC-173	Biolegend	400212
Mouse IgG2b	PE	MPC-11	Biolegend	400312
Rat IgG2a	PE	RTK2758	Biolegend	400508
Rat IgG2b	PE	RTK4530	Biolegend	400608

3.1.11 Oligonucleotide primers

Table 2.11. Oligonucleotide primers.

Target	Forward sequence (5’ → 3’)	Reverse sequence (5’ → 3’)
mTGFβ1	GCTGAACCAAGGAGACGGAA	GGGGCTGATCCCGTTGATTT
mTGFβ2	TAAAATCGACATGCCGTCCCA	CTGGGACTGTCTGGAGCAAA
mTGFβ3	GGCCCTGGACACCAATTACT	AGGTTCGTGGACCCATTTCC
mRara	CCTCATCTGTGGAGACCGAC	CCGTTTCCGGACGTAGACTT
mRarb	GGGCATGTCCAAAGAGTCTGT	CGTCTAGCTCCGCTGTCATC
mRarg	CCAAGGAAGCTGTAAGGAACG	TGGTGATGAGTTCCTCTAACTGTG

mPpara	TCTGGGCAAGAGAATCCACG	CAAAAGGCGGGTTGTTGCTG
mPpard	GCACATCTACAACGCCTACCT	GTGGATGACAAAGGGTGCGT
mPparg	TGTCTCACAATGCCATCAGGT	GATCAGCAGACTCTGGGTTCA
mActb	CAGATGTGGATCAGCAAGCA	GGGTGTAAAACGCAGCTCAGTA
mB2m	TGCTATCCAGAAAACCCCTCA	GGCGGGTGGAACTGTGTTA
mAldh1a1	GGTGAGGAGGACTAGTTGTGAC	TCACAACACCTGGGGAACAG
mAldh1a2	TGGACAGATCATCCCGTGGAA	CTCAGCGGGTTTGATGACCA
mAldh1a3	TGGCACGAATCCAAGAGTGG	CCTTGTCCACATCGGGCTTAT
mAdora1	TACTACGGGAAGGAGCTCAAG	AAGAGGGTGATGCAGTTCAAGA
mAdora2a	CTTTGTCCTGGTCCTCACGC	ACCAAGCCATTGTACCGGAG
mAdora2b	GCGTCCCGCTCAGGTATAAAG	AACGGAGTCAATCCAATGCCA
mAdora3	GTGCTGCTGATCTTCACCCA	GTGGTAACCGTTCTATATCTGACTG

3.1.12 Tumor cell lines

Table 2.12. Tumor cell lines.

Cell line	Cell type	Medium
RMA-S	Mouse T cell lymphoma	Complete RPMI
YAC-1	Mouse lymphoma	Complete RPMI
B16	Mouse melanoma	Complete DMEM
MCA 1956	Mouse fibrosarcoma	Complete RPMI
LLC	Mouse lung carcinoma	Complete DMEM

MCA 1956 (MCA-induced fibrosarcoma) was kindly provided by Prof. Robert Schreiber.

3.1.13 Mouse lines

Table 2.13. mouse lines.

Mouse line	Source and housing
B6.(MF;129)-Rag2tm1Fwa, Rag2 ko	Haus 111, UMM
B6.Rag2tm1Fwa Ptprca, Rag2 x Ly5.1	Haus 111, UMM
C57BL/6NRj	Janvier Labs
NKp46-cre, Tg(Ncr1-icre)265Sxl	Haus 111, UMM,
PPARγloxP, B6.129-Ppargtm2Rev/J	Provided by Dr. Elke Burgermeister Haus 111, UMM

In this thesis, we called $Ncr1^{iCreTg}$ $PPAR\gamma^{f/f}$ mouse as PPARγ cKO, and $PPAR\gamma^{f/f}$ mice as PPARγ flox.

3.2 Methods

3.2.1 Preparation of single-cell suspension

Blood

Mice were sacrificed under the CO_2-asphyxiation. 0.5 - 1.0 mL of blood from ocular vein was collected into a tube, containing heparin. Blood was treated with 20 mL of buffered ammonium chloride potassium phosphate solution (ACK lysis buffer) for 10 min to lyse red blood cells. Cells were washed with PBS (1600 rpm for 10 min at 4°C), and re-suspended in an appropriate buffer.

Lymph nodes

Lymph nodes were excised and kept in ice-cold PBS. Lymph nodes were minced through a 70 µm-pore cell strainer, and washed with PBS (1500 rpm for 10 min at 4°C). Cells were filtered through a 40 µm-pore cell strainer, washed with PBS (1500 rpm for 10 min at 4°C), and re-suspended in an appropriate buffer.

Spleen

Spleens were excised and kept in ice-cold PBS. Spleens were minced through a 40 µm-pore cell strainer and washed with PBS (1500 rpm for 10 min at 4°C). Cells were incubated with 4 mL of ACK lysis buffer per spleen for 5 min to lyse red blood cells. Cells were washed through a 40 µm-pore cell strainer with PBS (1500 rpm for 10 min at 4°C) and re-suspended in an appropriate buffer.

Liver (Manual dissociation)

Livers were excised and kept in ice-cold PBS. Gall bladders and connective tissues were removed, and liver was cut into small pieces using scalpels. Liver tissue was treated with 0.7 mg/mL of Hyaluronidase and 0.5 mg/mL of DNase in 10 mL of PBS, and incubated in water bath at 37ºC for 50 min with shaking. After the incubation, the digested liver tissue was centrifuged briefly and minced through a 100 µm-pore cell strainer, followed by washing with PBS (1500 rpm for 10 min at room temperature). Liver suspension was further filtered through a 70 µm-pore cell strainer and washed with PBS (1500 rpm for 10 min at room temperature). Cells were then re-suspended in 6 mL of PBS and layered on the top of 6 mL of mouse Lympholyte®-M solution. The gradient was centrifuged at 1500 g (acceleration rate: 1 and deceleration rate: 1) for 10 min at room temperature. Interphase enriched with liver mononuclear cells was collected, filtered through a 40 µm-pore cell strainer, and washed with PBS (1500 rpm for 10 min at 4°C). Cells were re-suspended in an appropriate buffer.

Liver (Liver Dissociation Kit)

Livers were excised and kept in ice-cold PBS. Gall bladders and connective tissues were removed and livers were cut into several pieces using scissors. Liver pieces were digested in DMEM media supplemented with 1% L-glutamine, using Liver Dissociation Kit, according to the manufacturer's protocol. The digested tissue was centrifuged shortly, and minced through a 100 µm-pore cell strainer, followed by washing with PBS (1500 rpm for 10 min at room temperature). 4 mL of ACK buffer per liver was added and cells were incubated for 5 min to lyse red blood cells. Liver suspension was filered through a 70 µm-pore cell strainer, washed with PBS (1500 rpm for 10 min at room temperature), and re-suspended in 3 mL of PBS. Isotonic Percoll® was prepared (nine parts of stock Percoll® and one part of 1.5M NaCl solution). 70% Percoll® and 40% Percoll® were prepared by diluting isotonic Percoll® with PBS. 70% Percoll®, 40% Percoll® and 3 mL of liver suspensions were layered and centrifuged at 1500 g (acceleration rate: 1 and deceleration rate: 1) for 10 min at room temperature. Interphase between 70% Percoll® and 40% Percoll®, enriched with liver mononuclear cells, was collected, filtered through a 40 µm-pore cell strainer, and washed with PBS (1500 rpm for 10 min at 4°C). Cells were re-suspended in an appropriate buffer.

Lung

Lungs were excised and kept in ice-cold PBS. Lungs were cut into pieces and digested in DMEM media supplemented with 1% L-glutamine, using Lung Dissociation Kit, according to the manufacturer's protocol. The digested tissue was centrifuged shortly, and minced through a 70 µm-pore cell strainer, followed by washing with PBS (1500 rpm for 10 min, at room temperature). 4 mL of ACK buffer per lung was added and cells were incubated for 5 min to lyse red blood cells. Cells were filtered through a 40 µm-pore cell strainer, washed with PBS (1500 rpm for 10 min at 4°C), and re-suspended in an appropriate buffer.

Bone Marrow

Hind legs were dissected and kept in ice-cold PBS. Muscle tissues were removed under the sterile condition. Tibia and femur were separated by disconnecting knee and heel. Tibia and femur were sterilized with 100% ethanol shortly and transferred to PBS. Both ends of tibia and femur were removed, and bone marrow was flushed and rinsed with PBS using a syringe with a 27G needle. Isolated bone marrow was minced through a 70 µm-pore cell strainer followed by washing with PBS (1500 rpm for 10 min at room temperature). 4 mL of ACK buffer per bone marrow was added, and cells were incubated for 5 min to lyse red blood cells. Cells were filtered through a 40 µm-pore cell strainer, washed with PBS (1500 rpm for 10 min at room temperature), and re-suspended in BM-DC media.

3.2.2 Magnetic cell sorting (MACS)

NK cells

Spleen single-cell suspension was washed with MACS buffer and re-suspended at a density of 1 X 10^7 cells in 40 µL of MACS buffer. NK cells were isolated using mouse NK cell isolation kit, according to manufacturer's protocol.

Naïve $CD4^+$ T cells

Spleen single-cell suspension was washed with MACS buffer and re-suspended at a density of 1 X 10^7 cells in 40 µL of MACS buffer. Naïve $CD62L^+CD44^-CD4^+$ T cells were isolated by using mouse Naïve T cell isolation kit, according to manufacturer's protocol.

3.2.3 Fluorescence activated cell sorting (FACS™)

NK cell sorting

Spleen single-cell suspension was washed and re-suspended in ice-cold Sort buffer at a density of 1 X 10^7 cells/mL. 10 µg/mL of anti-mouse CD16/CD32 was added and cells were incubated for 10 min at 4ºC to block antibody binding to Fc receptors. Antibody cocktail, including anti-mouse CD3ε-APC-Cy7, anti-mouse NK1.1-BV785, anti-mouse NKp46-BV421, anti-mouse TRAIL-PE, and anti-mouse CD200R-FITC, was added and incubated for 20 min at 4ºC. After the incubation, cells were washed with Sort buffer (1500 rpm for 10 min at 4°C) and re-suspended at density of 5 X 10^6 cells/mL. Cell suspension was filtered through a 35 µm-pore cell strainer, and 7AAD was added before sorting to distinguish live and dead cells. Splenic NK cells were sorted as live $CD3\varepsilon^-$ $NK1.1^+$ $NKp46^+$ $CD200R^-$ $TRAIL^-$ cells. The purity was confirmed to be higher than 98% after each sorting. Sorted cells were collected in PCCM, centrifuged (1500 rpm for 10 min at 4ºC) and re-suspended in pre-warmed PCCM.

3.2.4 Cell counting

Cell suspension was mixed with 0.05% Trypan blue solution (w/v) in a ratio of 1:1. Viable cells were counted using a Neubauer counting chamber (0.1mm depth). Number of viable cells per solution (mL) was calculated as:

$$Total\ cell\ number = \frac{cell\ count}{counted\ squares} \times dilution\ factor \times 10^4 \times volume\ (mL)$$

3.2.5 Primary cell culture

Splenocyte culture

Spleen single-cell suspension from Rag2$^{-/-}$ or Rag2$^{-/-}$Ly5.1 mice was re-suspended in 30 mL of fresh PCCM and incubated in T175 flask for 2 hours at 37°C in order to remove adherent cells. Suspension cells were collected, centrifuged (1500 rpm for 10 min at room temperature), and re-suspended in pre-warmed PCCM at a density of 1 X 10^6 cells/mL with 1500 U/mL of rhIL-2. Fresh PCCM with rhIL-2 was added every 2-3 days. After 5-7 days of culture, the purity of CD3ε$^-$NK1.1$^+$ NK cells were higher than 90%. 1 µM of *at*RA diluted in DMSO or the equivalent volume of DMSO (0.01%, v/v) was added to the culture as a solvent control. Freshly prepared *at*RA or DMSO were added every 2-3 days. In some experiments (mentioned in figure legends), 10 µM of Ro-415253, MM-11253, T0070907, or 10 µg/mL of anti-TGFβ antibody were added every 2-3 days.

NK cell culture

Isolated NK cells were cultured in PCCM at a density of 1 X 10^6 cells/mL with 1500 U/mL of rhIL-2. Fresh PCCM with rhIL-2 was added every 2-3 days. 1 µM of *at*RA diluted in DMSO or the equivalent volume of DMSO (0.01%, v/v) was added to the culture as a solvent control. Freshly prepared *at*RA or DMSO were added every 2-3 days.

Naïve CD4$^+$ T cell culture and polarizing conditions

Isolated naïve CD$^+$ T cells were re-suspended in PCCM at a density of 1 X 10^6 cells/mL and cultured in flat-bottomed well plate pre-coated with 2 µg/mL of anti-mouse CD3ε antibody (overnight at 4°C). 0.5 µg/mL of soluble anti-mouse CD28 antibody was added to the culture. Type 1 helper T (T_H1) cell-, type 2 helper T (T_H2) cell-, type 17 helper (T_H17) cell- and regulatory T cell (Treg)-polarizing conditions are described in table 2.14.

Table 2.14. CD4$^+$ T cells polarizing conditions.

T_H1	T_H2	T_H17	Treg
2 µg/mL anti-CD3ε 0.5 µg/mL anti-CD28 1 µg/mL anti-IL-4 30 U/mL rhIL-2 10 ng/mL IL-12	2 µg/mL anti-CD3ε 0.5 µg/mL anti-CD28 1 µg/mL anti-IFN-γ 30 U/mL rhIL-2 10 ng/mL IL-4	2 µg/mL anti-CD3ε 0.5 µg/mL anti-CD28 1 µg/mL anti-IFN-γ 1 µg/mL anti-IL2 1 µg/mL anti-IL4 20ng/mL IL-6 1 ng/mL TGFß1 10 ng/mL IL-23 20 ng/mL IL-1b	2 µg/mL anti-CD3ε 0.5 µg/mL anti-CD28 1 µg/mL anti-IFN-γ 1 µg/mL anti-IL4 30 U/mL rhIL-2 2 ng/mL TGFß1

NK cells co-culture with naïve CD4$^+$ T cells

Naïve CD4$^+$ T cells were re-suspended in PCCM at a density of 1 X 10^6 cells/mL and seeded as described above. NK cells pre-cultured with *at*RA (or DMSO) for 5 days were collected and washed with PBS twice (1500 rpm for 10 min at room temperature). NK cells were re-suspended in PCCM at a density of 1 X 10^6 cells/mL and added to naïve CD4$^+$ cells in a ratio of 1:1. Co-culture was conducted for two days. In some experiments (mentioned in figure legends), 5 μM of ZM 241385, 5 μM of SCH 58261, 7.5 μg/mL of anti-IL-10 antibody, 4 μg/mL of anti-CCL5 antibody, or 4 μg/mL of anti-CCL1 antibody were added upon two days of co-culture. In some experiments (mentioned in figure legends), transwell inserts were applied to separate naïve CD4$^+$ T cells and NK cells. Naïve CD4$^+$ T cells were re-suspended in PCCM at a density of 0.33 X 10^6 cells/mL, and 600 μL of cell suspension was seeded in the lower well. NK cells cultured with atRA (or DMSO) for 5 days were re-suspended in PCCM at a density of 2 X 10^6 cells/mL and 100 μL of cell suspension was seeded into the upper well. Co-culture was conducted for two days.

Bone marrow-derived dendritic cell (BM-DC) culture

Bone marrow single-cell suspensions were re-suspended in 30 mL of BM-DC media and incubated in T175 flask overnight to deplete adherent cells. On day 1, suspension cells were collected and distributed into flat-bottomed 6-well plate (1 mL/well). Pre-warmed BM-DC media was added into each well (2 mL/well). 2mL of fresh BM-DC media was added every 2-3 days.

NK cells co-cultured with BM-DCs

After the aspiration of media, BM-DC layer was rinsed with pre-warmed PBS. 1mL of non-enzymatic cell-dissociation buffer was added per well and incubated for 10 min at 37°C. BM-DCs were gently scrapped using a cell lifter and collected. 1mL of pre-warmed BM-DC media was used to wash out the well. BM-DCs were washed with BM-DC media (1500 rpm for 10 min at room temperature). Cells were re-suspended in PCCM at a density of 1 X 10^6 cells/mL and seeded in non-treated cell culture 24-well plate. NK cells pre-cultured with *at*RA (or DMSO) for 5 days were collected and washed with PBS twice (1500 rpm for 10 min at room temperature). NK cells were re-suspended in PCCM at a density of 1 X 10^6 cells/mL and added to BM-DC in ratios of 1:1, 1:2, and 1:4. 5 hours of co-culture was conducted for DC apoptosis assay, and 14-16 hours of co-culture was conducted for DC maturation assay. In some experiments (mentioned in figure legends), 1 μg/mL of anti-IFN-γ was added during 14-16 hours of co-culture.

3.2.6 Tumor cell culture

Cell thawing

Cryovial was thawed with gentle agitation in 37°C water bath and taken out as soon as 90% of content was thawed. The content was transferred to pre-warmed media and centrifuged (1500 rpm for 10 min at room temperature). Cell pellets were re-suspended in an appropriate media.

Suspension tumor cell culture

The density of suspension cells was maintained by splitting cells and adding fresh media every 2-3 days.

Adherent tumor cell culture

Media was aspirated and cell layers were rinsed with PBS. Pre-warmed Trypsin-EDTA was added and incubated at 37°C until all cells were detached. Pre-warmed media was added to stop the reaction. Cells were centrifuged (1500 rpm for 10 min at room temperature), and re-suspended at an appropriate density.

Cell freezing

Cells were harvested and centrifuged (1500 rpm for 10 min at room temperature). Cell pellets were re-suspended in Cell-Freezing Media at a density of 3 X 10^6 cells/mL, and 1 mL of cell suspension was aliquoted in cryovial. Cryovials were placed in freezing container and transferred at -80°C freezer. For the long-term storage, vials were transferred into liquid nitrogen tank.

3.2.7 Functional assays of NK cells

Stimulation with pro-inflammatory cytokines

NK cells pre-cultured with *at*RA (or DMSO) for 6-7 days were collected and washed with PBS (1500 rpm for 10 min at room temperature). Cells were re-suspended in PCCM at a density of 1 X 10^6 cells/mL, and seeded in round-bottomed 96-well plate. NK cells were stimulated with 1 ng/mL of mIL-12 and/or 20 ng/mL of mIL-18 for 5 hours. After 1 hours of stimulation, 1 µL of GolgiPlug™ containing Brefeldin A was added to stop intracellular protein transport processes. After the stimulation, cells were harvested and stained for detection of intracellular cytokines.

NK cell receptor triggering

10 µg/mL of anti-NK1.1 antibody, anti-NKG2D antibody, anti-NKp46 antibody, or 2 µg/mL of CD155 fusion protein were prepared in PBS. 50 µL of each solution was distributed to flat-bottomed 96-well plate and incubated overnight at 4°C. NK cells cultured with *at*RA (or DMSO) for 6-7 days were collected and washed with PBS (1500 rpm for 10 min at room temperature). Cells were re-suspended in PCCM at a density of 1 X 10^6 cells/mL, and seeded in pre-coated 96-well plate. 1 µL of FITC-CD107a antibody (or equal amount of Rat IgG2a as isotype control) was added into each well. After 1 hour of stimulation, GolgiPlug™ containing Brefeldin A was added to stop intracellular protein transport processes. After the stimulation, cells were harvested and stained for detection of intracellular cytokines.

Co-culture with tumor cells

Tumor cells were re-suspended in PCCM at a density of 1 X 10^6 cells/mL, and seeded in 96-well plate. NK cells cultured with *at*RA (or DMSO) for 6-7 days were collected and washed with PBS twice (1500 rpm for 10 min at room temperature). NK cells were re-suspended in PCCM at a density of 1 X 10^6 cells/mL, and added to tumor cells in a ratio of 1:1. Co-culture was conducted for 5 hours.

3.2.8 Flow cytometry

Analysis of surface molecules

Cells from single-cell suspension or from culture were re-suspended in PBS and distributed into 96-well plate at an appropriate density (0.1 X 10^6 - 0.2 X 10^6 cells/mL). Cells were treated with 30 µL of PBS containing 0.2 µL of Aqua Zombie™ and incubated for 20 min at room temperature in the dark. 20 µL of Fc blocking buffer was added to each well and incubated for 15 min at 4°C in the dark. Antibody cocktail, containing antibodies against surface molecule, diluted in 50 µL of FACS buffer (BD Horizon™ Brilliant Stain buffer was used for staining with antibodies conjugated with BUV- fluorochromes) was added and incubated for 20 min at 4°C in the dark. Cells were washed with FACS buffer twice (2100 rpm for 4 min at 4°C). In some experiments, if cell fixation is not required, instead of Aqua Zombie™, 5 µL of 7AAD was added before flow cytometry analysis, to distinguish live/dead cells.

Analysis of intracellular molecules

After surface staining, cells were fixed with using Fixation/Permeabilization Solution Kit. Cells were centrifuged (2100 rpm for 4 min at 4°C), and washed with Perm buffer. 25 µL of Perm buffer and 25 µL of Fc blocking buffer were added to each well and incubated for 20 min at 4°C. Antibody cocktail, containing antibodies against intracellular molecule, diluted in 50 µL of

Perm buffer, was added and incubated for 20 min at 4°C in the dark. Cells were washed with Perm buffer (2100 rpm for 4 min at 4°C), and re-suspended in FACS buffer for flow cytometry analysis.

Analysis of cell apoptosis

Cultured cells were harvested and treated with 20 µL of Fc blocking buffer for 15 min at 4°C. Antibody cocktail, containing antibodies against surface molecule, diluted in 50 µL of PBS was added and cells were incubated for 20 min at 4°C in the dark. Cells were washed with PBS (2100 rpm for 4 min at 4°C) and stained with master mix, containing Annexin V and 7ADD, diluted in Annexin V binding buffer, for 20 min at room temperature in the dark. 150 µL of Annexin V binding buffer was added for flow cytometry analysis.

Analysis of phosphorylated proteins

BD Cytofix/Cytoperm™ buffer was pre-warmed to 37°C, and BD phosflow™ perm buffer III was pre-cooled at -20°C. Cells were collected and stimulated with cytokines in 100 µL of PCCM. After the stimulation, cells were fixed immediately by adding an equal volume of 100 µL pre-warmed BD cytofix/cytoperm™ buffer and incubated for 10 min at 37°C. Cells were centrifuged (2100 rpm for 4 min at 4°C). 100 µL of pre-cooled BD phosflow™ perm-buffer III was added and incubated for 30 min on ice. Cells were washed with FACS buffer twice (2100 rpm for 4 min at 4°C), and treated with 20 µL of Fc-blocking buffer for 10 min on the ice in the dark. Antibody cocktail, containing antibodies against surface molecule or phospho-protein, diluted in FACS buffer was added and cells were incubated for 60 min at room temperature in the dark. Cells were washed with FACS buffer twice (2100 rpm for 4 min at 4°C) and re-suspended in FACS buffer for the flow cytometric analysis.

Analysis of cell division

Up to 1 X 10^6 cells were re-suspended in 1 mL of PBS and 5mM of CellTrace™ Violet stock solution was added to cell suspension in a ratio of 1:1000. Cells were incubated for 20 min at 37°C in the dark. Five times of staining volume of complete media was added to the cells, and cells were incubated for 5 min at 37°C in the dark. Cells were washed (1500 rpm for 4 min at room temperature) and re-suspended in pre-warmed PCCM. Cells were incubated for 10 min before co-culture or stimulation.

Analysis of mitochondria fitness or lipid uptake

Cultured cells were re-suspended in pre-warmed PCCM and distributed into 96-well plate at a density of 1 X 10^6 cells. 200nM of MitoTracker™ Green FM dye (for measurement of mitochondrial mass), 20 nM of MitoProbe™ TMRM dye (for of mitochondrial membrane potential),

500 µM of CellROX™ Deep Red dye (for measurement of reactive oxygen species production), or 5 nM of BODIPY™ FL C16 (for measurement of lipid uptake) was added. Cells were incubated for 30 min at 37°C in the dark and washed with PBS 3 times (2100 rpm for 4 min at room temperature). Surface molecules were stained for further analyses.

3.2.9 Flow cytometric analysis

Samples were meausred with LSR Fortessa™ or FACSAria™ fusion. Data were analyzed with FlowJo™_v10.7.1. Gating strategy was as follow:

Table 2.15. Gating strategy of cells using flow cytometry.

Cells	Gating strategy
Cultured NK cells	$CD3\varepsilon^-NK1.1^+NKp46^+$ or $CD3^-Eomes^+$
Cultured BM-DCs (upon co-culture with NK cells)	$NK1.1^-CD11b^+CD11c^+$
Naïve T cells	$CD3\varepsilon^+CD62L^+CD44^-$
Cultured $CD4^+$ T cells (upon co-culture with NK cells)	$CD45.2^+CD4^+$ or $CD45.2^+TCR\beta^+$
Cultured NK cells (upon co-culture with $CD4^+$ T cells)	$CD45.1^+Eomes^+$ or $CD45.1^+NK1.1^+$
ILC1s in liver	$CD45^+CD3\varepsilon^-CD19^-Ly6G^-Ter119^-$ $NK1.1^+NKp46^+Eomes^-CD49a^+$
NK cells in liver, lung, spleen	$CD45^+CD3\varepsilon^-$ $CD19^-Ly6G^-Ter119^-$ $NK1.1^+NKp46^+Eomes^+$
ILC1s in gut	$CD45^+CD3\varepsilon^-CD19^-Ly6G^-Ter119^-TCR\beta^-TCR\gamma\delta^-$ $CD127^+$T-bet$^+$
ILC2s in gut	$CD45^+CD3\varepsilon^-CD19^-Ly6G^-Ter119^-TCR\beta^-TCR\gamma\delta^-$ $CD127^+GATA3^+$
ILC3s in gut	$CD45^+CD3\varepsilon^-CD19^-Ly6G^-Ter119^-TCR\beta^-TCR\gamma\delta^-$ $CD127^+Ror\gamma t^+$
NK cells in gut	$CD45^+CD3\varepsilon^-CD19^-TCR\beta^-TCR\gamma\delta^-CD127^-$ $NK1.1^+NKp46^+Eomes^+$
$CD127^-$ ILCs in gut	$CD45^+CD3\varepsilon^-CD19^-TCR\beta^-TCR\gamma\delta^-CD127^-$ $NK1.1^+NKp46^+Eomes^-$
NK cells in tumor	$CD45.1^+CD3\varepsilon^-CD19^-Ly6G^-F4/80^-SiglecF^-FceRI^-$ $Ter111^-NK1.1^+NKp46^+Eomes^+$
ILC1s in tumor	$CD45.1^+CD3\varepsilon^-CD19^-Ly6G^-F4/80^-SiglecF^-FceRI^-$ $Ter111^-NK1.1^+NKp46^+Eomes^-CD49a^+$

3.2.10 Measurment of cytokine amount

NK cells were incubated for 5 hours upon stimulation with cytokine and for 24 hours upon co-culture with dendritic cells. At the end of the incubation, supernatants were collected and centrifuged (2100 rpm for 4 min at 4°C). Supernatant were stored at -20°C until the assay. The amount of released IFN-γ was measured using Mouse IFN-γ ELISA MAX™ Standard set (Biolegend), according to the manufacturer's instruction.

3.2.11 RNA extraction

Cultured cells or single-cell suspensions from tissues were collected in 1.5mL-tube and washed with sterile PBS (5000 rpm for 5 min at room temperature). After the aspiration of PBS, cell pellet was lysed with RLT buffer containing 1% of β-mercaptoethanol, and vortexed for 2 min. Lysates were stored at -20°C until the isolation. RNA extracting process was performed using RNeasy® Mini Kit according to manufacturer's instructions. To rule out contamination with genomic DNA, obtained RNA was treated with TURBO DNA-free® Kit according to manufacturer's instructions. RNA concentration was measured using TECAN Plate reader Infinite 200 pro.

3.2.12 cDNA Synthesis and quantitative real-time-PCR

Frist strand cDNA was synthesized from total RNA using ProtoScript® II First Strand cDNA Synthesis Kit, according to manufacturer's instructions. Master mix, containing appropriate primers, was added to cDNA, using PowerUp™ SYBR™ Green Mastermix, according to manufacturer's instructions. qRT-PCR was performed using in a QuantStudio™ 5 Real-Time PCR System with the following program: hold stage with 50ºC for 20min and 95ºC for 2 min, 40 cycles of amplification at 95ºC for 1s and 60 ºC for 30s, and melt curve stage at 95ºC for 15s, 60ºC for 1 min and 95ºC for 15s. The gene expression was quantified using the ΔΔCT method and Actb or B2m was used as a reference gene.
For RT² Profiler™ PCR Array Mouse Cytokines & Chemokines or RT² Profiler™ PCR Array Mouse Retinoic Acid Signaling, first strand cDNA was synthesized 400 ng of total RNA using RT^2 First Strand Kit according to manufacturer's instructions. Achieved cDNA was mixed with RT² SYBR™ Green qPCR Mastermix, and ROX as a reference dye according to manufacturer's instructions. qRT-PCR array was performed using in a QuantStudio™ 5 Real-Time PCR System with the program provided in RT² Profiler™ PCR Array.

3.2.13 Gene expression analysis

Gene expression analysis, including bioinformatics, was processed by the bioinformatics core facility of Medical faculty Mannheim (ZMF).

Gene expression

RNA quality test was performed using capillary electrophoresis on an Agilent 2100 bioanalyzer. The high-quality RNA samples (RIN = 10) were used. Gene-expression profiling was performed using Affymetrix GeneChip™ Mouse Gene 2.0 ST Arrays. Biotinylated antisense cDNA was prepared according to Affymetrix standard labelling protocol with the GeneChip™ Hybridization oven 640, dyed in the GeneChip™ Fluidics Station 450 and thereafter scanned with a GeneChip™ Scanner 3000.

Bioinformatics

A Custom CDF Version 21 with ENTREZ based gene definitions was used to annotate the arrays (Dai et. al, 2005). The Raw fluorescence intensity values were normalized applying quantile-normalization and RMA background correction. OneWay-ANOVA™ was performed to identify differentially expressed genes using a commercial software package SAS JMP10 Genomics, version 6, from SAS (SAS Institute, Cary, NC, USA). A false positive rate of a=0.05 with FDR correction was taken as the level of significance.

Gene Set Enrichment Analysis (GSEA)

GSEA was used to determine whether ranked-gene lists exhibit a statistically significant bias in their distribution using the software R v3.4.0 (R Core Team 2017), RStudio®: Integrated development environment for R (RStudio® Boston, MA, USA) and the fgsea package (Sergushichev, 2016). Annotations were pathways obtained from public external databases (KEGG, http://www.genome.jp/kegg).

3.2.14 Real-time metabolic analysis

Prior to the assay, Seahorse™ sensor cartridge was hydrated in an incubator overnight in the absence of CO_2. On the day of assay, the miniplate was coated with 100 µg/mL poly-D-lysine for 20 min. After the aspiration of Poly-D-lysine, miniplate was washed with water twice, followed by air-dryinig for for 30 min. Harvested cells were washed with PBS (1500 rpm for 10 min at room temperature), and re-suspended at density of 1 X 10^5 cells in 30 µL of XF RPMI media supplemented with glucose and pyruvate. 30 µL of cell suspension was added in the miniplate and loaded to Seahorse™ XF HS Mini Analyzer (Agilent). Oxygen consumption rate

(OCR) and extracellular acidification rate (ECAR) were measured in intervals of every 6 minutes. After the third, sixth, and ninth acquisition, 1.5 µM of oligomycin (ATP synthase inhibitor), 1 µM of FCCP (depolarizer of mitochondrial membrane), and 0.5 µM of Rotenon/Antimycin A (complex III and I inhibitor) were added, respectively. OCR was quantified in “pmol/min” and ECAR was quantified in “mpH/min”.

3.2.15 Mouse genotyping

Collected piece from murine tail or ear were lysed using MyTaq™ Extract-PCR Kit according to the manufacturer’s protocol. PCR was performed in C1000 Touch™ Thermal Cycler using lysate, optimized primers and MyTaq™ HS Red Mix, as described in Table 2.16. PCR products were separated on 2% of agarose Gel. Separated bands on the gel was detected using 200 Gel Imaging Workstation. The protocol of genotyping PCR for B6.129-Ppargtm2Rev/J was kindly provided by Dr. Elke Burgermeister.

Table 2.16. Genotyping PCR steps.

Step		**1**	**2**	**3**	**4**	**5**	**6**	**7**
NKp46-cre, Tg(Ncr1-icre) 265Sxl	Temp (°C)	94	94	60	72	Repeat 37x (step 2-4)	72	12
	Time	3 min	45 sec	45 sec	1 min		7 min	hold
PPARγloxP, B6.129-Ppargtm2Rev/J	Temp (°C)	94	94	60	68	Repeat 34x (step 2-4)	72	4
	Time	3 min	30 sec	30 sec	1 min		5 min	hold

3.2.16 Mouse tumor models

Preparation of tumor cells for injection

Adeherent tumor cells were harvested in the exponential growth phase after 5-7 days of culture using non-enzymatic cell-dissociation buffer, and centrifuged (1200 rpm for 5 min at room temperature). Cells were washed with media without FCS (1200 rpm for 5 min at room temperature), and washed with fresh PBS twice (1200 rpm for 5 min at room temperature).

Subcutaneous inoculation of tumor cells

Cells were re-suspended at density of 1 X 10^7 cells in 1 mL of PBS. Mice were injected with 100 µL of tumor cell suspension subcutaneously in the left flank. Tumor growth was assessed every 2-3 days with a caliper measuring the height, width and depth of the tumors and tumor volume was calculated. Mice were sacrificed to obtain tumor tissue, when the size of tumor reached ~1.5cm.

Metastases model

Cells were re-suspended at density of 1 X 10^6 cells in 1 mL of PBS. Mice were injected with 100 µL of tumor cell suspension through tail vein. Mice were sacrificed three weeks post-injection and lungs were excised.

3.2.17 Statistical analysis

Statistical analysis was performed using paired or unpaired two-tailed student's t-test, or one-way ANOVA with Tukey's multiple comparisons test. Data were considered to be significant, if p-value < 0.05 (*), p < 0.01 (**), p < 0.001 (***), p < 0.0001 (****) and to be not significant (n.s), if p-value > 0.05.

4 RESULTS

4.1 Effect of vitamin A on NK cell phenotype *in vitro*

NK cells are found in organs enriched with lipid-soluble vitamins, such as liver and adipose tissue (Kane et al., 2008; Peng & Tian, 2017), and can be further recruited during tissue inflammation. The impact of the lipid-soluble micronutrient, vitamin A, on NK cells remains unclear. Here, we investigated whether vitamin A metabolites can regulate NK cell phenotype and effector functions.

4.1.1 Transcriptomic reprogramming of NK cells induced by *at*RA

We treated NK cells with all-*trans* retinoic acid (*at*RA), a potent metabolite of vitamin A (Erkelens & Mebius, 2017) (Figure 3.1A). Based on the literature (Bidad, Salehi, Oraei, Saboor-Yaraghi, & Nicknam, 2011; Candia et al., 2017; Morita et al., 2019), we treated NK cells with three doses (0.01 µM, 0.1 µM, or 1 µM) of *at*RA for 7 days in the presence of IL-2, and afterwards re-stimulated cells with IL-12 and IL-18. The production of IFN-γ, a pro-inflammatory cytokine, was dose-dependently downregulated by *at*RA-treatment (Figure 3.1B). Furthermore, to optimize the duration of treatment, NK cells were exposed to 1 µM of *at*RA for 3 days, 5 days, or 7 days, and analyzed for the phenotype. We observed DNAM-1 and CD200R-expressing NK cells after 5 days of *at*RA-treatment (Figure 3.1C). Therefore, NK cells were treated with 1 µM of *at*RA for 5-7 days for subsequent experiments.

In order to elucidate a global impact of *at*RA on NK cell transcriptome, we performed transcriptome analysis of *at*RA-treated NK cells and control NK cells. The volcano-plot and heatmap shown in Figure 3.1D and E illustrate the distinct transcriptional phenotype of *at*RA-treated NK cells compared to control NK cells. Gene pathway analysis, based on Kyoto Encyclopedia of Genes and Genomes (KEGG), revealed that *at*RA-treated NK cells reduced the expression of genes involved in NFκB signaling pathway and NK cell-mediated cytotoxicity (Figure 3.1F and G). These results indicate that effector functions of NK cells might be attenuated by *at*RA-treatment. On the other hand, *at*RA-treated NK cells increased the expression of genes involved in retinol metabolism (Figure 3.1F and G). In a line with gene pathway analysis, *at*RA-treated NK cells showed reduction in Ifng (transcript encoding Interferon gamma, IFN-γ), Tnf (transcript encoding tumor necrosis factor alpha, TNF-α), Il18ra (transcript encoding interleukin-18 receptor alpha, IL-18Rα), Klrk1 (transcript encoding NKG2D), and Klrb1c (transcript encoding NK1.1) expression (Figure 3.1E).

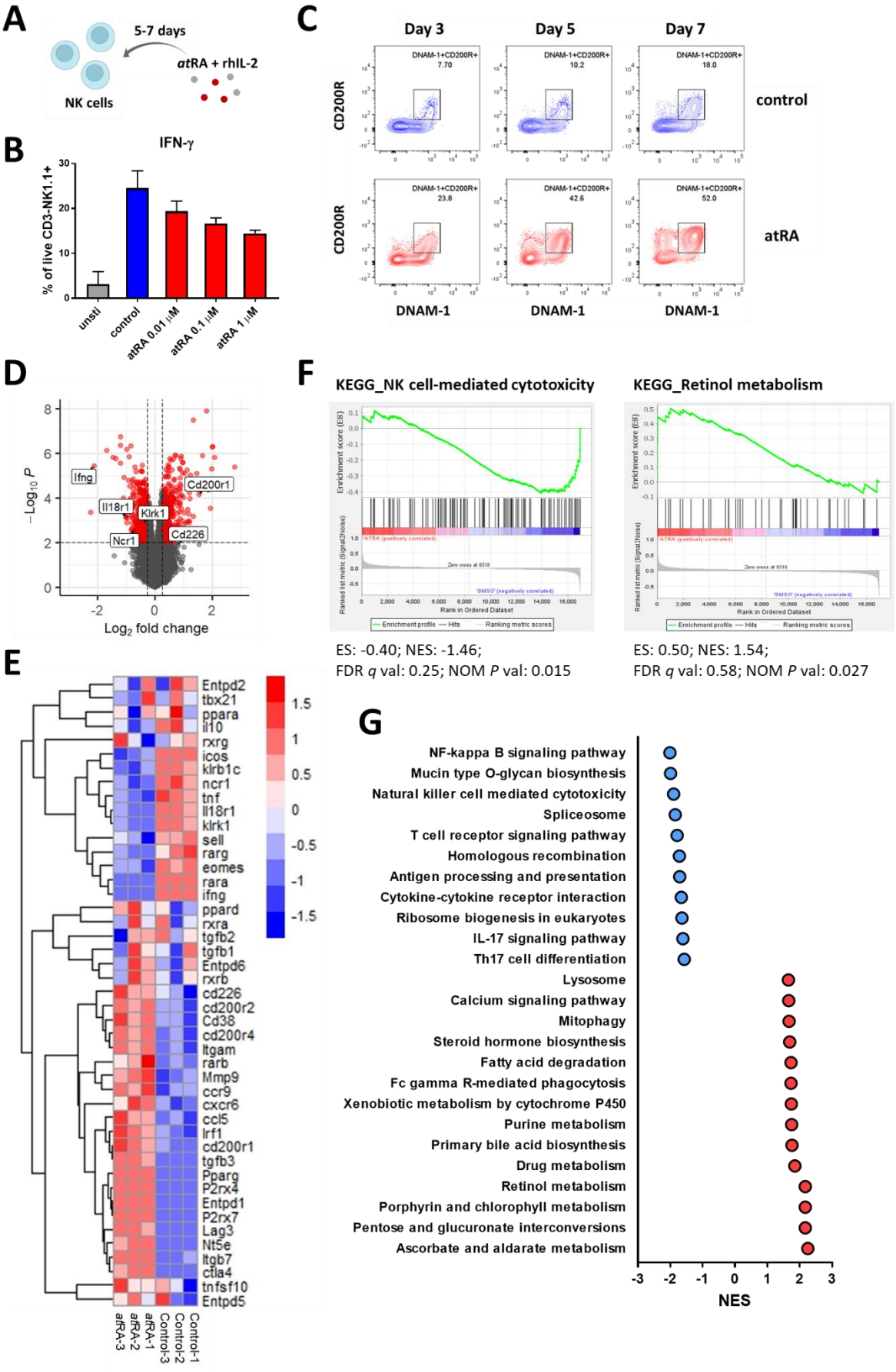

(Figure legend in the next page)

Figure 3.1 *at*RA induces transcriptomic reprogramming of NK cells. (A) Schematic illustration of *at*RA-treatment of NK cells (Created with BioRender.com). (B) Splenic NK cells were cultured with 0.01, 0.1 or 1µM of *at*RA in the presence of IL-2 for 7 days (the equivalent volume of DMSO was used as a solvent control), and re-stimulated with IL-12 and IL-18 for 5 hours. Production of IFN-γ was analyzed by flow cytometry (n=2). (C) Splenic NK cells were cultured with 1µM of *at*RA in the presence of IL-2 for 3 days, 5 days, or 7 days (the equivalent volume of DMSO was used as a solvent control). Representative contour-plots of DNAM-1 and CD200R expression on *at*RA-treated and control NK cells**.** (D-G) Splenic NK cells were isolated as live, $CD3\varepsilon^-$, $NKp46^+$, $CD200R^-$, and $TRAIL^-$ cells, and cultured with 1µM of *at*RA in the presence of IL-2 for 7 days (The equivalent volume of DMSO was used as a solvent control) (n=3). RNA was extracted to perform transcriptome analysis. (D) Differential transcript expression of *at*RA-treated NK cells compared to control NK cells shown in volcano-plot and (E) Heatmap. (F) Enrichment-plots of NK cell mediated cytotoxicity (left) and retinol metabolism (right) pathways in *at*RA-treated NK cells compared to control NK cells, generated with GSEA (www.gsea-msigdb.org). (G) Pathway enrichment analysis based on k for *at*RA-treated NK cells compared to control NK cells. Unsti, unstimulated cells; NES, normalized enrichment score; ES, enrichment score; FDR, false discovery rate; NOM P val, nominal p-value. Graphs indicate mean ± SEM.

4.1.2 Effect of all-*trans* retinoic acid on NK cell phenotype

Based on transcriptional alterations in NK cells upon *at*RA-treatment, we selected several molecules, including NK cell activating and inhibitory receptors, maturation markers, death-receptor ligands, and adenosine metabolizing enzymes, in order to evaluate the expression on NK cells. The exposure to *at*RA increased expression of DNAM-1, CD200R, CD11b, LAG3 and TRAIL at protein level, and decreased expression of CD62L and KLRG1 on the surface of NK cells (Figure 3.2A). Upon *at*RA-treatment, expression of activating receptors, such as NK1.1 and NKG2D, was significantly downregulated (Figure 3.2B), and expression of CD73, CD39 and CD38 was significantly upregulated (Figure 3.2C).

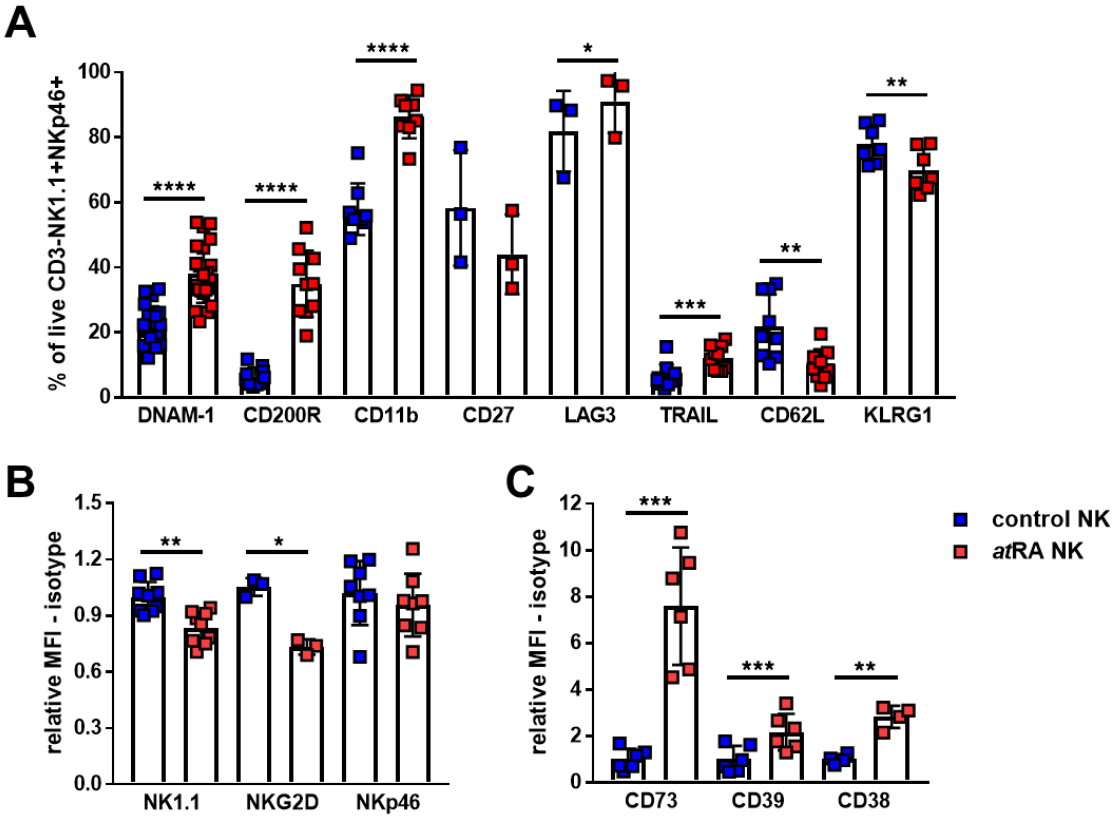

(Figure legend in the next page)

Figure 3.2. *at*RA induces phenotypic changes on NK cells. NK cells were cultured with 1µM of *at*RA in the presence of IL-2 for 7 days (the equivalent volume of DMSO was used as a solvent control), and analyzed by flow cytometry. NK cells were gated as live, CD3ε$^-$, NK1.1$^+$ and NKp46$^+$ cells. (A) Quantification of NK cells expressing DNAM-1, CD200R, CD11b, CD27, LAG3, TRAIL, CD62L, and KLRG1 upon *at*RA- or control-treatment (n≥3). (B-C) Geometric mean florescence intensity (MFI) of (B) activating receptor expression on NK cells (n≥3) and (C) adenosine ecto-enzymes expression on NK cells (n=4-6) upon *at*RA- or control-treatment. Graphs indicate mean ± SEM. *, p<0.05; **, p<0.01; ***, p<0.001; ****, p<0.0001 by paired Student's t-test.

4.1.3 Metabolic changes induced by *at*RA in NK cells

The pathway enrichment analysis from transcriptomic data revealed that *at*RA modified transcription of genes related to metabolism, for example, pentose interconversion and cytochrome P450 pathway (Figure 3.1A). To study the impact of *at*RA on NK cell metabolism, we measured the mitochondrial fitness and the metabolic profile of *at*RA-treated NK cells. We observed that *at*RA-treatment significantly diminished the cell size and the mitochondrial mass of NK cells, measured by the reduction on the forward scatter and florescence intensity of staining with Mitotracker ™ dye (Figure 3.3A and C). Despite the reduced cell size and mitochondrial mass, *at*RA-treated NK cells proliferated at a comparable level as control NK cells (Figure 3.3B). *at*RA-treatment also resulted in reduced mitochondrial membrane potential and production of reactive oxygen species (ROS) by NK cells (Figure 3.3D and E). As transcripts encoding proteins involved in fatty acid degradation, were enriched in *at*RA-treated NK cells (Figure 3.1A), we expected that *at*RA-treated NK cells might uptake higher amount of lipids compared to control NK cells. However, lipid uptake by *at*RA-treated NK cells was comparable to lipid uptake by control NK cells (Figure 3.3F). *at*RA-treatment induced higher basal oxygen consumption rate (OCR) and increased maximum OCR of NK cells (Figure 3.3G, I and J). These results indicates improved oxidative phosphorylation (OXPHOS). Glycolytic activity, measured by extracellular acidification rate (ECAR), was comparable between *at*RA-treated NK cells and control NK cells (Figure 3.3H and K).

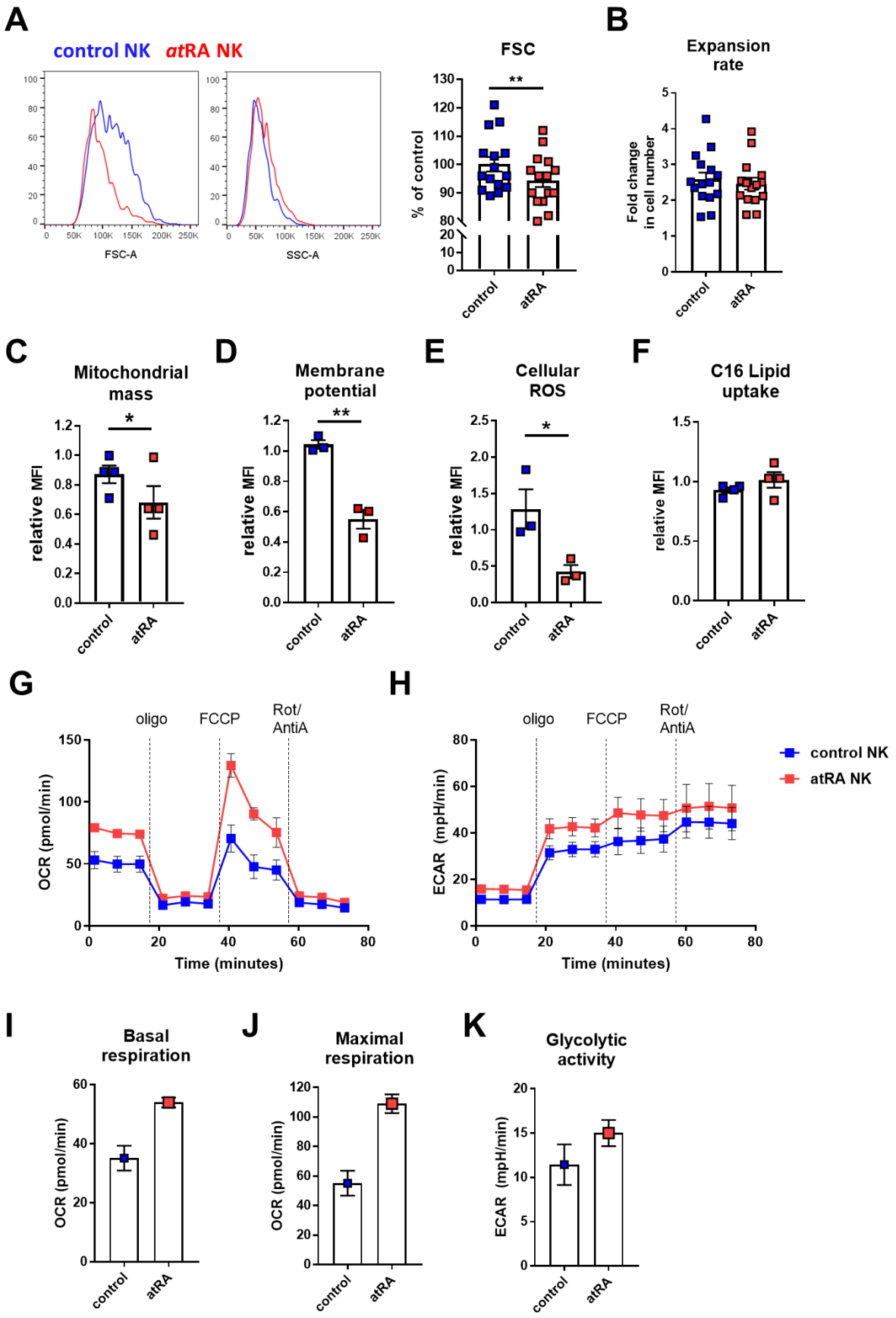

(Figure legend in the next page)

Figure 3.3 *at*RA-treated NK cells show differential mitochondrial phenotype and improved oxidative phosphorylation (OXPHOS). (A-F) NK cells were cultured with 1µM of *at*RA in the presence of IL-2 for 7 days (The equivalent volume of DMSO was used as a solvent control). Mitotracker™ dye, MitoProbe™ TMRM dye, CellRox™ dye, or Bodipy™ FL C16 were used for measuring mitochondrial mass, mitochondrial membrane potential, production of reactive oxygen species (ROS), or lipid uptake, respectively. NK cells were gated as live, CD3ε$^-$, NK1.1$^+$ and NKp46$^+$ cells. (A) Representative histogram (left) and quantification (right) of cell size depicted with forward scatter area (FSC-A), and cellular granularity depicted with side scatter area (SSC-A) (n=15). (B) Quantification of cell expansion rate calculated as final cell numbers divided by starting cell numbers (day 0). (C-F) Geometric mean fluorescence intensity (MFI) of (C) Mitotracker™, (D) TMRM, (E) CellRox™, and (F) Bodipy™ Fl C16 stainings. (n=3-4). (G-K) Oxygen consumption rate (OCR) and extracellular acidification rate (ECAR) of *at*RA-treated NK cells and control NK cells were measured upon oligomycin, FCCP, and Rotenone/Antimycin A-treatment. Quantification of (G) OCR, (H) ECAR, (I) basal respiration, (J) maximal respiration, and (K) baseline glycolytic activity (n=3 for control NK cells and n=2 for *at*RA-treated NK cells). Graphs indicate mean ± SEM. *, p<0.05; **, p<0.01 by paired Student's t-test.

4.1.4 Expression of RA-binding receptors on *at*RA-treated NK cells

Previous studies demonstrated that *at*RA-treatment mediated immune cell development and responses via retinoic acid (RA)-binding receptors. The blockade of RA receptors could prevent RA-induced effects (Dawson, Collins, Pyle, Key, & Taub, 2008; T. Feng et al., 2010; Wansley, Yin, & Prussin, 2013). Therefore, we assessed RA-binding receptors, e.g. retinoic acid receptors (RARs), retinoic X receptors (RXRs) and peroxisome proliferator-activated receptors (PPARs) expression. The transcriptome analysis illustrated higher expression of Pparg and Rarb, and lower expression of Rara and Rarg by NK cells upon *at*RA-treatment (Figure 3.4A). Ppard, Ppara, Rxra, Rxrb and Rxrg expression was comparable upon *at*RA-treatment (Figure 3.4A). In control NK cells, relative mRNA expression of Rara was highest among Rar and Ppar isoforms. *at*RA-treatment downregulated Rara and Rarg mRNA expression, and upregulated Pparg mRNA expression in NK cells (Figure 3.4B).

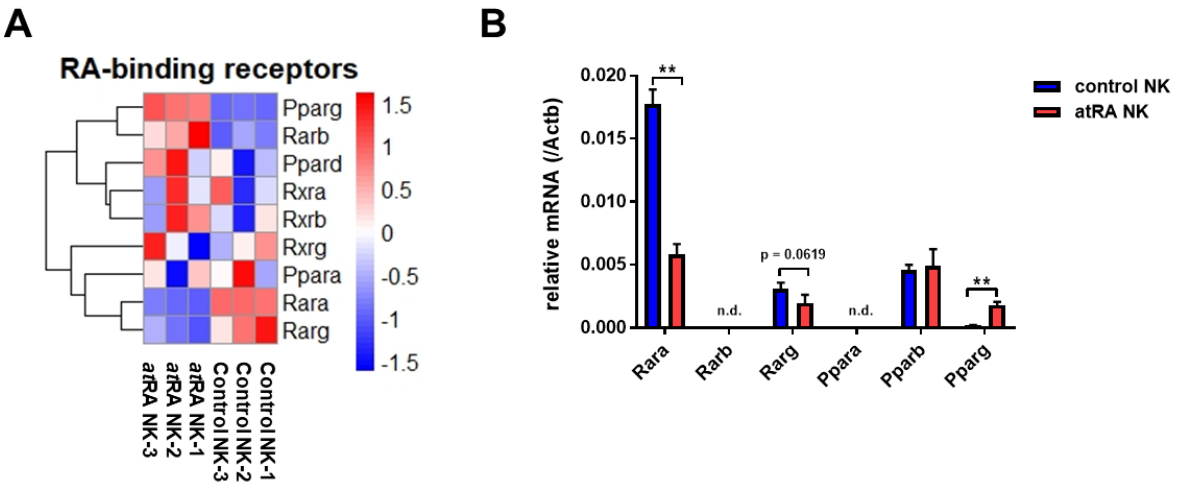

Figure 3.4. *at*RA downregulates expression of Rara and Rarg, and upregulates Pparg expression on NK cells. Data was acquired and analyzed by the transcriptome analysis as in Figure 3.1. (A) Heatmap displays gene expression of RA-binding receptors in *at*RA-treated NK cells and control NK cells. Data are scaled per row. (B) Relative mRNA expression of RA-binding receptors analyzed by qRT-PCR (n=3). Graphs indicate mean ± SEM. **, p<0.01 by paired Student's t-test. n.d. not detected.

4.1.5 Blockade of RA-binding receptor in *at*RA-induced NK cells

To investigate whether blockade of RARα or RARγ can prevent *at*RA-induced reprogramming on NK cells, we treated NK cells with selective RARα antagonist (Ro-415253) or RARγ antagonist (MM-11253) in the presence of *at*RA. Representative markers of the *at*RA-induced phenotype, DNAM-1 and CD200R, were measured on NK cells. In accordance with the previous results, *at*RA-treated NK cells expressed higher amounts of DNAM-1 and CD200R compared to control NK cells; however, these phenotypes were not changed by neither blocking RARα (Figure 3.5A and B), nor by blocking RARγ (Figure 3.6A and B) with selective antagonists.

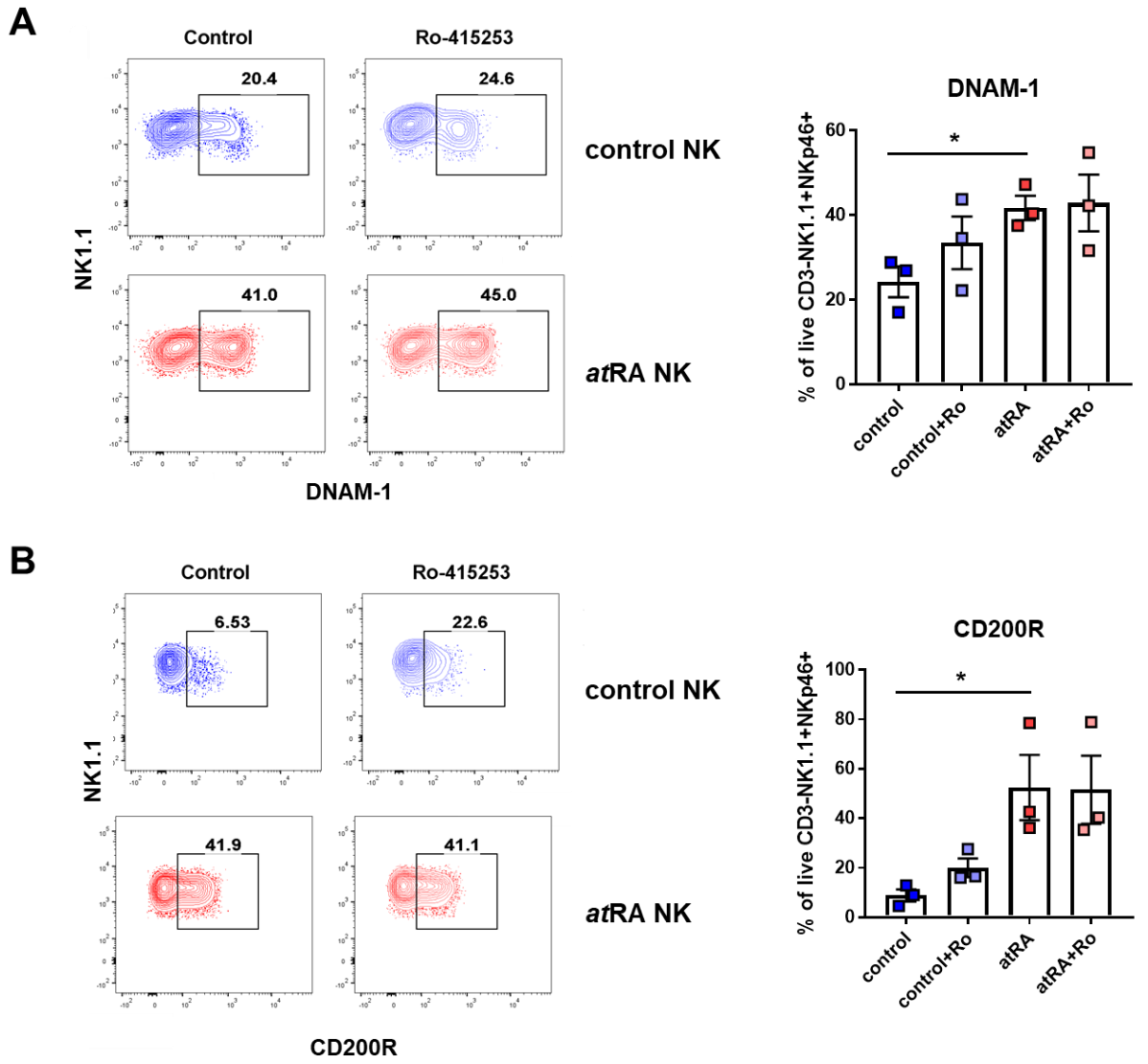

Figure 3.5. RARα inhibition does not regulate DNAM-1 and CD200R expression on *at*RA-treated NK cells. NK cells were cultured with 10 µM of selective RARα antagonist (Ro-415253) in the presence of 1 µM of *at*RA and IL-2 for 7 days. Cells were analyzed by flow cytometry for DNAM-1 and CD200R expression, and gated as live, CD3ε$^-$, NK1.1$^+$, and NKp46$^+$ cells. Representative contour-plots (left) and quantification (right) of NK cells expressing DNAM-1 (A) and CD200R (B) upon *at*RA- or control-treatment with or without Ro-415253 (n=3). Graphs indicate mean ± SEM. *, p<0.05 by one-way ANOVA (Tukey's multiple comparisons test). Ro, Ro-415253.

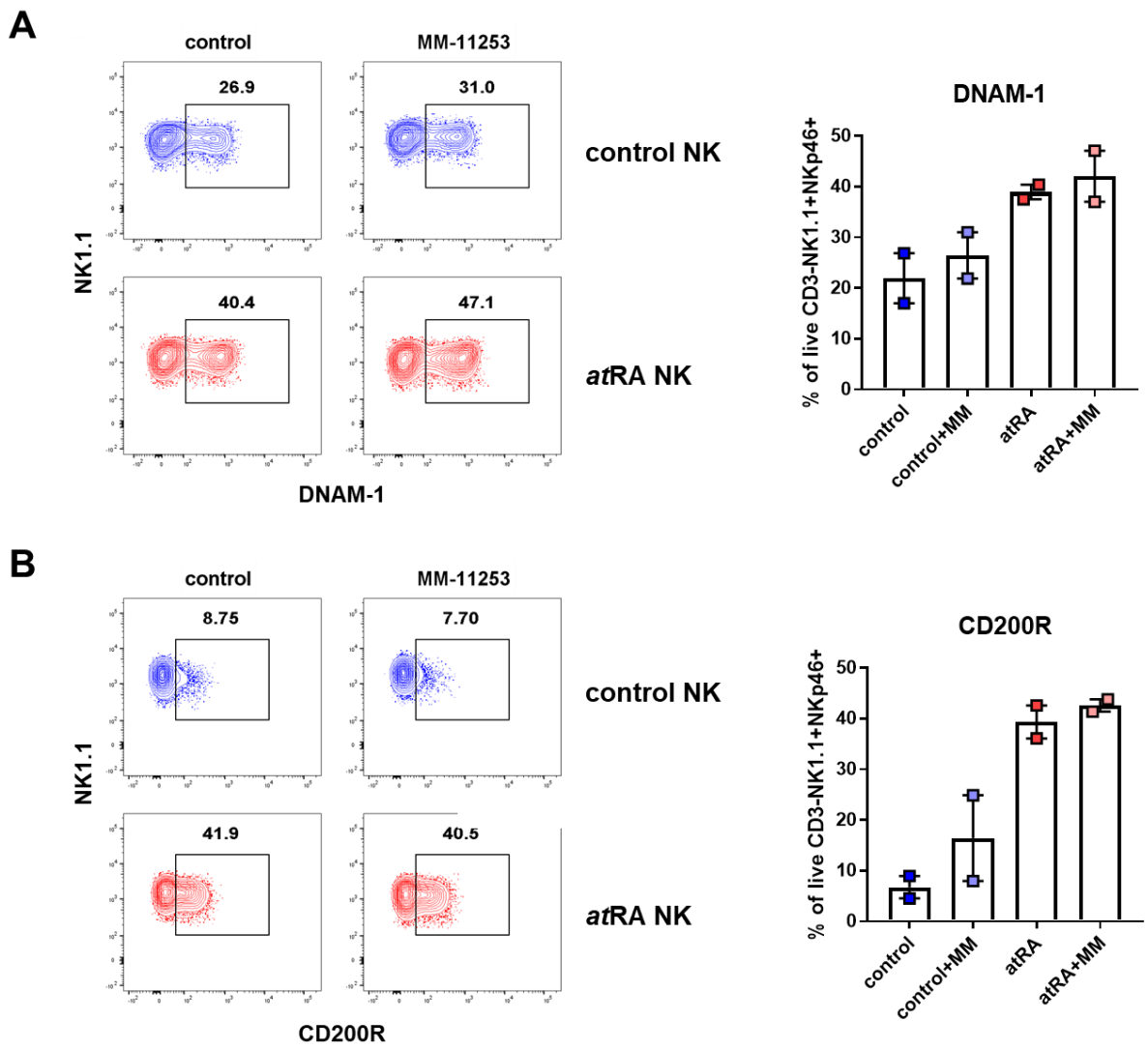

Figure 3.6. RARγ inhibition does not regulate DNAM-1 and CD200R expression on *at*RA-treated NK cells. NK cells were cultured with 10 µM of selective RARγ antagonist (MM-11253) in the presence of 1 µM of *at*RA and IL-2 for 7 days. Cells were analyzed by flow cytometry for DNAM-1 and CD200R expression, and gated as live$^-$, CD3ε$^-$, NK1.1$^+$, and NKp46$^+$ cells. Representative contour-plots (left) and quantification (right) of DNAM-1 (A) and CD200R (B) expression on *at*RA-treated NK cells and control NK cells with or without MM-11253 (n=2). Graphs indicate mean ± SEM. MM, MM-11253.

Nuclear receptors PPARβ/δ were reported to bind RA (Shaw, Elholm, & Noy, 2003), and their mRNA expression was highest among PPAR isoforms in cultured NK cells (Fig3.4B). Treatment with *at*RA did not change Ppard mRNA expression, while Pparg expression was upregulated upon *at*RA-treatment (Fig3.4B). Although PPARγ does not directly bind to RA, it heterodimerizes with retinoic X receptor (RXR) that can bind to RA, and can modulate PPARγ-mediated transcription (DiRenzo et al., 1997). We treated NK cells with selective PPARγ antagonist (T0070907) in the presence of *at*RA. Inhibition of PPARγ signaling prevented the elevated DNAM-1 and CD200R expression on *at*RA-treated NK cells, and did not have an effect on control NK cells (Figure 3.7B and C).

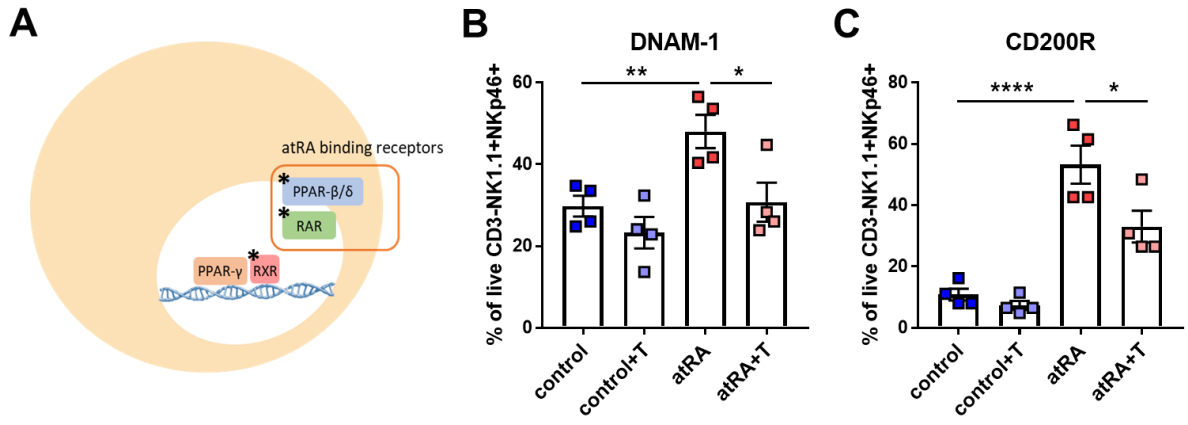

Figure 3.7. PPARγ inhibition reduces expression of DNAM-1 and CD200R on *at*RA-treated NK cells. (A) Graphic scheme of RA-binding receptors (marked with * in the scheme). (B-C) NK cells were cultured with 10 μM of selective PPARγ antagonist (T0070907) in the presence of 1 μM of *at*RA and IL-2 for 7 days. Cells were analyzed by flow cytometry for DNAM-1 and CD200R expression, and gated as live, CD3ε$^-$, NK1.1$^+$, and NKp46$^+$ cells. Quantification of DNAM-1 (B) and CD200R (C) expression on *at*RA-treated NK cells and control NK cells, treated or not with T0070907 (+T). Graphs indicate mean ± SEM. p<0.05; **, p<0.01; ****, p<0.0001 by paired Student's t-test.

4.1.6 Role of TGFβ in *at*RA-induced reprogramming of NK cells

Previous study demonstrated that TGFβ signaling in tumor microenvironment could induce NK cell conversion to an intermediate ILC1-like phenotype, which shared similaralities with *at*RA-treated NK cells, e.g. increased DNAM-1 and TRAIL expression, and decreased CD62L and Eomes expression (Gao et al., 2017). Our transcriptome analysis showed enhanced Tgfb3 transcription by *at*RA-treated NK cells (Figure 3.1C). Relative mRNA expression analysis showed that *at*RA-treatment enhanced Tgfb3 expression in NK cells (Figure 3.8A). To examine whether TGFβ modulates *at*RA-induced phenotype in an autocrine manner, we cultured NK cells with anti-TGFβ antibody in the presence of *at*RA. NK cells enhanced DNAM-1 and CD200R expression in the presence of *at*RA, and TGFβ neutralization did not affect this phenotype (Figure 3.8B).

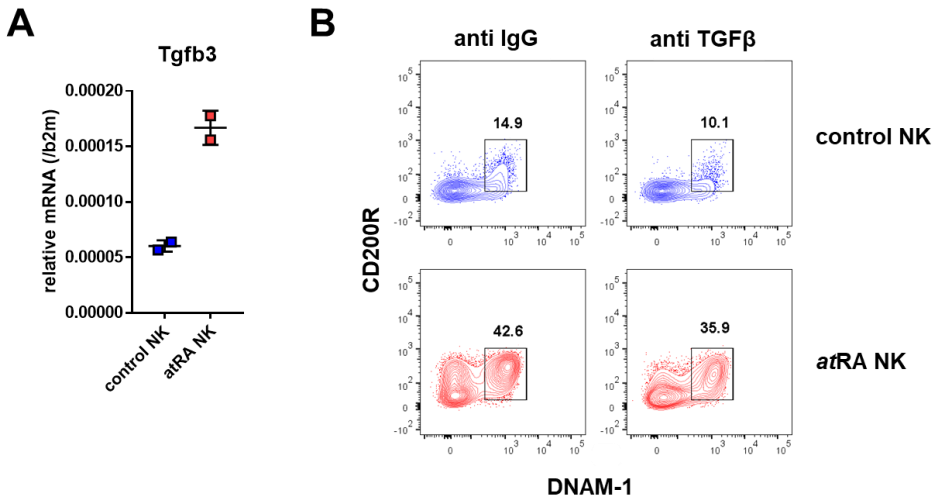

Figure 3.8. TGFβ neutralization does not affect the expression of DNAM-1 and CD200R on *at*RA-treated NK cells. (A) NK cells were cultured with 1 µM of *at*RA for 7 days in the presence of IL-2, and RNA was isolated to analyze Tgfb3 mRNA expression. Graph shows the quantification of Tgfb3 transcript in *at*RA-treated NK cells and control NK cells. (B) NK cells were cultured with 10 µg/mL of anti-TGFβ antibody in the presence of 1 µM of *at*RA and IL-2 for 7 days. NK cells were analyzed by flow cytometry for DNAM-1 and CD200R expression, and gated as live, $CD3\varepsilon^-$, $NK1.1^+$, and $NKp46^+$ cells. Representative contour-plots display DNAM-1 and CD200R expression. Graph indicates mean ± SD (n=2).

4.2 Effect of all-*trans* retinoic acid on NK cell effector functions

4.2.1 IFN-γ production of NK cells is reduced by *at*RA

Gene pathway analysis indicated downregulation of transcripts involved in NFκB pathway and NK cell mediated-cytotoxicity, in NK cells upon *at*RA-treatment (Figure 3.1A). Additionally, surface molecules, which play important roles in NK cell activation and cytotoxicity, such as NK1.1, NKG2D, CD226 (DNAM-1), TRAIL and IL-18Rα, were differentially expressed in NK cells exposed to *at*RA (Figure 3.2). Thus, we hypothesized that *at*RA might influence not only phenotype, but also effector functions of NK cells.

Upon NK cell stimulation with anti-NK1.1 antibody, anti-NKG2D antibody, anti-NKp46 antibody, or with CD155 fusion-protein (which stimulates the receptor DNAM-1), or with recombinant mouse IL-12 and IL-18, *at*RA-treated NK cells downregulated production of IFN-γ, compared to control NK cells (Figure 3.9A). The surface expression of the IL-18 receptor alpha (IL-18Rα) was diminished on NK cells upon *at*RA-treatment (Figure 3.9C). In accordance with the reduced IL-18Rα expression, *at*RA-treated NK cells decreased IFN-γ production in response to IL-18, but not in the response to IL-12 (Figure 3.9D). The expression of IκBζ, the transcriptional regulator of IFN-γ in the NFκB signaling pathway, was induced in control NK cells upon stimulation with IL-18, and IκBζ expression was lower in *at*RA-treated NK cells (Figure 3.9E). However, upon stimulation with IL-12, IκBζ expression was not induced, and not changed upon *at*RA-treatment. STAT4, a regulator of IL-12-induced IFN-γ production, was phosphorylated in control NK cells upon stimulation with IL-12, and the phosphorylation of STAT4 was equivalent between NK cells treated with *at*RA or control solvent (Figure 3.9F). Expression of NFκB p65 and pIKKα/β, molecules involved in the NFκB signaling pathway, did not change neither in control NK cells, nor in *at*RA-treated NK cells upon simulation with IL-12 or IL-18 (Figure 3.9G and H). These results indicate that *at*RA reduced IL-18Rα expression, along with the downstream of NFκB signaling pathway, and IκBζ expression, which resulted in diminished IFN-γ production upon NK cell activation.

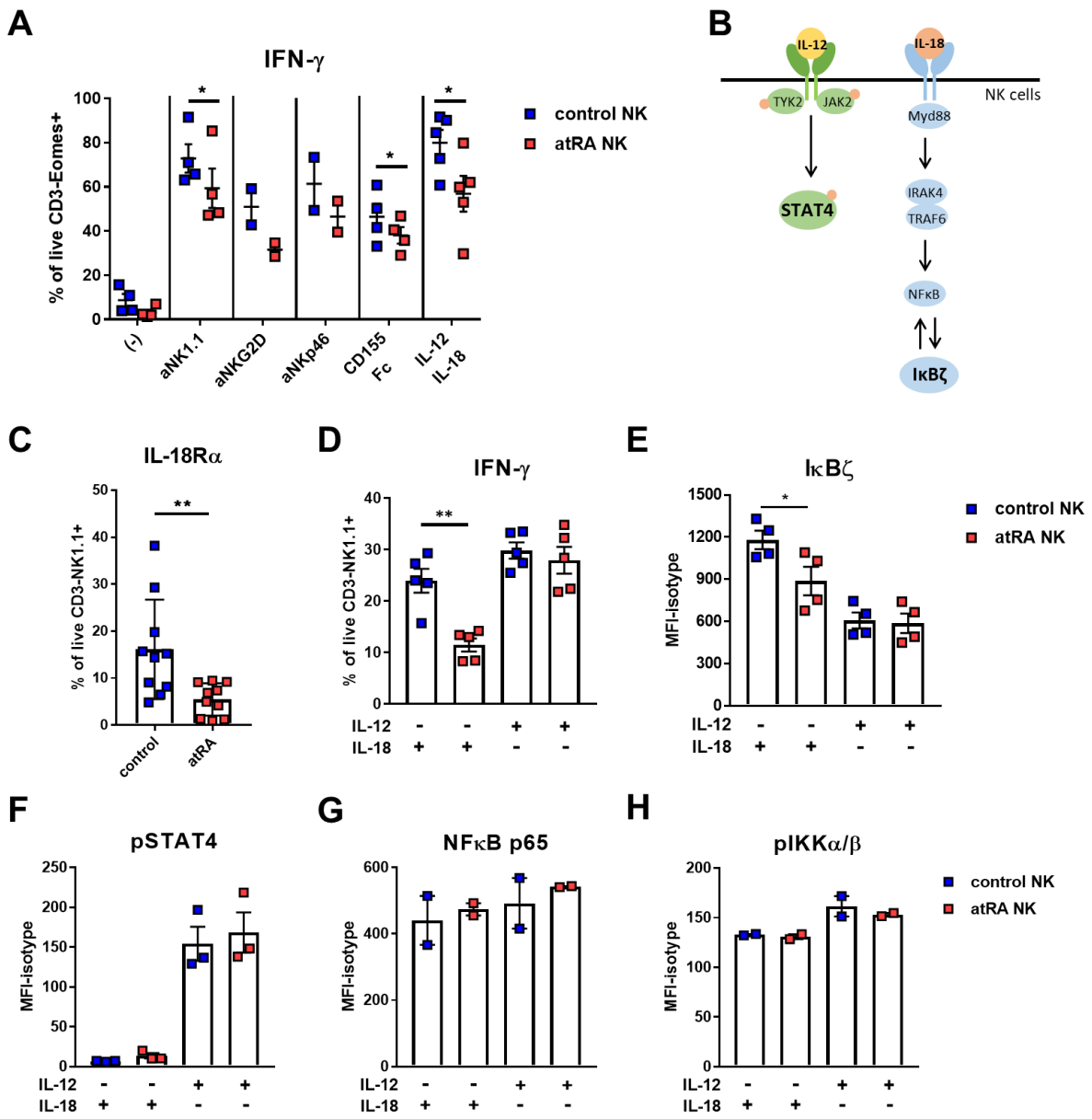

Figure 3.9. *at*RA reduces IFN-γ production by NK cells. (A) NK cells were cultured with 1 µM of *at*RA in the presence of IL-2 for 7 days, and then re-stimulated with anti-NK1.1 antibody, anti-NKG2D antibody, anti-NKp46 antibody, CD155 fusion-protein (CD155 Fc), or mouse IL-12 and/or IL-18 for 5 hours. NK cells were gated as live, CD3ε$^-$, NK1.1$^+$, and NKp46$^+$ cells, and analyzed by flow cytometry. (A) Quantification of IFN-γ-producing NK cells upon different stimuli (n=2-5). (B) Graphical scheme of signaling induced by IL-12 or IL-18 in NK cells. (C) Quantification of IL-18Rα expression on NK cells (n=11). (D-H) *at*RA-treated NK cells and control NK cells were stimulated with IL-12 or IL-18, and analyzed by flow cytometry. Quantification of (D) IFN-γ, (E) IκBζ, (F) phosphorylated (p)-STAT4, (G) NFκB p65, and (H) pIKKα/β expression in NK cells (n=2-5). Graphs indicate mean ± SEM. *, p<0.05; **, p<0.01 by paired Student's t-test; MFI, mean florescence intensity.

4.2.2 Reduced IFN-γ production and enhanced degranulation of *at*RA-treated NK cell in response to tumor cells

Tumor cells, such as YAC-1 lymphoma and B16 melanoma cells, were reported to express ligands of NK cell receptors (Chan et al., 2010; Ogawa et al., 2011). The engagement of ligands on tumor cells by activating receptors of NK cells can induce activation, cytokine production, and cytotoxicity against tumor cells. To elucidate the impact of *at*RA on effector functions of NK cells in response to tumor cells, we co-cultured *at*RA-treated NK cells with RMA-S lymphoma, YAC-1 lymphoma or B16 melanoma cells. *at*RA-treated NK cells displayed the reduced IFN-γ production upon co-culture with RMA-S or YAC-1, compared to control NK cells (Figure 3.10A and B). *at*RA-treated NK cells increased degranulation compared to control NK cells, during co-culture with RMA-S, YAC-1 or B16 tumor cells. (Figure 3.10A and C).

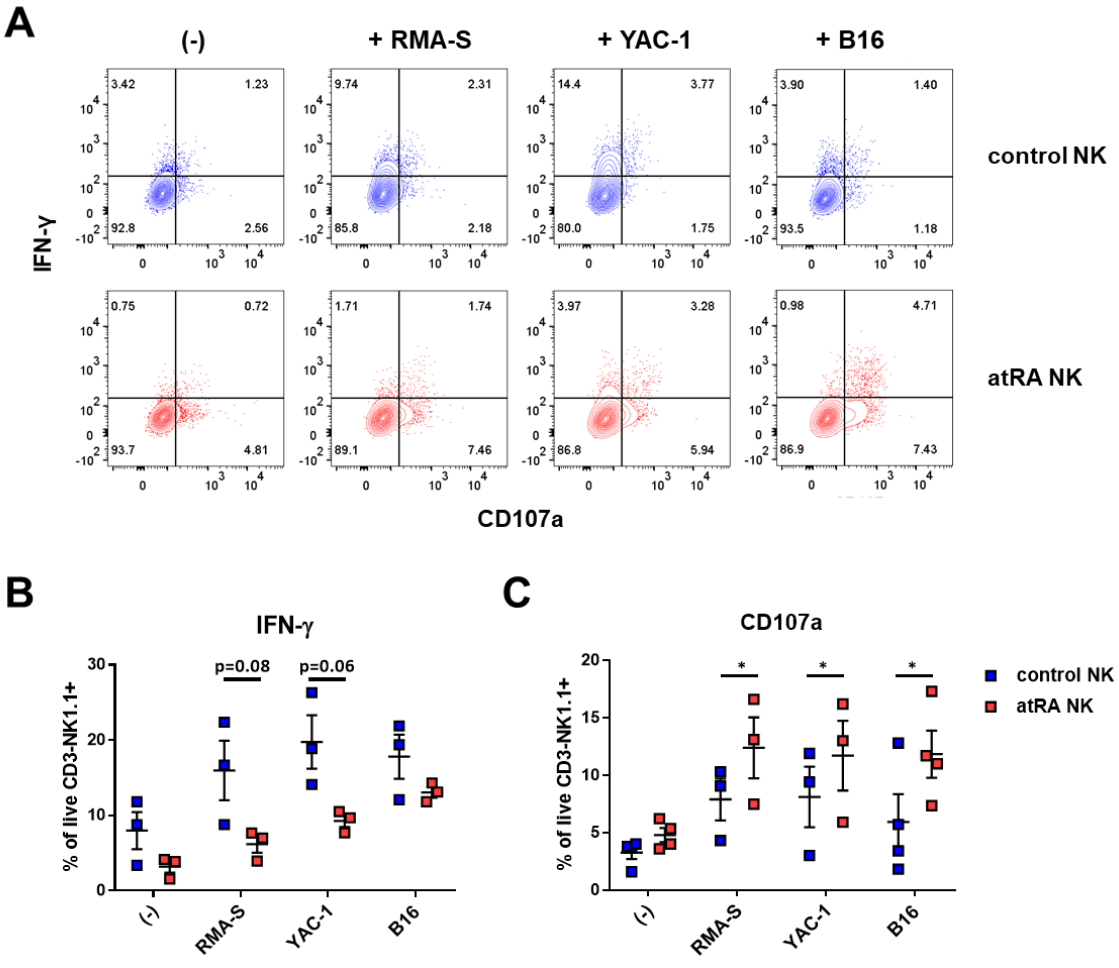

Figure 3.10. *at*RA reduces IFN-γ production and enhances degranulation of NK cells in response to tumor cells. (A-C) NK cells were cultured with 1 µM of *at*RA in the presence of IL-2 for 7 days and then co-cultured with RMA-S lymphoma, YAC-1 lymphoma, and B16 melanoma cells for 6 hours. FITC anti-CD107a was added into the co-culture. NK cells were gated as live, $CD3\varepsilon^-$ and $NK1.1^+$ cells, and analyzed by flow cytometry for IFN-γ and CD107a expression. (A) Representative dot-plots of IFN-γ and CD107a expression by *at*RA-treated NK cells and control NK cells upon co-culture with tumor cells. Quantification of (B) IFN-γ and (C) CD107a-expressing NK cells upon co-culture with tumor cells (n=3). Graphs indicate mean ± SEM. *, $p<0.05$ by paired Student's t-test.

4.2.3 Cytokine and chemokine expression of *at*RA-treated NK cells

To uncover which molecules might be secreted by NK cells upon *at*RA-treatment, we measured mRNA expression of various cytokines and chemokines in control NK cells and in *at*RA-treated NK cell upon stimulation. Control NK cells and *at*RA-treated NK cell were stimulated via receptor DNAM-1 (stimulation with CD155 fusion-protein) or receptor NK1.1 (simulation with anti-NK1.1 antibody), which were differentially regulated by *at*RA in NK cells (Figure 3.2). Unstimulated NK cells exposed to *at*RA upregulated mRNA expression of Csf2, Ccl5, Ccl1, Tnfsf10 and Tnfsf11, and downregulated mRNA expression of Ifng, Il23a, Ccl3, Tnfsf11b and Osm, compared to control NK cells (Figure 3.11A). Upon DNAM-1 triggering, *at*RA-treated NK cells further elevated expression of Tnfsf11, Tnfsf10, Ccl5, Cxcl10, Ccl1 and Csf2 compared to control NK cells (Figure 3.11B). Upon NK1.1 triggering, *at*RA-treated NK cells elevated expression of Fasl, Tnfsf11, Csf2, Cxcl10, Ccl5, Mif, Gpi1, Vegfa, and Xcl1 compared to control NK cells (Figure 3.11C).

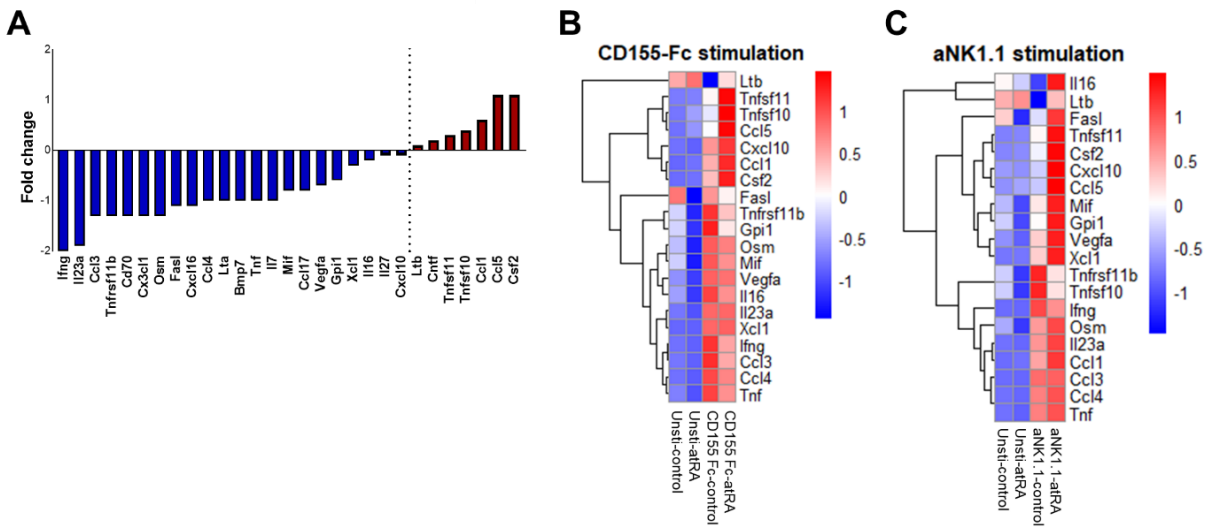

Figure 3.11. *at*RA elevates Csf2, Ccl5, Ccl1, Tnfsf10 and Tnfsf11 expression of NK cells upon stimulation. NK cells were cultured with 1 µM of *at*RA in the presence of IL-2 for 7 days, and then stimulated with plate-bound CD155 fusion-protein (CD155-Fc) or anti-NK1.1 antibody for 5 hours. qPCR was performed with RNA isolated from unstimulated and re-stimulated NK cells, to screen expression of 84 different transcripts encoding chemokines and cytokines. Genes, which displayed cycle threshold (CT) value higher than 35, were removed, and twenty genes were selected, based on expression levels. (A) Quantification of relative mRNA expression by unstimulated *at*RA-treated NK cells normalized to expression of unstimulated control NK cells. (B-C) Heatmap of relative mRNA expression by *at*RA-treated NK cells and control NK cells, which were unstimulated (Unsti-) or with (B) CD155 Fc-triggering or (C) anti-NK1.1 triggering.

4.3 Interaction of *at*RA-treated NK cells and immune cells

4.3.1 Crosstalk of *at*RA-treated NK cells with dendritic cells

Previous studies evidenced the importance of NK cells in regulating adaptive immunity via the interaction with dendritic cells (DCs) (Ferlazzo & Morandi, 2014). The crosstalk of NK cells with immature dendritic cells (iDCs) can induce iDC maturation or elimination. Several molecules, which play important roles in the interaction of NK cells and DCs, were differentially regulated in NK cells upon *at*RA-treatment. For instance, the expression of receptor DNAM-1 and death-receptor ligand TRAIL, which are reported to mediate DC elimination, were upregulated on the surface of *at*RA-treated NK cells (Figure 3.2A). *at*RA-treated NK cells produced lower amount of IFN-γ, an inflammatory cytokine that can induce maturation of DCs. Therefore, we hypothesized that *at*RA could affect the crosstalk of NK cells with DCs.

4.3.1.1 Phenotype of bone marrow-derived dendritic cells

Bone marrow-derived dendritic cells (BM-DCs) were generated from bone-marrow precursors in the presence of GM-CSF, and expressed integrins, CD11b and CD11c (Figure 3.12A). Expression of surface molecules, which are used as maturation markers of DCs, such as CD80, CD86, and major histocompatibility complex II (MHC II), were analyzed in BM-DCs upon treatment with LPS. The expression of these molecules was increased in BM-DCs treated with LPS (Figure 3.12B), indicating their maturation. DR5 and Rae-1 were not detected on BM-DCs before or after LPS-treatment, while expression of CD155 was upregulated upon LPS-treatment (Figure 3.12B). These results indicate that the maturation of BM-DCs can be detected by analyzing the expression of CD80, CD86, MHC II, and CD155.

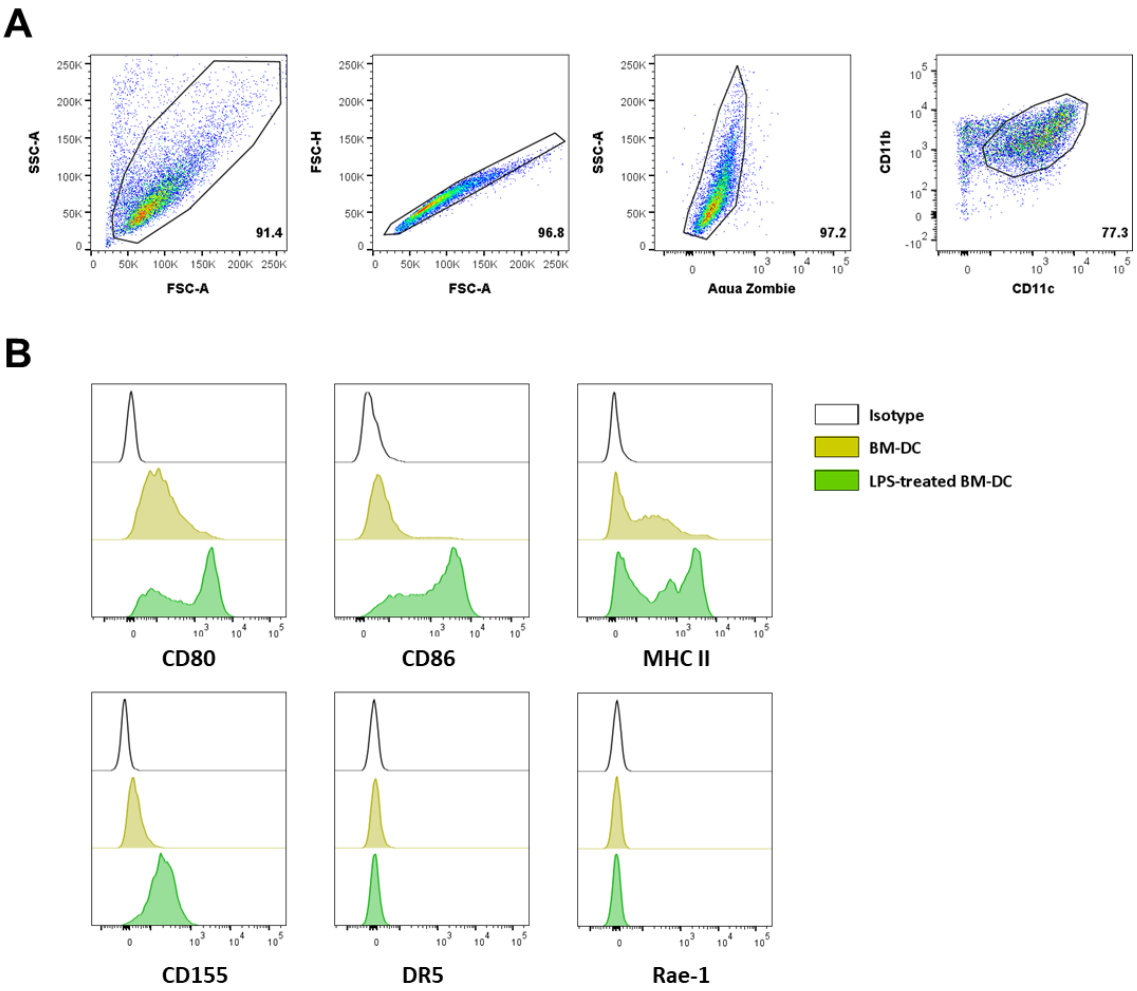

Figure 3.12. Gating strategy and phenotype of bone marrow-derived dendritic cells (BM-DCs). Non-adherent cells derived from bone marrow of C57BL/6N mice were cultured in media containing GM-CSF for 7-8 days. BM-DCs were analyzed by flow cytometry, and gated as live, $CD11b^+$ and $CD11c^+$ cells. (A) Representative dot-plots of BM-DCs gating strategy. (B) Representative histograms of CD80, CD86, MHC II, CD155, DR5, and Rae-1 expression on BM-DCs and LPS-treated BM-DCs. DR5, death receptor 5; Rae-1, Retinoic acid early inducible 1.

4.3.1.2 Reduced ability of *at*RA-treated NK cells to induce BM-DC maturation and apoptosis

To investigate the effect of *at*RA on NK cell ability to induce DC maturation, we co-cultured NK cells pre-treated with *at*RA, and BM-DCs at the different ratios (2:1, 1:1, and 1:2) (Figure 3.13A). Flow cytometric analysis showed that co-culture at ratios of 2:1 and 1:1 was not suitable for the analysis of BM-DC maturation, as the percentage of BM-DCs was very low (less than 5% among live cells) (Figure3.13B). Thus, the co-culture in a 1:2 ratio of NK cells to BM-DCs was performed. CD80, CD86, and MHC II expression was increased in BM-DCs in the presence of control NK cells, compared to BM-DCs alone (Figure 3.13C). The ability of *at*RA-treated NK cells to induce the expression of these molecules was lower, compared to the ability of control NK cells (Figure 3.13C).

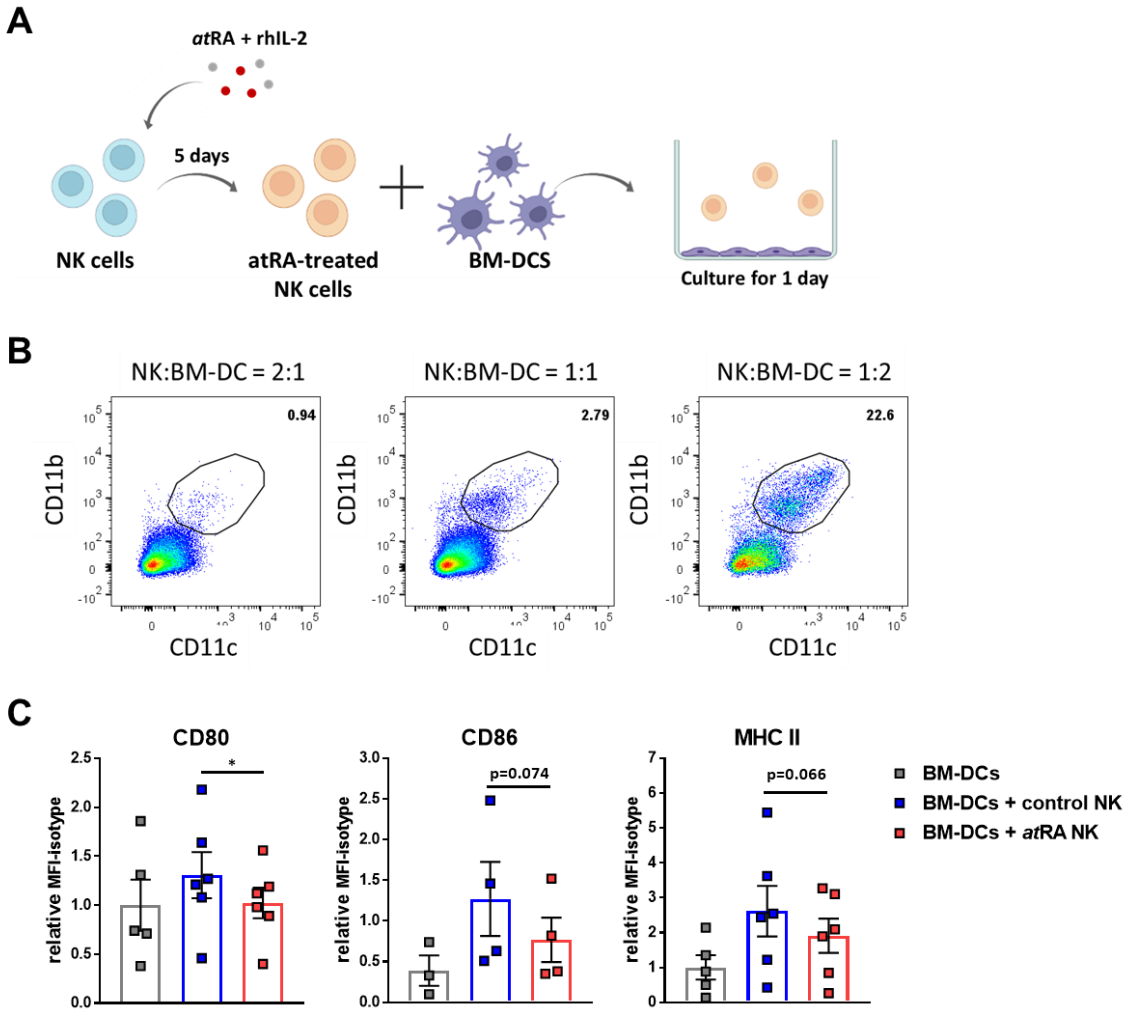

Figure 3.13. Reduced ability of *at*RA-treated NK cells to induce maturation of BM-DCs. BM-DCs were co-cultured with *at*RA-treated NK cells or control NK cells for 24 hours. BM-DCs were analyzed by flow cytometry for CD80, CD86 and MHC II expression, and gated as live, NK1.1$^-$, CD11b$^+$ and CD11c$^+$ cells. (A) Schematic illustration depicting the co-culture of BM-DCs and NK cells (Created with BioRender.com). (B) Representative dot-plots showing the percentage of CD11b$^+$CD11c$^+$ BM-DCs upon co-culture with NK cells at different ratios (2:1, 1:1, and 1:2 of NK cells to DCs). (C) Quantification of CD80, CD86, and MHC II expression on BM-DCs upon co-culture with *at*RA-treated NK cells or control NK cells (n=4-6). Graphs indicate mean ± SEM. *, p<0.05 by paired Student's t-test; MFI, mean florescence intensity.

One of the possible explanations for the reduced ability to induce maturation of BM-DCs is the lower capacity of *at*RA-treated NK cells to produce IFN-γ (Figure 3.9). IFN-γ is reported to support DC maturation (Martin-Fontecha et al., 2004; Vitale et al., 2005). Thus, we measured IFN-γ production by *at*RA-treated or control NK cells upon co-culture with BM-DCs. We observed that BM-DCs alone did not produce IFN-γ, and NK cells produced IFN-γ, in the presence of BM-DCs. *at*RA-treated NK cells produced significantly lower amounts of IFN-γ compared to control NK cells (Figure 3.14A). BM-DCs displayed the highest expression of MHC II in the presence of control NK cells, which was diminished in the presence of IFN-γ-neutralizing antibodies (Figure 3.14B). MHC II expression induced by *at*RA-treated NK cells was also decreased on BM-DCs with IFN-γ neutralization (Figure 3.14B). These results demonstrate that IFN-γ is a mediator of increased MHC II expression on BM-DCs, and due to reduced amount of IFN-γ secreted by *at*RA-treated NK cells, BM-DCs displayed lower maturation upon co-culture with *at*RA-treated NK cells.

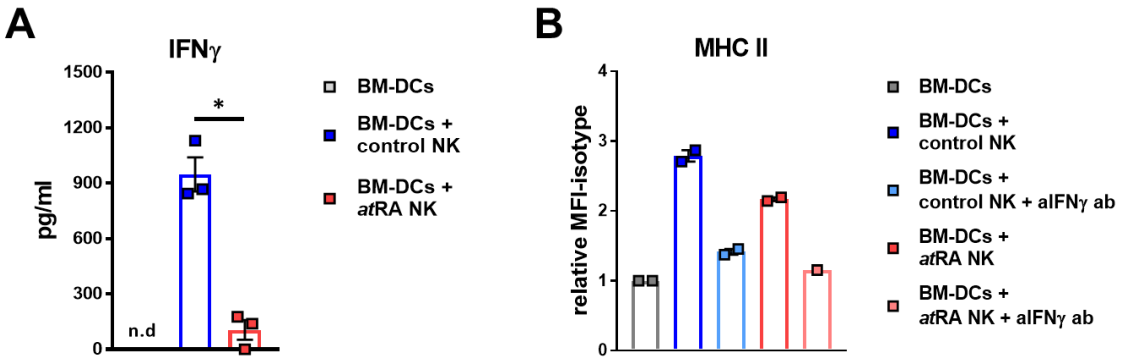

Figure 3.14. IFN-γ produced by NK cells affects MHC II expression on BM-DCs. (A) BM-DCs were cultured alone, with *at*RA-treated NK cells, or with control NK cells for 24 hours. Supernatant was collected to measure the amount of IFN-γ using ELISA. Quantification of IFN-γ upon co-culture (n=3). (B) 1 µg/mL of anti-IFN-γ antibody (+aIFNg ab) was added into the co-culture of BM-DCs and NK cells. BM-DCs were analyzed by flow cytometry for MHC II expression, and gated as live, NK1.1^{-}, CD11b^{+} and CD11c^{+} cells. Quantification of MHC II expression on BM-DCs upon co-culture with *at*RA-treated NK cells or control NK cells (n=2). Graphs indicate mean ± SEM. *, $p<0.05$ by paired Student's t-test.

Next, we assessed the apoptosis of DCs in the presence of NK cells. Compared to BM-DCs alone, the amount of apoptotic BM-DCs, measured as Annexin V^+ cells, were higher in the presence of control NK cells (Figure 3.15A), indicating the ability of control NK cells to eliminate immature BM-DCs. Upon co-culture with *at*RA-treated NK cells, the amount of apoptotic BM-DCs was significantly lower, compared to co-culture with control NK cells (Figure 3.15B). These results implies that the NK cell ability to induce apoptosis of immature BM-DCs is impaired by *at*RA.

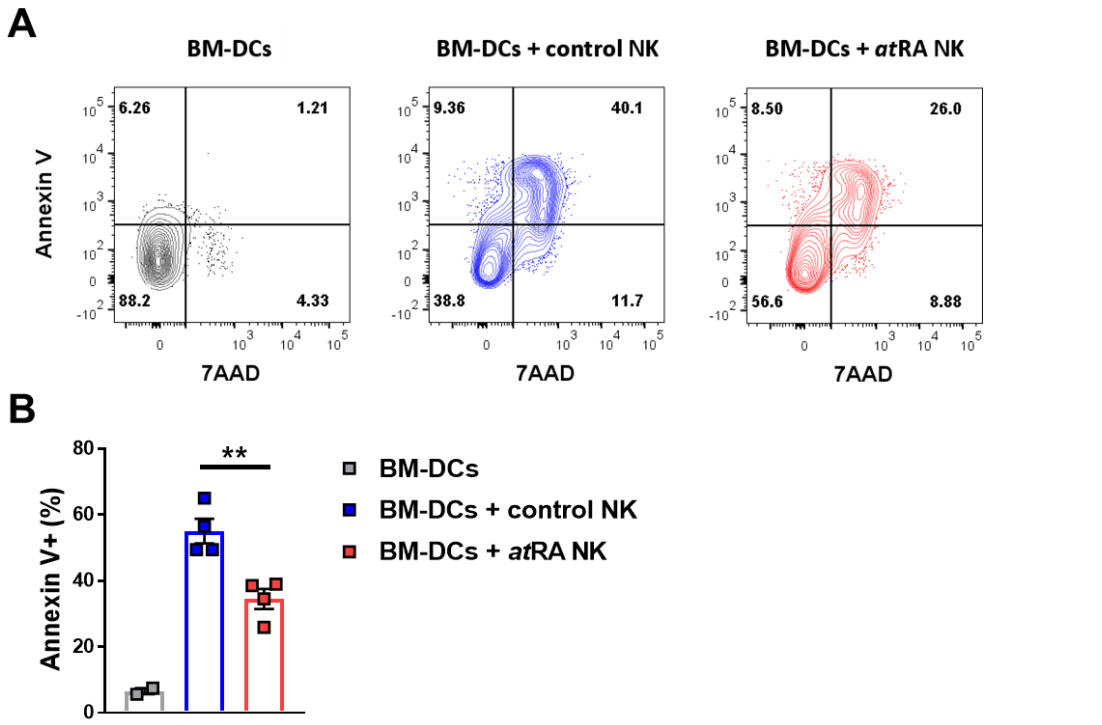

Figure 3.15. Reduced ability of *at*RA-treated NK cells to induce apoptosis of BM-DCs. Co-culture of NK cells and *at*RA-treated NK cells or control NK cells was performed at a 1:2 ratio for 6 hours. BM-DCs were analyzed by flow cytometry, and gated as $NK1.1^-$, $CD11b^+$ and $CD11c^+$ cells. (A) Representative contour-plots of apoptotic BM-DCs in the absence of NK cells, in the presence of control NK cells or *at*RA-treated NK cells. (B) Quantification of Annexin V-expressing BM-DCs (n=2-4). Graphs indicate mean ± SEM. **, $p<0.01$ by paired Student's t-test.

4.3.2 Influence of *at*RA-treated NK cells on CD4⁺ T cell polarization

NK cells are reported to regulate T cell differentiation, activation and elimination via direct interaction with T cells or through DCs conditioned by crosstalk with NK cells (Ferlazzo & Morandi, 2014; Pallmer & Oxenius, 2016). Here, we investigated the impact of *at*RA on the role of NK cells to regulate differentiation of CD4⁺ T cells.

4.3.2.1 Polarization of CD4⁺ T cells

Naïve CD4⁺ T cells were isolated (purity higher than 90%) (Figure 3.16A) and cultured in four different polarizing conditions; type 1 T helper (T_H1)-, type 2 T helper (T_H2)-, type 17 T helper (T_H17)- and regulatory T (Treg)-polarizing conditions. We analyzed the expression of transcription factors in T cells, in order to validate the polarization of CD4⁺ T cells. CD4⁺ T cells upregulated expression of T-bet in T_H1-polarzing condition, GATA-3 in T_H2-polarzing condition, RORγt in T_H17-polarzing condition, and FoxP3 in Treg-polarizing condition, compared to non-polarized T cells (T_H0) (Figure 3.16B).

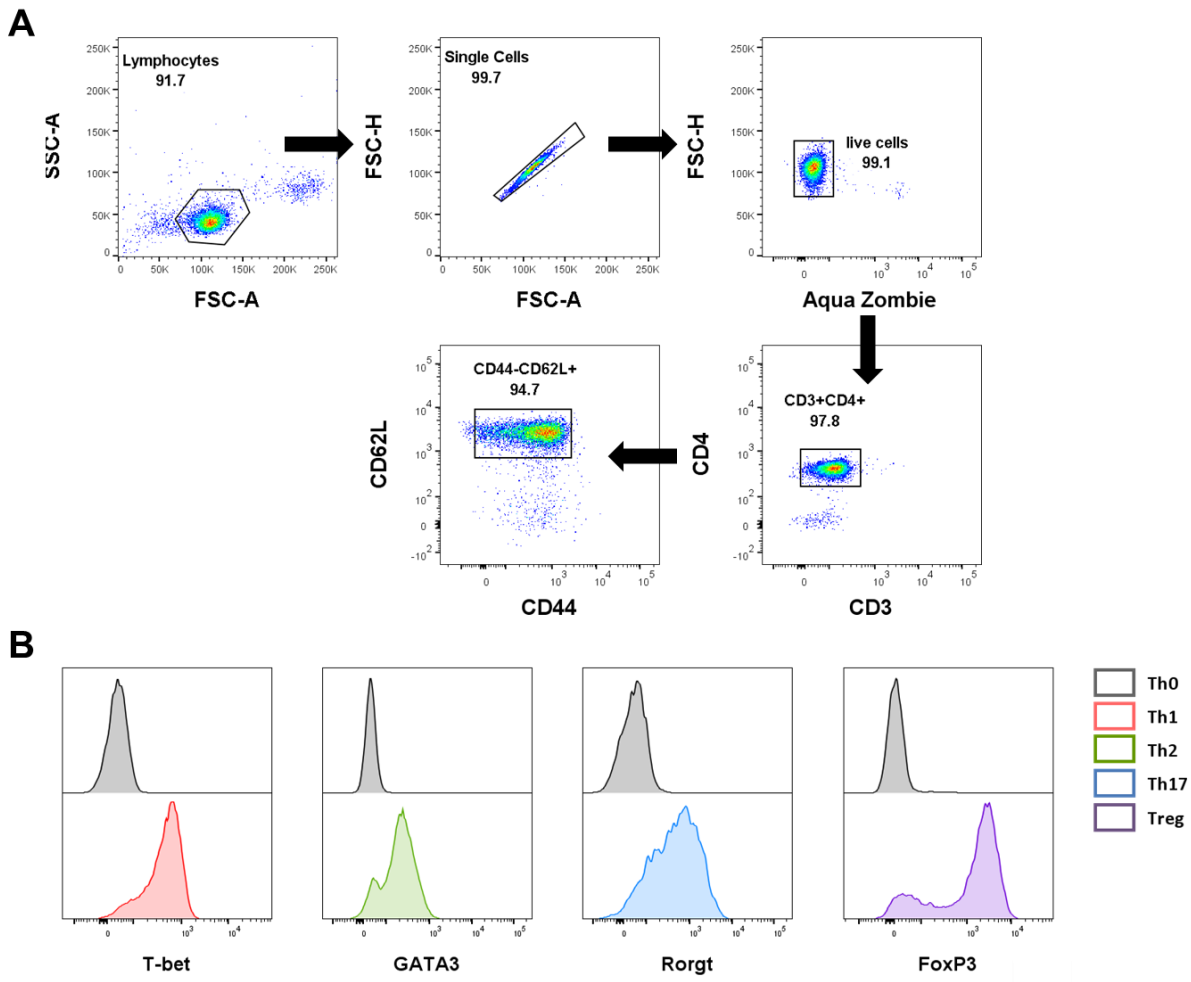

Figure 3.16. Gating strategy for naïve CD4⁺ T cells and expression of transcription factors upon T cell polarization. Naïve CD4⁺ T cells were isolated from spleen and lymph nodes of C57BL/6N-Ly5.2 mice, and cultured in different polarizing conditions in the presence of plate-bound anti-CD3ε antibody and soluble anti-CD28 antibody

for 2 days; type 1 T helper (T_H1)-, type 2 T helper (T_H2)-, type 17 T helper (T_H17)- and regulatory T (Treg)-polarizing conditions. (A) Representative dot-plots showing the gating strategy of naïve $CD4^+$ T cells. Cells were analyzed by flow cytometry, and gated as live, $CD3\varepsilon^+$, $CD4^+$, $CD44^-$ and $CD62L^+$ cells. (B) Representative histograms of T-bet, GATA-3, RORγt, and FoxP3 expression in $CD4^+$ T cells upon polarization. Cells were analyzed by flow cytometry, and gated as live, $CD45.2^+$ and $CD4^+$ cells (CD45.2 is an alloantigen of CD45, expressed by Ly5.2 congenic mouse strain).

4.3.2.2 Enhanced FoxP3 expression in $CD4^+$ T cells in the presence of *at*RA-treated NK cells

To further investigate the interaction between *at*RA-treated NK cells and T cells, we performed a 1:1 ratio co-culture of NK cells and $CD4^+$ T cells in different polarizing conditions (Figure 3.17A). $CD4^+$ T cells displayed T-bet expression and IFN-γ secretion in the presence of T_H1-polarizing cytokines, such as IL-2 and IL-12 (Figure 3.17B). Co-culture with control- or *at*RA-treated NK cells did not change this phenotype of $CD4^+$ T cells (Figure 3.17B and C). $CD4^+$ T cells expressed GATA3 in the presence of T_H2-polarizing cytokines, such as IL-2 and IL-4, and the presence of control- or *at*RA-treated NK cells did not change GATA3 expression of $CD4^+$ T cells (Figure 3.17D).

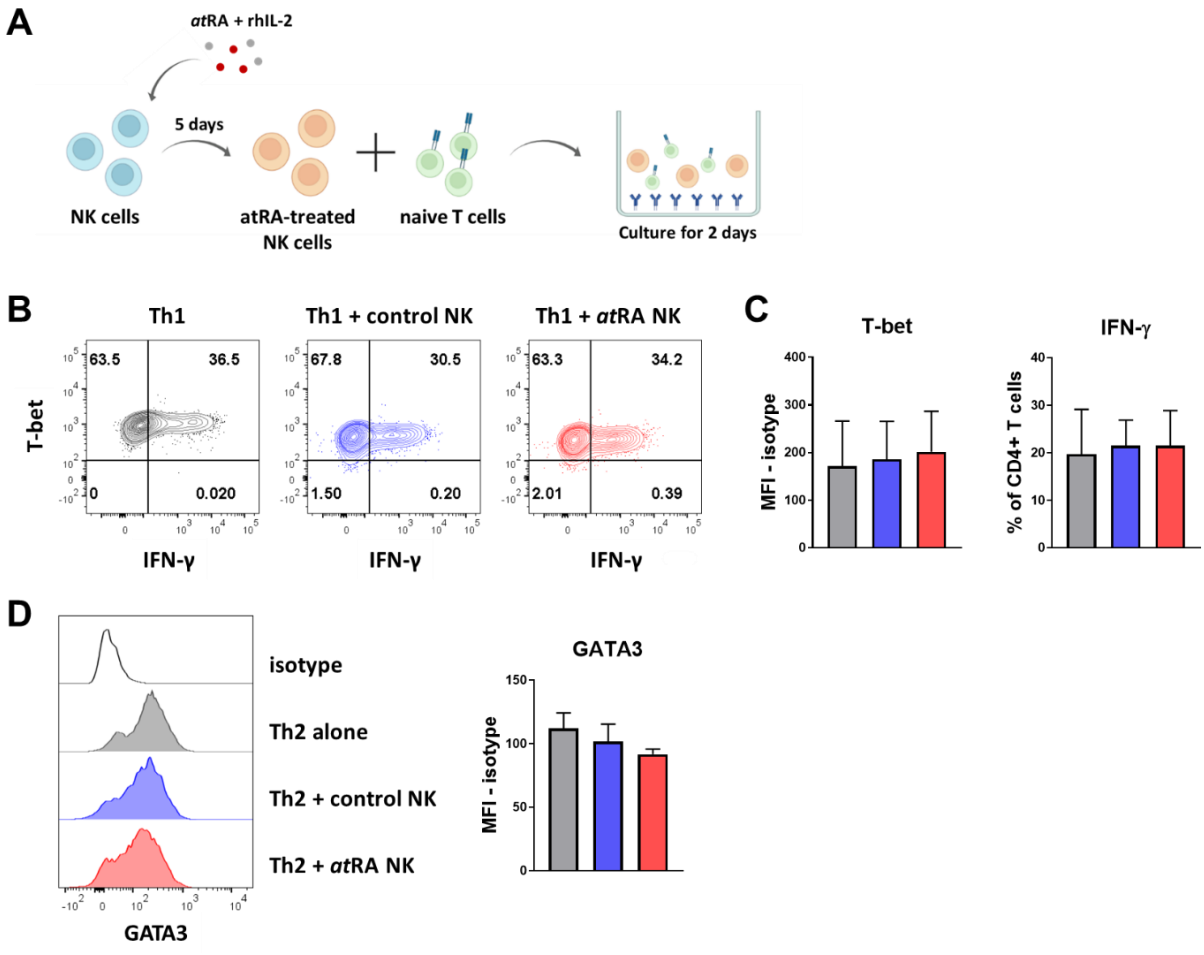

(Figure legend in the next page)

Figure 3.17. T_H1 and T_H2 cell polarization in the presence of control- or *at*RA-treated NK cells. CD45.1$^+$ NK cells pre-treated with *at*RA or control solvent were co-cultured with freshly-isolated naïve CD45.2$^+$CD4$^+$ T cells in T_H1- or T_H2-polarizing conditions in the presence of plate-bound anti-CD3ε antibody and soluble anti-CD28 antibody for 2 days. 50 ng/mL of PMA and 1µM of Ionomycin were added to the last 4 hours of co-culture. Cells were analyzed by flow cytometry, and T cells were gated as live, CD45.1$^-$, CD45.2$^+$, and CD4$^+$ cells. (A) Schematic illustration depicting the co-culture of naïve CD4$^+$ T cells and NK cells (Created with BioRender.com). (B) Representative contour-plots and (C) quantification of T-bet and IFN-γ expression of CD4$^+$ T cells in T_H1-polarizing condition (n=3). (D) Representative histogram and quantification of GATA3 expression of CD4$^+$ T cells in T_H2-polarizing conditions (n=3). Graphs indicate mean ± SEM.

CD4$^+$ cells exposed to cytokines IL-1b, IL-6, IL-23, and TGFβ in T_H17-polarizing condition, displayed RORγt expression (Figure 3.18A). The frequency of RORγt-expressing T cells was not changed in the presence of control- or *at*RA-treated NK cells (Figure 3.18B). The percentage of FoxP3-expressing cells was comparable in CD4$^+$ T cells cultured alone or co-cultured with control NK cells (Figure 3.18B). In the presence of *at*RA-treated NK cells, the percentage of FoxP3-expressing CD4$^+$ T cells was significantly increased (Figure 3.18B). Furthermore, CD4$^+$ T cells released pro-inflammatory cytokines IL-17A and IL-17F, when polarized to T_H17 phenotype, and in the presence of control- or *at*RA-treated NK cells, the production of IL-17A and IL-17F was not detected in CD4$^+$ T cells (Figure 3.18C).

In Treg-polarizing condition, CD4$^+$ cells were cultured in the presence of IL-2 and TGF-β. The proportion of T cells expressing FoxP3 was higher in Treg-polarizing condition, compared to T_H17-polarizing condition (Figure 3.18A and D). The frequency of FoxP3-expressing T cells was decreased in the presence of control NK cells (Figure 3.18D). However, the frequency of FoxP3-expressing T cells was significantly upregulated in the presence of *at*RA-treated NK cells (Figure 3.18D and E). FoxP3-expressing T cells co-expressed RORγt in Treg-polarizing condition and the expression of RORγt was decreased in the presence of control or *at*RA-treated NK cells (Figure 3.18D and E). Altogether, these results indicate that *at*RA-treated NK cells can support or maintain regulatory phenotype of CD4$^+$ T cells.

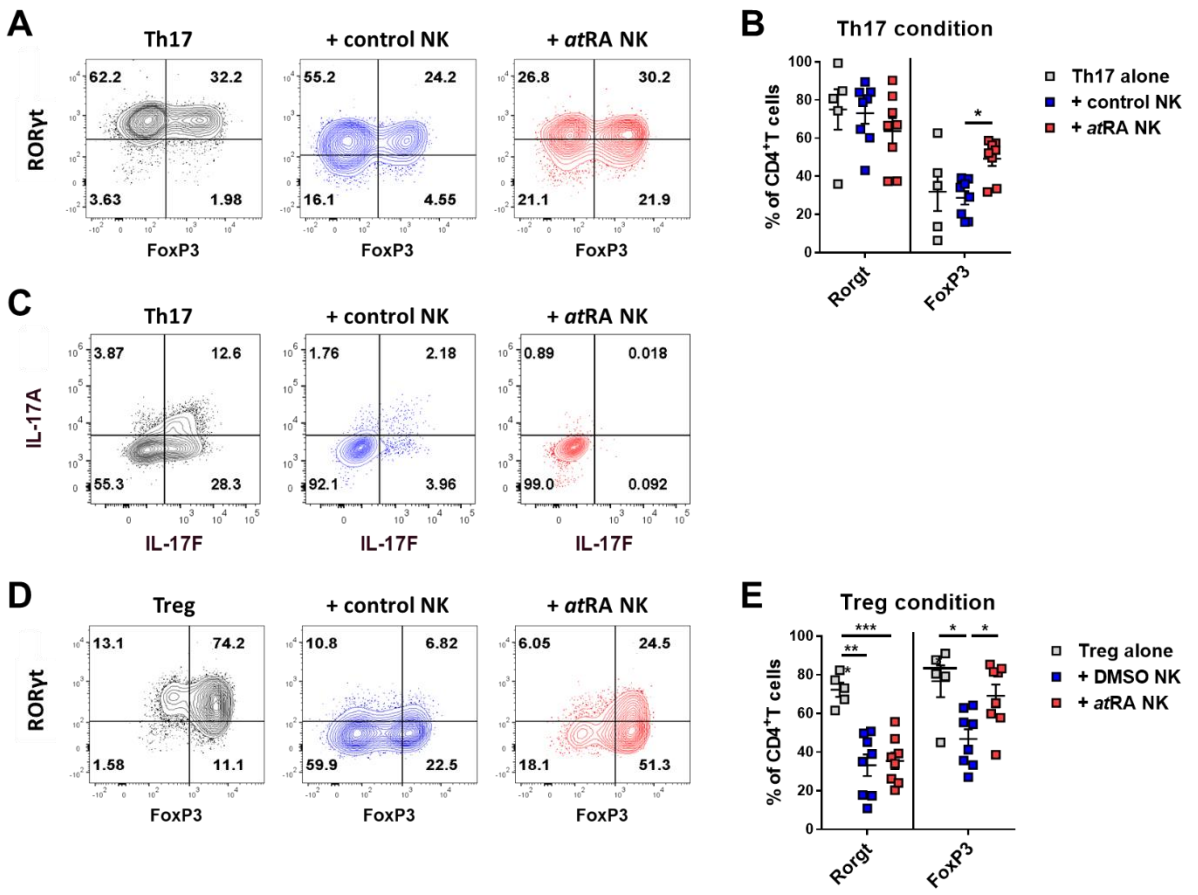

Figure 3.18. RORγt and FoxP3 expression in cells polarized in T_H17- or Treg- conditions in the presence of control- or *at*RA-treated NK cells. (A-E) CD45.1$^+$ NK cells pre-treated with *at*RA or control solvent were co-cultured with freshly-isolated naïve CD45.2$^+$CD4$^+$ T cells in T_H17- or Treg-polarizing conditions in the presence of plate-bound anti-CD3ε antibody and soluble anti-CD28 antibody for 2 days. For the analysis of cytokine production, 50 ng/mL of PMA and 1µM of Ionomycin were added to the last 4 hours of co-culture. Cells were analyzed by flow cytometry and gated as live, CD45.1$^-$, CD45.2$^+$, and CD4$^+$ cells. (A) Representative contour-plots and (B) quantification of RORγt- or FoxP3-expressing CD4$^+$ T cells in T_H17-polarizing conditions (n=5-8). (C) Representative contour-plots of IL-17A- and IL-17F-producing CD4$^+$ T cells in T_H17-polarizing conditions. (D) Representative contour-plots and (E) quantification of RORγt- or FoxP3-expressing CD4$^+$ T cells in Treg-polarizing conditions (n=5-8). Graphs indicate mean ± SEM. *, p<0.05; ***, p<0.001 by one-way ANOVA (Tukey's multiple comparisons test).

4.3.2.3 Mechanism of enhanced FoxP3 expression in CD4$^+$ T cells in the presence of *at*RA-treated NK cells

To dissect how *at*RA-treated NK cells could support FoxP3-expressing CD4$^+$ T cells, we first performed co-culture of NK cells and CD4$^+$ T cells using a transwell system, which could block direct cell-to-cell contacts. In T_H17-polarizing condition, the percentage of FoxP3-expressing T cells was increased in the presence of *at*RA-treated NK cells, compared to co-culture with control NK cells (Figure 3.19A). Prevention of cell-to-cell contacts did not affect the percentage of FoxP3-expressing T cells (Figure 3.19A and C). These data indicate that the effect of *at*RA-treated NK cells was contact-independently regulated.

In Treg-polarizing condition, the percentage of FoxP3-expressing CD4$^+$ T cells was lower in the presence of control NK cells, compared to T cells cultured alone (Figure 3.19B). When cell-to-cell contacts were prevented, the frequency of FoxP3-expressing CD4$^+$ T cells in the presence of control NK cells was increased (Figure 3.19B and D), which indicates that the effect of control NK cells required direct contacts between cells. In the presence of *at*RA-treated NK cells, the frequency of FoxP3-expressing T cells was significantly increased, compared to co-culture with control NK cells (Figure 3.19D). Prevention of cell-to-cell contacts did not change this frequency. These data imply that *at*RA-treated NK cells could support FoxP3 expression in T cells in a contact-independent manner.

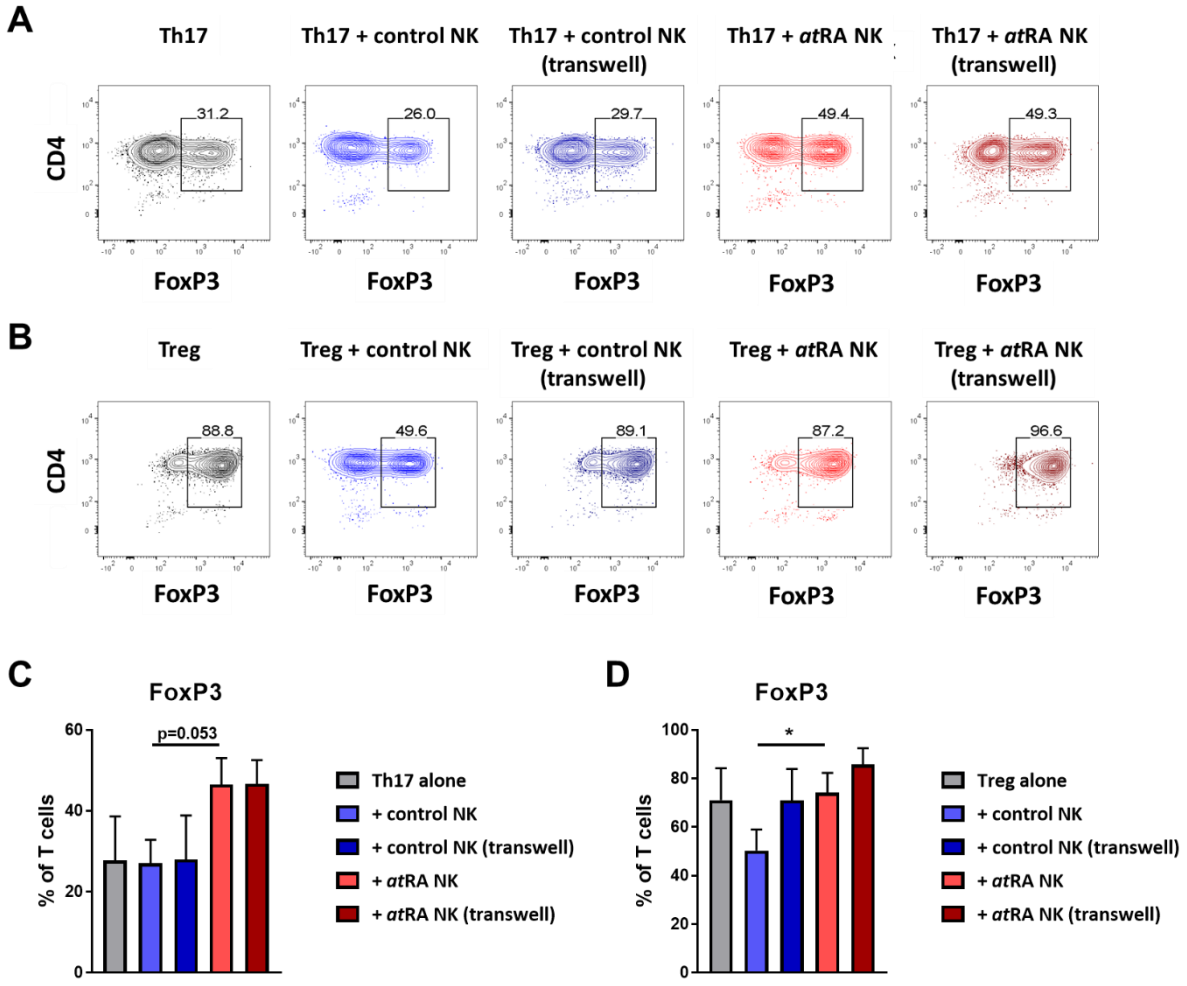

Figure 3.19. *at*RA-treated NK cells support Treg cell differentiation in a contact-independent manner. CD45.1$^+$ NK cells pre-treated with *at*RA or control solvent were co-cultured with freshly-isolated naïve CD45.2$^+$CD4$^+$ T cells in T_H17- or Treg-polarizing conditions in the presence of plate-bound anti-CD3ε antibody and soluble anti-CD28 antibody for 2 days. In certain conditions (transwell), transwell inserts were applied to separate naïve CD4$^+$ T cells and NK cells. NK cells were seeded into the upper chamber of transwell inserts. Cells were analyzed by flow cytometry and T cells were gated as live, CD45.1$^-$, CD45.2$^+$, and CD4$^+$ cells (A-B) Representative contour-plots of FoxP3 expression by CD4$^+$ T cells in (A) T_H17-polarizing and (B) Treg-polarizing conditions co-cultured with NK cells. (C-D) Quantification of FoxP3-expressing CD4$^+$ T cells in (C) T_H17-polarizing and (D) Treg-polarizing conditions upon culture alone, or co-culture with control or *at*RA-treated NK cells (n=3). Graphs indicate mean ± SEM. *, p<0.05 by one-way ANOVA (Tukey's multiple comparisons test).

To uncover which molecules secreted by *at*RA-treated NK cells support FoxP3 expression in $CD4^+$ T cells, we examined several candidates that were reported to regulate FoxP3 expression. One candidate was adenosine, which was reported to support Treg polarization and proliferation (Ohta & Sitkovsky, 2014). The expression of adenosine ectoenzymes, CD73, CD39 and CD38, was enhanced by *at*RA-treatment in NK cells (Figure 3.2C), demonstrating the potential production of adenosine by *at*RA-treated NK cells. Among four isoforms of adenosine receptors, mRNA expression of adenosine A_{2A} receptor (A2AR) was highest in T_H17- and Treg-polarized $CD4^+$ T cells (Figure 3.20A). To block the binding of A2AR and adenosine, we used two A2AR antagonists (ZM 241385 and SCH 58261) that were added to co-culture of $CD4^+$ T cells and NK cells. The presence of A2AR antagonists did not affect FoxP3 expression in $CD4^+$ T cells co-cultured with *at*RA-treated NK cells (Figure 3.20B). The next candidate was IL-10, which was reported to promote FoxP3 expression in T cells (Hsu et al., 2015). In addition, human ILC2s treated with *at*RA-treatment *in vitro* produced IL-10 (Morita et al., 2019). Thus, we hypothesized that IL-10 could be secreted by *at*RA-treated NK cells. IL-10 neutralization using anti-IL-10 antibody did not influence FoxP3 expression in $CD4^+$ T cells (Figure 3.20C). Additionally, results obtained from mRNA-expression analysis revealed that *at*RA increased Ccl1 and Ccl5 expression by NK cells (Figure 3.11A), implying the potential CCL1 or CCL5 production by *at*RA-treated NK cells. Chemokines CCL1 and CCL5 found in the gut and tumor microenvironment were shown to attract Treg cells (Kuehnemuth et al., 2018; Tan et al., 2009; X. Wang et al., 2017), and CCL1 neutralization during Treg-polarization reduced FoxP3 expression (Hoelzinger et al., 2010). Therefore, we added anti-CCL1 and anti-CCL5 antibodies during the co-culture of $CD4^+$ T cells and NK cells. Neutralization of CCL5 and CCL1 did not change FoxP3 expression by $CD4^+$ T cells (Figure 3.20D).

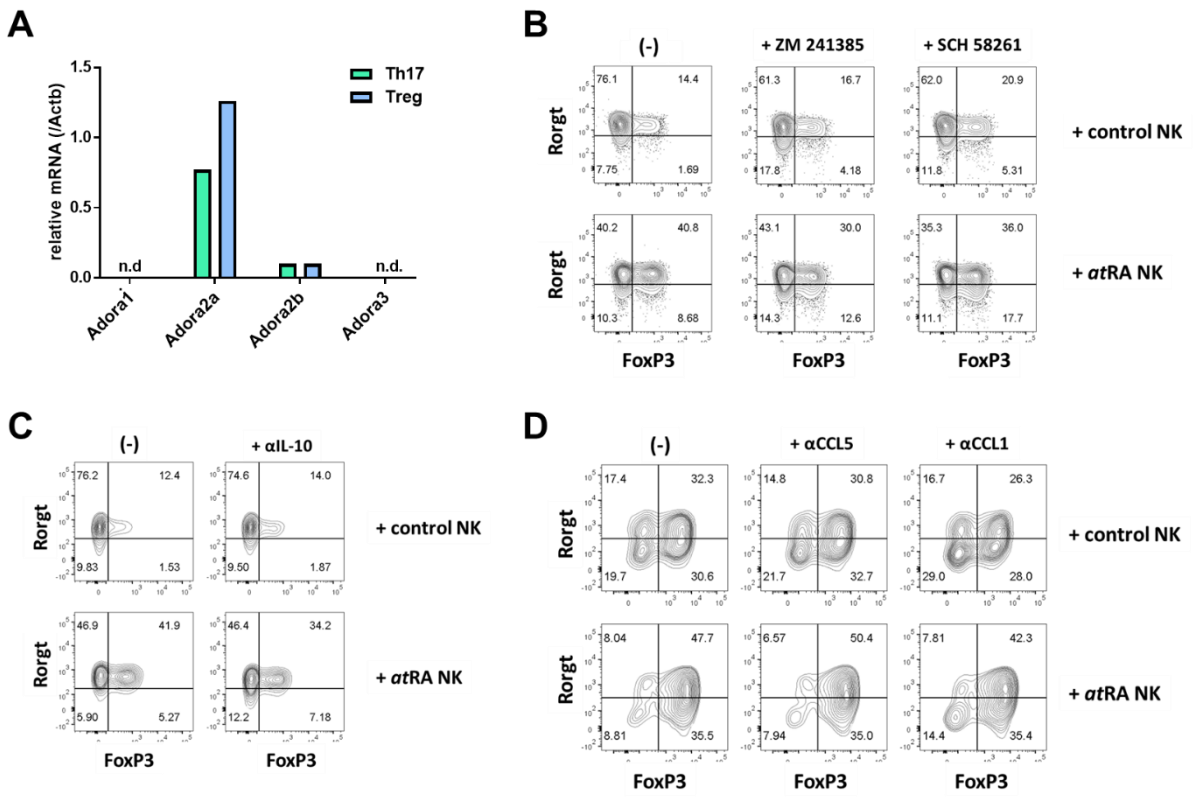

Figure 3.20. Inhibition of adenosine receptor, IL-10, CCL1, and CCL5 did not change FoxP3 expression by CD4$^+$ T cells co-cultureD with control NK cells or *at*RA-treated NK cells. (A) Naïve CD4$^+$ T cells were cultured in T$_H$17- or Treg-polarizing conditions, and mRNA expression of Adora1, Adora2a, Adora2b, and Adora3 in T$_H$17- or Treg-polarized CD4$^+$ T cells was analyzed by qRT-PCR. (B-D) CD45.1$^+$ NK cells pre-treated with *at*RA or control solvent were co-cultured with freshly-isolated naïve CD45.2$^+$CD4$^+$ T cells in T$_H$17-polarizing condition in the presence of plate-bound anti-CD3ε antibody and soluble anti-CD28 antibody for 2 days. 5 μM of adenosine receptor antagonists (ZM 241385 and SCH 58261), 7.5 μg/mL of anti-IL-10 antibody, 4 μg/mL of anti-CCL5 antibody, or 4 μg/mL of anti-CCL1 antibody were added during co-culture. Cells were analyzed by flow cytometry, and T cells were gated as live, CD45.1$^-$, CD45.2$^+$, and CD4$^+$ cells. Representative contour-plots showing the expression of FoxP3 and RORγt in T$_H$17 cells co-cultured with control- or *at*RA-treated NK cells in the presence of (B) adenosine receptor antagonists, (C) anti-IL-10 antibody, (D) anti-CCL5 antibody or anti-CCL1 antibody.

We could not identify the soluble factor produced by *at*RA-treated NK cells that could regulate FoxP3 expression in CD4$^+$ T cells; however, we hypothesized that *at*RA-treated NK cells could create microenvironment, which supported the proliferation of FoxP3-expressing T cells. Thus, we stained Ki67, a protein expressed during active phases of cell cycles, but not in resting cells, in order to analyze proliferation of CD4$^+$ T cells. In both T$_H$17- and Treg-polarizing conditions, the frequency of FoxP3$^+$Ki67$^+$ population was significantly increased, and the frequency of FoxP3$^-$Ki67$^+$ population was significantly reduced in co-culture with *at*RA-treated NK cells, compared to co-culture with control NK cells (Figure 3.21A and B). The amounts of FoxP3$^+$Ki67$^-$ T cells and FoxP3$^-$Ki67$^-$ T cells were comparable in the presence of control- or *at*RA-treated NK cells (Figure 3.21A).

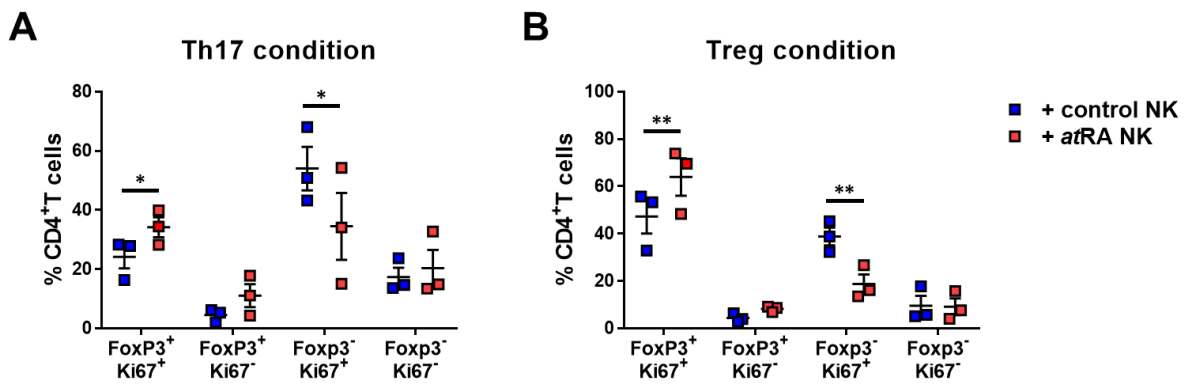

Figure 3.21. Increased proliferation of FoxP3$^+$ T cells supported by *at*RA-treated NK cells. CD45.1$^+$ NK cells pre-treated with *at*RA or control solvent were co-cultured with naïve CD45.2$^+$CD4$^+$ T cells in T_H17- or Treg-polarizing conditions in the presence of plate-bound anti-CD3ε antibody and soluble anti-CD28 antibody for 2 days. Cells were analyzed by flow cytometry, and T cells were gated as live, CD45.1$^-$, CD45.2$^+$, and CD4$^+$ cells. (A-B) Frequency of FoxP3$^+$Ki67$^+$ and FoxP3$^-$Ki67$^+$ CD4$^+$ T cells upon co-culture with control- or *at*RA-treated NK cells in (A) T_H17-polarizing condition (n=3) and (B) Treg-polarizing condition (n=3). Graphs indicate mean ± SEM. *, p<0.05; **, p<0.01 by paired Student's t-test.

4.4 Tumor microenvironment enriched with vitamin A metabolites

In addition to the digestive system, which is enriched with vitamin A metabolites (Kane et al., 2008), murine sarcoma tissues were reported to show high expression of Raldh (encoding retinaldehyde dehydrogenase, RALDH), compared to other tissues, and to promote RA-abundant tumor microenvironment (TME), which resulted in immune suppression through impairing tumor-associated macrophages (Devalaraja et al., 2020). NK cells can be recruited to tumor tissues, where they can recognize and eliminate tumor cells via receptor-ligand engagement (Vivier, Tomasello, Baratin, Walzer, & Ugolini, 2008). Thus, we hypothesized that a vitamin A-enriched TME could regulate the phenotype of NK cells.

4.4.1 Expression of RA-metabolizing enzymes by tumor cells

It was reported that mRNA expression of Raldh correlated with concentration of RA in tumor tissues (Devalaraja et al., 2020). Thus, we analyzed relative mRNA expression of RA-metabolizing enzymes in tumor cells, including B16 melanoma, Lewis lung carcinoma (LL2), MCA-induced fibrosarcoma (MCA 1956), and MC38 colon carcinoma. Relative expression of Raldh1 and Raldh3 was higher in B16 melanoma cells, compared to other tumor cells, while Raldh2 expression was not detected (Figure 3.22). These results suggest a potential RA-production by B16 melanoma cells.

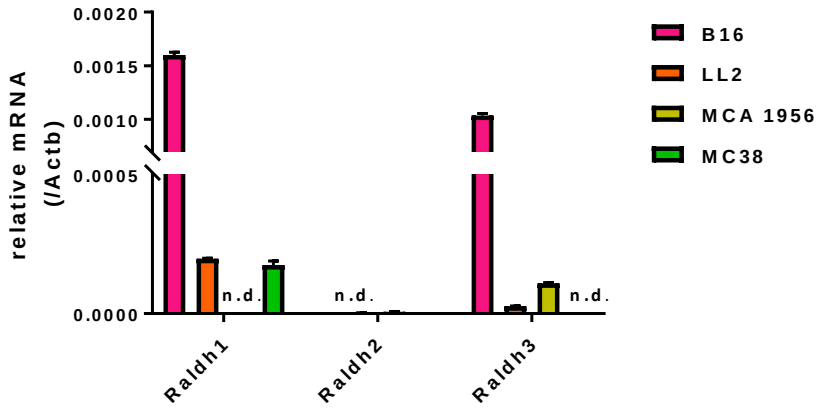

Figure 3.22. B16 melanoma cells express higher amounts of Raldh transcript, compared to other tumor cells. (A-B) Tumor cells were cultured in medium for one week (*in vitro*). RNA isolated from tumor cells was used to perform qRT-PCR analysis. Quantification of Raldh1, Raldh2 and Raldh3 relative expression of *in vitro* cultured tumor cells. Graph indicates mean ± SEM. Raldh, retinaldehyde dehydrogenase. B16, B16 melanoma; LL2, Lewis lung carcinoma; MCA 1956, MCA-induced fibrosarcoma; MC38, MC38 colon adenocarcinoma.

4.4.2 RA-signatures in liver, lung, lymph node and spleen

Next, we analyzed the “RA-signatures” in different organs in steady-state, such as liver, lung, mesenteric lymph node (mLN) and spleen, by analyzing mRNA expression of RA-receptors, genes involved in RA-metabolism, and target genes of retinoic acid receptors (RARs). We noted that transcription of RA-receptors and genes involved in RA-metabolism was enriched in the lung, compared to other organs (Figure 3.23A and B). Among target genes of RARs, relative expression of Efnb1, Plat, Hoxb4, Rara, Meis2, Egr1, Rarb, Rarg, Cyp26c1, and Hnf1b, was highest in the lung (Figure 3.23C). Relative expression of Dhrs9, Srebf1, Adh1, Apoa2 and Rbp4 was highest in the liver (Figure 3.23C), which is considered a main storage of vitamin A metabolites (Kane et al., 2008)

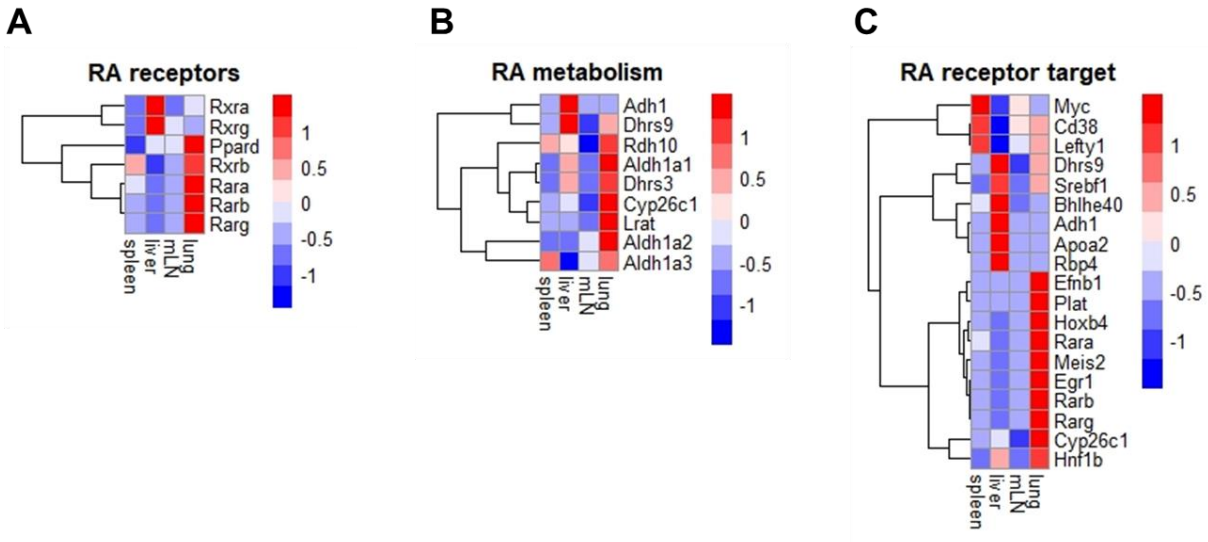

Figure 3.23. Relative expression of RA-receptors, genes involved in RA-metabolism, and target genes of RARs is enriched in the lung. (A-C) RNA isolated from the spleen, liver, mesenteric lymph node (mLN), and lung, was used for qRT-PCR analysis. Heatmaps illustrate the relative mRNA expression of (A) RA-receptors, (B) genes involved in RA-metabolism, and (C) target genes of RARs. Data are scaled per row. RA, retinoic acid; RAR, retinoic acid receptors; mLN, mesenteric lymph nodes.

4.4.3 Group 1 ILC phenotype in MCA-induced fibrosarcoma

A recent study reported that several types of sarcoma cells, including synovial sarcoma, undifferentiated pleomorphic sarcoma and fibrosarcoma cells, could release *at*RA in TME, leading to immunosuppressive effects of immune cells (Devalaraja et al., 2020). In addition, it was reported that NK cells in fibrosarcoma tumor tissues displayed an intermediate ILC1-like phenotype, characterized by the increased expression of TRAIL, CD49a, and CD69, and the decreased expression of CD62L and Eomes (Gao et al., 2017). Hence, we aimed to investigate whether MCA-induced fibrosarcoma could induce an intermediate ILC1-like phenotype of NK cells, in a vitamin A-dependent manner.

As described in Gao et al. (Gao et al., 2017), MCA-induced fibrosarcoma (MCA1956) was subcutaneously injected to C57BL/6N mice. Compared to PBS-injected mice, MCA1956-bearing mice displayed comparable weights of liver, and higher weights of spleens (Figure 3.24B). Group 1 ILCs were gated as $CD45^+CD3\varepsilon^-NK1.1^+NKp46^+$ cells. Two subpopulation of group 1 ILCs were identified, $Eomes^+$ NK cells (NK cells) and $Eomes^-$ ILC1s (ILC1s) (Figure 3.24C). Based on the flow cytometric results shown in Figure 3.2, we selected candidate proteins and assessed their expression in NK cells and ILC1s in the TME. As an internal control, group 1 ILCs in liver were analyzed. The expression of CD49a, CD39, CD160, CD38, CD200R, and CXCR6 was higher in liver ILC1s, compared to liver NK cells, tumor NK cells and tumor ILC1s (Figure 3.24D). T-bet expression was comparable in both liver NK cells and ILC1s, which was higher than the expression in tumor NK cells and ILC1s (Figure 3.24D). Tumor NK cells displayed higher expression of Eomes, RANKL and IRF8 than other analyzed cell populations (Figure 3.24D). NK cells and ILC1s in tumor tissues shared similarities in protein expression, for instance the higher expression of NKG2D, CD96, NK1.1, CD61, CD69, CD27, and CXCR3, compared to NK cells and ILC1s in livers. However, based on our analysis, NK cells did not display an intermediate ILC1-like phenotype in fibrosarcoma tumor tissues.

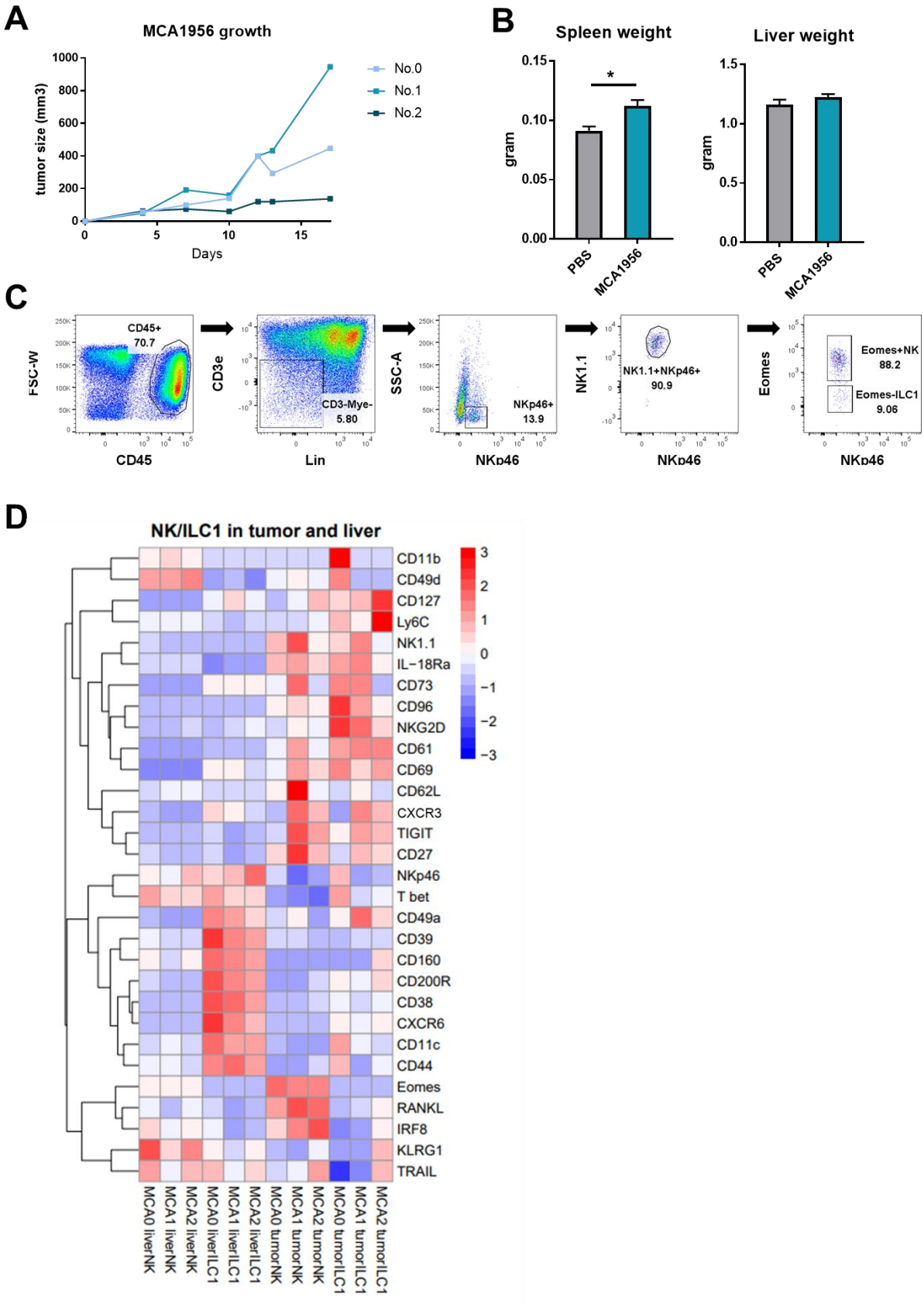

Figure 3.24. The growth of MCA1956 tumor and the phenotype of group 1 ILCs in tumor-tissue and liver. MCA-induced fibrosarcoma (MCA1956, 1 x 10^6 cells/100 µL) was subcutaneously injected into C57BL/6N mice (female, 8 weeks old, n=3), and the equivalent volume of PBS was injected as control solvent to mice (female, 8 weeks old, n=3). (A) Quantification of tumor growth. (B) Spleen and liver weight (n=3). (C) Single-cell suspensions were prepared from the collected tumor tissues and livers. Group 1 ILCs were analyzed by flow cytometry, and

gated as live, CD45$^+$, CD3ε$^-$, lineage$^-$, NK1.1$^+$, and NKp46$^+$ cells (For the lineage markers, Ly6G, F4/80, SiglecF, FcεRI, Ter119 and CD19 were used). Representative plots show the gating strategy of Eomes$^+$ NK cells and Eomes$^-$ ILC1s in tumor. (D) Heatmap depicts the geometric mean florescence intensity (MFI) of CD11b, CD49d, CD127, Ly6C, NK1.1, IL-18Rα, CD73, CD96, NKG2D, CD61, CD69, CD62L, CXCR3, TIGIT, CD27, NKp46, T-bet, CD49a, CD39, CD160, CD200R, CD38, CXCR6, CD11c, CD44, Eomes, RANKL, IRF8, KLRG1, and TRAIL in liver NK cells, liver ILC1s, tumor NK cells and tumor ILC1s of MCA1956-injected mice. Data are scaled per row. Graphs indicate mean ± SEM. *, $p<0.05$ by non-paired Student's t-test.

4.4.4 NK cell phenotype in B16 melanoma tumors

We observed enriched "RA-signatures" in lung (Figure 3.23), and the highest expression of Raldh1 in B16 melanoma cells (Figure 3.22), which might correlate with their ability to produce RA. To create a vitamin A-enriched TME, we utilized animal model of lung metastasis, and investigated how this microenvironment could affect tumor-infiltrating NK cell phenotype. Body weight, lung weight, and spleen weight were comparable in PBS-injected and B16 lung metastases-bearing mice (Figure 3.25A). Group 1 ILCs (CD45$^+$ CD3ε$^-$ NK1.1$^+$ NKp46$^+$ cells) comprised mainly Eomes$^+$ NK cells in lungs (Figure 3.25C), and the absolute number of NK cells in the lung from tumor-bearing mice was comparable to PBS-injected mice (Figure 3.25B).

Based on the flow cytometric analysis in Figure 3.2 and the intermediate ILC1-like phenotype demonstrated in Gao et al. (Gao et al., 2017), we chose several proteins and examined their expression in lung NK cells of B16-bearing and PBS-injected mice. DNAM-1, CD200R, CD38, CD49a, TRAIL, CD160, and TIGIT expression was not detected, and the expression of CD73, CD39, CD49d, IL-18Rα, CD62L, and CD96 was similar in NK cells from control lungs and tumor-bearing lungs (Figure 3.25D). Compared to lung NK cells from PBS-injected mice, the expression of KLRG1, an inhibitory receptor, was downregulated in NK cells from tumor-bearing mice (Figure 3.25D). These data indicate that the TME of B16 melanoma metastases did not induce an ILC1-like phenotype in lung NK cells.

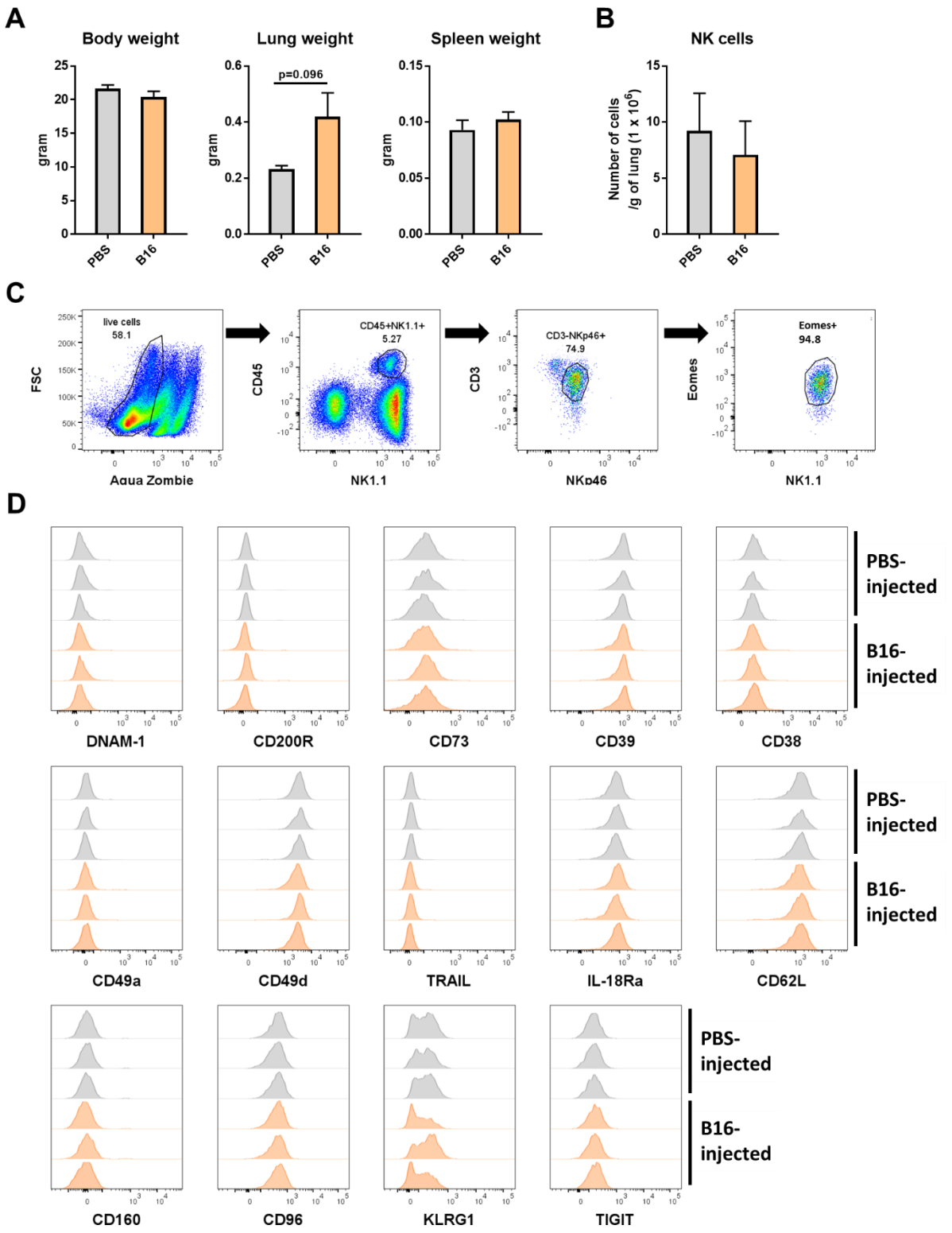

Figure 3.25. Number and phenotype of NK cells in B16 melanoma metastases-bearing lungs. B16 melanoma cells (1 x 10^5/100 µL) or the equivalent volume of PBS (as a control) were intravenously injected into C57BL/6N mice (female, 10 weeks old, n=3 for each group). After 21 days of tumor-injection, single-cell suspensions were prepared from lungs and analyzed by flow cytometry. NK cells were gated as live, CD45$^+$, CD3ε$^-$, lineage$^-$, NK1.1$^+$, NKp46$^+$, and Eomes$^+$ cells (For the lineage markers, Ly6G, F4/80, SiglecF, FcεRI, Ter119 and CD19 were used). (A) Quantification of body, lung and spleen weights. (B) Absolute number of NK cells in lungs. (C) Representative plots of gating strategy of NK cells in lungs. (D) Histogram plots depict the expression of DNAM-1, CD200R, CD73, CD39, CD38, CD49a, CD49d, TRAIL, IL-18Rα, CD62L, CD160, CD96, KLRG1 and TIGIT in lung NK cells from PBS-injected mice (in gray color, n=3) and B16-bearing mice (in orange color, n=3). Graphs indicate mean ± SEM. Statistical analysis was performed by non-paired Student's t-test.

4.5 PPARγ as regulators of *at*RA-induced NK cell reprogramming

We observed that Pparg expression was increased in NK cells upon *at*RA-treatment (Figure 3.4A and B), and the enhanced DNAM-1 and CD200R expression in *at*RA-treated NK cells was partially prevented by the inhibition of PPARγ (Figure 3.7B and C). Thus, we hypothesized that PPARγ might be a key regulator of *at*RA-induced reprogramming in NK cells. Thus, we generated mice with a conditional deletion of PPARγ in NKp46-expressing cells, by crossing $Ncr1^{iCre}$ mice with $PPAR\gamma^{f/f}$ mice. In this thesis, we will call $Ncr1^{iCreTg}$ $PPAR\gamma^{f/f}$ mice as PPARγ cKO, and $PPAR\gamma^{f/f}$ mice as PPARγ flox.

4.5.1 Phenotype of PPARγ-deficient ILCs

NKp46-expressing cells, mainly NK cells, ILC1s and ILC3s, are found in the lung, liver and gut, where “RA-signatures” are enriched (Figure 3.23), vitamin A metabolites are stored (Kane et al., 2008), and vitamin A is metabolized (Erkelens & Mebius, 2017). To investigate the impact of PPARγ deletion in NKp46-expressing cells, we analyzed the numbers and phenotype of these cells in the lung, liver and gut, as well as spleen of PPARγ cKO and PPARγ flox mice. Two males and one female mouse in each group were taken for analysis.

First, we examined spleens and showed that the weights of spleens were comparable between PPARγ flox mice and PPARγ cKO mice (Figure 3.26A). In the spleen, $Eomes^{+}$ NK cells were identified as a major population of group 1 ILCs, and comprised 2% of CD45-expressing immune cells (Figure 3.26C and D). PPARγ deletion did not affect the number and percentage of splenic NK cells among immune cells (Figure 3.26B and C). Based on the flow cytometric analysis shown in Figure 3.2, several molecules were selected and measured in splenic NK cells from PPARγ flox and PPARγ cKO mice. The expression of DNAM-1, CD200R, TRAIL, CD73, CD39, CD11b, CD62L, CD127, CD160, IL-18Rα, and KLRG1, was similar in the two groups (Figure 3.26D), suggesting that PPARγ deletion did not cause differences in the phenotype of splenic NK cells.

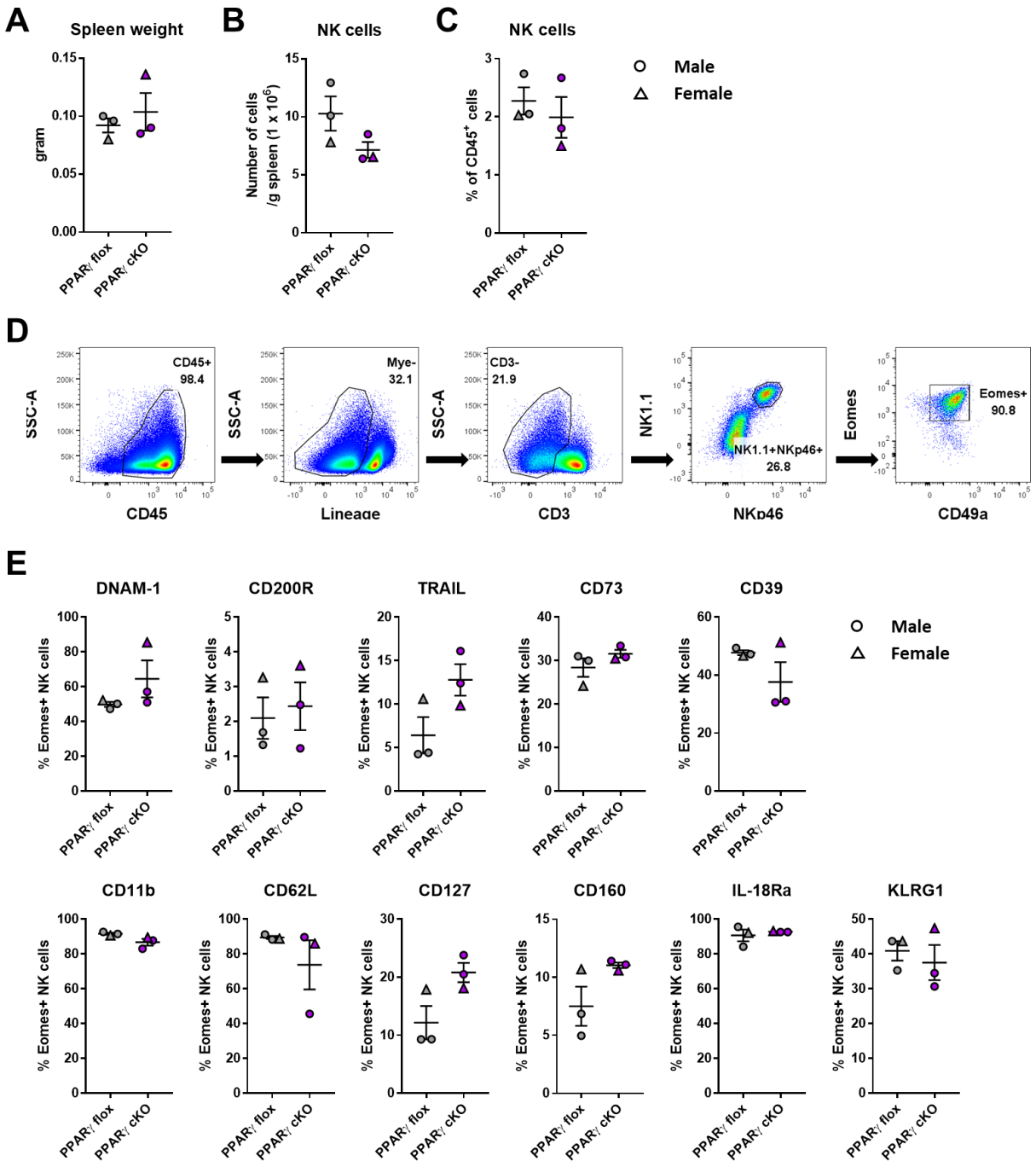

Figure 3.26. Splenic NK cell number and phenotype in PPARγ flox mice and PPARγ cKO mice. Spleens were collected from PPARγ flox mice (PPARγ$^{f/f}$ mice) and PPARγ cKO mice (Ncr1^{iCreTg} PPARγ$^{f/f}$ mice) (Male mice, depicted as a circle mark in the graphs, and female mice, depicted as a triangle mark in the graphs, 11-13 weeks old, n=3 for each group). Single-cell suspension was prepared from spleens of PPARγ flox and PPARγ cKO mice, and analyzed by flow cytometry. NK cells were gated as live, CD45$^+$, CD3ε$^-$, lineage$^-$, NK1.1$^+$, NKp46$^+$, and Eomes$^+$ cells (For the lineage markers, CD19, Ly6G, and Ter119 were used). (A) Quantification of spleen weight. (B) Absolute number and (C) percentage of NK cells in the spleen. (D) Representative dot plots show the gating strategy of Eomes$^+$ NK cells in the spleen. (E) Percentage of cells expressing DNAM-1, CD200R, TRAIL, CD73, CD39, CD11b, CD62L, CD127, CD160, IL-18Rα, and KLRG1 in spleens from PPARγ flox and PPARγ cKO mice. Graphs indicate mean ± SEM.

Next, we analyzed livers, which play important roles in metabolism and storage of vitamin A and its metabolites. PPARγ deletion did not cause differences in liver weight (Figure 3.27A). Hepatic group 1 ILCs comprise Eomes$^+$ NK cells and CD49a$^+$ ILC1s. In livers, both the number of NK cells and ILC1s, and the percentage of NK cells and ILC1s among CD45-expressing cells were comparable between PPARγ flox mice and PPARγ cKO mice (Figure 3.27B and C). Liver CD49$^+$ ILC1s displayed higher expression of CD73, CD39, CD38, DNAM-1, CD200R, TRAIL, CD127 and CXCR3, compared to Eomes$^+$ NK cells. On the other hand, Eomes$^+$ NK cells displayed higher expression of CD62L, KLRG1, IL-18Rα and CD11b, compared to CD49$^+$ ILC1s. The phenotype of liver ILC1s and NK cells was similar between PPARγ flox mice and PPARγ cKO mice (Figure 3.27D), indicating that PPARγ deletion did not modulated the expression of these proteins.

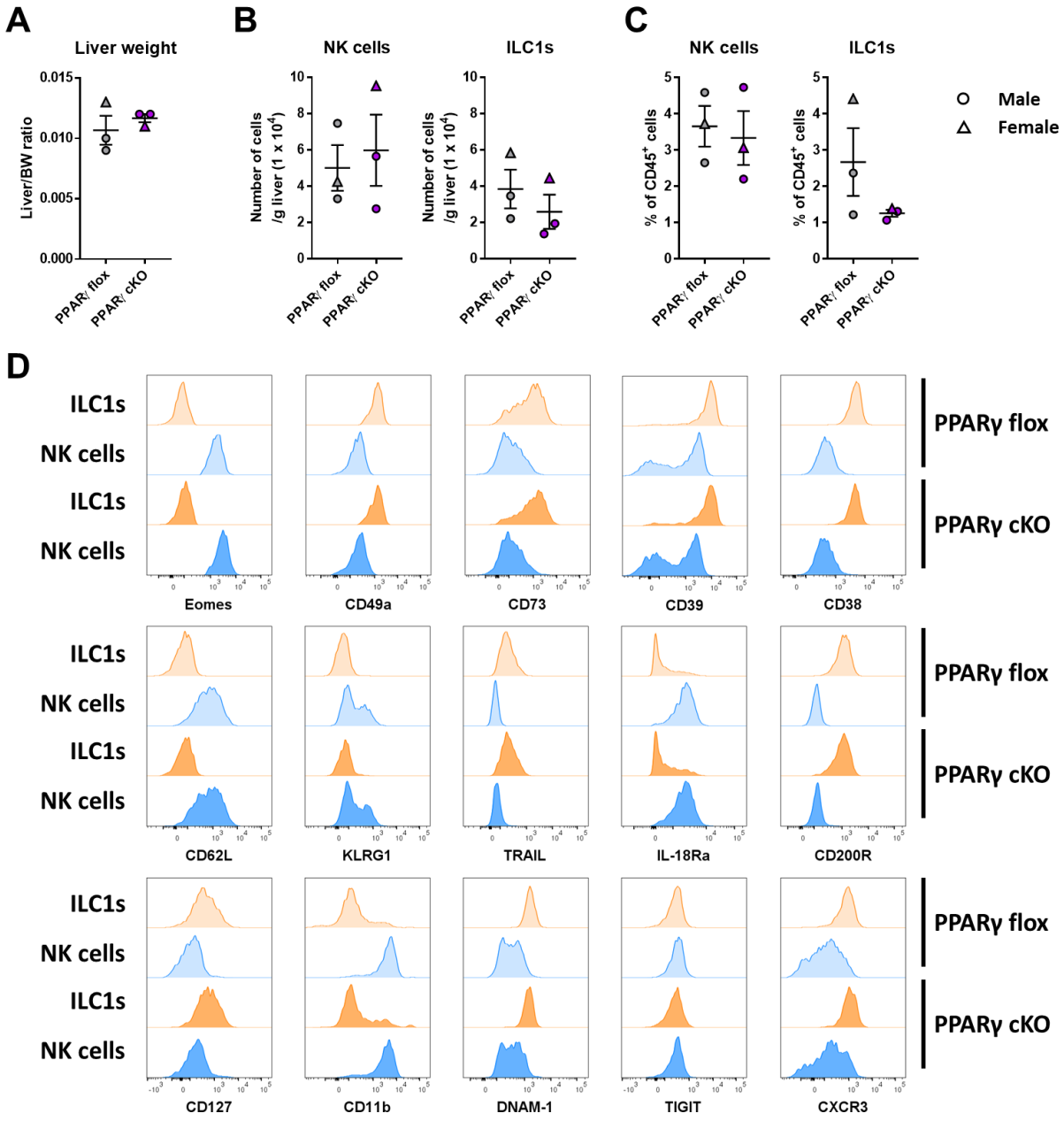

(Figure legend in the next page)

Figure 3.27. Hepatic ILC1 and NK cell number and phenotype in PPARγ flox mice and PPARγ cKO mice. Livers were collected from PPARγ flox mice (PPARγ$^{f/f}$ mice) and PPARγ cKO mice (Ncr1^{iCreTg} PPARγ$^{f/f}$ mice) (Male mice, depicted as a circle mark in the graphs, and female mice, depicted as a triangle mark in the graphs, 11-13 weeks old, n=3 for each group). Single-cell suspension was prepared from livers of PPARγ flox mice and PPARγ cKO mice, and analyzed by flow cytometry. Group 1 ILCs were gated as live, CD45$^+$, CD3ε$^-$, lineage$^-$, NK1.1$^+$, and NKp46$^+$ cells (For the lineage markers, CD19, Ly6G, and Ter119 were used). NK cells were gated Eomes$^+$ and CD49a$^-$, and ILC1s were gated CD49a$^+$ and Eomes$^-$. (A) Quantification of liver weight. (B) Absolute cell number of NK cells and ILC1s in the liver. (C) Percentage of NK cells and ILC1s among CD45-expressing cells. (D) Representative histograms show Eomes, CD49a, CD73, CD39, CD38, CD62L, KLRG1, TRAIL, IL-18Rα, CD200R, CD127, CD11b, DNAM-1, TIGIT, and CXCR3 expression in hepatic ILC1s and NK cells from PPARγ flox and PPARγ cKO mice. Graphs indicate mean ± SEM.

In a next step, we assessed lung, an organ enriched with “RA-signatures” (Figure 3.23). PPARγ deletion in NKp46-expressing cells did not induce differences of lung weights in mice (Figure 3.28A). We observed that the major population of group 1 ILCs in lungs are NK cells (Figure 3.28D). The number of NK cells and the percentage of NK cells among immune cells, gated as CD45-expressing cells, were similar in lungs of PPARγ cKO mice and PPARγ flox mice (Figure 3.28B). The expression of CD73, CD38, CD127, CXCR3, CD39, CD62L, KLRG1 and IL-18Rα was detected in lung NK cells (Figure 3.28E). Their expression by NK cells were comparable in lungs of PPARγ cKO mice and PPARγ flox.

Our results showed that the weights of spleen, lung, and liver did not show differences in PPARγ flox mice and PPARγ cKO mice. The number of NK cells in the spleen, lung or liver, and ILC1s in the liver, were similar in in PPARγ flox mice and PPARγ cKO mice. In addition, the phenotype of NK cells and ILC1s was not affected by the deletion of PPARγ.

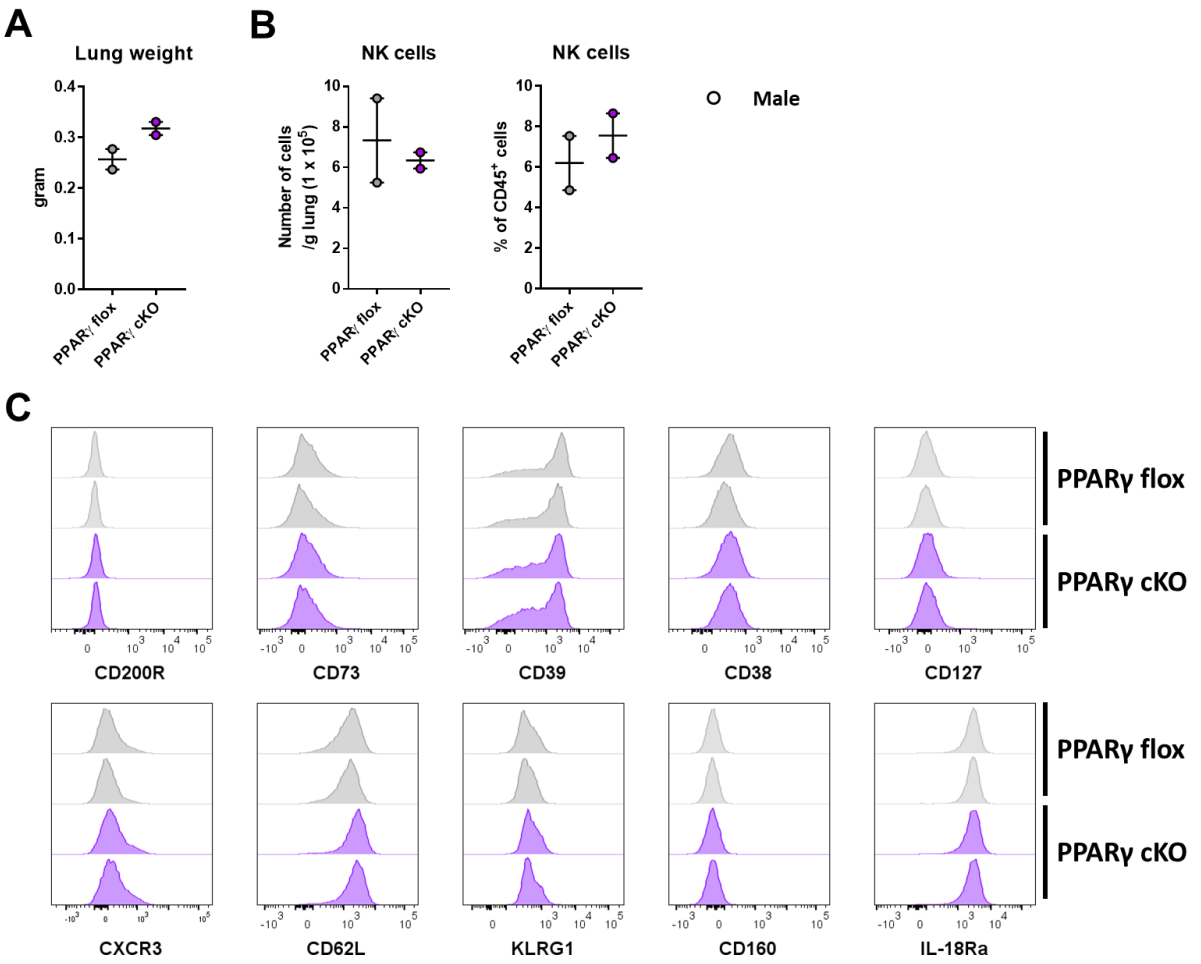

Figure 3.28. Lung NK cell number and phenotype in PPARγ flox mice and PPARγ cKO mice. Lungs were collected from PPARγ flox mice (PPARγ$^{f/f}$ mice) and PPARγ cKO mice (Ncr1^{iCreTg} PPARγ$^{f/f}$ mice) (Male mice, depicted as a circle mark in the graphs, 11-13 weeks old, n=3 for each group). Single cell suspension was prepared from lungs of PPARγ flox and PPARγ cKO mice, and analyzed by flow cytometry. NK cells were gated as live, CD45$^+$, CD3ε$^-$, lineage$^-$, NK1.1$^+$, NKp46$^+$, and Eomes$^+$ cells (For the lineage markers, CD19, Ly6G, and Ter119 were used). (A) Quantification of lung weight. (B) Absolute number and percentage of NK cells among CD45-expressing cells in the lung. (D) Representative dot plots show the gating strategy of Eomes$^+$ NK cells in the lung. (E) Quantification of CD200R, CD73, CD39, CD38, CD127, CXCR3, CD62L, KLRG1, CD160, and IL-18Rα expression in lung NK cells from PPARγ flox and PPARγ cKO mice. Graphs indicate mean ± SEM.

Lastly, we explored guts, where vitamin A precursors in food are oxidized and absorbed by intestinal epithelium (Oliveira, Teixeira, & Sato, 2018). In PPARγ flox mice and PPARγ cKO mice, we examined the weight of small intestine, the length of small and large intestine, and the number of Peyer's patches. PPARγ deletion in NKp46-expressing cells did not influence the weight and length of intestines, and the number of Peyer's patches (Figure 3.9A, B and C). The different subpopulation of tissue-resident ILCs are found in the small intestine. Thus, we analyzed the subsets of CD127-expressing ILCs, such as T-bet^{+} ILC1s (ILC1), GATA3^{+} ILC2s (ILC2), and RORγt^{+} ILC3s (ILC3) (gated in the blue frames in Figure 3.29D), and CD127^{-} NK cells and ILCs (gated in the red frames in Figure 3.29D).

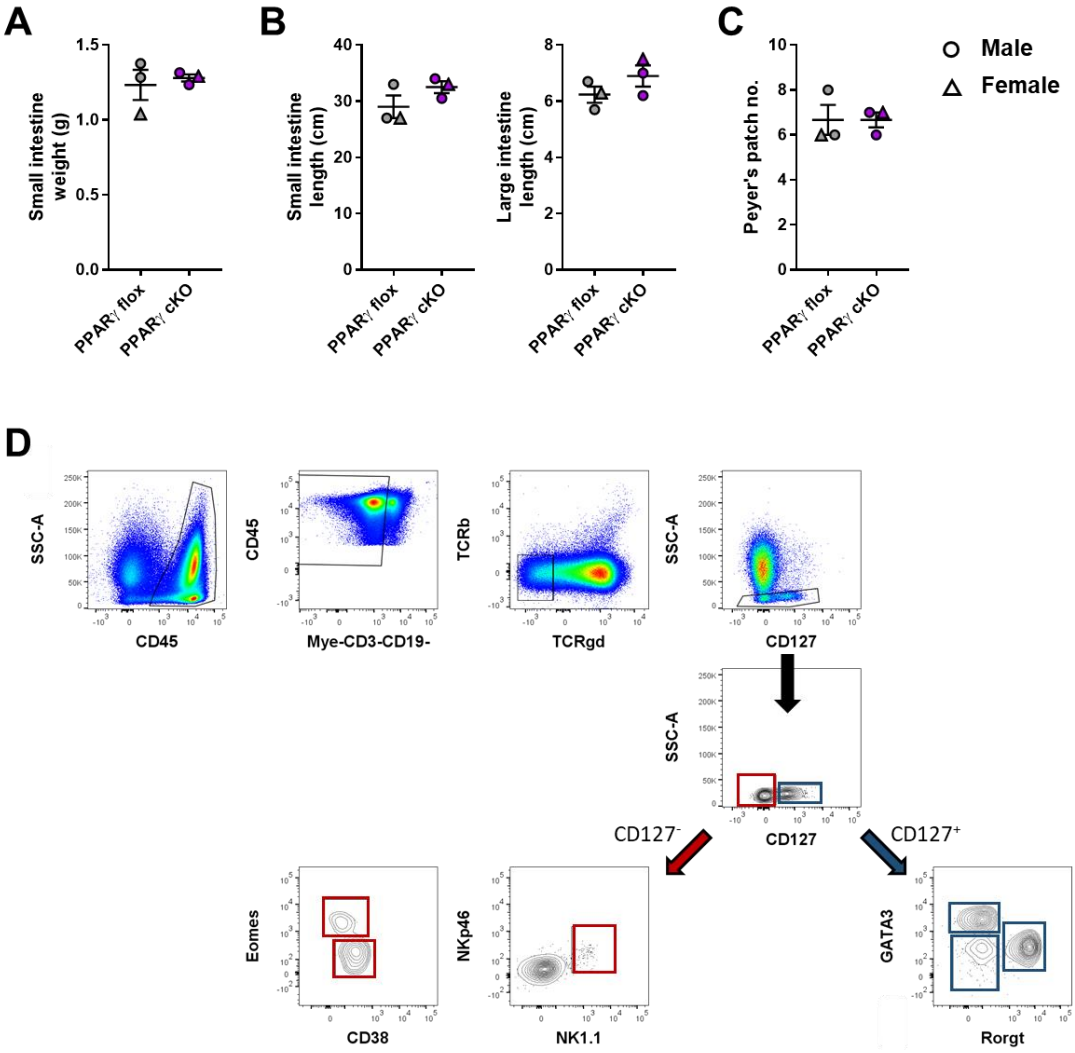

Figure 3.29. The phenotype of gut, and the gating strategy of ILCs in PPARγ flox mice and PPARγ cKO mice. Intestines were collected from PPARγ flox mice (PPARγ$^{f/f}$ mice) and PPARγ cKO mice (Ncr1^{iCreTg} PPARγ$^{f/f}$ mice) (Male mice, depicted as a circle mark in the graphs, and female mice, depicted as a triangle mark in the graphs, 11-13 weeks old, n=3 for each group). Single-cell suspension was prepared from guts of PPARγ flox and PPARγ cKO mice, and analyzed by flow cytometry. ILCs were gated as live CD45^{+}, CD3ε^{-}, CD19^{-}, Ly6G^{-}, Ter119^{-}, TCRβ^{-}, TCRγδ^{-}, and CD127^{+} cells. ILC1s were gated as RORγt^{-}, GATA3^{-}, and T-bet^{+} cells, ILC2s as GATA3^{+} cells, and ILC3s as RORγt^{+} cells. NK cells were gated as CD45^{+}, CD3ε^{-}, CD19^{-}, Ly6G^{-}, Ter119^{-} , TCRβ^{-}, TCRγδ^{-}, CD127^{-} , and Eomes^{+} cells. CD127^{-} ILCs were gated as CD45^{+}, CD3ε^{-}, CD19^{-}, Ly6G^{-}, Ter119^{-}, TCRβ^{-}, TCRγδ^{-}, CD127^{-}, and Eomes^{-} cells. (A) Small intestine weight, (B) small intestine and large intestine length, and (C) number of Peyer's patches in small intestine of PPARγ flox mice and PPARγ cKO mice. (D) Representative plots depict the gating strategy of CD127^{+} ILC1s, ILC2s, and ILC3s, and CD127^{-} NK cells and ILCs. Graphs indicate mean ± SEM.

CD127-expressing ILCs and CD127$^-$ NK cells and ILCs were analyzed in the three compartments of the small intestine, which are intraepithelial part, intestinal lamina propria and Peyer's patches. First, we analyzed the intraepithelial compartment and observed that the absolute number of RORγt$^+$ ILC3s was increased in the absence of PPARγ (Figure 3.30A). The number of ILC1s, ILC2s, CD127$^-$ NK cells, and CD127$^-$ ILCs were comparable between PPARγ flox mice and PPARγ cKO mice (Figure 3.30A and B). As we detected the elevated number of intraepithelial ILC3s, we investigated the three subpopulations of ILC3s. Figure 3.30C depicts the subpopulation of RORγt$^+$ ILC3s, including NKp46$^+$ CD4$^-$ ILC3s (NKp46$^+$ ILC3), NKp46$^-$ CD4$^-$ ILC3s (NKp46$^-$ ILC3), and CD4$^+$ LTi (LTi) cells. The absolute number of NKp46$^-$ ILC3 was significantly increased and contributed to the elevated number of RORγt$^+$ ILC3s (Figure 3.30D).

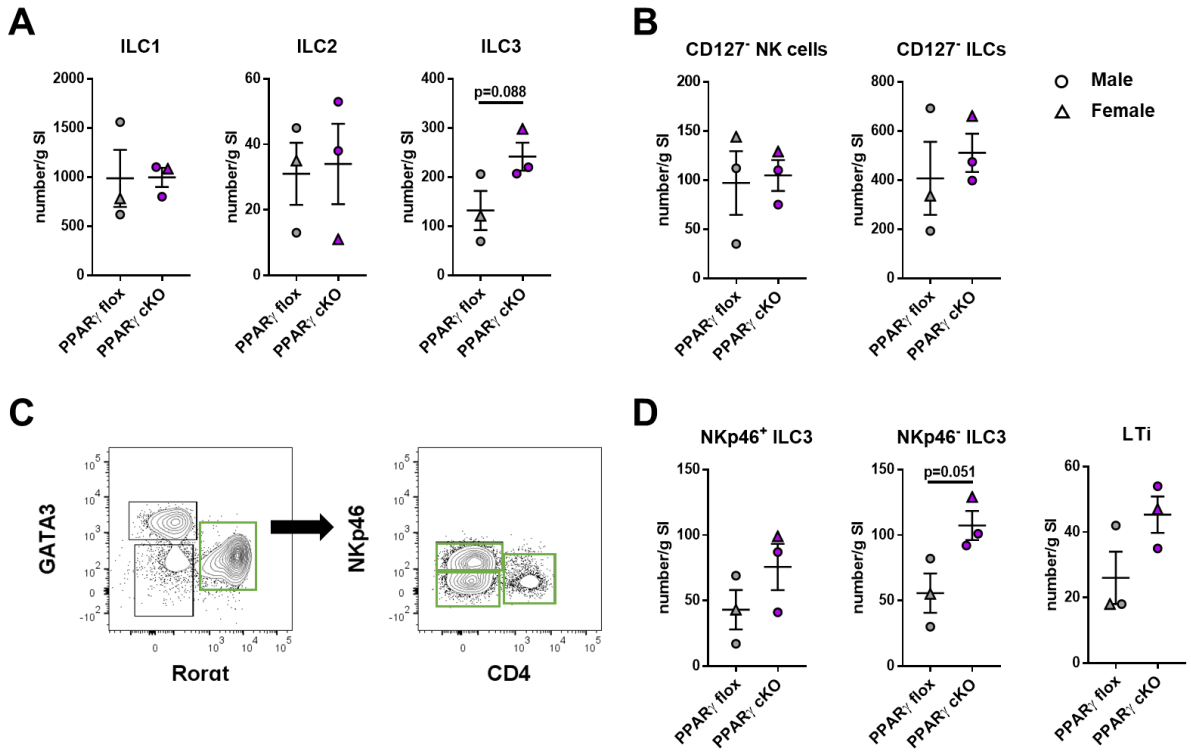

Figure 3.30. Absolute number of ILCs in the intraepithelial compartment of PPARγ flox mice and PPARγ cKO mice. Intestines were collected from PPARγ flox mice (PPARγ$^{f/f}$ mice) and PPARγ cKO mice (Ncr1^{iCreTg} PPARγ$^{f/f}$ mice) (Male mice, depicted as a circle mark in the graphs, and female mice, depicted as a triangle mark in the graphs, 11-13 weeks old, n=3 for each group). ILCs were analyzed by flow cytometry and gated as live CD45$^+$, CD3ε$^-$, CD19$^-$, Ly6G$^-$, Ter119$^-$, TCRβ$^-$, and TCRγδ$^-$ cells. (A) Absolute number of CD127$^+$ ILC1s, ILC2s, and ILC3s. (B) Absolute number of CD127$^-$ NK cells and ILCs. (C) Representative contour plots display a gating strategy of intraepithelial ILC3 subpopulations. (D) Absolute number of NKp46$^+$ ILC3s (gated CD127$^+$, RORγt$^+$, NKp46$^+$ and CD4$^-$ cells), NKp46$^-$ ILC3s (gated CD127$^+$, RORγt$^+$, NKp46$^-$ and CD4$^-$ cells), and LTi cells (gated CD127$^+$, RORγt$^+$, NKp46$^-$ and CD4$^+$ ILC3s). Graphs indicate mean ± SEM. Statistical analysis was performed by non-paired Student's t-test. ILC, innate lymphoid cells; LTi, lymphoid tissue inducer.

Next, we examined ILCs in the intestinal lamina propria. The absolute numbers of ILC1s, ILC3s, CD127$^-$ NK cells, and CD127$^-$ ILCs in lamina propria were higher in PPARγ cKO mice, compared to PPARγ flox mice (Figure 3.31A and B). In addition, the number of NKp46$^+$ ILC3s, NKp46$^-$ ILC3, and LTi cells, were higher in PPARγ cKO mice, compared to PPARγ flox mice (Figure 3.31C).

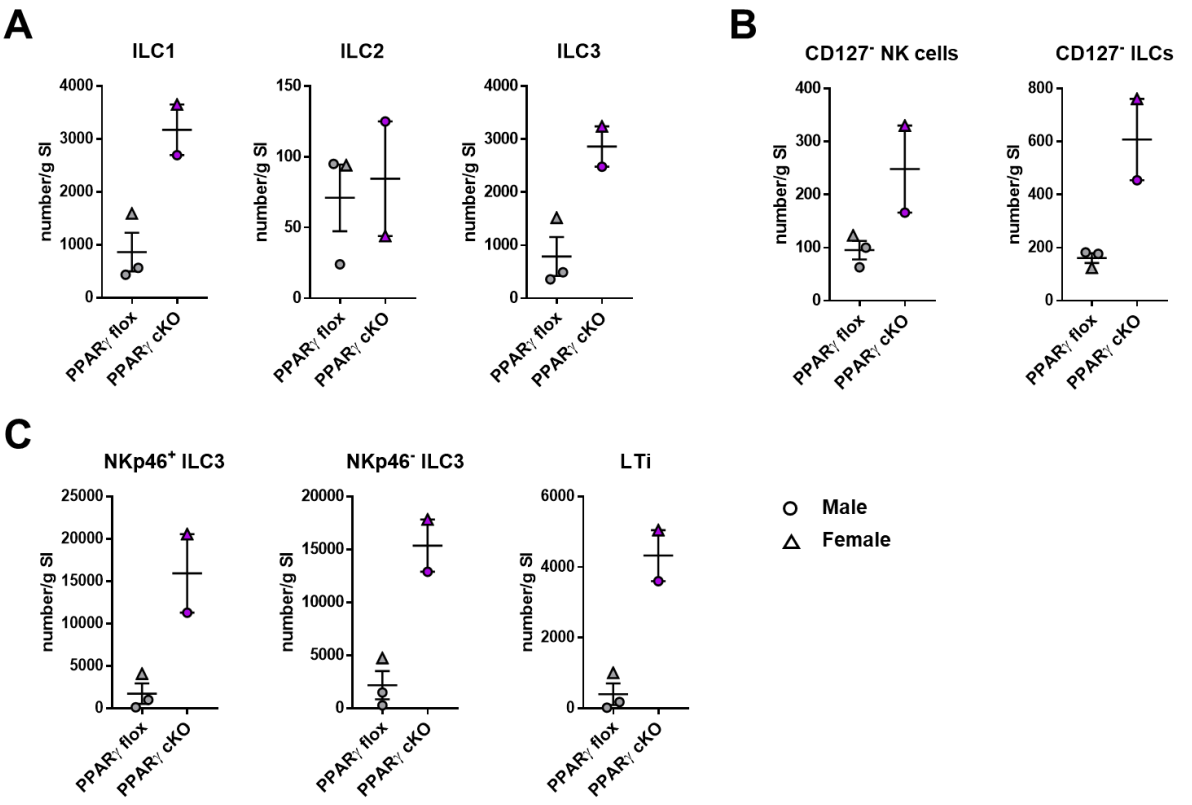

Figure 3.31. Absolute number of ILCs in the lamina propria of PPARγ flox mice and PPARγ cKO mice. Intestines were collected from PPARγ flox mice (PPARγ$^{f/f}$ mice) and PPARγ cKO mice (Ncr1^{iCreTg} PPARγ$^{f/f}$ mice) (Male mice, depicted as a circle mark in the graphs, and female mice, depicted as a triangle mark in the graphs, 11-13 weeks old, n=2-3 for each group). ILCs were analyzed by flow cytometry and gated as live CD45$^+$, CD3ε$^-$, CD19$^-$, Ly6G$^-$, Ter119$^-$, TCRβ$^-$, and TCRγδ$^-$ cells. (A) Absolute number of CD127$^+$ ILC1s, ILC2s, and ILC3s. (B) Absolute number of CD127$^-$ NK cells and ILCs. (C) Absolute number of NKp46$^+$ ILC3s (gated CD127$^+$, RORγt$^+$, NKp46$^+$ and CD4$^-$ cells), NKp46$^-$ ILC3s (gated CD127$^+$, RORγt$^+$, NKp46$^-$ and CD4$^-$ cells), and LTi cells (gated CD127$^+$, RORγt$^+$, NKp46$^-$ and CD4$^+$ ILC3s). Graphs indicate mean ± SEM. ILC, innate lymphoid cells; LTi, lymphoid tissue inducer.

Lastly, Peyer's patches, lymphoid follicles lining along the small intestine, were assessed. The absolute numbers of ILC1s, ILC2s, ILC3s, CD127$^-$ NK cells, and CD127$^-$ ILCs were comparable between Peyer's patches obtained from PPARγ cKO mice and PPARγ flox mice (Figure 3.32A and B). Furthermore, the absolute number of three ILC3 subsets did not show difference between two groups of mice (Figure 3.32C).

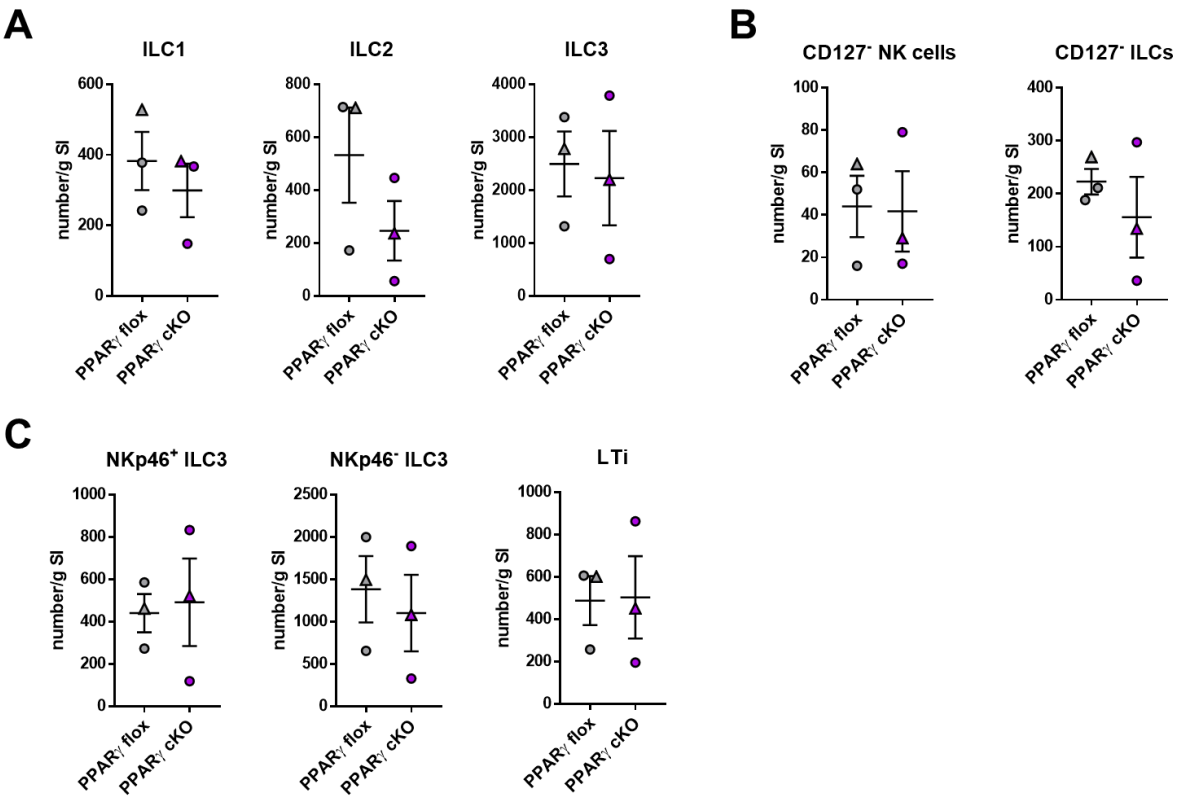

Figure 3.32. Absolute number of ILCs in the Peyer's patches of PPARγ flox mice and PPARγ cKO mice. Intestines were collected from PPARγ flox mice (PPARγ$^{f/f}$ mice) and PPARγ cKO mice (Ncr1^{iCreTg} PPARγ$^{f/f}$ mice) (Male mice, depicted as a circle mark in the graphs, and female mice, depicted as a triangle mark in the graphs, 11-13 weeks old, n=3 for each group). ILCs were analyzed by flow cytometry and gated as live CD45$^+$, CD3ε$^-$, CD19$^-$, Ly6G$^-$, Ter119$^-$, TCRβ$^-$, and TCRγδ$^-$ cells. (A) Absolute number of CD127$^+$ ILC1s, ILC2s, and ILC3s. (B) Absolute number of CD127$^-$ NK cells and ILCs. (C) Absolute number of NKp46$^+$ ILC3s (gated CD127$^+$, RORγt$^+$, NKp46$^+$ and CD4$^-$ cells), NKp46$^-$ ILC3s (gated CD127$^+$, RORγt$^+$, NKp46$^-$ and CD4$^-$ cells), and LTi cells (gated CD127$^+$, RORγt$^+$, NKp46$^-$ and CD4$^+$ ILC3s). Graphs indicate mean ± SEM. ILC, innate lymphoid cells; LTi, lymphoid tissue inducer.

In conclusion, PPARγ cKO and PPARγ flox mice showed similar weights of analyzed organs, including spleens, livers, lungs, small intestines, and large intestines. Furthermore, the number and phenotype of NK cells and ILC1s were comparable in spleens, livers, and lungs of PPARγ cKO and PPARγ flox mice. In gut, PPARγ cKO mice displayed the increased number of intraepithelial ILC3s as well as the elevated numbers of ILC1s, ILC3s, NK cells, and CD127$^-$ ILCs in lamina propria, compared to PPARγ flox mice.

4.5.2 PPARγ-deletion on *at*RA-induced reprogramming of NK cells

NK cells isolated from spleens of PPARγ cKO mice and PPARγ flox mice were treated with *at*RA in the presence of IL-2. The expression of DNAM-1, CD200R, TRAIL, RANKL, CD11b, CD73, CD39, and CD38 was upregulated and the expression of IL-18Rα was downregulated on PPARγ flox NK cells upon *at*RA-treatment (Figure 3.33). PPARγ deletion in NK cells did not affect these changes (Figure 3.33). The expression of CD62L and KLRG1 on both PPARγ flox NK cells and PPARγ cKO NK cells in both control- and atRA-treated NK cells was comparable (Figure 3.33).

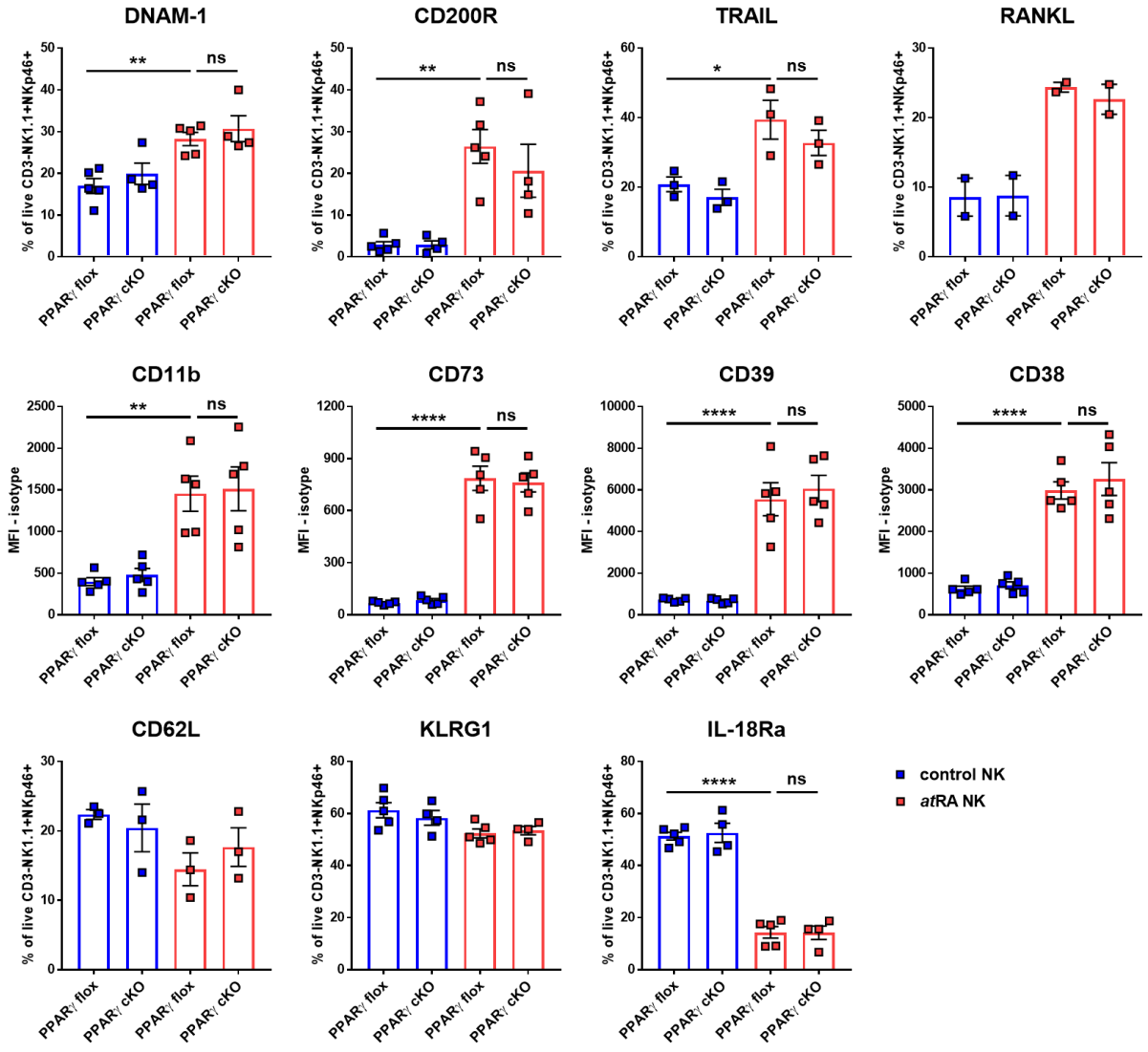

Figure 3.33. PPARγ conditional deletion did not alter *at*RA-induced phenotype of NK cells. NK cells were isolated from spleens of PPARγ flox mice (PPARγ$^{f/f}$ mice) and PPARγ cKO mice (Ncr1^{iCreTg} PPARγ$^{f/f}$ mice) (Both male and female mice were used, 6, 11, or 13 weeks old, n=2 or 5 for each group), and treated with 1 µM of *at*RA for 7 days in the presence of IL-2. The equivalent volume of DMSO was used as a solvent control. NK cells were analyzed by flow cytometry, and gated as live, CD3ε$^-$, NK1.1$^+$ and NKp46$^+$ cells. Percentage of PPARγ flox or PPARγ cKO NK cells expressing DNAM-1, CD200R, TRAIL, RANKL, CD11b, CD73, CD39, CD38, CD62L, KLRG1, and IL-18Rα. Graphs indicate mean ± SEM. *, p<0.05; **, p<0.01; ****, p<0.0001 by one-way ANOVA (Tukey's multiple comparisons test); MFI, mean florescence intensity; ns: not significant.

4.5.3 PPARγ-deletion on *at*RA-induced metabolic changes in NK cells

NK cells obtained from PPARγ cKO mice (PPARγ cKO NK cells) displayed similar basal oxygen consumption rate (OCR), compared to NK cells obtained from PPARγ flox mice (PPARγ flox NK cells) (Figure 3.34A and C), indicating comparable mitochondrial respiration. The basal level of aerobic glycolysis, measured as extracellular acidification rates (ECAR), did not change between PPARγ cKO NK cells and PPARγ flox NK cells (Figure 3.34B and C). After the FCCP-treatment, which triggers the depolarization of mitochondrial membrane and induces the maximal mitochondrial respiration, PPARγ cKO NK cells were unable to engage maximal respiration, compared to PPARγ flox NK cells (Figure 3.34D). In addition, ECR dropped to basal level in PPARγ cKO NK cells, while it was maintained in PPARγ flox NK cells (Figure 3.34B and D). These results suggest that the deletion of PPARγ alters NK cell metabolism.

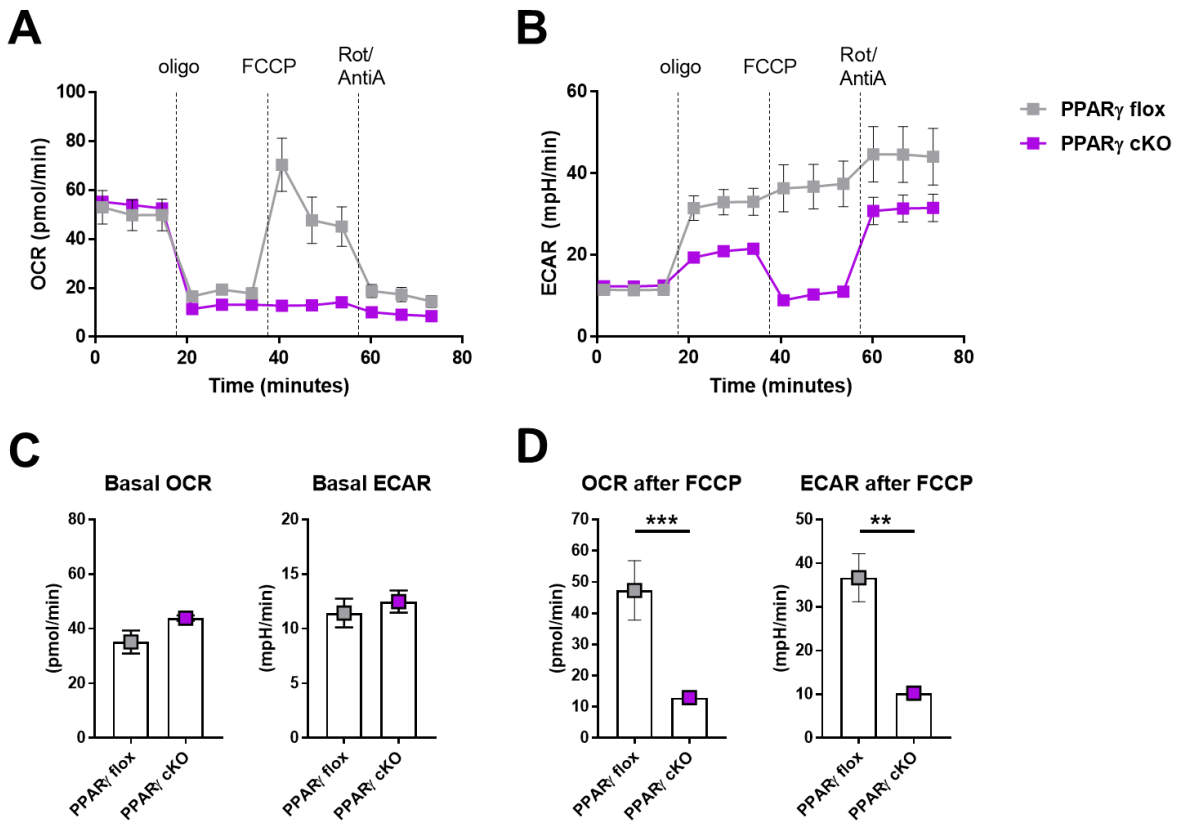

Figure 3.34. PPARγ deletion affects NK cell metabolism. NK cells were isolated from spleens of PPARγ flox mice (PPARγ$^{f/f}$ mice) and PPARγ cKO mice (Ncr1^{iCreTg} PPARγ$^{f/f}$ mice), and cultured for 7 days in the presence of IL-2. Oxygen consumption rate (OCR) and extracellular acidification rate (ECAR) of PPARγ flox or PPARγ cKO NK cells were measured upon oligomycin, FCCP, and Rotenone/Antimycin A-treatment. Quantification of (A) OCR, (B) ECAR, (C) basal OCR and ECAR, and (D) OCR and ECAR upon FCCP-treatment. Graphs indicate mean ± SEM. **, p<0.01; ***, p<0.001 by non-paired Student's t-test.

Basal and maximal mitochondrial respirations of NK cells were upregulated upon *at*RA-treatment (Figure 3.3I and J). To elucidate whether *at*RA can affect metabolism of PPARγ-deficient NK cells, we cultured both PPARγ cKO NK cells with or without *at*RA for 7 days in the presence of IL-2. Similar to previous results shown in Figure 3.3, *at*RA elevated basal OCR and ECAR of PPARγ cKO NK cells (Figure 3.35A, B and C). Upon FCCP-treatment, *at*RA-treated PPARγ cKO NK cells exhibited higher OCR and higher ECAR, compared to control-treated PPARγ cKO NK cells, which failed to engage OXPHOS and glycolysis (Figure 3.35D). These data indicate that *at*RA can alter NK cell metabolism independent of PPARγ.

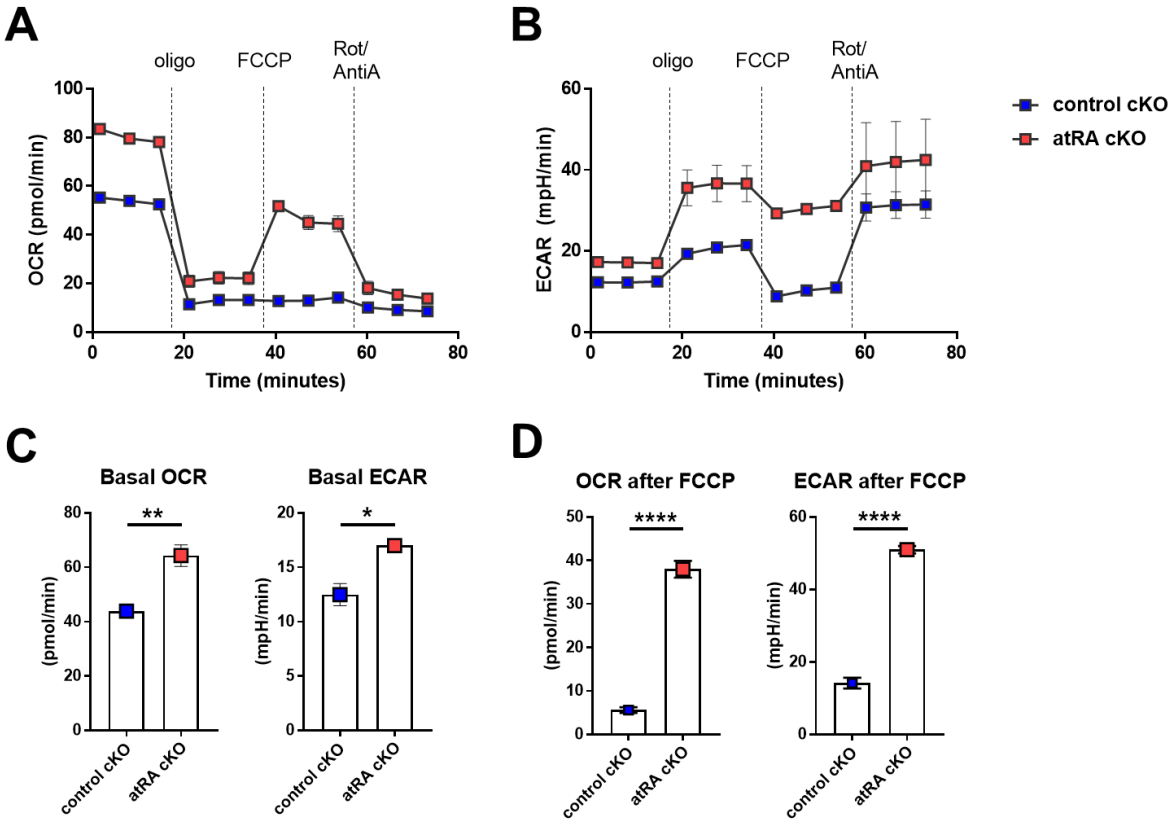

Figure 3.35. *at*RA affects oxidative phosphorylation and aerobic glycolysis in PPARγ-deficient NK cells. NK cells were isolated from spleens of PPARγ flox mice (PPARγ$^{f/f}$ mice) and PPARγ cKO mice (Ncr1^{iCreTg} PPARγ$^{f/f}$ mice), and cultured with 1µM of *at*RA for 7 days in the presence of IL-2. The equivalent volume of DMSO was used as a solvent control. Oxygen consumption rate (OCR) and extracellular acidification rate (ECAR) of were measured upon oligomycin, FCCP, and Rotenone/Antimycin A-treatment. Quantification of (A) OCR, (B) ECAR, (C) basal OCR and ECAR, and (D) OCR and ECAR upon FCCP-treatment. Graphs indicate mean ± SEM. *, p<0.05; **, p<0.01; ****, p<0.0001 by non-paired Student's t-test.

5 DISCUSSION

A lipid-soluble micronutrient, vitamin A, is absorbed in the small intestine, and stored mainly in the liver and adipose tissue (Chelstowska, Widjaja-Adhi, Silvaroli, & Golczak, 2016; Kane et al., 2008). Previous studies highlighted that vitamin A metabolites played an important role in tissue homeostasis. For instance, retinoic acid (RA) was reported to induce the expression of gut-homing chemokine and integrin receptors on T cells and innate lymphoid cells (ILCs), which facilitated the migration of T cells and ILCs towards the gut (Iwata et al., 2004; Jaensson et al., 2008; Kim et al., 2015). The tissue-specific migration of cells contributes to the local immunological milieu and to the balance of immune responses in the gut. Moreover, vitamin A regulates the developmental balance of ILC populations in the small intestine, as vitamin A deficiency was shown to cause a decrease in number of ILC3s and an increase in number of ILC2s (Spencer et al., 2014). The decreased number of ILC3s, which produce IL-22, led to an impaired immune responses against *Citrobacter rodentium* infection. In the liver, hepatic stellate cells (HSCs), a major reservoir of retinol, can release retinol in conditions of liver damage (Higashi et al., 2005; Yanagitani et al., 2004). Immune responses, which contribute to tissue regeneration, are regulated by the vitamin A-enriched environment during liver damage (Natarajan, Thomas, Ramachandran, Pulimood, & Balasubramanian, 2005; Yanagitani et al., 2004). In addition to the role of vitamin A in the gut and liver, many studies demonstrated the impact of vitamin A on adipose tissues (Kawada et al., 2000; Pairault, Quignard-Boulange, Dugail, & Lasnier, 1988; M. Sato, Hiragun, & Mitsui, 1980; Schwarz, Reginato, Shao, Krakow, & Lazar, 1997). For example, vitamin A metabolites could inhibit the differentiation of adipocytes and adipogenesis by blocking C/EBPβ-mediated transcriptional activation.

NK cells are innate lymphocytes, circulating in the body. During tissue inflammation, NK cells are recruited to tissues, e.g. gut, liver, and lung, and can produce inflammatory cytokines and exert cytotoxicity against abnormal cells. The recruitment of NK cells can promote tissue repair and host defense (Tosello-Trampont, Surette, Ewald, & Hahn, 2017). However, the role of a vitamin A-enriched environment in regulating NK cell-mediated immune responses remains unknown. Therefore, in this project, we investigated the impact of vitamin A on NK cell phenotype and effector functions.

5.1 *at*RA induces ILC1-like phenotype

NK cells exposed to all-*trans* retinoic acid *(at*RA) for 6-7 days, displayed a differential expression of multiple genes, which were involved in different metabolism pathways and NK cell effector functions (Figure 3.1). Furthermore, *at*RA altered the expression of molecules selected from the transcript analysis and metabolic activities of NK cells (Figure 3.2 and 3.3). Among them, several proteins expressed on the surface of liver ILC1s were detected on *at*RA-treated

NK cells. For instance, the increased expression of DNAM-1, CD200R, TRAIL, CD73, CD39, and LAG3 was observed on the surface of NK cells upon *at*RA-treatment. Furthermore, the transcription factor Eomes, selectively expressed by NK cells, but not by ILC1s (Tang et al., 2016), was downregulated in NK cells exposed to *at*RA. The expression of the activating receptor NKG2D and the adhesion molecule CD62L was reported to be lower on liver ILC1s, compared to circulating NK cells (Tang et al., 2016). In accordance, *at*RA-treated NK cells downregulated the transcript Klrk1 and Sell, and the protein expression of NKG2D and CD62L on the cell surface.

ILC1s are known as helper ILCs, and NK cells are cytotoxic ILCs, which are able to eliminate infected cells and tumor cells (Vivier et al., 2018). It was reported that liver ILC1s expressed a lower amount of CD107a (a marker of degranulation) and IFN-γ (an inflammatory cytokine), compared to NK cells, upon stimulation with PMA and Ionomycin. (Tang et al., 2016). Indeed, similar to the cytokine production of liver ILC1s, the production of IFN-γ by NK cells upon *at*RA-treatment was downregulated in response to different stimuli, including cytokine activation, receptor-engagement, or co-culture with tumor cells (Figure 3.9 and 3.10). Our results showed that *at*RA-treated NK cells had an increased expression of Csf2 (encoding GM-CSF) at mRNA level, as well as intracellular production of GM-CSF in the presence of $CD4^+$ T cells (Data not shown).

Taken together, these results demonstrate that NK cells conditioned by *at*RA share similar features with liver ILC1s. One possible explanation of why *at*RA-treated NK cells displayed similarities with liver ILC1s is the liver microenvironment, which is enriched with vitamin A metabolites. A main difference between NK cells and ILC1s is that NK cells are circulating, while ILC1s are tissue-resident. A recent study showed that liver ILC1s developed locally (L. Bai et al., 2021) and remained in the liver. Thus, ILC1s are constantly exposed to vitamin A metabolites, such as retinol and retinoic acid, because liver is the major storage organ of vitamin A. In steady-state, vitamin A absorbed in the small intestine is transported to the liver, metabolized and stored (Erkelens & Mebius, 2017). Therefore, the culture of NK cells in the presence of *at*RA could mimic the vitamin A-enriched liver microenvironment, enabling NK cells to show similar features as liver ILC1s.

It was also shown that a subset of NK cells, found in tumor microenvironment (TME), could acquire an intermediate ILC1-like phenotype (Gao et al., 2017). These intermediate ILC1-like NK cells expressed Eomes and CD49a. Concurrently, they expressed DNAM-1, TRAIL, CD69, and CD62L, which were expressed by tumor-infiltrating ILC1s. The TGFβ signaling pathway mediated the acquisition of the intermediate ILC1-like phenotype by NK cells. As NK cells exposed to *at*RA resembled the phenotype of intermediate ILC1-like NK cells, we hypothesized that NK cells might produce TGFβ in the presence of *at*RA, and TGFβ might regulate *at*RA-

induced reprogramming of NK cells in the autocrine manner. NK cells exposed to *at*RA expressed the increased amount of Tgfb3 transcript (encoding TGFβ3, which is a member of the TGFβ family). However, the pan-TGFβ neutralization did not change the phenotype of *at*RA-treated NK cells. These results indicate that even though Tgfb3 expression was enhanced, either it might not result in the production of TGFβ or TGFβ was not involved in *at*RA-induced reprogramming in NK cells.

5.2 Regulatory features of a*t*RA-treated NK cells

Previous studies demonstrated that vitamin A metabolites induced regulatory features in lymphocytes (Elias et al., 2008; Mucida et al., 2007; S. Xiao et al., 2008). For instance, $CD4^+$ T cells exposed to all-*trans* retinoic acid (*at*RA) *in vitro* displayed enhanced FoxP3 expression, which is commonly expressed by regulatory T (Treg) cells (Elias et al., 2008; Mucida et al., 2007). Besides, the expression of RORγt, a transcription factor expressed by Type 17 helper T (T_H17) cells, and IL-17, a pro-inflammatory cytokine, was reduced by these cells. Additionally, ILC2s, an ILC subset expressing the transcription factor GATA3, could produce IL-10 upon *at*RA-treatment in the presence of IL-2 and IL-33 (Morita et al., 2019). Based on previous findings, we hypothesized that *at*RA could promote regulatory features in NK cells.

Upon *at*RA-treatment, NK cells displayed features, which are observed in Treg cells, such as increased expression of Ctla4 (encoding CTLA4) and Tgfb3. CTLA4 is a negative regulator of T lymphocyte activation. For instance, CTLA4 expressed on $CD4^+$ and $CD8^+$ T cells was involved in the inhibition of T cell proliferation and activation (McCoy & Le Gros, 1999). CTLA4 is also expressed on the cell surface of NK cells activated with IL-2. Upon CD80/CTLA4 engagement, IFN-γ production by NK cells was decreased (Stojanovic, Fiegler, Brunner-Weinzierl, & Cerwenka, 2014). We detected the decreased IFN-γ production by *at*RA-treated NK cells upon co-culture with BM-DCs, which express CD80. Although the expression of CTLA4 at protein level was not confirmed, the Clta4 expression might explain a lower IFN-γ production by *at*RA-treated NK cells upon co-culture with BM-DCs. Furthermore, CD38 (NAD-hydrolase), which is expressed by Treg cells and crucial for the cell viability, phenotype, and function of Tregs in homeostasis and disease (X. Feng et al., 2017; Hubert et al., 2010), was upregulated in NK cells upon *at*RA-treatment. In the context of NK cell-mediated immune responses, CD38 is crucial for antibody-dependent cellular cytotoxicity (ADCC) (Lejeune et al., 2021; Naeimi Kararoudi et al., 2020). For example, studies showed that CD38 ligation with an agonistic monoclonal antibody increased the expression of MHC class II molecules and CD25 on NK cells, and induced the production of inflammatory cytokines by NK cells (Mallone et al., 2001). Thus, the role of CD38 in Treg cells and *at*RA-treated NK cells appeared to be different.

Another regulatory feature detected on *at*RA-treated NK cells was elevated cell surface expression of the nucleotide metabolizing enzymes, CD39 and CD73. CD39 (ecto-nucleoside triphosphate diphosphohydrolase) can convert adenosine triphosphate (ATP) to adenosine diphosphate (ADP) or adenosine monophosphate (AMP), and CD73 (ecto-5'-nucleotidase) can convert AMP to adenosine (Airas et al., 1997; Kaczmarek et al., 1996). Studies reported that FoxP3$^+$ Treg cells expressed CD39 and CD73 on the cell surface, and adenosine contributed to the inhibition of CD4$^+$ T cells in both human and mouse (Deaglio et al., 2007; Kobie et al., 2006; Mandapathil et al., 2010). Our results show that CD39 and CD73 expression on the cell surface of NK cells was upregulated upon *at*RA-treatment (Figure 3.2), indicating the increased potential ability of NK cells to metabolize adenosine. However, we could not detect adenosine in the supernatant collected during NK cell culture in the presence of *at*RA (Data not shown). Previous studies demonstrated ATP molecules had to be added in the cell culture to confirm whether cells can metabolize ATP to adenosine (Perrot et al., 2019; Schneider et al., 2021). Therefore, we cannot exclude that *at*RA-treated NK cells do not have the ability to metabolize ATP to adenosine.

IL-10, a pleiotropic cytokine, can be released by regulatory immune cells. It was reported that a vitamin A-enriched microenvironment and vitamin A-conditioned dendritic cells (DCs) could induce IL-10 production by lymphocytes (Bakdash, Vogelpoel, van Capel, Kapsenberg, & de Jong, 2015; Morita et al., 2019). However, we could not detect IL-10 production by NK cells upon *at*RA-treatment.

PPARγ, a nuclear receptor, plays an important role in inducing the Treg phenotype, such as FoxP3 expression, and in accumulation of Treg cells in adipose tissue (Cipolletta et al., 2012). In addition, the metabolism of Treg cells was regulated by PPARγ-mediated transcription (Field et al., 2020). Another study showed that the expression of fatty acid binding protein 5 (FABP5), a direct target gene of PPARγ, was higher in Treg cells, compared to naïve T cells, and FABP5 could regulate mitochondrial respiration and lipid metabolism of Treg cells (Kempkes, Joosten, Koenen, & He, 2019). Similarly, our results showed that NK cells had increased Pparg (encoding PPARγ) expression upon *at*RA-treatment (Figure 3.4). Moreover, *at*RA-treated NK cells displayed increased mitochondrial respiration and showed no difference in glycolysis (Figure 3.3).

Taken together, we observed that vitamin A-treated NK cells displayed a unique regulatory transcriptomic, metabolic, and phenotypic profile resembling regulatory T cells. These data suggest that NK cells exposed to a vitamin A-enriched microenvironment in steady-state and during disease could negatively regulate immune responses.

5.3 PPARγ, a key mediator of a*t*RA-induced NK cell phenotype?

Studies reported that RA could bind to nuclear receptors, such as retinoic acid receptors (RARs) and peroxisome proliferator-activated receptors (PPARs) (Repa, Hanson, & Clagett-Dame, 1993; Rieck, Meissner, Ries, Muller-Brusselbach, & Muller, 2008). More importantly, *at*RA was demonstrated to promote the production of Type 2 helper T (T_H2) cytokine production by T_H2 cells and PBMCs (Dawson et al., 2008; Wansley et al., 2013). The blockade of the binding of RA to RARs could reverse *at*RA-induced features in different immune cells. For instance, the exposure to Ro 41-5253, which selectively inhibits the binding between RA and RARα, reversed the increased T_H2 cytokine production by T_H2 cells and PBMCs (Dawson et al., 2008; Wansley et al., 2013). Additionally, T cells displayed increased expression of FoxP3 and CCR9 in the presence of *at*RA-shaped DCs, and the usage of LE135, which selectively inhibits the binding of RA to RARα and RARβ, could reduce their expression (T. Feng et al., 2010). Based on these findings, we hypothesized that RA-binding nuclear receptors might regulate *at*RA-induce NK cell phenotype.

We detected the Rara and Rarg expression in NK cells cultured in the presence of IL-2. Upon *at*RA-treatment, the expression of Rara and Rarg was downregulated (Figure 3.4). Based on the changes in mRNA expression, we added the selective antagonist of RARα (Ro 41-5253) or RARγ (MM-11253) to NK cell culture in the presence of *at*RA. The inhibition of RARα or RARγ did not affect the expression of CD200R and DNAM-1, which was increased in *at*RA-treated NK cell. These results imply that RARα or RARγ do not mediate *at*RA-induced phenotype.

Next, we analyzed the expression of three isoforms of PPAR, which are PPARα, PPARβ/δ, and PPARγ, as RARs can compete with PPARs to form a heterodimer with retinoic X receptor (RXR) (Szanto et al., 2004). In NK cells cultured in the presence of IL-2, mRNA expression of Ppard and Pparg was detected. *at*RA-treatment did not affect Ppard expression, while Pparg expression was upregulated. As we detected elevated Pparg expression in *at*RA-treated NK cell, we added the selective antagonist of PPARγ (T0070907) during NK cell culture in the presence of *at*RA. CD200R and DNAM-1 expression by NK cells was increased by *at*RA. Upon the inhibition of PPARγ, CD200R and DNAM-1 expression in *at*RA-treated NK cells was detected comparable to control NK cells. One explanation for observed effect might be the availability of the nuclear receptor RXR to form heterodimers with PPARγ. In *at*RA-treated NK cells, the expression of Rxr was unchanged, the expression of Rara and Rarg was downregulated, while the expression of Pparg was upregulated, compared to control NK cells. As RARs compete with PPARs to bind RXR, there might be more available PPARγ protein to bind RXR in *at*RA-treated NK cells. We hypothesized that PPARγ engages RXR protein, mediating the *at*RA-induced NK cell phenotype.

5.4 The deletion of PPARγ in NKp46-expressing cells

To investigate the role of PPARγ in NK cells exposed to vitamin A metabolites, we generated PPARγ$^{f/f}$Ncr1^{iCreTg} mice (PPARγ cKO) and used PPARγ$^{f/f}$ mice (PPARγ flox) as a control. PPARγ cKO mice bear a conditional deletion of PPARγ in NKp46-expressing cells. NK cells and ILC1s are the main populations of NKp46-expressing cells found in vitamin A-enriched organs, such as liver and lung (Chelstowska et al., 2016; Kane et al., 2008). We hypothesized that the deletion of PPARγ would block vitamin A signaling in NK cells and ILC1s in these organs, which might result in phenotypic and/or functional changes of NK cells and ILC1s. Thus, we examined the phenotype of NK cells and ILC1s in livers and lungs (vitamin A-enriched organs), and spleen (an internal control organ, storing low amounts of vitamin A) in PPARγ cKO and PPARγ flox mice.

Spleen, as a secondary lymphoid organ, contains numerous immune cells and does not provide a vitamin A-enriched microenvironment. Our data showed that the spleen weight, the number and percentage of NK cells, and the phenotype of NK cells did not change in PPARγ cKO mice, compared to PPARγ flox mice (Figure 3.26). We hypothesized that vitamin A is abundant in lungs and livers, as we detected the high expression of genes involved in RA-receptors and RA-metabolism in lungs, and liver is a main storage of vitamin A metabolites. Our results revealed that organ weight, the number and phenotype of NK cells or ILC1s were comparable in the lungs of PPARγ cKO and PPARγ flox mice, as well as in the livers (Figure 3.27 and 3.28). Based on these data, we postulate followings: 1) the nuclear receptor PPARγ might not mediate the a*t*RA-induced reprogramming of NKp46-expressing cells, 2) NK cells and ILC1s in such tissues might not be conditioned by vitamin A due to the low amount of vitmain A metabolites at a physiological level, compared to the concentration of *at*RA we used *in vitro*. Furthermore, as we analyzed the expression of a limited number of molecules, to establish an overview of alterations induced by the deletion of PPARγ in NKp46-expressing cells, transcriptome analysis would be required.

Furthermore, small intestine, a part of gastrointestinal tract constantly encountering precursors and metabolites of vitamin A (Erkelens & Mebius, 2017), were analyzed in PPARγ cKO and PPARγ flox mice (Figure 3.29 - 3.32). We observed that the weight and length of intestine, and the number of Peyer's patches were comparable in PPARγ cKO and PPARγ flox mice. Previous studies showed that the vitamin A regulated the distribution of ILCs in the gut (Goverse et al., 2016; Spencer et al., 2014). For instance, mice fed with vitamin A-deficient diet showed altered distribution of ILC subsets, such as a reduction in ILC3 number and an increase in ILC2 number, in the intestine (Spencer et al., 2014). In addition, the absence of vitamin A downregulated the percentage of RORγt$^+$ NKp46$^-$ and RORγt$^+$ NKp46$^+$ ILCs in the gut, and RA injection significantly increased the percentage of RORγt$^+$ NKp46$^-$ cells (Goverse et al., 2016). Thus, we

expected that the genetic ablation of PPARγ, which potentially inhibits the vitamin A signaling, would result in a similar distribution of ILC subsets. However, surprisingly, the number of ILCs, which comprise ILC1s, ILC2s, ILC3s, NK cells, and CD127$^-$ ILCs, was higher in PPARγ cKO mice, compared to PPARγ flox mice. One explanation is that PPARγ is not involved in vitamin A signaling, thus, the deletion of PPARγ would affect NKp46-expressing cells differently than vitamin A deficieny. Another possiblitiy is that the genetic ablation of PPARγ in NKp46-expressing cells might cause congenital changes in mice, while feeding of modified diet was executed for certain length of time. Besides, diet regimes might induce microenvionmental alterations by influencing other cells and microbiota, which might cause the reduction of ILC3s.

Previously, studies reported that PPARγ could play a role in cellular apoptosis. For instance, the absence of PPARγ resulted in diminished apoptosis of lymphocytes, including T cells and B cells, resulting in the increased proliferation of cells (Y. H. Liu et al., 2016; Schmidt et al., 2011). Apart from the role of PPARγ in regulating vitamin A signaling, the deletion of PPARγ in NKp46-expressing cells might reduce apoptosis, thus, we detected higher numbers of NKp46-expressing NK cells, ILC1s and ILC3s in the gut of PPARγ cKO mice, compared to PPARγ flox mice. Moreover, the numbers of ILCs, which do not express NKp46, were increased, indicating that extrinsic effects were induced by the altered microenvironment or interaction with other cells. Further investigations on apoptosis and proliferation of intestinal ILCs will be necessary, to understand the mechanism of increased numbers of intestinal ILCs in PPARγ cKO mice.

In addition, it was shown that the deletion of PPARγ in lymphocytes affected their immune responses. The genetic ablation of PPARγ or PPARγ blockade in ILC2s led to impaired production of type 2 cytokine (Ercolano et al., 2021; Q. Xiao et al., 2021). Furthermore, the deletion of PPARγ in T cells mediated cell activation and upregulated production of inflammatory cytokines, resulting in exacerbation of autoimmune diseases (Guri, Mohapatra, Horne, Hontecillas, & Bassaganya-Riera, 2010; H. J. Park et al., 2014). Therefore, research on the role of PPARγ in immune responses of NKp46-expressing cells is warranted.

To investigate whether PPARγ is a key regulator of *at*RA-induced reprogramming of NK cells, splenic NK cells, obtained from PPARγ cKO or PPARγ flox mice, were exposed to *at*RA for 7 days. Based on phenotypic changes in *at*RA-treated NK cells shown in Figure 3.2, we selected various proteins, such as DNAM-1, CD200R, TRAIL, RANKL, CD11b, CD73, CD39, CD38, CD62L, KLRG1, and IL-18Rα, and analyzed their expression in NK cells. NK cells obtained from PPARγ flox mice showed *at*RA-induced phenotype, for example, increased expression of DNAM-1, CD200R, TRAIL, RANKL, CD11b, CD73, CD39 and CD38, and decreased expression of IL-18Rα (Figure 3.33). NK cells obtained from PPARγ cKO mice showed similar

expression of these proteins on the surface upon *at*RA-treatment, compared to NK cells obtained from PPARγ flox mice. The data are opposed to the results, which showed that the treatment of selective PPARγ antagonist could regulate DNAM-1 and CD200R expression by NK cells upon *at*RA-treatment. Supposedly, despite the high selectivity, antagonists can bind to other receptors, resulting difference outcome compared to genetic ablation.

5.5 a*t*RA-induced metabolic changes of NK cells

Previous studies demonstrated that vitamin A could regulate mitochondrial size, structure and membrane potential (Chidipi et al., 2021; Rigobello et al., 1999; Silva et al., 2013; Tourniaire et al., 2015). Furthermore, vitamin A metabolites or synthesized retinoid could affect cellular oxidative stress, mitochondrial functions, and oxidative phosphorylation of cells (H. J. Chiu, Fischman, & Hammerling, 2008; Seward, Vaughan, & Hove, 1966). Our transcriptomic data demonstrated that many of transcripts, which take part in metabolism, such as fatty acid degradation, pentose interconversion, and cytochrome P450 pathway, were up- or down-regulated in NK cells upon a*t*RA-treatment (Figure 3.1). Thus, we hypothesized that the exposure to a*t*RA might influence NK cell metabolism.

First, we observed that the size of the cells and mitochondrial mass decreased in NK cells upon a*t*RA-treatment (Figure 3.3). Studies showed that upon activtaion, lymphocytes displayed an elevated mitochondrial membrane potential (Gergely, Grossman, et al., 2002; Gergely, Niland, et al., 2002; Surace et al., 2021). NK cells treated with a*t*RA showed a decreased membrane potential, which might be an indicator of reduced function. Reactive oxygen species (ROS) production by NK cells were significantly decreased in the presence of a*t*RA, which can be explained by the antioxidant role of vitamin A. It was reported that vitamin A could remove radicals by breaking chain reactions (Ahlemeyer et al., 2001; T. K. Hong & Lee-Kim, 2009; Jackson, Morgan, Werrbach-Perez, & Perez-Polo, 1991). This correlates with the upregulated expression of transcripts involved in ascorbate (Vitamin C) metabolism and cytochrome P450 pathway, as these pathways are important for antioxidant reactions (Brown & Borutaite, 2008).

Our data showed that NK cells exposed to a*t*RA displayed enriched expression of fatty acid degradation-related transcripts. We postulate that this might be because vitamin A metabolites require lipoproteins in order to be transported in the aqueous environment (Goodman, Huang, & Shiratori, 1965; H. S. Huang & Goodman, 1965), which might be facilitated by the usage of lipids. Thus, we hypothesized that a*t*RA-treated NK cells would increase fatty acid uptake to fulfill their functions. However, a*t*RA-exposure did not affect fatty acid uptake by NK cells, which can potentially be explained by postulating that a*t*RA-treated NK cells use intrisic lipids produced by other metabolites. In addition, for analyzing fatty acid uptake, we used BODIPY™

FL C16, which can mimic long chain fatty acids. Therefore, uptake of short chain fatty acid and cholesterol has to be further investigated.

Futhermore, vitamin A could regulate the carbohydrate metabolic pathways by affecting enzmye acitivies in the liver (W. Chen & Chen, 2014). For example, glycolysis of hepatic cells was impaired by the deficiency of vitamin A, due to the reduced acitivtiy of glucokinase and hexokinase. However, in NK cells, we did not observe changes in glycolytic activities in the presence of a*t*RA. The effect of vitamin A on mitochondrial resipration in immune cells is unknown. However, studies showed that excessive or insufficient amounts of vitamin A could impair the capacity of mitochondrial oxidative phosphorylation in the liver (Seward, Vaughan, & Hove, 1964; Seward et al., 1966). In our experimental settings, *at*RA-treatment increased oxidative phosphorylation (OXPHOS) of cultured NK cells. We also detected that the exposure to a*t*RA elevated the enrichedment score of glucoronate interconversion pathway, in which non-carbohydrate substrates, such as amino acid or fat, are utilized to generate glucose (Exton, 1972). Moreover, vitamin A was reported to modulate amino acid metabolism (W. Chen & Chen, 2014) Hence, future investigation of protein metabolism in a*t*RA-treated NK cells is warranted.

PPARγ is a nuclear receptor that modulates lipid metabolism and adipogenesis (Ahmadian et al., 2013). Studies showed that PPARγ could regulate the uptake of lipid into T cells in an mTOR-dependent manner (Angela et al., 2016), and the deletion of PPARγ-coactivator-1α (PGC-1α) in NK cells altered their metabolism and effector functions (Gerbec et al., 2020). For example, OXPHOS of NK cells was impaired in the absence of PGC-1α. Thus, we hypothesized that the absence of PPARγ in NK cells might induce metabolic changes. PPARγ cKO NK cells exposed to IL-2 showed comparable glycolysis and OXPHOS, compared to PPARγ flox NK cells. However, when cells were treated with FCCP, which induces the release of uncoupled protons through the inner mitochondrial membrane, PPARγ cKO NK cells displayed low glycolytic activity and OXPHOS, compared to PPARγ flox NK cells (Figure 3.35). Upon FCCP-treatment, PPARγ cKO NK cells remained metabolically quiescent with utilizing low glycolysis and OXPHOS. On the contrary, PPARγ flox NK cells showed the maximal oxidative respiration upon FCCP-treatment. After the treatment with Rotenone/Antimycin A, which inhibits the activities of complex I and IV, PPARγ cKO NK cells used glycolysis to generate energy, but the activity of OXPHOS remained very low. Previously, agonists of PPARγ, such as thiazolidinedione and pioglitazone, were shown to elevate mitochondrial oxidative respiration and to prevent the loss of mitochondrial membrane potential (Corona & Duchen, 2016), indicating the importance of PPARγ in mitochondrial metabolism. However, in our study, the role of PPARγ in the metabolism of immune cells was not extensively studied, thus, the further understanding of these aspects is required.

5.6 *at*RA regulates NK cell effector functions

5.6.1 Cytokine production by a*t*RA-treated NK cells

The effects of vitamin A on NK cell effector functions remains unclear. Studies showed that *at*RA could promote NK cell cytotoxicity, by elevating the ligand expression on target cells (Grudzien & Rapak, 2018). For example, *at*RA induces retinoic acid early inducible (RAE-1) expression on embryonic carcinoma cell line F9 (Nomura, Takihara, & Shimada, 1994), which triggers NK cell cytotoxicity via engagement with NKG2D (Cerwenka et al., 2000). However, other studies demonstrated that *at*RA directly impaired effector functions of NK cells. For instance, after 5 days of exposure to *at*RA, NK cells showed impaired cytolytic activities, due to downregulated expression of cathepsin C, which regulates the production of granzyme (Sanchez-Martinez et al., 2014). To elucidate the direct impact of vitamin A on NK cell effector functions, we performed functional assays with NK cells exposed to *at*RA.

NK cell activation can be induced by various mechanisms of interaction with target cells. Thus, we co-cultured NK cells and tumor cells, including YAC-1 lymphoma cells, RMA-S lymphoma cells, or B16 melanoma cells, which can differentially activate NK cells. YAC-1 lymphoma cells were reported to express ligands of NKG2D, such as Rae-1 and MULT-1(Ogawa et al., 2011). The engagement of NKG2D and these ligands can facilitate NK cell cytotoxicity and cytokine production. B16 melanoma cells express CD155, a ligand of DNAM-1, and the interaction between CD155 and DNAM-1 was required for anti-metastasis activities of NK cells (Chan et al., 2010). RMA-S lymphoma cells is a subline of RMA, which can trigger NK cell cytotoxicity due to low MHC class I surface expression (Karre, Ljunggren, Piontek, & Kiessling, 1986). Our data showed that NK cells exposed to *at*RA produced lower amounts of IFN-γ upon stimulation with different tumor cells (Figure 3.10). The results indicate that differentially regulated expression of the activating receptors DNAM-1 and NKG2D by *at*RA-treatment did not affect the amounts of cytokine, and implies that the downstream signal of cytokine production in NK cells might be regulated by *at*RA. In accordance, *at*RA-treated NK cells released less amounts of IFN-γ in response to cytokine receptor-activation or activating NK cell receptor-engagement (Figure 3.9). We observed that the expression of genes involved in NFκB signaling pathway were enriched in *at*RA-treated NK cells (Figure 3.1), which are important for the development, proliferation and cytokine production of NK cells (Hayden & Ghosh, 2011). Indeed, upon stimulation with IL-18, a pro-inflammatory cytokine, the expression of IκBζ, which is a mediator of NFκB transcriptional programs, was downregulated in *at*RA-treated NK cells.

Upon co-culture with tumor cells, NK cells expressed CD107a, indicating degranulation of cells, and the degranulation of *at*RA-treated NK cells was higher compared to control NK cells. The degranulating subset of NK cells did not produce with IFN-γ, indicating that $CD107a^+$ NK

cells might release other secretory molecules upon degranulation. Thus, we hypothesized that *at*RA-treatment might reprogram the cytokine profile of NK cells. Our data showed that the relative mRNA expression of several inflammatory cytokines was upregulated in *at*RA-treated NK cells (Figure 3.11). For instance, Csf2 (encoding GM-CSF), and Tnfsf10 (encoding TRAIL), and Tnfsf11 (encoding RANKL) were increased. Additionally, the expression of genes that encode chemokines, such as Ccl5 and Ccl1, was increased. It was unexpected that *at*RA-treatment upregulated the mRNA expression of pro-inflammatory cytokines upon activating NK cell receptor-engagement, as vitamin A was reported to induce regulatory phenotypes of immune cells (Elias et al., 2008; Mucida et al., 2007; S. Xiao et al., 2008). It has to be further confirmed whether the altered mRNA expression could lead to the production of protein.

5.6.2 Crosstalk between *at*RA-treated NK cells and dendritic cells

NK cells, a part of the innate immune system, can regulate the adaptive immune responses via the crosstalk with dendritic cells (DCs). The crosstalk between NK cells and DCs can lead to NK cell activation, DC maturation or DC apoptosis (Walzer et al., 2005). For instance, pro-inflammatory cytokines derived from DCs, such as IL-12 and IL-18, can enhance IFN-γ production and lytic activity of NK cells (Borg et al., 2004; Gerosa et al., 2002; Yu et al., 2001). The production of IFN-γ and TNF-α by NK cells can induce the maturation of immature DCs, including increased expression of CD83, CD86 and MHC class I molecules (Piccioli et al., 2002; Vitale et al., 2005).

At a high ratio of NK to DCs, NK cells were shown to eliminate immature DCs (Ferlazzo et al., 2002; Piccioli et al., 2002), and the killing of DCs was mediated via a DNAM-1/CD155 axis or TRAIL-pathway (Hayakawa et al., 2004; Seth et al., 2009). Our results showed that the expression of several molecules, which play important roles in the interaction of NK cells and DCs, were altered in NK cells upon *at*RA-treatment. For instance, IFN-γ production was decreased, and TRAIL, DNAM-1, and GM-CSF expression was increased in *at*RA-treated NK cells. Therefore, we hypothesized that *at*RA-induced reprogramming might affect the crosstalk between NK cells and DCs.

Our data illustrate that control NK cells could enhance the expression of co-stimulatory molecules, such as CD80, CD86, and MHC class I molecules, on bone marrow-derived dendritic cells (BM-DCs) (Figure 3.13 and 3.14), indicating the maturation of DCs. However, *at*RA-treatment reduced the ability of NK cells to induce the maturation of BM-DCs. Co-stimulatory molecules are essential for antigen presentation of DCs and further T cell priming, thus, immature DCs with low expression of these molecules are considered less immunogenic or tolerogenic DCs (Ferlazzo & Morandi, 2014). We observed that the maturation of BM-DCs was mediated by IFN-γ secreted by NK cells, and due to a diminished production of IFN-γ, the maturation of

DCs induced by *at*RA-treated NK cells was lower than the maturation induced by control NK cells. Cytokines released by DCs, such as IL-12 and IL-18, can induce NK cell activation and cytokine production (Ferlazzo & Morandi, 2014). Upon stimulation with IL-12, the amount of IFN-γ produced by control NK cells and *at*RA-treated NK cells was comparable; on the other hand, upon stimulation with IL-18, *at*RA-treated NK cells produced lower amounts of IFN-γ. To understand the reciprocal interaction between BM-DCs and *at*RA-treated NK cells, more research on the mechanism mediating IFN-γ production by NK cells is needed.

In addition, our data showed that *at*RA-treated NK cells displayed increased expression of DNAM-1 and TRAIL, thus, we expected that the elimination of DCs by *at*RA-treated NK cells might be enhanced. However, *at*RA-treated NK cells displayed a reduced ability to eliminate immature DCs. Together, NK cells exposed to a vitamin A-enriched microenvironment might impair inflammatory responses.

5.6.3 Interaction between *at*RA-treated NK cells and T cells

The dual role of NK cells in T cell differentiation, proliferation and effector functions was largely explored. First, NK cells were shown to affect the functions and differentiation of T cells via crosstalk with DCs. For instance, DCs matured by activated NK cells could promote the proliferation of $CD4^+$ T cells, which was comparable to DCs-exposed to LPS (Gerosa et al., 2002). Previous studies showed that pro-inflammatory-cytokine-activated NK cells could support the differentiation of T_H1 cells and their IFN-γ production. Monocyte-derived DCs (MoDCs) that were co-cultured with IL-2- or IL-12-stimulated NK cells could induce IFN-γ-producing T cells (Agaugue, Marcenaro, Ferranti, Moretta, & Moretta, 2008). In lymphoid organs, the recruitment and activation of NK cells was required for T_H1 polarization and proliferation (Martin-Fontecha et al., 2004; Morandi et al., 2006). NK cells exposed to TGF-β induced inhibition of T_H1 polarization and IFN-γ production by T cells (Laouar et al., 2005).

On the contrary, NK cells were reported to inhibit T cell responses by eliminating T cells. In murine cytomegalovirus (MCMV) and lymphocytic choriomeningitis virus (LCMV) infection, NK cells eliminated $CD4^+$ T cells and $CD8^+$ T cells via TRAIL-induced apoptosis (Schuster et al., 2014), and limited the development of $CD8^+$ T cells via NKG2D-engagement (Lang et al., 2012). Moreover, the engagement of receptor 2B4 on NK cells could inhibit NK cell activation, and 2B4-deficient NK cells lysed activated $CD8^+$ T cells in a perforin-dependent manner (Waggoner et al., 2010). In homeostasis, NK cells and T cells are found in vitamin A-enriched tissues, and they can be further re-located to the tissues during inflammation. As several proteins involved in the interaction between NK cells and T cells were up- or down-regulated in NK cells upon *at*RA-treatment, such as NKG2D, TRAIL and IFN-γ, we hypothesize that *at*RA might affect NK cells and T cells interaction. To investigate the role of *at*RA-treated NK cells in $CD4^+$ T cell

differentiation, we co-cultured these NK cells with naïve $CD4^+$ T cells in different T cell-polarizing conditions.

We expected that control NK cells might support T_H1 differentiation, and that *at*RA-treated NK cells could not do so, due to a reduced production of IFN-γ. However, T_H1 differentiation and IFN-γ production by T cells were affected neither by the presence of control NK cells nor of *at*RA-treated NK cells (Figure 3.17) *at*RA-treated NK cells produced a similar amount of IFN-γ compared to control NK cells in response to IL-12, but not IL-18 (Figure 3.9), and T_H1-polarizing condition included IL-2 and IL-12. Hence, the support of T_H1 differentiation mediated by IFN-γ is comparable upon co-culture with control NK cells or *at*RA-treated NK cells.

Our data revealed that *at*RA-treated NK cells could upregulate or maintain the FoxP3 expression, a transcription factor expressed by regulatory T (Treg) cells, in a contact-independent manner (Figure 3.18 and 3.19). Furthermore, both control NK cells and *at*RA-treated NK cells inhibited RORγt expression in T cells in the T_H17-polarizing condition. We aimed to elucidate, which soluble factor produced by *at*RA-treated NK cells could regulate FoxP3 expression of T cells. The first candidate was adenosine, as *at*RA-treated NK cells displayed increased adenosine ecto-enzyme expression, such as CD73, CD39 and CD38, which implies a potential production of adenosine. Adenosine was reported to modulate the activation and responses of Treg cells (S. R. Ma et al., 2017; Martinez-Navio et al., 2011; Ring, Oliver, Cronstein, Enk, & Mahnke, 2009). The second candidate was IL-10, as the differentiation of Treg cells is supported by IL-10 (Hsu et al., 2015), and it was reported that *at*RA converted human ILC2s to IL-10-producing ILCs *in vitro* (Morita et al., 2019). The third and fourth candidates were chemokines CCL1 and CCL5. Studies showed that CCL1 and CCL5 played an important role in the recruitment of Treg cells to the gut and tumor microenvironment (TME) (Kuehnemuth et al., 2018; Tan et al., 2009; X. Wang et al., 2017). We detected increased Ccl1 and Ccl5 relative mRNA expression in *at*RA-treated NK cells. We inhibited the function of four candidates as outlined above by using antibodies or antagonists; however, this did not result in differential FoxP3 expression in T cells (Figure 3.20)

Although we could not decipher which molecule supported FoxP3 expression on T cells upon co-culture with *at*RA-treated NK cells, we observed that the proliferation of FoxP3-expressing T cells was enhanced in the presence of *at*RA-treated NK cells (Figure 3.19). As IL-2 was reported to support expansion of Treg cells (Fontenot, Rasmussen, Gavin, & Rudensky, 2005; Zorn et al., 2006), we postulated that the affinity of the IL-2 receptors (IL-2R) on T cells could support FoxP3 expression and proliferation. Furthermore, studies indicated that $CD25^+CD4^+$ Treg cells competed with other types of T cells for IL-2, due to the high affinity of IL-2R on Treg cells (Barthlott et al., 2005; Busse et al., 2010; Salinas, Olguin, Castellanos, & Saavedra, 2014). As both NK cells and T cells express IL-2 receptors and respond to IL-2 (Farrar,

Johnson, & Farrar, 1981; Handa, Suzuki, Matsui, Shimizu, & Kumagai, 1983; Wagner et al., 1980), the competition between T cells and *at*RA-treated NK cells might regulate the differentiation of Treg cells. Accordingly, the expression of IL-2 receptors and the downstream signal of IL-2, such as signal transducer and activator of transcription-5 (STAT5) should be further studied.

The balance between pro-inflammatory T_H17 cells and negative immune regulator Treg cells is important for the tissue homeostasis and immunity to infections. It was demonstrated that different combinations of cytokines could modulate the T_H17/Treg balance (Deknuydt, Bioley, Valmori, & Ayyoub, 2009; Koenen et al., 2008; Yang et al., 2008). In gut, intestinal microbiota-derived short chain fatty acid support the differentiation and homeostasis of Treg cells (Arpaia et al., 2013; Furusawa et al., 2013; P. M. Smith et al., 2013). During yeast infection and in inflammatory bowel disease, IL-17A production by FoxP3-expressing Treg cells was observed in the lamina propria and in the intraepithelial area (Bhaskaran, Cohen, Zhang, Weinberg, & Pandiyan, 2015), indicating the conversion between inflammatory and regulatory features of T cells. Based on our NK cells/T cells co-culture assays, we anticipate that NK cells could play an important role in regulating balance between T_H17/Treg in vitamin A-enriched microenvironments.

5.7 Physiological relevance of *at*RA-treated NK cells

We showed that *at*RA reprogramed NK cells during *in vitro* culture, for example, inducing phenotypic changes, affecting metabolism, and altering effector functions. To find the physiological relevance of our findings, we examined the phenotype of NK cells in tissues, enriched with vitamin A.

In 8-16 week-old mice, the average physiological concentrations of retinol are 560 nmol/g in liver, 1.2 nmol/g in spleen, and 0.22 nmol/g in serum; the physiological concentrations of *at*RA are 15 pmol/g in liver and 4 pmol/mL (=4 nM) in serum (Kane et al., 2008; Obrochta, Kane, & Napoli, 2014). In murine spleens, NK cells did not display an *at*RA-induced phenotype. In murine livers and lungs, where abundant vitamin A metabolites are found, we also did not observe NK cells displaying *at*RA-induced phenotype. We postulated that *at*RA-exposure *in vitro* might be not comparable to the physiological concentrations of *at*RA, as we cultured murine NK cells in the presence of 1 µM of *at*RA for 7 days. Another reason is that NK cells in organs might be exposed to dynamic changes of microenvironment, compared to NK cells cultured *in vitro*. This might explain that one micronutrient could not modulate NK cell features in steady-state.

In addition to homeostatic conditions, RA signaling is demonstrated to affect metabolic disorders and non-alcoholic fatty liver disease (NAFLD). Studies demonstrated that patients with

metabolic disorders and NAFLD showed significantly lower RA concertation in the serum, compared to healthy individuals (Godala et al., 2017; Y. Liu et al., 2016; Y. Liu et al., 2015). On the other hand, one study reported that the concentration of RA in livers was upregulated, and the concentrations of retinol and retinaldehyde in livers were downregulated in mice with liver cirrhosis (Natarajan et al., 2005). Multiple studies reported that *at*RA-treatment alleviated the symptoms of liver fibrosis and hepatitis via modulating the collagen production by hepatic stellate cells (HSCs), γδT cell and NKT cell responses, and TGFβ production (Hisamori et al., 2008; Jie et al., 2017; K. A. Lee et al., 2012; Seguin-Devaux et al., 2005). Mouse injected with Con A displayed liver damage, and RA injection alleviated the damage via inhibiting effector functions of NKT cells (K. A. Lee et al., 2012). In liver disease stated above, NK cells are recruited to liver and serve important a role in immune responses. For instance, NK cells alleviated liver fibrosis by exerting cytotoxicity against hepatocytes and HSCs via TRAIL-, FasL- or NKG2D-pathway (Y. Chen et al., 2007; Cheng et al., 2011; Dunn et al., 2007; Lassen et al., 2010; Ochi et al., 2004; Radaeva et al., 2007; Stegmann et al., 2010; Zou et al., 2010). In addition, we observed that a vitamin A could modulate expression of cell surface proteins and production of cytokines of NK cells. These differentially reguated molecules play important roles in NK cell functions upon liver diseases. Therefore, it is required to investigate whether vitamin A-treatment for liver diseases could modulate NK cell activities in future studies.

A recent study demonstrated that sarcoma tissues were enriched with *at*RA, resulting in the differentiation of immunosuppressive myeloid cells (Devalaraja et al., 2020). Together with myeloid cells in TME, lymphocytes, such as NK cells, can perform anti-tumor activities by recognizing and killing tumor cells. Thus, it is essential to elucidate effector functions and anti-tumor activities of NK cells in the vitamin A-enriched TME. However, in our experimental settings, fibrosarcoma tissues did not express higher amounts of the retinoic acid-metabolizing enzyme, Raldh, compared to other types of tumor tissues (Figure 3.22).

In contrast to the immunosuppressive effect of vitamin A on immune cells in the TME, studies suggested anti-tumor effects of vitamin A metabolites. For example, it was reported that *at*RA could suppress the cell growth of breast cancer, prostate cancer, and lung cancer cells by inducing apoptosis of tumor cells *in vitro* and *in vivo* (Koshiuka et al., 2000; Manna & Aggarwal, 2000; Niu, Menard, Reed, Krajewski, & Pratt, 2001; S. Y. Sun, Wan, Yue, Hong, & Lotan, 2000; Q. Wang, Yang, Uytingco, Christakos, & Wieder, 2000). These results provide potential use of vitamin A as an anti-cancer treatment. Large trials conducted in Europe, Japan and the United States, have concluded that the administration of β-carotene, a precursor of vitamin A, does not have beneficial effects for cancer-patients (Miller, 1998). On the contrary, retinoids were shown to suppress carcinogenesis (Lotan, 1996). Additionally, chronic administration of high concentrations of retinoids induced toxicity, resulting in anorexia, fever, alopecia, or joint pain

(Chytil, 1984). Therefore, further studies have to be conducted to understand the clinical impact of vitamin A metabolites on anti-tumor effects.

In co-culture assays, *at*RA-reprogrammed NK cells induced immaturities of DCs and supported the differentiation and proliferation of Treg cells, which might result in tolerogenic immune responses. This might not be beneficial for immune responses, where anti-tumor or anti-viral activities are required. However, in autoimmune diseases or hypersensitivity, where immune cells are over-activated, the impact of *at*RA on NK cells might contribute to therapeutic effects. Studies illustrated that *at*RA-treatment supported Treg cells to suppress IFN-γ production in patients with type 1 diabetes (Van et al., 2009; Y. Wang, Zhong, Wang, Xing, & Wang, 2016). Furthermore, *at*RA was found to alleviate the intestinal inflammation in colitis (A. Bai et al., 2010; K. Hong et al., 2014) and the adenomatous polyposis models (Penny et al., 2016). As *at*RA-treated NK cells promoted Treg cells, we anticipate that NK cells exposed to and shaped by vitamin A metabolites might play a protective role in autoimmune diseases.

In conclusion, we demonstrated that *at*RA, a prevalent vitamin A metabolite, could induce the transcriptional, phenotypical and functional reprogramming of NK cells *in vitro*. It is difficult to relate experimental results directly to the physiological settings in steady-state due to the high concentration of *at*RA used in *in vitro* studies. However, numerous studies illustrated that RA-signaling could regulate immune responses in liver disease, cancer and autoimmune disease. Thus, the understanding of how vitamin A can influence NK cell-mediated immune responses in these diseases will broaden the knowledge of the effect of essential nutrients on the immune system function.

6 SUMMARY

Vitamin A, a fat-soluble micronutrient, plays an indispensable role in embryogenesis and development, and was also reported to regulate immune responses. In mammals, Vitamin A-enriched tissues, such as liver, gut or fat, comprise various immune cells. NK cells, circulating innate lymphocytes, are frequently recruited to tissues during inflammatory responses. NK cells contribute to tissue homeostasis by eliminating abnormal cells and modulating immune responses. However, the influence of vitamin A in regulating NK cell-mediated immune responses remains unclear.

Here, we investigated the effect of the vitamin A metabolite, all-*trans* retinoic acid (*at*RA) on murine NK cells. We showed that *at*RA induced transcriptional and phenotypic reprogramming of NK cells, depicted as altered expression of transcription factors, receptors, adhesion molecules and metabolizing-enzymes. In addition, *at*RA altered effector functions of NK cells, which led to a reduced production of inflammatory cytokines, such as interferon gamma (IFN-γ), in response to various stimuli. Our data revealed that *at*RA reduced ability of NK cells to induce maturation of dendritic cells (DCs) or to remove immature DCs, resulting in an increased number of immature antigen-presenting cells. NK cells treated with *at*RA supported FoxP3 expression and proliferation of regulatory T cells, promoting immune-regulatory microenvironment.

Furthermore, *at*RA altered mitochondrial fitness and metabolisms of NK cells by enhancing mitochondrial respiration. Peroxisome proliferator-activated receptor gamma (PPARγ), a nuclear receptor, was upregulated by NK cells upon exposure to *at*RA. The conditional deletion of PPARγ in NK cells caused impaired glycolysis and mitochondrial respiration, and the malfunction of metabolism of PPARγ-deficient NK cells could be rescued by *at*RA.

In summary, we identify a novel role of vitamin A in shaping molecular and functional characteristics of NK cells. We demonstrate regulatory functions of vitamin A-exposed NK cells and their ability to regulate other immune cells, which might contribute to tolerogenic immune responses.

7 CURRICULUM VITAE AND PUBLICATIONS

PERSONAL INFORMATION

Name und surname:	Mingeum Jeong.....
Birthday:	04.12.1991.....
Birthplace:	Cheongju-si, Republic of Korea.....
Nationality	Korean

EDUCATION

02.2018 - Present	**Promotion, Dr. sc. hum. (scientiarum humanarum)** Majored in Immunology Medical Faculty of Mannheim Heidelberg University, Germany Thesis: The impact of vitamin A metabolites on natural killer cell functions
09.2013 - 08.2015	**Master of Science** in Integrated Biomedical and Life Sciences Majored in Food and Nutritional Science Korea University in Seoul, South Korea GPA 4.5/4.5 Thesis: Beneficial effect of *Aspergillus oryzae*-fermented Germinated Soybeans Extract on perimenopausal symptoms in ovariectomized rats
03.1910 - 08.2013	**Bachelor of Science** in Food and Nutritional Sciences Korea University in Seoul, South Korea GPA 4.02/4.5 (Summa cum laude)

WORK EXPERIENCE

04.2016 – 08.2017 **Postgraduate associate**

Yale University in New Haven, CT, USA

PUBLICATION

E Berdyshev, E Goleva, I Bronova, N Dyjack, C Rios, J Jung, P Taylor, **M Jeong**, C F Hall, B N Richers, K A Norquest, T Zheng, M A Seibold, D YM Leung, “Lipid abnormalities in atopic skin are driven by type 2 cytokines”, *The Journal of Clinical Investigation Insight* (2018)

H Lou, J Lu, EB Choi, MH Oh, **M Jeong**, S Barmettler, Z Zhu, T Zheng, “Expression of IL-22 in the skin causes Th2-biased immunity, epidermal barrier dysfunction, and pruritus via stimulating epithelial Th2 cytokines and the GRP pathway“, *Journal of Immunology* (2017)

M Jeong, DS Lee, HJ Suh, Y Park, “*Aspergillus oryzae* fermented germinated soybean extract alleviates perimenopausal symptoms in ovariectomised rats”, *Journal of the Science of Food and Agriculture* (2016)

K Hong, **M Jeong**, KS Han, JH Kim, Y Park, HJ Suh, “Photoprotective effects of galacto-oligosaccharide and/or *Bifidobacterium longum* supplementation against skin damage induced by ultraviolet irradiation in hairless mice”, *International Journal of Food Sciences and Nutrition* (2015)

8 REFERENCE

Abel, A. M., Yang, C., Thakar, M. S., & Malarkannan, S. (2018). Natural Killer Cells: Development, Maturation, and Clinical Utilization. *Front Immunol, 9*, 1869. doi:10.3389/fimmu.2018.01869

Aderem, A., & Underhill, D. M. (1999). Mechanisms of phagocytosis in macrophages. *Annu Rev Immunol, 17*, 593-623. doi:10.1146/annurev.immunol.17.1.593

Agaugue, S., Marcenaro, E., Ferranti, B., Moretta, L., & Moretta, A. (2008). Human natural killer cells exposed to IL-2, IL-12, IL-18, or IL-4 differently modulate priming of naive T cells by monocyte-derived dendritic cells. *Blood, 112*(5), 1776-1783. doi:10.1182/blood-2008-02-135871

Ahlemeyer, B., Bauerbach, E., Plath, M., Steuber, M., Heers, C., Tegtmeier, F., & Krieglstein, J. (2001). Retinoic acid reduces apoptosis and oxidative stress by preservation of SOD protein level. *Free Radic Biol Med, 30*(10), 1067-1077. doi:10.1016/s0891-5849(01)00495-6

Ahmadian, M., Suh, J. M., Hah, N., Liddle, C., Atkins, A. R., Downes, M., & Evans, R. M. (2013). PPARgamma signaling and metabolism: the good, the bad and the future. *Nat Med, 19*(5), 557-566. doi:10.1038/nm.3159

Airas, L., Niemela, J., Salmi, M., Puurunen, T., Smith, D. J., & Jalkanen, S. (1997). Differential regulation and function of CD73, a glycosyl-phosphatidylinositol-linked 70-kD adhesion molecule, on lymphocytes and endothelial cells. *J Cell Biol, 136*(2), 421-431. doi:10.1083/jcb.136.2.421

Akira, S., Hoshino, K., & Kaisho, T. (2000). The role of Toll-like receptors and MyD88 in innate immune responses. *J Endotoxin Res, 6*(5), 383-387. Retrieved from https://www.ncbi.nlm.nih.gov/pubmed/11521059

Akira, S., & Takeda, K. (2004). Toll-like receptor signalling. *Nat Rev Immunol, 4*(7), 499-511. doi:10.1038/nri1391

Aktas, E., Kucuksezer, U. C., Bilgic, S., Erten, G., & Deniz, G. (2009). Relationship between CD107a expression and cytotoxic activity. *Cell Immunol, 254*(2), 149-154. doi:10.1016/j.cellimm.2008.08.007

Ali, A. K., Komal, A. K., Almutairi, S. M., & Lee, S. H. (2019). Natural Killer Cell-Derived IL-10 Prevents Liver Damage During Sustained Murine Cytomegalovirus Infection. *Front Immunol, 10*, 2688. doi:10.3389/fimmu.2019.02688

Alimonti, J. B., Shi, L., Baijal, P. K., & Greenberg, A. H. (2001). Granzyme B induces BID-mediated cytochrome c release and mitochondrial permeability transition. *J Biol Chem, 276*(10), 6974-6982. doi:10.1074/jbc.M008444200

Alter, G., Malenfant, J. M., & Altfeld, M. (2004). CD107a as a functional marker for the identification of natural killer cell activity. *J Immunol Methods, 294*(1-2), 15-22. doi:10.1016/j.jim.2004.08.008

Amengual, J., Ribot, J., Bonet, M. L., & Palou, A. (2010). Retinoic acid treatment enhances lipid oxidation and inhibits lipid biosynthesis capacities in the liver of mice. *Cell Physiol Biochem, 25*(6), 657-666. doi:10.1159/000315085

Andoniou, C. E., Sutton, V. R., Wikstrom, M. E., Fleming, P., Thia, K. Y., Matthews, A. Y., . . . Degli-Esposti, M. A. (2014). A natural genetic variant of granzyme B confers lethality to a common viral infection. *PLoS Pathog, 10*(12), e1004526. doi:10.1371/journal.ppat.1004526

Andrews, D. M., Scalzo, A. A., Yokoyama, W. M., Smyth, M. J., & Degli-Esposti, M. A. (2003). Functional interactions between dendritic cells and NK cells during viral infection. *Nat Immunol, 4*(2), 175-181. doi:10.1038/ni880

Angela, M., Endo, Y., Asou, H. K., Yamamoto, T., Tumes, D. J., Tokuyama, H., . . . Nakayama, T. (2016). Fatty acid metabolic reprogramming via mTOR-mediated

inductions of PPARgamma directs early activation of T cells. *Nat Commun, 7*, 13683. doi:10.1038/ncomms13683

Aparicio-Domingo, P., Romera-Hernandez, M., Karrich, J. J., Cornelissen, F., Papazian, N., Lindenbergh-Kortleve, D. J., . . . Cupedo, T. (2015). Type 3 innate lymphoid cells maintain intestinal epithelial stem cells after tissue damage. *J Exp Med, 212*(11), 1783-1791. doi:10.1084/jem.20150318

Arango Duque, G., & Descoteaux, A. (2014). Macrophage cytokines: involvement in immunity and infectious diseases. *Front Immunol, 5*, 491. doi:10.3389/fimmu.2014.00491

Arpaia, N., Campbell, C., Fan, X., Dikiy, S., van der Veeken, J., deRoos, P., . . . Rudensky, A. Y. (2013). Metabolites produced by commensal bacteria promote peripheral regulatory T-cell generation. *Nature, 504*(7480), 451-455. doi:10.1038/nature12726

Assmann, N., O'Brien, K. L., Donnelly, R. P., Dyck, L., Zaiatz-Bittencourt, V., Loftus, R. M., . . . Finlay, D. K. (2017). Srebp-controlled glucose metabolism is essential for NK cell functional responses. *Nat Immunol, 18*(11), 1197-1206. doi:10.1038/ni.3838

Aste-Amezaga, M., D'Andrea, A., Kubin, M., & Trinchieri, G. (1994). Cooperation of natural killer cell stimulatory factor/interleukin-12 with other stimuli in the induction of cytokines and cytotoxic cell-associated molecules in human T and NK cells. *Cell Immunol, 156*(2), 480-492. doi:10.1006/cimm.1994.1192

Bai, A., Lu, N., Zeng, H., Li, Z., Zhou, X., Chen, J., . . . Guo, Y. (2010). All-trans retinoic acid ameliorates trinitrobenzene sulfonic acid-induced colitis by shifting Th1 to Th2 profile. *J Interferon Cytokine Res, 30*(6), 399-406. doi:10.1089/jir.2009.0028

Bai, L., Vienne, M., Tang, L., Kerdiles, Y., Etiennot, M., Escaliere, B., . . . Tian, Z. (2021). Liver type 1 innate lymphoid cells develop locally via an interferon-gamma-dependent loop. *Science, 371*(6536). doi:10.1126/science.aba4177

Bakdash, G., Vogelpoel, L. T., van Capel, T. M., Kapsenberg, M. L., & de Jong, E. C. (2015). Retinoic acid primes human dendritic cells to induce gut-homing, IL-10-producing regulatory T cells. *Mucosal Immunol, 8*(2), 265-278. doi:10.1038/mi.2014.64

Barthlott, T., Moncrieffe, H., Veldhoen, M., Atkins, C. J., Christensen, J., O'Garra, A., & Stockinger, B. (2005). CD25+ CD4+ T cells compete with naive CD4+ T cells for IL-2 and exploit it for the induction of IL-10 production. *Int Immunol, 17*(3), 279-288. doi:10.1093/intimm/dxh207

Becher, B., Tugues, S., & Greter, M. (2016). GM-CSF: From Growth Factor to Central Mediator of Tissue Inflammation. *Immunity, 45*(5), 963-973. doi:10.1016/j.immuni.2016.10.026

Beijer, M. R., Molenaar, R., Goverse, G., Mebius, R. E., Kraal, G., & den Haan, J. M. (2013). A crucial role for retinoic acid in the development of Notch-dependent murine splenic CD8- CD4- and CD4+ dendritic cells. *Eur J Immunol, 43*(6), 1608-1616. doi:10.1002/eji.201343325

Bernardini, G., Gismondi, A., & Santoni, A. (2012). Chemokines and NK cells: regulators of development, trafficking and functions. *Immunol Lett, 145*(1-2), 39-46. doi:10.1016/j.imlet.2012.04.014

Bhaskaran, N., Cohen, S., Zhang, Y., Weinberg, A., & Pandiyan, P. (2015). TLR-2 Signaling Promotes IL-17A Production in CD4+CD25+Foxp3+ Regulatory Cells during Oropharyngeal Candidiasis. *Pathogens, 4*(1), 90-110. doi:10.3390/pathogens4010090

Bidad, K., Salehi, E., Oraei, M., Saboor-Yaraghi, A. A., & Nicknam, M. H. (2011). Effect of all-trans retinoic acid (ATRA) on viability, proliferation, activation and lineage-specific transcription factors of CD4+ T cells. *Iran J Allergy Asthma Immunol, 10*(4), 243-249. doi:010.04/ijaai.243249

Birch, H. E., & Schreiber, G. (1986). Transcriptional regulation of plasma protein synthesis during inflammation. *J Biol Chem, 261*(18), 8077-8080. Retrieved from https://www.ncbi.nlm.nih.gov/pubmed/2424892

Blomhoff, R., Green, M. H., Berg, T., & Norum, K. R. (1990). Transport and storage of vitamin A. *Science, 250*(4979), 399-404. doi:10.1126/science.2218545

Blomhoff, R., Helgerud, P., Rasmussen, M., Berg, T., & Norum, K. R. (1982). In vivo uptake of chylomicron [3H]retinyl ester by rat liver: evidence for retinol transfer from parenchymal to nonparenchymal cells. *Proc Natl Acad Sci U S A, 79*(23), 7326-7330. doi:10.1073/pnas.79.23.7326

Borg, C., Jalil, A., Laderach, D., Maruyama, K., Wakasugi, H., Charrier, S., . . . Zitvogel, L. (2004). NK cell activation by dendritic cells (DCs) requires the formation of a synapse leading to IL-12 polarization in DCs. *Blood, 104*(10), 3267-3275. doi:10.1182/blood-2004-01-0380

Bouchery, T., Kyle, R., Camberis, M., Shepherd, A., Filbey, K., Smith, A., . . . Le Gros, G. (2015). ILC2s and T cells cooperate to ensure maintenance of M2 macrophages for lung immunity against hookworms. *Nat Commun, 6*, 6970. doi:10.1038/ncomms7970

Brady, J., Carotta, S., Thong, R. P., Chan, C. J., Hayakawa, Y., Smyth, M. J., & Nutt, S. L. (2010). The interactions of multiple cytokines control NK cell maturation. *J Immunol, 185*(11), 6679-6688. doi:10.4049/jimmunol.0903354

Brand, A., Singer, K., Koehl, G. E., Kolitzus, M., Schoenhammer, G., Thiel, A., . . . Kreutz, M. (2016). LDHA-Associated Lactic Acid Production Blunts Tumor Immunosurveillance by T and NK Cells. *Cell Metab, 24*(5), 657-671. doi:10.1016/j.cmet.2016.08.011

Brockman, M. A., Kwon, D. S., Tighe, D. P., Pavlik, D. F., Rosato, P. C., Sela, J., . . . Kaufmann, D. E. (2009). IL-10 is up-regulated in multiple cell types during viremic HIV infection and reversibly inhibits virus-specific T cells. *Blood, 114*(2), 346-356. doi:10.1182/blood-2008-12-191296

Brown, G. C., & Borutaite, V. (2008). Regulation of apoptosis by the redox state of cytochrome c. *Biochim Biophys Acta, 1777*(7-8), 877-881. doi:10.1016/j.bbabio.2008.03.024

Buentke, E., Heffler, L. C., Wilson, J. L., Wallin, R. P., Lofman, C., Chambers, B. J., . . . Scheynius, A. (2002). Natural killer and dendritic cell contact in lesional atopic dermatitis skin--Malassezia-influenced cell interaction. *J Invest Dermatol, 119*(4), 850-857. doi:10.1046/j.1523-1747.2002.00132.x

Bushue, N., & Wan, Y. Y. (2009). Retinoic Acid-mediated Nuclear Receptor Activation and Hepatocyte Proliferation. *J Exp Clin Med, 1*(1), 23-30. doi:10.1016/S1878-3317(09)60007-3

Busse, D., de la Rosa, M., Hobiger, K., Thurley, K., Flossdorf, M., Scheffold, A., & Hofer, T. (2010). Competing feedback loops shape IL-2 signaling between helper and regulatory T lymphocytes in cellular microenvironments. *Proc Natl Acad Sci U S A, 107*(7), 3058-3063. doi:10.1073/pnas.0812851107

Cai, G., Kastelein, R. A., & Hunter, C. A. (1999). IL-10 enhances NK cell proliferation, cytotoxicity and production of IFN-gamma when combined with IL-18. *Eur J Immunol, 29*(9), 2658-2665. doi:10.1002/(SICI)1521-4141(199909)29:09<2658::AID-IMMU2658>3.0.CO;2-G

Campbell, I. K., Rich, M. J., Bischof, R. J., Dunn, A. R., Grail, D., & Hamilton, J. A. (1998). Protection from collagen-induced arthritis in granulocyte-macrophage colony-stimulating factor-deficient mice. *J Immunol, 161*(7), 3639-3644. Retrieved from https://www.ncbi.nlm.nih.gov/pubmed/9759887

Candia, E., Reyes, P., Covian, C., Rodriguez, F., Wainstein, N., Morales, J., . . . Fierro, J. A. (2017). Single and combined effect of retinoic acid and rapamycin modulate the generation, activity and homing potential of induced human regulatory T cells. *PLoS One, 12*(7), e0182009. doi:10.1371/journal.pone.0182009

Carbone, E., Terrazzano, G., Ruggiero, G., Zanzi, D., Ottaiano, A., Manzo, C., . . . Zappacosta, S. (1999). Recognition of autologous dendritic cells by human NK cells. *Eur J Immunol, 29*(12), 4022-4029. doi:10.1002/(SICI)1521-4141(199912)29:12<4022::AID-IMMU4022>3.0.CO;2-O

Castriconi, R., Cantoni, C., Della Chiesa, M., Vitale, M., Marcenaro, E., Conte, R., . . . Moretta, A. (2003). Transforming growth factor beta 1 inhibits expression of NKp30 and NKG2D receptors: consequences for the NK-mediated killing of dendritic cells. *Proc Natl Acad Sci U S A, 100*(7), 4120-4125. doi:10.1073/pnas.0730640100

Caux, C., Vanbervliet, B., Massacrier, C., Dezutter-Dambuyant, C., de Saint-Vis, B., Jacquet, C., . . . Banchereau, J. (1996). CD34+ hematopoietic progenitors from human cord blood differentiate along two independent dendritic cell pathways in response to GM-CSF+TNF alpha. *J Exp Med, 184*(2), 695-706. doi:10.1084/jem.184.2.695

Cerboni, C., Zingoni, A., Cippitelli, M., Piccoli, M., Frati, L., & Santoni, A. (2007). Antigen-activated human T lymphocytes express cell-surface NKG2D ligands via an ATM/ATR-dependent mechanism and become susceptible to autologous NK- cell lysis. *Blood, 110*(2), 606-615. doi:10.1182/blood-2006-10-052720

Cerwenka, A., Bakker, A. B., McClanahan, T., Wagner, J., Wu, J., Phillips, J. H., & Lanier, L. L. (2000). Retinoic acid early inducible genes define a ligand family for the activating NKG2D receptor in mice. *Immunity, 12*(6), 721-727. doi:10.1016/s1074-7613(00)80222-8

Chan, C. J., Andrews, D. M., McLaughlin, N. M., Yagita, H., Gilfillan, S., Colonna, M., & Smyth, M. J. (2010). DNAM-1/CD155 interactions promote cytokine and NK cell-mediated suppression of poorly immunogenic melanoma metastases. *J Immunol, 184*(2), 902-911. doi:10.4049/jimmunol.0903225

Chea, S., Schmutz, S., Berthault, C., Perchet, T., Petit, M., Burlen-Defranoux, O., . . . Golub, R. (2016). Single-Cell Gene Expression Analyses Reveal Heterogeneous Responsiveness of Fetal Innate Lymphoid Progenitors to Notch Signaling. *Cell Rep, 14*(6), 1500-1516. doi:10.1016/j.celrep.2016.01.015

Chelstowska, S., Widjaja-Adhi, M. A., Silvaroli, J. A., & Golczak, M. (2016). Molecular Basis for Vitamin A Uptake and Storage in Vertebrates. *Nutrients, 8*(11). doi:10.3390/nu8110676

Chen, M. C., Hsu, S. L., Lin, H., & Yang, T. Y. (2014). Retinoic acid and cancer treatment. *Biomedicine (Taipei), 4*, 22. doi:10.7603/s40681-014-0022-1

Chen, W., & Chen, G. (2014). The Roles of Vitamin A in the Regulation of Carbohydrate, Lipid, and Protein Metabolism. *J Clin Med, 3*(2), 453-479. doi:10.3390/jcm3020453

Chen, Y., Wei, H., Sun, R., Dong, Z., Zhang, J., & Tian, Z. (2007). Increased susceptibility to liver injury in hepatitis B virus transgenic mice involves NKG2D-ligand interaction and natural killer cells. *Hepatology, 46*(3), 706-715. doi:10.1002/hep.21872

Cheng, C. W., Duwaerts, C. C., Rooijen, N., Wintermeyer, P., Mott, S., & Gregory, S. H. (2011). NK cells suppress experimental cholestatic liver injury by an interleukin-6-mediated, Kupffer cell-dependent mechanism. *J Hepatol, 54*(4), 746-752. doi:10.1016/j.jhep.2010.07.018

Chidipi, B., Shah, S. I., Reiser, M., Kanithi, M., Garces, A., Cha, B. J., . . . Noujaim, S. F. (2021). All-Trans Retinoic Acid Increases DRP1 Levels and Promotes Mitochondrial Fission. *Cells, 10*(5). doi:10.3390/cells10051202

Chiu, H. J., Fischman, D. A., & Hammerling, U. (2008). Vitamin A depletion causes oxidative stress, mitochondrial dysfunction, and PARP-1-dependent energy deprivation. *FASEB J, 22*(11), 3878-3887. doi:10.1096/fj.08-112375

Chiu, V. K., Walsh, C. M., Liu, C. C., Reed, J. C., & Clark, W. R. (1995). Bcl-2 blocks degranulation but not fas-based cell-mediated cytotoxicity. *J Immunol, 154*(5), 2023-2032. Retrieved from https://www.ncbi.nlm.nih.gov/pubmed/7532659

Chong, W. P., van Panhuys, N., Chen, J., Silver, P. B., Jittayasothorn, Y., Mattapallil, M. J., . . . Caspi, R. R. (2015). NK-DC crosstalk controls the autopathogenic Th17 response through an innate IFN-gamma-IL-27 axis. *J Exp Med, 212*(10), 1739-1752. doi:10.1084/jem.20141678

Chytil, F. (1984). Retinoic acid: biochemistry, pharmacology, toxicology, and therapeutic use. *Pharmacol Rev, 36*(2 Suppl), 93S-100S. Retrieved from https://www.ncbi.nlm.nih.gov/pubmed/6382359

Cipolletta, D., Feuerer, M., Li, A., Kamei, N., Lee, J., Shoelson, S. E., . . . Mathis, D. (2012). PPAR-gamma is a major driver of the accumulation and phenotype of adipose tissue Treg cells. *Nature, 486*(7404), 549-553. doi:10.1038/nature11132

Clark, S. E., Burrack, K. S., Jameson, S. C., Hamilton, S. E., & Lenz, L. L. (2019). NK Cell IL-10 Production Requires IL-15 and IL-10 Driven STAT3 Activation. *Front Immunol, 10*, 2087. doi:10.3389/fimmu.2019.02087

Clark, S. E., Filak, H. C., Guthrie, B. S., Schmidt, R. L., Jamieson, A., Merkel, P., . . . Lenz, L. L. (2016). Bacterial Manipulation of NK Cell Regulatory Activity Increases Susceptibility to Listeria monocytogenes Infection. *PLoS Pathog, 12*(6), e1005708. doi:10.1371/journal.ppat.1005708

Clark, S. E., Schmidt, R. L., Aguilera, E. R., & Lenz, L. L. (2020). IL-10-producing NK cells exacerbate sublethal Streptococcus pneumoniae infection in the lung. *Transl Res, 226*, 70-82. doi:10.1016/j.trsl.2020.07.001

Clemente, C., Elba, S., Buongiorno, G., Berloco, P., Guerra, V., & Di Leo, A. (2002). Serum retinol and risk of hepatocellular carcinoma in patients with child-Pugh class A cirrhosis. *Cancer Lett, 178*(2), 123-129. doi:10.1016/s0304-3835(01)00843-6

Constantinides, M. G., McDonald, B. D., Verhoef, P. A., & Bendelac, A. (2014). A committed precursor to innate lymphoid cells. *Nature, 508*(7496), 397-401. doi:10.1038/nature13047

Cook, A. D., Pobjoy, J., Steidl, S., Durr, M., Braine, E. L., Turner, A. L., . . . Hamilton, J. A. (2012). Granulocyte-macrophage colony-stimulating factor is a key mediator in experimental osteoarthritis pain and disease development. *Arthritis Res Ther, 14*(5), R199. doi:10.1186/ar4037

Coombes, J. L., Siddiqui, K. R., Arancibia-Carcamo, C. V., Hall, J., Sun, C. M., Belkaid, Y., & Powrie, F. (2007). A functionally specialized population of mucosal CD103+ DCs induces Foxp3+ regulatory T cells via a TGF-beta and retinoic acid-dependent mechanism. *J Exp Med, 204*(8), 1757-1764. doi:10.1084/jem.20070590

Cooper, M. A., Elliott, J. M., Keyel, P. A., Yang, L., Carrero, J. A., & Yokoyama, W. M. (2009). Cytokine-induced memory-like natural killer cells. *Proc Natl Acad Sci U S A, 106*(6), 1915-1919. doi:10.1073/pnas.0813192106

Corona, J. C., & Duchen, M. R. (2016). PPARgamma as a therapeutic target to rescue mitochondrial function in neurological disease. *Free Radic Biol Med, 100*, 153-163. doi:10.1016/j.freeradbiomed.2016.06.023

Crouse, J., Bedenikovic, G., Wiesel, M., Ibberson, M., Xenarios, I., Von Laer, D., . . . Oxenius, A. (2014). Type I interferons protect T cells against NK cell attack mediated by the activating receptor NCR1. *Immunity, 40*(6), 961-973. doi:10.1016/j.immuni.2014.05.003

Cuturi, M. C., Anegon, I., Sherman, F., Loudon, R., Clark, S. C., Perussia, B., & Trinchieri, G. (1989). Production of hematopoietic colony-stimulating factors by human natural killer cells. *J Exp Med, 169*(2), 569-583. doi:10.1084/jem.169.2.569

D'Andrea, A., Aste-Amezaga, M., Valiante, N. M., Ma, X., Kubin, M., & Trinchieri, G. (1993). Interleukin 10 (IL-10) inhibits human lymphocyte interferon gamma-production by suppressing natural killer cell stimulatory factor/IL-12 synthesis in accessory cells. *J Exp Med, 178*(3), 1041-1048. doi:10.1084/jem.178.3.1041

Daussy, C., Faure, F., Mayol, K., Viel, S., Gasteiger, G., Charrier, E., . . . Walzer, T. (2014). T-bet and Eomes instruct the development of two distinct natural killer cell lineages in the liver and in the bone marrow. *J Exp Med, 211*(3), 563-577. doi:10.1084/jem.20131560

Dawson, H. D., Collins, G., Pyle, R., Key, M., & Taub, D. D. (2008). The Retinoic Acid Receptor-alpha mediates human T-cell activation and Th2 cytokine and chemokine production. *BMC Immunol, 9*, 16. doi:10.1186/1471-2172-9-16

Deaglio, S., Dwyer, K. M., Gao, W., Friedman, D., Usheva, A., Erat, A., . . . Robson, S. C. (2007). Adenosine generation catalyzed by CD39 and CD73 expressed on regulatory T cells mediates immune suppression. *J Exp Med, 204*(6), 1257-1265. doi:10.1084/jem.20062512

Deknuydt, F., Bioley, G., Valmori, D., & Ayyoub, M. (2009). IL-1beta and IL-2 convert human Treg into T(H)17 cells. *Clin Immunol, 131*(2), 298-307. doi:10.1016/j.clim.2008.12.008

Della Chiesa, M., Vitale, M., Carlomagno, S., Ferlazzo, G., Moretta, L., & Moretta, A. (2003). The natural killer cell-mediated killing of autologous dendritic cells is confined to a cell subset expressing CD94/NKG2A, but lacking inhibitory killer Ig-like receptors. *Eur J Immunol, 33*(6), 1657-1666. doi:10.1002/eji.200323986

Derebe, M. G., Zlatkov, C. M., Gattu, S., Ruhn, K. A., Vaishnava, S., Diehl, G. E., . . . Hooper, L. V. (2014). Serum amyloid A is a retinol binding protein that transports retinol during bacterial infection. *Elife, 3*, e03206. doi:10.7554/eLife.03206

Devalaraja, S., To, T. K. J., Folkert, I. W., Natesan, R., Alam, M. Z., Li, M., . . . Haldar, M. (2020). Tumor-Derived Retinoic Acid Regulates Intratumoral Monocyte Differentiation to Promote Immune Suppression. *Cell, 180*(6), 1098-1114 e1016. doi:10.1016/j.cell.2020.02.042

Diefenbach, A., Colonna, M., & Koyasu, S. (2014). Development, differentiation, and diversity of innate lymphoid cells. *Immunity, 41*(3), 354-365. doi:10.1016/j.immuni.2014.09.005

DiRenzo, J., Soderstrom, M., Kurokawa, R., Ogliastro, M. H., Ricote, M., Ingrey, S., . . . Glass, C. K. (1997). Peroxisome proliferator-activated receptors and retinoic acid receptors differentially control the interactions of retinoid X receptor heterodimers with ligands, coactivators, and corepressors. *Mol Cell Biol, 17*(4), 2166-2176. doi:10.1128/MCB.17.4.2166

Doherty, G. M., Lange, J. R., Langstein, H. N., Alexander, H. R., Buresh, C. M., & Norton, J. A. (1992). Evidence for IFN-gamma as a mediator of the lethality of endotoxin and tumor necrosis factor-alpha. *J Immunol, 149*(5), 1666-1670. Retrieved from https://www.ncbi.nlm.nih.gov/pubmed/1506688

Domagala, J., Lachota, M., Klopotowska, M., Graczyk-Jarzynka, A., Domagala, A., Zhylko, A., . . . Winiarska, M. (2020). The Tumor Microenvironment-A Metabolic Obstacle to NK Cells' Activity. *Cancers (Basel), 12*(12). doi:10.3390/cancers12123542

Donnelly, R. P., Loftus, R. M., Keating, S. E., Liou, K. T., Biron, C. A., Gardiner, C. M., & Finlay, D. K. (2014). mTORC1-dependent metabolic reprogramming is a prerequisite for NK cell effector function. *J Immunol, 193*(9), 4477-4484. doi:10.4049/jimmunol.1401558

Dostert, C., Grusdat, M., Letellier, E., & Brenner, D. (2019). The TNF Family of Ligands and Receptors: Communication Modules in the Immune System and Beyond. *Physiol Rev, 99*(1), 115-160. doi:10.1152/physrev.00045.2017

Draghi, M., Pashine, A., Sanjanwala, B., Gendzekhadze, K., Cantoni, C., Cosman, D., . . . Parham, P. (2007). NKp46 and NKG2D recognition of infected dendritic cells is necessary for NK cell activation in the human response to influenza infection. *J Immunol, 178*(5), 2688-2698. doi:10.4049/jimmunol.178.5.2688

Dunn, C., Brunetto, M., Reynolds, G., Christophides, T., Kennedy, P. T., Lampertico, P., . . . Maini, M. K. (2007). Cytokines induced during chronic hepatitis B virus infection promote a pathway for NK cell-mediated liver damage. *J Exp Med, 204*(3), 667-680. doi:10.1084/jem.20061287

Duriancik, D. M., & Hoag, K. A. (2010). Vitamin A deficiency alters splenic dendritic cell subsets and increases CD8(+)Gr-1(+) memory T lymphocytes in C57BL/6J mice. *Cell Immunol, 265*(2), 156-163. doi:10.1016/j.cellimm.2010.08.006

Eberl, G., Di Santo, J. P., & Vivier, E. (2015). The brave new world of innate lymphoid cells. *Nat Immunol, 16*(1), 1-5. doi:10.1038/ni.3059

Einspahr, K. J., Abraham, R. T., Binstadt, B. A., Uehara, Y., & Leibson, P. J. (1991). Tyrosine phosphorylation provides an early and requisite signal for the activation of natural killer cell cytotoxic function. *Proc Natl Acad Sci U S A, 88*(14), 6279-6283. doi:10.1073/pnas.88.14.6279

Eisenhauer, P. B., Harwig, S. S., & Lehrer, R. I. (1992). Cryptdins: antimicrobial defensins of the murine small intestine. *Infect Immun, 60*(9), 3556-3565. doi:10.1128/iai.60.9.3556-3565.1992

El Costa, H., Casemayou, A., Aguerre-Girr, M., Rabot, M., Berrebi, A., Parant, O., . . . Tabiasco, J. (2008). Critical and differential roles of NKp46- and NKp30-activating receptors expressed by uterine NK cells in early pregnancy. *J Immunol, 181*(5), 3009-3017. doi:10.4049/jimmunol.181.5.3009

Elias, K. M., Laurence, A., Davidson, T. S., Stephens, G., Kanno, Y., Shevach, E. M., & O'Shea, J. J. (2008). Retinoic acid inhibits Th17 polarization and enhances FoxP3 expression through a Stat-3/Stat-5 independent signaling pathway. *Blood, 111*(3), 1013-1020. doi:10.1182/blood-2007-06-096438

Ercolano, G., Gomez-Cadena, A., Dumauthioz, N., Vanoni, G., Kreutzfeldt, M., Wyss, T., . . . Jandus, C. (2021). PPAR drives IL-33-dependent ILC2 pro-tumoral functions. *Nat Commun, 12*(1), 2538. doi:10.1038/s41467-021-22764-2

Erkelens, M. N., & Mebius, R. E. (2017). Retinoic Acid and Immune Homeostasis: A Balancing Act. *Trends Immunol, 38*(3), 168-180. doi:10.1016/j.it.2016.12.006

Exton, J. H. (1972). Gluconeogenesis. *Metabolism, 21*(10), 945-990. doi:10.1016/0026-0495(72)90028-5

Farrar, W. L., Johnson, H. M., & Farrar, J. J. (1981). Regulation of the production of immune interferon and cytotoxic T lymphocytes by interleukin 2. *J Immunol, 126*(3), 1120-1125. Retrieved from https://www.ncbi.nlm.nih.gov/pubmed/6161959

Feng, T., Cong, Y., Qin, H., Benveniste, E. N., & Elson, C. O. (2010). Generation of mucosal dendritic cells from bone marrow reveals a critical role of retinoic acid. *J Immunol, 185*(10), 5915-5925. doi:10.4049/jimmunol.1001233

Feng, X., Zhang, L., Acharya, C., An, G., Wen, K., Qiu, L., . . . Anderson, K. C. (2017). Targeting CD38 Suppresses Induction and Function of T Regulatory Cells to Mitigate Immunosuppression in Multiple Myeloma. *Clin Cancer Res, 23*(15), 4290-4300. doi:10.1158/1078-0432.CCR-16-3192

Ferlazzo, G., & Morandi, B. (2014). Cross-Talks between Natural Killer Cells and Distinct Subsets of Dendritic Cells. *Front Immunol, 5*, 159. doi:10.3389/fimmu.2014.00159

Ferlazzo, G., Morandi, B., D'Agostino, A., Meazza, R., Melioli, G., Moretta, A., & Moretta, L. (2003). The interaction between NK cells and dendritic cells in bacterial infections results in rapid induction of NK cell activation and in the lysis of uninfected dendritic cells. *Eur J Immunol, 33*(2), 306-313. doi:10.1002/immu.200310004

Ferlazzo, G., Pack, M., Thomas, D., Paludan, C., Schmid, D., Strowig, T., . . . Munz, C. (2004). Distinct roles of IL-12 and IL-15 in human natural killer cell activation by dendritic cells from secondary lymphoid organs. *Proc Natl Acad Sci U S A, 101*(47), 16606-16611. doi:10.1073/pnas.0407522101

Ferlazzo, G., Tsang, M. L., Moretta, L., Melioli, G., Steinman, R. M., & Munz, C. (2002). Human dendritic cells activate resting natural killer (NK) cells and are recognized via the NKp30 receptor by activated NK cells. *J Exp Med, 195*(3), 343-351. doi:10.1084/jem.20011149

Fernandez, N. C., Lozier, A., Flament, C., Ricciardi-Castagnoli, P., Bellet, D., Suter, M., . . . Zitvogel, L. (1999). Dendritic cells directly trigger NK cell functions: cross-talk relevant in innate anti-tumor immune responses in vivo. *Nat Med, 5*(4), 405-411. doi:10.1038/7403

Field, C. S., Baixauli, F., Kyle, R. L., Puleston, D. J., Cameron, A. M., Sanin, D. E., . . . Pearce, E. L. (2020). Mitochondrial Integrity Regulated by Lipid Metabolism Is a Cell-Intrinsic Checkpoint for Treg Suppressive Function. *Cell Metab, 31*(2), 422-437 e425. doi:10.1016/j.cmet.2019.11.021

Fontenot, J. D., Rasmussen, J. P., Gavin, M. A., & Rudensky, A. Y. (2005). A function for interleukin 2 in Foxp3-expressing regulatory T cells. *Nat Immunol, 6*(11), 1142-1151. doi:10.1038/ni1263

Friedman, S. L. (2008). Hepatic stellate cells: protean, multifunctional, and enigmatic cells of the liver. *Physiol Rev, 88*(1), 125-172. doi:10.1152/physrev.00013.2007

Furusawa, Y., Obata, Y., Fukuda, S., Endo, T. A., Nakato, G., Takahashi, D., . . . Ohno, H. (2013). Commensal microbe-derived butyrate induces the differentiation of colonic regulatory T cells. *Nature, 504*(7480), 446-450. doi:10.1038/nature12721

Gao, Y., Souza-Fonseca-Guimaraes, F., Bald, T., Ng, S. S., Young, A., Ngiow, S. F., . . . Smyth, M. J. (2017). Tumor immunoevasion by the conversion of effector NK cells into type 1 innate lymphoid cells. *Nat Immunol, 18*(9), 1004-1015. doi:10.1038/ni.3800

Gardiner, C. M., & Finlay, D. K. (2017). What Fuels Natural Killers? Metabolism and NK Cell Responses. *Front Immunol, 8*, 367. doi:10.3389/fimmu.2017.00367

Gasteiger, G., Fan, X., Dikiy, S., Lee, S. Y., & Rudensky, A. Y. (2015). Tissue residency of innate lymphoid cells in lymphoid and nonlymphoid organs. *Science, 350*(6263), 981-985. doi:10.1126/science.aac9593

Gazzinelli, R. T., Wysocka, M., Hayashi, S., Denkers, E. Y., Hieny, S., Caspar, P., . . . Sher, A. (1994). Parasite-induced IL-12 stimulates early IFN-gamma synthesis and resistance during acute infection with Toxoplasma gondii. *J Immunol, 153*(6), 2533-2543. Retrieved from https://www.ncbi.nlm.nih.gov/pubmed/7915739

Gerbec, Z. J., Hashemi, E., Nanbakhsh, A., Holzhauer, S., Yang, C., Mei, A., . . . Malarkannan, S. (2020). Conditional Deletion of PGC-1alpha Results in Energetic and Functional Defects in NK Cells. *iScience, 23*(9), 101454. doi:10.1016/j.isci.2020.101454

Gergely, P., Jr., Grossman, C., Niland, B., Puskas, F., Neupane, H., Allam, F., . . . Perl, A. (2002). Mitochondrial hyperpolarization and ATP depletion in patients with systemic lupus erythematosus. *Arthritis Rheum, 46*(1), 175-190. doi:10.1002/1529-0131(200201)46:1<175::AID-ART10015>3.0.CO;2-H

Gergely, P., Jr., Niland, B., Gonchoroff, N., Pullmann, R., Jr., Phillips, P. E., & Perl, A. (2002). Persistent mitochondrial hyperpolarization, increased reactive oxygen intermediate production, and cytoplasmic alkalinization characterize altered IL-10 signaling in patients with systemic lupus erythematosus. *J Immunol, 169*(2), 1092-1101. doi:10.4049/jimmunol.169.2.1092

Gerosa, F., Baldani-Guerra, B., Nisii, C., Marchesini, V., Carra, G., & Trinchieri, G. (2002). Reciprocal activating interaction between natural killer cells and dendritic cells. *J Exp Med, 195*(3), 327-333. doi:10.1084/jem.20010938

Godala, M., Materek-Kusmierkiewicz, I., Moczulski, D., Rutkowski, M., Szatko, F., Gaszynska, E., . . . Kowalski, J. (2017). The risk of plasma vitamin A, C, E and D deficiency in patients with metabolic syndrome: A case-control study. *Adv Clin Exp Med, 26*(4), 581-586. doi:10.17219/acem/62453

Goodman, D. W., Huang, H. S., & Shiratori, T. (1965). Tissue Distribution and Metabolism of Newly Absorbed Vitamin a in the Rat. *J Lipid Res, 6*, 390-396. Retrieved from https://www.ncbi.nlm.nih.gov/pubmed/14336210

Goodnow, C. C., Crosbie, J., Jorgensen, H., Brink, R. A., & Basten, A. (1989). Induction of self-tolerance in mature peripheral B lymphocytes. *Nature, 342*(6248), 385-391. doi:10.1038/342385a0

Gordon, S. M., Chaix, J., Rupp, L. J., Wu, J., Madera, S., Sun, J. C., . . . Reiner, S. L. (2012). The transcription factors T-bet and Eomes control key checkpoints of natural killer cell maturation. *Immunity, 36*(1), 55-67. doi:10.1016/j.immuni.2011.11.016

Goto, Y., Obata, T., Kunisawa, J., Sato, S., Ivanov, II, Lamichhane, A., . . . Kiyono, H. (2014). Innate lymphoid cells regulate intestinal epithelial cell glycosylation. *Science, 345*(6202), 1254009. doi:10.1126/science.1254009

Goverse, G., Labao-Almeida, C., Ferreira, M., Molenaar, R., Wahlen, S., Konijn, T., . . . Mebius, R. E. (2016). Vitamin A Controls the Presence of RORgamma+ Innate Lymphoid Cells and Lymphoid Tissue in the Small Intestine. *J Immunol, 196*(12), 5148-5155. doi:10.4049/jimmunol.1501106

Grant, L. R., Yao, Z. J., Hedrich, C. M., Wang, F., Moorthy, A., Wilson, K., . . . Bream, J. H. (2008). Stat4-dependent, T-bet-independent regulation of IL-10 in NK cells. *Genes Immun, 9*(4), 316-327. doi:10.1038/gene.2008.20

Greter, M., Helft, J., Chow, A., Hashimoto, D., Mortha, A., Agudo-Cantero, J., . . . Merad, M. (2012). GM-CSF controls nonlymphoid tissue dendritic cell

homeostasis but is dispensable for the differentiation of inflammatory dendritic cells. *Immunity, 36*(6), 1031-1046. doi:10.1016/j.immuni.2012.03.027

Grizotte-Lake, M., Zhong, G., Duncan, K., Kirkwood, J., Iyer, N., Smolenski, I., . . . Vaishnava, S. (2018). Commensals Suppress Intestinal Epithelial Cell Retinoic Acid Synthesis to Regulate Interleukin-22 Activity and Prevent Microbial Dysbiosis. *Immunity, 49*(6), 1103-1115 e1106. doi:10.1016/j.immuni.2018.11.018

Gronke, K., Hernandez, P. P., Zimmermann, J., Klose, C. S. N., Kofoed-Branzk, M., Guendel, F., . . . Diefenbach, A. (2019). Interleukin-22 protects intestinal stem cells against genotoxic stress. *Nature, 566*(7743), 249-253. doi:10.1038/s41586-019-0899-7

Grudzien, M., & Rapak, A. (2018). Effect of Natural Compounds on NK Cell Activation. *J Immunol Res, 2018*, 4868417. doi:10.1155/2018/4868417

Guia, S., Fenis, A., Vivier, E., & Narni-Mancinelli, E. (2018). Activating and inhibitory receptors expressed on innate lymphoid cells. *Semin Immunopathol, 40*(4), 331-341. doi:10.1007/s00281-018-0685-x

Guri, A. J., Mohapatra, S. K., Horne, W. T., 2nd, Hontecillas, R., & Bassaganya-Riera, J. (2010). The role of T cell PPAR gamma in mice with experimental inflammatory bowel disease. *BMC Gastroenterol, 10*, 60. doi:10.1186/1471-230X-10-60

Halgunset, J., Sunde, A., & Lundmo, P. I. (1987). Retinoic acid (RA): an inhibitor of 5 alpha-reductase in human prostatic cancer cells. *J Steroid Biochem, 28*(6), 731-736. doi:10.1016/0022-4731(87)90405-5

Halim, T. Y., Steer, C. A., Matha, L., Gold, M. J., Martinez-Gonzalez, I., McNagny, K. M., . . . Takei, F. (2014). Group 2 innate lymphoid cells are critical for the initiation of adaptive T helper 2 cell-mediated allergic lung inflammation. *Immunity, 40*(3), 425-435. doi:10.1016/j.immuni.2014.01.011

Handa, K., Suzuki, R., Matsui, H., Shimizu, Y., & Kumagai, K. (1983). Natural killer (NK) cells as a responder to interleukin 2 (IL 2). II. IL 2-induced interferon gamma production. *J Immunol, 130*(2), 988-992. Retrieved from https://www.ncbi.nlm.nih.gov/pubmed/6294182

Hashimoto, W., Osaki, T., Okamura, H., Robbins, P. D., Kurimoto, M., Nagata, S., . . . Tahara, H. (1999). Differential antitumor effects of administration of recombinant IL-18 or recombinant IL-12 are mediated primarily by Fas-Fas ligand- and perforin-induced tumor apoptosis, respectively. *J Immunol, 163*(2), 583-589. Retrieved from https://www.ncbi.nlm.nih.gov/pubmed/10395644

Hayakawa, Y., Screpanti, V., Yagita, H., Grandien, A., Ljunggren, H. G., Smyth, M. J., & Chambers, B. J. (2004). NK cell TRAIL eliminates immature dendritic cells in vivo and limits dendritic cell vaccination efficacy. *J Immunol, 172*(1), 123-129. doi:10.4049/jimmunol.172.1.123

Hayden, M. S., & Ghosh, S. (2011). NF-kappaB in immunobiology. *Cell Res, 21*(2), 223-244. doi:10.1038/cr.2011.13

Hepworth, M. R., Fung, T. C., Masur, S. H., Kelsen, J. R., McConnell, F. M., Dubrot, J., . . . Sonnenberg, G. F. (2015). Immune tolerance. Group 3 innate lymphoid cells mediate intestinal selection of commensal bacteria-specific CD4(+) T cells. *Science, 348*(6238), 1031-1035. doi:10.1126/science.aaa4812

Hiemstra, I. H., Beijer, M. R., Veninga, H., Vrijland, K., Borg, E. G., Olivier, B. J., . . . den Haan, J. M. (2014). The identification and developmental requirements of colonic CD169(+) macrophages. *Immunology, 142*(2), 269-278. doi:10.1111/imm.12251

Higashi, N., Sato, M., Kojima, N., Irie, T., Kawamura, K., Mabuchi, A., & Senoo, H. (2005). Vitamin A storage in hepatic stellate cells in the regenerating rat liver: with special reference to zonal heterogeneity. *Anat Rec A Discov Mol Cell Evol Biol, 286*(2), 899-907. doi:10.1002/ar.a.20230

Hisamori, S., Tabata, C., Kadokawa, Y., Okoshi, K., Tabata, R., Mori, A., . . . Sakai, Y. (2008). All-trans-retinoic acid ameliorates carbon tetrachloride-induced liver fibrosis in mice through modulating cytokine production. *Liver Int, 28*(9), 1217-1225. doi:10.1111/j.1478-3231.2008.01745.x

Hoelzinger, D. B., Smith, S. E., Mirza, N., Dominguez, A. L., Manrique, S. Z., & Lustgarten, J. (2010). Blockade of CCL1 inhibits T regulatory cell suppressive function enhancing tumor immunity without affecting T effector responses. *J Immunol, 184*(12), 6833-6842. doi:10.4049/jimmunol.0904084

Hong, K., Zhang, Y., Guo, Y., Xie, J., Wang, J., He, X., . . . Bai, A. (2014). All-trans retinoic acid attenuates experimental colitis through inhibition of NF-kappaB signaling. *Immunol Lett, 162*(1 Pt A), 34-40. doi:10.1016/j.imlet.2014.06.011

Hong, T. K., & Lee-Kim, Y. C. (2009). Effects of retinoic acid isomers on apoptosis and enzymatic antioxidant system in human breast cancer cells. *Nutr Res Pract, 3*(2), 77-83. doi:10.4162/nrp.2009.3.2.77

Hoshino, K., Takeuchi, O., Kawai, T., Sanjo, H., Ogawa, T., Takeda, Y., . . . Akira, S. (1999). Cutting edge: Toll-like receptor 4 (TLR4)-deficient mice are hyporesponsive to lipopolysaccharide: evidence for TLR4 as the Lps gene product. *J Immunol, 162*(7), 3749-3752. Retrieved from https://www.ncbi.nlm.nih.gov/pubmed/10201887

Hsu, P., Santner-Nanan, B., Hu, M., Skarratt, K., Lee, C. H., Stormon, M., . . . Nanan, R. (2015). IL-10 Potentiates Differentiation of Human Induced Regulatory T Cells via STAT3 and Foxo1. *J Immunol, 195*(8), 3665-3674. doi:10.4049/jimmunol.1402898

Huang, H. S., & Goodman, D. S. (1965). Vitamin a and Carotenoids. I. Intestinal Absorption and Metabolism of 14c-Labelled Vitamin a Alcohol and Beta-Carotene in the Rat. *J Biol Chem, 240*, 2839-2844. Retrieved from https://www.ncbi.nlm.nih.gov/pubmed/14342304

Huang, S., Hendriks, W., Althage, A., Hemmi, S., Bluethmann, H., Kamijo, R., . . . Aguet, M. (1993). Immune response in mice that lack the interferon-gamma receptor. *Science, 259*(5102), 1742-1745. doi:10.1126/science.8456301

Huang, Y., Mao, K., Chen, X., Sun, M. A., Kawabe, T., Li, W., . . . Germain, R. N. (2018). S1P-dependent interorgan trafficking of group 2 innate lymphoid cells supports host defense. *Science, 359*(6371), 114-119. doi:10.1126/science.aam5809

Huber, S., Gagliani, N., Zenewicz, L. A., Huber, F. J., Bosurgi, L., Hu, B., . . . Flavell, R. A. (2012). IL-22BP is regulated by the inflammasome and modulates tumorigenesis in the intestine. *Nature, 491*(7423), 259-263. doi:10.1038/nature11535

Hubert, S., Rissiek, B., Klages, K., Huehn, J., Sparwasser, T., Haag, F., . . . Adriouch, S. (2010). Extracellular NAD+ shapes the Foxp3+ regulatory T cell compartment through the ART2-P2X7 pathway. *J Exp Med, 207*(12), 2561-2568. doi:10.1084/jem.20091154

Hussain, M. M., Mahley, R. W., Boyles, J. K., Fainaru, M., Brecht, W. J., & Lindquist, P. A. (1989). Chylomicron-chylomicron remnant clearance by liver and bone marrow in rabbits. Factors that modify tissue-specific uptake. *J Biol Chem, 264*(16), 9571-9582. Retrieved from https://www.ncbi.nlm.nih.gov/pubmed/2722852

Hyodo, Y., Matsui, K., Hayashi, N., Tsutsui, H., Kashiwamura, S., Yamauchi, H., . . . Higashino, K. (1999). IL-18 up-regulates perforin-mediated NK activity without increasing perforin messenger RNA expression by binding to constitutively expressed IL-18 receptor. *J Immunol, 162*(3), 1662-1668. Retrieved from https://www.ncbi.nlm.nih.gov/pubmed/9973427

Ichikawa, S., Mucida, D., Tyznik, A. J., Kronenberg, M., & Cheroutre, H. (2011). Hepatic stellate cells function as regulatory bystanders. *J Immunol, 186*(10), 5549-5555. doi:10.4049/jimmunol.1003917

Imai, K., Sato, M., Kojima, N., Miura, M., Sato, T., Sugiyama, T., . . . Senoo, H. (2000). Storage of lipid droplets in and production of extracellular matrix by hepatic stellate cells (vitamin A-storing cells) in Long-Evans cinnamon-like colored (LEC) rats. *Anat Rec, 258*(4), 338-348. doi:10.1002/(SICI)1097-0185(20000401)258:4<338::AID-AR2>3.0.CO;2-G

Inaba, K., Inaba, M., Romani, N., Aya, H., Deguchi, M., Ikehara, S., . . . Steinman, R. M. (1992). Generation of large numbers of dendritic cells from mouse bone marrow cultures supplemented with granulocyte/macrophage colony-stimulating factor. *J Exp Med, 176*(6), 1693-1702. doi:10.1084/jem.176.6.1693

Inaba, K., Steinman, R. M., Pack, M. W., Aya, H., Inaba, M., Sudo, T., . . . Schuler, G. (1992). Identification of proliferating dendritic cell precursors in mouse blood. *J Exp Med, 175*(5), 1157-1167. doi:10.1084/jem.175.5.1157

Ishizuka, I. E., Chea, S., Gudjonson, H., Constantinides, M. G., Dinner, A. R., Bendelac, A., & Golub, R. (2016). Single-cell analysis defines the divergence between the innate lymphoid cell lineage and lymphoid tissue-inducer cell lineage. *Nat Immunol, 17*(3), 269-276. doi:10.1038/ni.3344

Ivanov, II, & Littman, D. R. (2011). Modulation of immune homeostasis by commensal bacteria. *Curr Opin Microbiol, 14*(1), 106-114. doi:10.1016/j.mib.2010.12.003

Iwata, M., Hirakiyama, A., Eshima, Y., Kagechika, H., Kato, C., & Song, S. Y. (2004). Retinoic acid imprints gut-homing specificity on T cells. *Immunity, 21*(4), 527-538. doi:10.1016/j.immuni.2004.08.011

Iyer, N., & Vaishnava, S. (2019). Vitamin A at the interface of host-commensal-pathogen interactions. *PLoS Pathog, 15*(6), e1007750. doi:10.1371/journal.ppat.1007750

Jackson, G. R., Morgan, B. C., Werrbach-Perez, K., & Perez-Polo, J. R. (1991). Antioxidant effect of retinoic acid on PC12 rat pheochromocytoma. *Int J Dev Neurosci, 9*(2), 161-170. doi:10.1016/0736-5748(91)90007-9

Jaensson, E., Uronen-Hansson, H., Pabst, O., Eksteen, B., Tian, J., Coombes, J. L., . . . Agace, W. W. (2008). Small intestinal CD103+ dendritic cells display unique functional properties that are conserved between mice and humans. *J Exp Med, 205*(9), 2139-2149. doi:10.1084/jem.20080414

Jamieson, A. M., Diefenbach, A., McMahon, C. W., Xiong, N., Carlyle, J. R., & Raulet, D. H. (2002). The role of the NKG2D immunoreceptor in immune cell activation and natural killing. *Immunity, 17*(1), 19-29. doi:10.1016/s1074-7613(02)00333-3

Janeway, C. A., Jr. (1989). The role of CD4 in T-cell activation: accessory molecule or co-receptor? *Immunol Today, 10*(7), 234-238. doi:10.1016/0167-5699(89)90260-0

Jang, M. H., Sougawa, N., Tanaka, T., Hirata, T., Hiroi, T., Tohya, K., . . . Miyasaka, M. (2006). CCR7 is critically important for migration of dendritic cells in intestinal lamina propria to mesenteric lymph nodes. *J Immunol, 176*(2), 803-810. doi:10.4049/jimmunol.176.2.803

Jensen, I. J., McGonagill, P. W., Butler, N. S., Harty, J. T., Griffith, T. S., & Badovinac, V. P. (2021). NK Cell-Derived IL-10 Supports Host Survival during Sepsis. *J Immunol, 206*(6), 1171-1180. doi:10.4049/jimmunol.2001131

Jiao, Y., Huntington, N. D., Belz, G. T., & Seillet, C. (2016). Type 1 Innate Lymphoid Cell Biology: Lessons Learnt from Natural Killer Cells. *Front Immunol, 7*, 426. doi:10.3389/fimmu.2016.00426

Jie, Z., Liang, Y., Yi, P., Tang, H., Soong, L., Cong, Y., . . . Sun, J. (2017). Retinoic Acid Regulates Immune Responses by Promoting IL-22 and Modulating S100 Proteins in Viral Hepatitis. *J Immunol, 198*(9), 3448-3460. doi:10.4049/jimmunol.1601891

Jinushi, M., Takehara, T., Tatsumi, T., Kanto, T., Miyagi, T., Suzuki, T., . . . Hayashi, N. (2004). Negative regulation of NK cell activities by inhibitory receptor CD94/NKG2A leads to altered NK cell-induced modulation of dendritic cell functions in chronic hepatitis C virus infection. *J Immunol, 173*(10), 6072-6081. doi:10.4049/jimmunol.173.10.6072

Jokhi, P. P., King, A., Sharkey, A. M., Smith, S. K., & Loke, Y. W. (1994). Screening for cytokine messenger ribonucleic acids in purified human decidual lymphocyte populations by the reverse-transcriptase polymerase chain reaction. *J Immunol, 153*(10), 4427-4435. Retrieved from https://www.ncbi.nlm.nih.gov/pubmed/7525703

Jorgovanovic, D., Song, M., Wang, L., & Zhang, Y. (2020). Roles of IFN-gamma in tumor progression and regression: a review. *Biomark Res, 8*, 49. doi:10.1186/s40364-020-00228-x

Jutley, J. K., Reaney, S., Kelleher, J., & Whelan, P. (1990). Interactions of retinoic acid and androgens in human prostatic tissue. *Prostate, 16*(4), 299-304. doi:10.1002/pros.2990160404

Kaczmarek, E., Koziak, K., Sevigny, J., Siegel, J. B., Anrather, J., Beaudoin, A. R., . . . Robson, S. C. (1996). Identification and characterization of CD39/vascular ATP diphosphohydrolase. *J Biol Chem, 271*(51), 33116-33122. doi:10.1074/jbc.271.51.33116

Kane, M. A., Folias, A. E., & Napoli, J. L. (2008). HPLC/UV quantitation of retinal, retinol, and retinyl esters in serum and tissues. *Anal Biochem, 378*(1), 71-79. doi:10.1016/j.ab.2008.03.038

Kannan, K., Stewart, R. M., Bounds, W., Carlsson, S. R., Fukuda, M., Betzing, K. W., & Holcombe, R. F. (1996). Lysosome-associated membrane proteins h-LAMP1 (CD107a) and h-LAMP2 (CD107b) are activation-dependent cell surface glycoproteins in human peripheral blood mononuclear cells which mediate cell adhesion to vascular endothelium. *Cell Immunol, 171*(1), 10-19. doi:10.1006/cimm.1996.0167

Karlhofer, F. M., Ribaudo, R. K., & Yokoyama, W. M. (1992). MHC class I alloantigen specificity of Ly-49+ IL-2-activated natural killer cells. *Nature, 358*(6381), 66-70. doi:10.1038/358066a0

Karre, K., Ljunggren, H. G., Piontek, G., & Kiessling, R. (1986). Selective rejection of H-2-deficient lymphoma variants suggests alternative immune defence strategy. *Nature, 319*(6055), 675-678. doi:10.1038/319675a0

Kashii, Y., Giorda, R., Herberman, R. B., Whiteside, T. L., & Vujanovic, N. L. (1999). Constitutive expression and role of the TNF family ligands in apoptotic killing of tumor cells by human NK cells. *J Immunol, 163*(10), 5358-5366. Retrieved from https://www.ncbi.nlm.nih.gov/pubmed/10553060

Kato, Y., Ozawa, S., Miyamoto, C., Maehata, Y., Suzuki, A., Maeda, T., & Baba, Y. (2013). Acidic extracellular microenvironment and cancer. *Cancer Cell Int, 13*(1), 89. doi:10.1186/1475-2867-13-89

Kawada, T., Kamei, Y., Fujita, A., Hida, Y., Takahashi, N., Sugimoto, E., & Fushiki, T. (2000). Carotenoids and retinoids as suppressors on adipocyte differentiation via nuclear receptors. *Biofactors, 13*(1-4), 103-109. doi:10.1002/biof.5520130117

Kayagaki, N., Yamaguchi, N., Nakayama, M., Takeda, K., Akiba, H., Tsutsui, H., . . . Yagita, H. (1999). Expression and function of TNF-related apoptosis-inducing ligand on murine activated NK cells. *J Immunol, 163*(4), 1906-1913. Retrieved from https://www.ncbi.nlm.nih.gov/pubmed/10438925

Keating, S. E., Zaiatz-Bittencourt, V., Loftus, R. M., Keane, C., Brennan, K., Finlay, D. K., & Gardiner, C. M. (2016). Metabolic Reprogramming Supports IFN-gamma Production by CD56bright NK Cells. *J Immunol, 196*(6), 2552-2560. doi:10.4049/jimmunol.1501783

Kedia-Mehta, N., Tobin, L., Zaiatz-Bittencourt, V., Pisarska, M. M., De Barra, C., Choi, C., . . . Hogan, A. E. (2021). Cytokine-induced natural killer cell training is dependent on cellular metabolism and is defective in obesity. *Blood Adv, 5*(21), 4447-4455. doi:10.1182/bloodadvances.2021005047

Kempkes, R. W. M., Joosten, I., Koenen, H., & He, X. (2019). Metabolic Pathways Involved in Regulatory T Cell Functionality. *Front Immunol, 10*, 2839. doi:10.3389/fimmu.2019.02839

Keppel, M. P., Saucier, N., Mah, A. Y., Vogel, T. P., & Cooper, M. A. (2015). Activation-specific metabolic requirements for NK Cell IFN-gamma production. *J Immunol, 194*(4), 1954-1962. doi:10.4049/jimmunol.1402099

Kim, M. H., Taparowsky, E. J., & Kim, C. H. (2015). Retinoic Acid Differentially Regulates the Migration of Innate Lymphoid Cell Subsets to the Gut. *Immunity, 43*(1), 107-119. doi:10.1016/j.immuni.2015.06.009

Kinchen, J. M., & Ravichandran, K. S. (2008). Phagosome maturation: going through the acid test. *Nat Rev Mol Cell Biol, 9*(10), 781-795. doi:10.1038/nrm2515

Klebanoff, C. A., Spencer, S. P., Torabi-Parizi, P., Grainger, J. R., Roychoudhuri, R., Ji, Y., . . . Restifo, N. P. (2013). Retinoic acid controls the homeostasis of pre-cDC-derived splenic and intestinal dendritic cells. *J Exp Med, 210*(10), 1961-1976. doi:10.1084/jem.20122508

Klose, C. S. N., & Artis, D. (2020). Innate lymphoid cells control signaling circuits to regulate tissue-specific immunity. *Cell Res, 30*(6), 475-491. doi:10.1038/s41422-020-0323-8

Klose, C. S. N., Flach, M., Mohle, L., Rogell, L., Hoyler, T., Ebert, K., . . . Diefenbach, A. (2014). Differentiation of type 1 ILCs from a common progenitor to all helper-like innate lymphoid cell lineages. *Cell, 157*(2), 340-356. doi:10.1016/j.cell.2014.03.030

Kobie, J. J., Shah, P. R., Yang, L., Rebhahn, J. A., Fowell, D. J., & Mosmann, T. R. (2006). T regulatory and primed uncommitted CD4 T cells express CD73, which suppresses effector CD4 T cells by converting 5'-adenosine monophosphate to adenosine. *J Immunol, 177*(10), 6780-6786. doi:10.4049/jimmunol.177.10.6780

Kodama, T., Takeda, K., Shimozato, O., Hayakawa, Y., Atsuta, M., Kobayashi, K., . . . Okumura, K. (1999). Perforin-dependent NK cell cytotoxicity is sufficient for anti-metastatic effect of IL-12. *Eur J Immunol, 29*(4), 1390-1396. doi:10.1002/(SICI)1521-4141(199904)29:04<1390::AID-IMMU1390>3.0.CO;2-C

Koenen, H. J., Smeets, R. L., Vink, P. M., van Rijssen, E., Boots, A. M., & Joosten, I. (2008). Human CD25highFoxp3pos regulatory T cells differentiate into IL-17-producing cells. *Blood, 112*(6), 2340-2352. doi:10.1182/blood-2008-01-133967

Koshiuka, K., Elstner, E., Williamson, E., Said, J. W., Tada, Y., & Koeffler, H. P. (2000). Novel therapeutic approach: organic arsenical melarsoprol) alone or with all-trans-retinoic acid markedly inhibit growth of human breast and prostate cancer cells in vitro and in vivo. *Br J Cancer, 82*(2), 452-458. doi:10.1054/bjoc.1999.0942

Kruisbeek, A. M., Mond, J. J., Fowlkes, B. J., Carmen, J. A., Bridges, S., & Longo, D. L. (1985). Absence of the Lyt-2-,L3T4+ lineage of T cells in mice treated neonatally with anti-I-A correlates with absence of intrathymic I-A-bearing antigen-presenting cell function. *J Exp Med, 161*(5), 1029-1047. doi:10.1084/jem.161.5.1029

Kuehnemuth, B., Piseddu, I., Wiedemann, G. M., Lauseker, M., Kuhn, C., Hofmann, S., . . . Anz, D. (2018). CCL1 is a major regulatory T cell attracting factor in human breast cancer. *BMC Cancer, 18*(1), 1278. doi:10.1186/s12885-018-5117-8

Kwaa, A. K. R., Talana, C. A. G., & Blankson, J. N. (2019). Interferon Alpha Enhances NK Cell Function and the Suppressive Capacity of HIV-Specific CD8(+) T Cells. *J Virol, 93*(3). doi:10.1128/JVI.01541-18

Kwok, S. K., Park, M. K., Cho, M. L., Oh, H. J., Park, E. M., Lee, D. G., . . . Park, S. H. (2012). Retinoic acid attenuates rheumatoid inflammation in mice. *J Immunol, 189*(2), 1062-1071. doi:10.4049/jimmunol.1102706

Lang, P. A., Lang, K. S., Xu, H. C., Grusdat, M., Parish, I. A., Recher, M., . . . Ohashi, P. S. (2012). Natural killer cell activation enhances immune pathology and promotes chronic infection by limiting CD8+ T-cell immunity. *Proc Natl Acad Sci U S A, 109*(4), 1210-1215. doi:10.1073/pnas.1118834109

Lanzavecchia, A., & Sallusto, F. (2001). Regulation of T cell immunity by dendritic cells. *Cell, 106*(3), 263-266. doi:10.1016/s0092-8674(01)00455-x

Laouar, Y., Sutterwala, F. S., Gorelik, L., & Flavell, R. A. (2005). Transforming growth factor-beta controls T helper type 1 cell development through regulation of natural killer cell interferon-gamma. *Nat Immunol, 6*(6), 600-607. doi:10.1038/ni1197

Lassen, M. G., Lukens, J. R., Dolina, J. S., Brown, M. G., & Hahn, Y. S. (2010). Intrahepatic IL-10 maintains NKG2A+Ly49- liver NK cells in a functionally hyporesponsive state. *J Immunol, 184*(5), 2693-2701. doi:10.4049/jimmunol.0901362

Lee, K. A., Song, Y. C., Kim, G. Y., Choi, G., Lee, Y. S., Lee, J. M., & Kang, C. Y. (2012). Retinoic acid alleviates Con A-induced hepatitis and differentially regulates effector production in NKT cells. *Eur J Immunol, 42*(7), 1685-1694. doi:10.1002/eji.201142322

Lee, S. H., Kim, K. S., Fodil-Cornu, N., Vidal, S. M., & Biron, C. A. (2009). Activating receptors promote NK cell expansion for maintenance, IL-10 production, and CD8 T cell regulation during viral infection. *J Exp Med, 206*(10), 2235-2251. doi:10.1084/jem.20082387

Lehrer, R. I., Selsted, M. E., Szklarek, D., & Fleischmann, J. (1983). Antibacterial activity of microbicidal cationic proteins 1 and 2, natural peptide antibiotics of rabbit lung macrophages. *Infect Immun, 42*(1), 10-14. doi:10.1128/iai.42.1.10-14.1983

Leibson, P. J. (1997). Signal transduction during natural killer cell activation: inside the mind of a killer. *Immunity, 6*(6), 655-661. doi:10.1016/s1074-7613(00)80441-0

Lejeune, M., Duray, E., Peipp, M., Clemenceau, B., Baron, F., Beguin, Y., & Caers, J. (2021). Balancing the CD38 Expression on Effector and Target Cells in Daratumumab-Mediated NK Cell ADCC against Multiple Myeloma. *Cancers (Basel), 13*(12). doi:10.3390/cancers13123072

Li, D., & Wu, M. (2021). Pattern recognition receptors in health and diseases. *Signal Transduct Target Ther, 6*(1), 291. doi:10.1038/s41392-021-00687-0

Li, H., Zhai, N., Wang, Z., Song, H., Yang, Y., Cui, A., . . . Tu, Z. (2018). Regulatory NK cells mediated between immunosuppressive monocytes and dysfunctional T cells in chronic HBV infection. *Gut, 67*(11), 2035-2044. doi:10.1136/gutjnl-2017-314098

Li, T., Zhang, Y., Meng, Y. P., Bo, L. S., & Ke, W. B. (2017). miR-542-3p Appended Sorafenib/All-trans Retinoic Acid (ATRA)-Loaded Lipid Nanoparticles to Enhance the Anticancer Efficacy in Gastric Cancers. *Pharm Res, 34*(12), 2710-2719. doi:10.1007/s11095-017-2202-7

Liang, Y., Yi, P., Wang, X., Zhang, B., Jie, Z., Soong, L., & Sun, J. (2020). Retinoic Acid Modulates Hyperactive T Cell Responses and Protects Vitamin A-Deficient Mice against Persistent Lymphocytic Choriomeningitis Virus Infection. *J Immunol, 204*(11), 2984-2994. doi:10.4049/jimmunol.1901091

Lieberman, J. (2003). The ABCs of granule-mediated cytotoxicity: new weapons in the arsenal. *Nat Rev Immunol, 3*(5), 361-370. doi:10.1038/nri1083

Liou, Y. H., Wang, S. W., Chang, C. L., Huang, P. L., Hou, M. S., Lai, Y. G., . . . Liao, N. S. (2014). Adipocyte IL-15 regulates local and systemic NK cell development. *J Immunol, 193*(4), 1747-1758. doi:10.4049/jimmunol.1400868

Littwitz-Salomon, E., Moreira, D., Frost, J. N., Choi, C., Liou, K. T., Ahern, D. K., . . . Finlay, D. K. (2021). Metabolic requirements of NK cells during the acute response against retroviral infection. *Nat Commun, 12*(1), 5376. doi:10.1038/s41467-021-25715-z

Liu, B., Mori, I., Hossain, M. J., Dong, L., Takeda, K., & Kimura, Y. (2004). Interleukin-18 improves the early defence system against influenza virus infection by augmenting natural killer cell-mediated cytotoxicity. *J Gen Virol, 85*(Pt 2), 423-428. doi:10.1099/vir.0.19596-0

Liu, Y., Chen, H., Mu, D., Fan, J., Song, J., Zhong, Y., . . . Xia, M. (2016). Circulating Retinoic Acid Levels and the Development of Metabolic Syndrome. *J Clin Endocrinol Metab, 101*(4), 1686-1692. doi:10.1210/jc.2015-4038

Liu, Y., Chen, H., Wang, J., Zhou, W., Sun, R., & Xia, M. (2015). Association of serum retinoic acid with hepatic steatosis and liver injury in nonalcoholic fatty liver disease. *Am J Clin Nutr, 102*(1), 130-137. doi:10.3945/ajcn.114.105155

Liu, Y. H., Tsai, Y. S., Lin, S. C., Liao, N. S., Jan, M. S., Liang, C. T., . . . Tsai, P. J. (2016). Quantitative PPARgamma expression affects the balance between tolerance and immunity. *Sci Rep, 6*, 26646. doi:10.1038/srep26646

Liu, Y. J., Zhang, J., Lane, P. J., Chan, E. Y., & MacLennan, I. C. (1991). Sites of specific B cell activation in primary and secondary responses to T cell-dependent and T cell-independent antigens. *Eur J Immunol, 21*(12), 2951-2962. doi:10.1002/eji.1830211209

Ljunggren, H. G., & Karre, K. (1990). In search of the 'missing self': MHC molecules and NK cell recognition. *Immunol Today, 11*(7), 237-244. doi:10.1016/0167-5699(90)90097-s

Loftus, R. M., Assmann, N., Kedia-Mehta, N., O'Brien, K. L., Garcia, A., Gillespie, C., . . . Finlay, D. K. (2018). Amino acid-dependent cMyc expression is essential for NK cell metabolic and functional responses in mice. *Nat Commun, 9*(1), 2341. doi:10.1038/s41467-018-04719-2

Lotan, R. (1996). Retinoids in cancer chemoprevention. *FASEB J, 10*(9), 1031-1039. doi:10.1096/fasebj.10.9.8801164

Lotan, R., Giotta, G., Nork, E., & Nicolson, G. L. (1978). Characterization of the inhibitory effects of retinoids on the in vitro growth of two malignant murine melanomas. *J Natl Cancer Inst, 60*(5), 1035-1041. doi:10.1093/jnci/60.5.1035

Louis, C., Souza-Fonseca-Guimaraes, F., Yang, Y., D'Silva, D., Kratina, T., Dagley, L., . . . Wicks, I. P. (2020). NK cell-derived GM-CSF potentiates inflammatory arthritis and is negatively regulated by CIS. *J Exp Med, 217*(5). doi:10.1084/jem.20191421

Lu, B., Ebensperger, C., Dembic, Z., Wang, Y., Kvatyuk, M., Lu, T., . . . Rothman, P. B. (1998). Targeted disruption of the interferon-gamma receptor 2 gene results in severe immune defects in mice. *Proc Natl Acad Sci U S A, 95*(14), 8233-8238. doi:10.1073/pnas.95.14.8233

Lu, L., Ikizawa, K., Hu, D., Werneck, M. B., Wucherpfennig, K. W., & Cantor, H. (2007). Regulation of activated CD4+ T cells by NK cells via the Qa-1-NKG2A inhibitory pathway. *Immunity, 26*(5), 593-604. doi:10.1016/j.immuni.2007.03.017

Ludwig, K. W., Lowey, B., & Niles, R. M. (1980). Retinoic acid increases cyclic AMP-dependent protein kinase activity in murine melanoma cells. *J Biol Chem, 255*(13), 5999-6002. Retrieved from https://www.ncbi.nlm.nih.gov/pubmed/6248511

Ma, J., Liu, Y., Li, Y., Gu, J., Liu, J., Tang, J., . . . Zheng, S. G. (2014). Differential role of all-trans retinoic acid in promoting the development of CD4+ and CD8+ regulatory T cells. *J Leukoc Biol, 95*(2), 275-283. doi:10.1189/jlb.0513297

Ma, S. R., Deng, W. W., Liu, J. F., Mao, L., Yu, G. T., Bu, L. L., . . . Sun, Z. J. (2017). Blockade of adenosine A2A receptor enhances CD8(+) T cells response and decreases regulatory T cells in head and neck squamous cell carcinoma. *Mol Cancer, 16*(1), 99. doi:10.1186/s12943-017-0665-0

Madera, S., Rapp, M., Firth, M. A., Beilke, J. N., Lanier, L. L., & Sun, J. C. (2016). Type I IFN promotes NK cell expansion during viral infection by protecting NK cells against fratricide. *J Exp Med, 213*(2), 225-233. doi:10.1084/jem.20150712

Maghazachi, A. A. (2010). Role of chemokines in the biology of natural killer cells. *Curr Top Microbiol Immunol, 341*, 37-58. doi:10.1007/82_2010_20

Mailliard, R. B., Son, Y. I., Redlinger, R., Coates, P. T., Giermasz, A., Morel, P. A., . . . Kalinski, P. (2003). Dendritic cells mediate NK cell help for Th1 and CTL responses: two-signal requirement for the induction of NK cell helper function. *J Immunol, 171*(5), 2366-2373. doi:10.4049/jimmunol.171.5.2366

Mallone, R., Funaro, A., Zubiaur, M., Baj, G., Ausiello, C. M., Tacchetti, C., . . . Malavasi, F. (2001). Signaling through CD38 induces NK cell activation. *Int Immunol, 13*(4), 397-409. doi:10.1093/intimm/13.4.397

Mandapathil, M., Hilldorfer, B., Szczepanski, M. J., Czystowska, M., Szajnik, M., Ren, J., . . . Whiteside, T. L. (2010). Generation and accumulation of immunosuppressive adenosine by human CD4+CD25highFOXP3+ regulatory T cells. *J Biol Chem, 285*(10), 7176-7186. doi:10.1074/jbc.M109.047423

Manna, S. K., & Aggarwal, B. B. (2000). All-trans-retinoic acid upregulates TNF receptors and potentiates TNF-induced activation of nuclear factors-kappaB, activated protein-1 and apoptosis in human lung cancer cells. *Oncogene, 19*(17), 2110-2119. doi:10.1038/sj.onc.1203547

Mao, Y., van Hoef, V., Zhang, X., Wennerberg, E., Lorent, J., Witt, K., . . . Lundqvist, A. (2016). IL-15 activates mTOR and primes stress-activated gene expression leading to prolonged antitumor capacity of NK cells. *Blood, 128*(11), 1475-1489. doi:10.1182/blood-2016-02-698027

Marcais, A., Cherfils-Vicini, J., Viant, C., Degouve, S., Viel, S., Fenis, A., . . . Walzer, T. (2014). The metabolic checkpoint kinase mTOR is essential for IL-15 signaling during the development and activation of NK cells. *Nat Immunol, 15*(8), 749-757. doi:10.1038/ni.2936

Martin-Fontecha, A., Thomsen, L. L., Brett, S., Gerard, C., Lipp, M., Lanzavecchia, A., & Sallusto, F. (2004). Induced recruitment of NK cells to lymph nodes provides IFN-gamma for T(H)1 priming. *Nat Immunol, 5*(12), 1260-1265. doi:10.1038/ni1138

Martinez-Navio, J. M., Casanova, V., Pacheco, R., Naval-Macabuhay, I., Climent, N., Garcia, F., . . . Franco, R. (2011). Adenosine deaminase potentiates the generation of effector, memory, and regulatory CD4+ T cells. *J Leukoc Biol, 89*(1), 127-136. doi:10.1189/jlb.1009696

McCoy, K. D., & Le Gros, G. (1999). The role of CTLA-4 in the regulation of T cell immune responses. *Immunol Cell Biol, 77*(1), 1-10. doi:10.1046/j.1440-1711.1999.00795.x

McDaniel, K. L., Restori, K. H., Dodds, J. W., Kennett, M. J., Ross, A. C., & Cantorna, M. T. (2015). Vitamin A-Deficient Hosts Become Nonsymptomatic Reservoirs of Escherichia coli-Like Enteric Infections. *Infect Immun, 83*(7), 2984-2991. doi:10.1128/IAI.00201-15

McQualter, J. L., Darwiche, R., Ewing, C., Onuki, M., Kay, T. W., Hamilton, J. A., . . . Bernard, C. C. (2001). Granulocyte macrophage colony-stimulating factor: a new putative therapeutic target in multiple sclerosis. *J Exp Med, 194*(7), 873-882. doi:10.1084/jem.194.7.873

Metkar, S. S., Wang, B., Ebbs, M. L., Kim, J. H., Lee, Y. J., Raja, S. M., & Froelich, C. J. (2003). Granzyme B activates procaspase-3 which signals a mitochondrial amplification loop for maximal apoptosis. *J Cell Biol, 160*(6), 875-885. doi:10.1083/jcb.200210158

Meyskens, F. L., Jr., & Salmon, S. E. (1979). Inhibition of human melanoma colony formation by retinoids. *Cancer Res, 39*(10), 4055-4057. Retrieved from https://www.ncbi.nlm.nih.gov/pubmed/476643

Michelet, X., Dyck, L., Hogan, A., Loftus, R. M., Duquette, D., Wei, K., . . . Lynch, L. (2018). Metabolic reprogramming of natural killer cells in obesity limits antitumor responses. *Nat Immunol, 19*(12), 1330-1340. doi:10.1038/s41590-018-0251-7

Mielke, L. A., Jones, S. A., Raverdeau, M., Higgs, R., Stefanska, A., Groom, J. R., . . . Mills, K. H. (2013). Retinoic acid expression associates with enhanced IL-22 production by gammadelta T cells and innate lymphoid cells and attenuation of intestinal inflammation. *J Exp Med, 210*(6), 1117-1124. doi:10.1084/jem.20121588

Miller, W. H., Jr. (1998). The emerging role of retinoids and retinoic acid metabolism blocking agents in the treatment of cancer. *Cancer, 83*(8), 1471-1482. doi:10.1002/(sici)1097-0142(19981015)83:8<1471::aid-cncr1>3.0.co;2-6

Mocellin, S., Panelli, M., Wang, E., Rossi, C. R., Pilati, P., Nitti, D., . . . Marincola, F. M. (2004). IL-10 stimulatory effects on human NK cells explored by gene profile analysis. *Genes Immun, 5*(8), 621-630. doi:10.1038/sj.gene.6364135

Mocikat, R., Braumuller, H., Gumy, A., Egeter, O., Ziegler, H., Reusch, U., . . . Rocken, M. (2003). Natural killer cells activated by MHC class I(low) targets prime dendritic cells to induce protective CD8 T cell responses. *Immunity, 19*(4), 561-569. doi:10.1016/s1074-7613(03)00264-4

Mombaerts, P., Iacomini, J., Johnson, R. S., Herrup, K., Tonegawa, S., & Papaioannou, V. E. (1992). RAG-1-deficient mice have no mature B and T lymphocytes. *Cell, 68*(5), 869-877. doi:10.1016/0092-8674(92)90030-g

Mondino, A., Khoruts, A., & Jenkins, M. K. (1996). The anatomy of T-cell activation and tolerance. *Proc Natl Acad Sci U S A, 93*(6), 2245-2252. doi:10.1073/pnas.93.6.2245

Morandi, B., Bougras, G., Muller, W. A., Ferlazzo, G., & Munz, C. (2006). NK cells of human secondary lymphoid tissues enhance T cell polarization via IFN-gamma secretion. *Eur J Immunol, 36*(9), 2394-2400. doi:10.1002/eji.200636290

Morita, H., Kubo, T., Ruckert, B., Ravindran, A., Soyka, M. B., Rinaldi, A. O., . . . Akdis, C. A. (2019). Induction of human regulatory innate lymphoid cells from group 2 innate lymphoid cells by retinoic acid. *J Allergy Clin Immunol, 143*(6), 2190-2201 e2199. doi:10.1016/j.jaci.2018.12.1018

Mortha, A., & Burrows, K. (2018). Cytokine Networks between Innate Lymphoid Cells and Myeloid Cells. *Front Immunol, 9*, 191. doi:10.3389/fimmu.2018.00191

Morvan, M. G., & Lanier, L. L. (2016). NK cells and cancer: you can teach innate cells new tricks. *Nat Rev Cancer, 16*(1), 7-19. doi:10.1038/nrc.2015.5

Mucida, D., Park, Y., Kim, G., Turovskaya, O., Scott, I., Kronenberg, M., & Cheroutre, H. (2007). Reciprocal TH17 and regulatory T cell differentiation mediated by retinoic acid. *Science, 317*(5835), 256-260. doi:10.1126/science.1145697

Muenzner, M., Tuvia, N., Deutschmann, C., Witte, N., Tolkachov, A., Valai, A., . . . Schupp, M. (2013). Retinol-binding protein 4 and its membrane receptor STRA6 control adipogenesis by regulating cellular retinoid homeostasis and retinoic acid receptor alpha activity. *Mol Cell Biol, 33*(20), 4068-4082. doi:10.1128/MCB.00221-13

Mugusi, F. M., Rusizoka, O., Habib, N., & Fawzi, W. (2003). Vitamin A status of patients presenting with pulmonary tuberculosis and asymptomatic HIV-infected individuals, Dar es Salaam, Tanzania. *Int J Tuberc Lung Dis, 7*(8), 804-807. Retrieved from https://www.ncbi.nlm.nih.gov/pubmed/12921158

Mullbacher, A., Waring, P., Tha Hla, R., Tran, T., Chin, S., Stehle, T., . . . Simon, M. M. (1999). Granzymes are the essential downstream effector molecules for the control of primary virus infections by cytolytic leukocytes. *Proc Natl Acad Sci U S A, 96*(24), 13950-13955. doi:10.1073/pnas.96.24.13950

Muller, E., Christopoulos, P. F., Halder, S., Lunde, A., Beraki, K., Speth, M., . . . Corthay, A. (2017). Toll-Like Receptor Ligands and Interferon-gamma Synergize for Induction of Antitumor M1 Macrophages. *Front Immunol, 8*, 1383. doi:10.3389/fimmu.2017.01383

Murakami, K., Kaji, T., Shimono, R., Hayashida, Y., Matsufuji, H., Tsuyama, S., . . . Takamatsu, H. (2011). Therapeutic effects of vitamin A on experimental cholestatic rats with hepatic fibrosis. *Pediatr Surg Int, 27*(8), 863-870. doi:10.1007/s00383-011-2853-0

Naeimi Kararoudi, M., Nagai, Y., Elmas, E., de Souza Fernandes Pereira, M., Ali, S. A., Imus, P. H., . . . Ghiaur, G. (2020). CD38 deletion of human primary NK cells eliminates daratumumab-induced fratricide and boosts their effector activity. *Blood, 136*(21), 2416-2427. doi:10.1182/blood.2020006200

Naka, K., Yokozaki, H., Domen, T., Hayashi, K., Kuniyasu, H., Yasui, W., . . . Tahara, E. (1997). Growth inhibition of cultured human gastric cancer cells by 9-cis-retinoic acid with induction of cdk inhibitor Waf1/Cip1/Sdi1/p21 protein. *Differentiation, 61*(5), 313-320. doi:10.1046/j.1432-0436.1997.6150313.x

Nakane, A., Okamoto, M., Asano, M., Kohanawa, M., & Minagawa, T. (1995). Endogenous gamma interferon, tumor necrosis factor, and interleukin-6 in Staphylococcus aureus infection in mice. *Infect Immun, 63*(4), 1165-1172. doi:10.1128/iai.63.4.1165-1172.1995

Nakano, Y., Onozuka, K., Terada, Y., Shinomiya, H., & Nakano, M. (1990). Protective effect of recombinant tumor necrosis factor-alpha in murine salmonellosis. *J Immunol, 144*(5), 1935-1941. Retrieved from https://www.ncbi.nlm.nih.gov/pubmed/2106556

Natarajan, S. K., Thomas, S., Ramachandran, A., Pulimood, A. B., & Balasubramanian, K. A. (2005). Retinoid metabolism during development of liver cirrhosis. *Arch Biochem Biophys, 443*(1-2), 93-100. doi:10.1016/j.abb.2005.09.008

Nathan, C. F., & Hibbs, J. B., Jr. (1991). Role of nitric oxide synthesis in macrophage antimicrobial activity. *Curr Opin Immunol, 3*(1), 65-70. doi:10.1016/0952-7915(91)90079-g

Nguyen, K. B., Salazar-Mather, T. P., Dalod, M. Y., Van Deusen, J. B., Wei, X. Q., Liew, F. Y., . . . Biron, C. A. (2002). Coordinated and distinct roles for IFN-alpha beta, IL-12, and IL-15 regulation of NK cell responses to viral infection. *J Immunol, 169*(8), 4279-4287. doi:10.4049/jimmunol.169.8.4279

Niu, M. Y., Menard, M., Reed, J. C., Krajewski, S., & Pratt, M. A. (2001). Ectopic expression of cyclin D1 amplifies a retinoic acid-induced mitochondrial death pathway in breast cancer cells. *Oncogene, 20*(27), 3506-3518. doi:10.1038/sj.onc.1204453

Nomura, M., Takihara, Y., & Shimada, K. (1994). Isolation and characterization of retinoic acid-inducible cDNA clones in F9 cells: one of the early inducible clones encodes a novel protein sharing several highly homologous regions with a Drosophila polyhomeotic protein. *Differentiation, 57*(1), 39-50. doi:10.1046/j.1432-0436.1994.5710039.x

O'Brien, K. L., Assmann, N., O'Connor, E., Keane, C., Walls, J., Choi, C., . . . Finlay, D. K. (2021). De novo polyamine synthesis supports metabolic and functional responses in activated murine NK cells. *Eur J Immunol, 51*(1), 91-102. doi:10.1002/eji.202048784

O'Sullivan, T. E., Johnson, L. R., Kang, H. H., & Sun, J. C. (2015). BNIP3- and BNIP3L-Mediated Mitophagy Promotes the Generation of Natural Killer Cell Memory. *Immunity, 43*(2), 331-342. doi:10.1016/j.immuni.2015.07.012

O'Sullivan, T. E., Rapp, M., Fan, X., Weizman, O. E., Bhardwaj, P., Adams, N. M., . . . Sun, J. C. (2016). Adipose-Resident Group 1 Innate Lymphoid Cells Promote Obesity-Associated Insulin Resistance. *Immunity, 45*(2), 428-441. doi:10.1016/j.immuni.2016.06.016

Obrochta, K. M., Kane, M. A., & Napoli, J. L. (2014). Effects of diet and strain on mouse serum and tissue retinoid concentrations. *PLoS One, 9*(6), e99435. doi:10.1371/journal.pone.0099435

Ochi, M., Ohdan, H., Mitsuta, H., Onoe, T., Tokita, D., Hara, H., . . . Asahara, T. (2004). Liver NK cells expressing TRAIL are toxic against self hepatocytes in mice. *Hepatology, 39*(5), 1321-1331. doi:10.1002/hep.20204

Ochoa, M. C., Minute, L., Rodriguez, I., Garasa, S., Perez-Ruiz, E., Inoges, S., . . . Berraondo, P. (2017). Antibody-dependent cell cytotoxicity: immunotherapy strategies enhancing effector NK cells. *Immunol Cell Biol, 95*(4), 347-355. doi:10.1038/icb.2017.6

Ogawa, T., Tsuji-Kawahara, S., Yuasa, T., Kinoshita, S., Chikaishi, T., Takamura, S., . . . Miyazawa, M. (2011). Natural killer cells recognize friend retrovirus-infected erythroid progenitor cells through NKG2D-RAE-1 interactions In Vivo. *J Virol, 85*(11), 5423-5435. doi:10.1128/JVI.02146-10

Ohl, L., Mohaupt, M., Czeloth, N., Hintzen, G., Kiafard, Z., Zwirner, J., . . . Forster, R. (2004). CCR7 governs skin dendritic cell migration under inflammatory and

steady-state conditions. *Immunity, 21*(2), 279-288. doi:10.1016/j.immuni.2004.06.014

Ohta, A., & Sitkovsky, M. (2014). Extracellular adenosine-mediated modulation of regulatory T cells. *Front Immunol, 5*, 304. doi:10.3389/fimmu.2014.00304

Oliveira, L. M., Teixeira, F. M. E., & Sato, M. N. (2018). Impact of Retinoic Acid on Immune Cells and Inflammatory Diseases. *Mediators Inflamm, 2018*, 3067126. doi:10.1155/2018/3067126

Orange, J. S., & Biron, C. A. (1996). Characterization of early IL-12, IFN-alphabeta, and TNF effects on antiviral state and NK cell responses during murine cytomegalovirus infection. *J Immunol, 156*(12), 4746-4756. Retrieved from https://www.ncbi.nlm.nih.gov/pubmed/8648121

Ortaldo, J. R., Mason, A. T., Gerard, J. P., Henderson, L. E., Farrar, W., Hopkins, R. F., 3rd, . . . Rabin, H. (1984). Effects of natural and recombinant IL 2 on regulation of IFN gamma production and natural killer activity: lack of involvement of the Tac antigen for these immunoregulatory effects. *J Immunol, 133*(2), 779-783. Retrieved from https://www.ncbi.nlm.nih.gov/pubmed/6203980

Osada, T., Nagawa, H., Kitayama, J., Tsuno, N. H., Ishihara, S., Takamizawa, M., & Shibata, Y. (2001). Peripheral blood dendritic cells, but not monocyte-derived dendritic cells, can augment human NK cell function. *Cell Immunol, 213*(1), 14-23. doi:10.1006/cimm.2001.1858

Pairault, J., Quignard-Boulange, A., Dugail, I., & Lasnier, F. (1988). Differential effects of retinoic acid upon early and late events in adipose conversion of 3T3 preadipocytes. *Exp Cell Res, 177*(1), 27-36. doi:10.1016/0014-4827(88)90022-5

Pallmer, K., & Oxenius, A. (2016). Recognition and Regulation of T Cells by NK Cells. *Front Immunol, 7*, 251. doi:10.3389/fimmu.2016.00251

Pan, J., Zhang, M., Wang, J., Wang, Q., Xia, D., Sun, W., . . . Cao, X. (2004). Interferon-gamma is an autocrine mediator for dendritic cell maturation. *Immunol Lett, 94*(1-2), 141-151. doi:10.1016/j.imlet.2004.05.003

Park, H. J., Kim, D. H., Choi, J. Y., Kim, W. J., Kim, J. Y., Senejani, A. G., . . . Choi, J. M. (2014). PPARgamma negatively regulates T cell activation to prevent follicular helper T cells and germinal center formation. *PLoS One, 9*(6), e99127. doi:10.1371/journal.pone.0099127

Park, J. Y., Lee, S. H., Yoon, S. R., Park, Y. J., Jung, H., Kim, T. D., & Choi, I. (2011). IL-15-induced IL-10 increases the cytolytic activity of human natural killer cells. *Mol Cells, 32*(3), 265-272. doi:10.1007/s10059-011-1057-8

Parker, D. C. (1993). T cell-dependent B cell activation. *Annu Rev Immunol, 11*, 331-360. doi:10.1146/annurev.iy.11.040193.001555

Parolini, S., Santoro, A., Marcenaro, E., Luini, W., Massardi, L., Facchetti, F., . . . Sozzani, S. (2007). The role of chemerin in the colocalization of NK and dendritic cell subsets into inflamed tissues. *Blood, 109*(9), 3625-3632. doi:10.1182/blood-2006-08-038844

Patrad, E., Niapour, A., Farassati, F., & Amani, M. (2018). Combination treatment of all-trans retinoic acid (ATRA) and gamma-secretase inhibitor (DAPT) cause growth inhibition and apoptosis induction in the human gastric cancer cell line. *Cytotechnology, 70*(2), 865-877. doi:10.1007/s10616-018-0199-3

Paul, S., & Lal, G. (2017). The Molecular Mechanism of Natural Killer Cells Function and Its Importance in Cancer Immunotherapy. *Front Immunol, 8*, 1124. doi:10.3389/fimmu.2017.01124

Paust, S., Gill, H. S., Wang, B. Z., Flynn, M. P., Moseman, E. A., Senman, B., . . . von Andrian, U. H. (2010). Critical role for the chemokine receptor CXCR6 in NK cell-mediated antigen-specific memory of haptens and viruses. *Nat Immunol, 11*(12), 1127-1135. doi:10.1038/ni.1953

Pelaseyed, T., Bergstrom, J. H., Gustafsson, J. K., Ermund, A., Birchenough, G. M., Schutte, A., . . . Hansson, G. C. (2014). The mucus and mucins of the goblet cells and enterocytes provide the first defense line of the gastrointestinal tract and interact with the immune system. *Immunol Rev, 260*(1), 8-20. doi:10.1111/imr.12182

Peng, H., & Tian, Z. (2017). Diversity of tissue-resident NK cells. *Semin Immunol, 31*, 3-10. doi:10.1016/j.smim.2017.07.006

Penny, H. L., Prestwood, T. R., Bhattacharya, N., Sun, F., Kenkel, J. A., Davidson, M. G., . . . Engleman, E. G. (2016). Restoring Retinoic Acid Attenuates Intestinal Inflammation and Tumorigenesis in APCMin/+ Mice. *Cancer Immunol Res, 4*(11), 917-926. doi:10.1158/2326-6066.CIR-15-0038

Peppa, D., Gill, U. S., Reynolds, G., Easom, N. J., Pallett, L. J., Schurich, A., . . . Maini, M. K. (2013). Up-regulation of a death receptor renders antiviral T cells susceptible to NK cell-mediated deletion. *J Exp Med, 210*(1), 99-114. doi:10.1084/jem.20121172

Perona-Wright, G., Mohrs, K., Szaba, F. M., Kummer, L. W., Madan, R., Karp, C. L., . . . Mohrs, M. (2009). Systemic but not local infections elicit immunosuppressive IL-10 production by natural killer cells. *Cell Host Microbe, 6*(6), 503-512. doi:10.1016/j.chom.2009.11.003

Perrot, I., Michaud, H. A., Giraudon-Paoli, M., Augier, S., Docquier, A., Gros, L., . . . Bonnefoy, N. (2019). Blocking Antibodies Targeting the CD39/CD73 Immunosuppressive Pathway Unleash Immune Responses in Combination Cancer Therapies. *Cell Rep, 27*(8), 2411-2425 e2419. doi:10.1016/j.celrep.2019.04.091

Perussia, B. (1996). The Cytokine Profile of Resting and Activated NK Cells. *Methods, 9*(2), 370-378. doi:10.1006/meth.1996.0042

Pham, T. A., Clare, S., Goulding, D., Arasteh, J. M., Stares, M. D., Browne, H. P., . . . Lawley, T. D. (2014). Epithelial IL-22RA1-mediated fucosylation promotes intestinal colonization resistance to an opportunistic pathogen. *Cell Host Microbe, 16*(4), 504-516. doi:10.1016/j.chom.2014.08.017

Piccioli, D., Sbrana, S., Melandri, E., & Valiante, N. M. (2002). Contact-dependent stimulation and inhibition of dendritic cells by natural killer cells. *J Exp Med, 195*(3), 335-341. doi:10.1084/jem.20010934

Poggi, A., Massaro, A. M., Negrini, S., Contini, P., & Zocchi, M. R. (2005). Tumor-induced apoptosis of human IL-2-activated NK cells: role of natural cytotoxicity receptors. *J Immunol, 174*(5), 2653-2660. doi:10.4049/jimmunol.174.5.2653

Prager, I., & Watzl, C. (2019). Mechanisms of natural killer cell-mediated cellular cytotoxicity. *J Leukoc Biol, 105*(6), 1319-1329. doi:10.1002/JLB.MR0718-269R

Qrafli, M., El Kari, K., Aguenaou, H., Bourkadi, J. E., Sadki, K., & El Mzibri, M. (2017). Low plasma vitamin A concentration is associated with tuberculosis in Moroccan population: a preliminary case control study. *BMC Res Notes, 10*(1), 421. doi:10.1186/s13104-017-2737-z

Rabinovich, B. A., Li, J., Shannon, J., Hurren, R., Chalupny, J., Cosman, D., & Miller, R. G. (2003). Activated, but not resting, T cells can be recognized and killed by syngeneic NK cells. *J Immunol, 170*(7), 3572-3576. doi:10.4049/jimmunol.170.7.3572

Radaeva, S., Wang, L., Radaev, S., Jeong, W. I., Park, O., & Gao, B. (2007). Retinoic acid signaling sensitizes hepatic stellate cells to NK cell killing via upregulation of NK cell activating ligand RAE1. *Am J Physiol Gastrointest Liver Physiol, 293*(4), G809-816. doi:10.1152/ajpgi.00212.2007

Ramachandran, G., Santha, T., Garg, R., Baskaran, D., Iliayas, S. A., Venkatesan, P., . . . Narayanan, P. R. (2004). Vitamin A levels in sputum-positive pulmonary tuberculosis patients in comparison with household contacts and healthy 'normals'. *Int J Tuberc Lung Dis, 8*(9), 1130-1133. Retrieved from https://www.ncbi.nlm.nih.gov/pubmed/15455600

Reichlin, A., & Yokoyama, W. M. (1998). Natural killer cell proliferation induced by anti-NK1.1 and IL-2. *Immunol Cell Biol, 76*(2), 143-152. doi:10.1046/j.1440-1711.1998.00726.x

Reiner, S. L. (2007). Development in motion: helper T cells at work. *Cell, 129*(1), 33-36. doi:10.1016/j.cell.2007.03.019

Repa, J. J., Hanson, K. K., & Clagett-Dame, M. (1993). All-trans-retinol is a ligand for the retinoic acid receptors. *Proc Natl Acad Sci U S A, 90*(15), 7293-7297. doi:10.1073/pnas.90.15.7293

Restori, K. H., McDaniel, K. L., Wray, A. E., Cantorna, M. T., & Ross, A. C. (2014). Streptococcus pneumoniae-induced pneumonia and Citrobacter rodentium-induced gut infection differentially alter vitamin A concentrations in the lung and liver of mice. *J Nutr, 144*(3), 392-398. doi:10.3945/jn.113.186569

Rieck, M., Meissner, W., Ries, S., Muller-Brusselbach, S., & Muller, R. (2008). Ligand-mediated regulation of peroxisome proliferator-activated receptor (PPAR) beta/delta: a comparative analysis of PPAR-selective agonists and all-trans retinoic acid. *Mol Pharmacol, 74*(5), 1269-1277. doi:10.1124/mol.108.050625

Rigobello, M. P., Scutari, G., Friso, A., Barzon, E., Artusi, S., & Bindoli, A. (1999). Mitochondrial permeability transition and release of cytochrome c induced by retinoic acids. *Biochem Pharmacol, 58*(4), 665-670. doi:10.1016/s0006-2952(99)00149-5

Ring, S., Oliver, S. J., Cronstein, B. N., Enk, A. H., & Mahnke, K. (2009). CD4+CD25+ regulatory T cells suppress contact hypersensitivity reactions through a CD39, adenosine-dependent mechanism. *J Allergy Clin Immunol, 123*(6), 1287-1296 e1282. doi:10.1016/j.jaci.2009.03.022

Robinette, M. L., Fuchs, A., Cortez, V. S., Lee, J. S., Wang, Y., Durum, S. K., . . . Immunological Genome, C. (2015). Transcriptional programs define molecular characteristics of innate lymphoid cell classes and subsets. *Nat Immunol, 16*(3), 306-317. doi:10.1038/ni.3094

Rojas, J. M., Avia, M., Martin, V., & Sevilla, N. (2017). IL-10: A Multifunctional Cytokine in Viral Infections. *J Immunol Res, 2017*, 6104054. doi:10.1155/2017/6104054

Rook, A. H., Kehrl, J. H., Wakefield, L. M., Roberts, A. B., Sporn, M. B., Burlington, D. B., . . . Fauci, A. S. (1986). Effects of transforming growth factor beta on the functions of natural killer cells: depressed cytolytic activity and blunting of interferon responsiveness. *J Immunol, 136*(10), 3916-3920. Retrieved from https://www.ncbi.nlm.nih.gov/pubmed/2871107

Ross, M. E., & Caligiuri, M. A. (1997). Cytokine-induced apoptosis of human natural killer cells identifies a novel mechanism to regulate the innate immune response. *Blood, 89*(3), 910-918. Retrieved from https://www.ncbi.nlm.nih.gov/pubmed/9028322

Ruane, D. T., & Lavelle, E. C. (2011). The role of CD103(+) dendritic cells in the intestinal mucosal immune system. *Front Immunol, 2*, 25. doi:10.3389/fimmu.2011.00025

Russell, M. S., Dudani, R., Krishnan, L., & Sad, S. (2009). IFN-gamma expressed by T cells regulates the persistence of antigen presentation by limiting the survival of dendritic cells. *J Immunol, 183*(12), 7710-7718. doi:10.4049/jimmunol.0901274

Saeed, A., Dullaart, R. P. F., Schreuder, T., Blokzijl, H., & Faber, K. N. (2017). Disturbed Vitamin A Metabolism in Non-Alcoholic Fatty Liver Disease (NAFLD). *Nutrients, 10*(1). doi:10.3390/nu10010029

Sag, D., Ayyildiz, Z. O., Gunalp, S., & Wingender, G. (2019). The Role of TRAIL/DRs in the Modulation of Immune Cells and Responses. *Cancers (Basel), 11*(10). doi:10.3390/cancers11101469

Salinas, N., Olguin, J. E., Castellanos, C., & Saavedra, R. (2014). T cell suppression in vitro during Toxoplasma gondii infection is the result of IL-2 competition between Tregs and T cells leading to death of proliferating T cells. *Scand J Immunol, 79*(1), 1-11. doi:10.1111/sji.12120

Sanchez-Martinez, D., Krzywinska, E., Rathore, M. G., Saumet, A., Cornillon, A., Lopez-Royuela, N., . . . Villalba, M. (2014). All-trans retinoic acid (ATRA) induces miR-23a expression, decreases CTSC expression and granzyme B activity leading to impaired NK cell cytotoxicity. *Int J Biochem Cell Biol, 49*, 42-52. doi:10.1016/j.biocel.2014.01.003

Sato, M., Hiragun, A., & Mitsui, H. (1980). Preadipocytes possess cellular retinoid binding proteins and their differentiation is inhibited by retinoids. *Biochem Biophys Res Commun, 95*(4), 1839-1845. doi:10.1016/s0006-291x(80)80113-6

Sato, Y., Murase, K., Kato, J., Kobune, M., Sato, T., Kawano, Y., . . . Niitsu, Y. (2008). Resolution of liver cirrhosis using vitamin A-coupled liposomes to deliver siRNA against a collagen-specific chaperone. *Nat Biotechnol, 26*(4), 431-442. doi:10.1038/nbt1396

Satoh-Takayama, N., Vosshenrich, C. A., Lesjean-Pottier, S., Sawa, S., Lochner, M., Rattis, F., . . . Di Santo, J. P. (2008). Microbial flora drives interleukin 22 production in intestinal NKp46+ cells that provide innate mucosal immune defense. *Immunity, 29*(6), 958-970. doi:10.1016/j.immuni.2008.11.001

Schambach, F., Schupp, M., Lazar, M. A., & Reiner, S. L. (2007). Activation of retinoic acid receptor-alpha favours regulatory T cell induction at the expense of IL-17-secreting T helper cell differentiation. *Eur J Immunol, 37*(9), 2396-2399. doi:10.1002/eji.200737621

Schmidt, M. V., Paulus, P., Kuhn, A. M., Weigert, A., Morbitzer, V., Zacharowski, K., . . . von Knethen, A. (2011). Peroxisome proliferator-activated receptor gamma-induced T cell apoptosis reduces survival during polymicrobial sepsis. *Am J Respir Crit Care Med, 184*(1), 64-74. doi:10.1164/rccm.201010-1585OC

Schneider, E., Winzer, R., Rissiek, A., Ricklefs, I., Meyer-Schwesinger, C., Ricklefs, F. L., . . . Tolosa, E. (2021). CD73-mediated adenosine production by CD8 T cell-derived extracellular vesicles constitutes an intrinsic mechanism of immune suppression. *Nat Commun, 12*(1), 5911. doi:10.1038/s41467-021-26134-w

Schulz, O., Jaensson, E., Persson, E. K., Liu, X., Worbs, T., Agace, W. W., & Pabst, O. (2009). Intestinal CD103+, but not CX3CR1+, antigen sampling cells migrate in lymph and serve classical dendritic cell functions. *J Exp Med, 206*(13), 3101-3114. doi:10.1084/jem.20091925

Schuster, I. S., Wikstrom, M. E., Brizard, G., Coudert, J. D., Estcourt, M. J., Manzur, M., . . . Degli-Esposti, M. A. (2014). TRAIL+ NK cells control CD4+ T cell responses during chronic viral infection to limit autoimmunity. *Immunity, 41*(4), 646-656. doi:10.1016/j.immuni.2014.09.013

Schwarz, E. J., Reginato, M. J., Shao, D., Krakow, S. L., & Lazar, M. A. (1997). Retinoic acid blocks adipogenesis by inhibiting C/EBPbeta-mediated transcription. *Mol Cell Biol, 17*(3), 1552-1561. doi:10.1128/MCB.17.3.1552

Screpanti, V., Wallin, R. P., Grandien, A., & Ljunggren, H. G. (2005). Impact of FASL-induced apoptosis in the elimination of tumor cells by NK cells. *Mol Immunol, 42*(4), 495-499. doi:10.1016/j.molimm.2004.07.033

Seguin-Devaux, C., Hanriot, D., Dailloux, M., Latger-Cannard, V., Zannad, F., Mertes, P. M., . . . Devaux, Y. (2005). Retinoic acid amplifies the host immune response to LPS through increased T lymphocytes number and LPS binding protein expression. *Mol Cell Endocrinol, 245*(1-2), 67-76. doi:10.1016/j.mce.2005.10.006

Sengupta, S., Ray, S., Chattopadhyay, N., Biswas, N., & Chatterjee, A. (2000). Effect of retinoic acid on integrin receptors of B16F10 melanoma cells. *J Exp Clin Cancer Res, 19*(1), 81-87. Retrieved from https://www.ncbi.nlm.nih.gov/pubmed/10840941

Senoo, H., & Wake, K. (1985). Suppression of experimental hepatic fibrosis by administration of vitamin A. *Lab Invest, 52*(2), 182-194. Retrieved from https://www.ncbi.nlm.nih.gov/pubmed/2578584

Serafini, N., Klein Wolterink, R. G., Satoh-Takayama, N., Xu, W., Vosshenrich, C. A., Hendriks, R. W., & Di Santo, J. P. (2014). Gata3 drives development of RORgammat+ group 3 innate lymphoid cells. *J Exp Med, 211*(2), 199-208. doi:10.1084/jem.20131038

Seth, S., Georgoudaki, A. M., Chambers, B. J., Qiu, Q., Kremmer, E., Maier, M. K., . . . Bernhardt, G. (2009). Heterogeneous expression of the adhesion receptor CD226 on murine NK and T cells and its function in NK-mediated killing of immature dendritic cells. *J Leukoc Biol, 86*(1), 91-101. doi:10.1189/jlb.1208745

Seward, C. R., Vaughan, G., & Hove, E. L. (1964). Respiratory Activities of Hypo- and Hypervitaminotic-a Rat Liver Homogenates. *Proc Soc Exp Biol Med, 117*, 477-480. doi:10.3181/00379727-117-29612

Seward, C. R., Vaughan, G., & Hove, E. L. (1966). Effect of vitamin A deficiency or excess on the oxidative phosphorylation by rat liver mitochondria. *J Biol Chem, 241*(5), 1229-1232. Retrieved from https://www.ncbi.nlm.nih.gov/pubmed/5933880

Sharpe, A. H., & Freeman, G. J. (2002). The B7-CD28 superfamily. *Nat Rev Immunol, 2*(2), 116-126. doi:10.1038/nri727

Shaw, N., Elholm, M., & Noy, N. (2003). Retinoic acid is a high affinity selective ligand for the peroxisome proliferator-activated receptor beta/delta. *J Biol Chem, 278*(43), 41589-41592. doi:10.1074/jbc.C300368200

Shinkai, Y., Rathbun, G., Lam, K. P., Oltz, E. M., Stewart, V., Mendelsohn, M., . . . et al. (1992). RAG-2-deficient mice lack mature lymphocytes owing to inability to initiate V(D)J rearrangement. *Cell, 68*(5), 855-867. doi:10.1016/0092-8674(92)90029-c

Siddikuzzaman, & Grace, V. M. (2012). Inhibition of metastatic lung cancer in C57BL/6 mice by liposome encapsulated all trans retinoic acid (ATRA). *Int Immunopharmacol, 14*(4), 570-579. doi:10.1016/j.intimp.2012.09.008

Siddikuzzaman, & Grace, V. M. (2014). Anti-metastatic study of liposome-encapsulated all trans retinoic acid (ATRA) in B16F10 melanoma cells-implanted C57BL/6 mice. *Cancer Invest, 32*(10), 507-517. doi:10.3109/07357907.2014.964408

Silva, F. S., Ribeiro, M. P., Santos, M. S., Rocha-Pereira, P., Santos-Silva, A., & Custodio, J. B. (2013). Acitretin affects bioenergetics of liver mitochondria and

promotes mitochondrial permeability transition: potential mechanisms of hepatotoxicity. *Toxicology, 306*, 93-100. doi:10.1016/j.tox.2013.01.020

Silver, J. S., Kearley, J., Copenhaver, A. M., Sanden, C., Mori, M., Yu, L., . . . Humbles, A. A. (2016). Inflammatory triggers associated with exacerbations of COPD orchestrate plasticity of group 2 innate lymphoid cells in the lungs. *Nat Immunol, 17*(6), 626-635. doi:10.1038/ni.3443

Sivakumar, B., & Reddy, V. (1972). Absorption of labelled vitamin A in children during infection. *Br J Nutr, 27*(2), 299-304. doi:10.1079/bjn19720094

Sivakumar, B., & Reddy, V. (1975). Absorption of vitamin A in children with ascariasis. *J Trop Med Hyg, 78*(5), 114-115. Retrieved from https://www.ncbi.nlm.nih.gov/pubmed/1152102

Slattery, K., Woods, E., Zaiatz-Bittencourt, V., Marks, S., Chew, S., Conroy, M., . . . Gardiner, C. M. (2021). TGFbeta drives NK cell metabolic dysfunction in human metastatic breast cancer. *J Immunother Cancer, 9*(2). doi:10.1136/jitc-2020-002044

Smith, C. A., Williams, G. T., Kingston, R., Jenkinson, E. J., & Owen, J. J. (1989). Antibodies to CD3/T-cell receptor complex induce death by apoptosis in immature T cells in thymic cultures. *Nature, 337*(6203), 181-184. doi:10.1038/337181a0

Smith, P. M., Howitt, M. R., Panikov, N., Michaud, M., Gallini, C. A., Bohlooly, Y. M., . . . Garrett, W. S. (2013). The microbial metabolites, short-chain fatty acids, regulate colonic Treg cell homeostasis. *Science, 341*(6145), 569-573. doi:10.1126/science.1241165

Smyth, M. J., Swann, J., Kelly, J. M., Cretney, E., Yokoyama, W. M., Diefenbach, A., . . . Hayakawa, Y. (2004). NKG2D recognition and perforin effector function mediate effective cytokine immunotherapy of cancer. *J Exp Med, 200*(10), 1325-1335. doi:10.1084/jem.20041522

Smyth, M. J., Thia, K. Y., Cretney, E., Kelly, J. M., Snook, M. B., Forbes, C. A., & Scalzo, A. A. (1999). Perforin is a major contributor to NK cell control of tumor metastasis. *J Immunol, 162*(11), 6658-6662. Retrieved from https://www.ncbi.nlm.nih.gov/pubmed/10352283

Sojka, D. K., Plougastel-Douglas, B., Yang, L., Pak-Wittel, M. A., Artyomov, M. N., Ivanova, Y., . . . Yokoyama, W. M. (2014). Tissue-resident natural killer (NK) cells are cell lineages distinct from thymic and conventional splenic NK cells. *Elife, 3*, e01659. doi:10.7554/eLife.01659

Sonnenberg, G. F., Fouser, L. A., & Artis, D. (2011). Border patrol: regulation of immunity, inflammation and tissue homeostasis at barrier surfaces by IL-22. *Nat Immunol, 12*(5), 383-390. doi:10.1038/ni.2025

Spencer, S. P., Wilhelm, C., Yang, Q., Hall, J. A., Bouladoux, N., Boyd, A., . . . Belkaid, Y. (2014). Adaptation of innate lymphoid cells to a micronutrient deficiency promotes type 2 barrier immunity. *Science, 343*(6169), 432-437. doi:10.1126/science.1247606

Stacey, M. A., Marsden, M., Wang, E. C., Wilkinson, G. W., & Humphreys, I. R. (2011). IL-10 restricts activation-induced death of NK cells during acute murine cytomegalovirus infection. *J Immunol, 187*(6), 2944-2952. doi:10.4049/jimmunol.1101021

Stegmann, K. A., Bjorkstrom, N. K., Veber, H., Ciesek, S., Riese, P., Wiegand, J., . . . Wedemeyer, H. (2010). Interferon-alpha-induced TRAIL on natural killer cells is associated with control of hepatitis C virus infection. *Gastroenterology, 138*(5), 1885-1897. doi:10.1053/j.gastro.2010.01.051

Stegmann, K. A., Robertson, F., Hansi, N., Gill, U., Pallant, C., Christophides, T., . . . Maini, M. K. (2016). CXCR6 marks a novel subset of T-bet(lo)Eomes(hi) natural killer cells residing in human liver. *Sci Rep, 6*, 26157. doi:10.1038/srep26157

Stojanovic, A., Fiegler, N., Brunner-Weinzierl, M., & Cerwenka, A. (2014). CTLA-4 is expressed by activated mouse NK cells and inhibits NK Cell IFN-gamma production in response to mature dendritic cells. *J Immunol, 192*(9), 4184-4191. doi:10.4049/jimmunol.1302091

Sun, C. M., Hall, J. A., Blank, R. B., Bouladoux, N., Oukka, M., Mora, J. R., & Belkaid, Y. (2007). Small intestine lamina propria dendritic cells promote de novo generation of Foxp3 T reg cells via retinoic acid. *J Exp Med, 204*(8), 1775-1785. doi:10.1084/jem.20070602

Sun, H., Sun, C., Tian, Z., & Xiao, W. (2013). NK cells in immunotolerant organs. *Cell Mol Immunol, 10*(3), 202-212. doi:10.1038/cmi.2013.9

Sun, J. C., Beilke, J. N., & Lanier, L. L. (2009). Adaptive immune features of natural killer cells. *Nature, 457*(7229), 557-561. doi:10.1038/nature07665

Sun, S. Y., Wan, H., Yue, P., Hong, W. K., & Lotan, R. (2000). Evidence that retinoic acid receptor beta induction by retinoids is important for tumor cell growth inhibition. *J Biol Chem, 275*(22), 17149-17153. doi:10.1074/jbc.M000527200

Surace, L., Doisne, J. M., Escoll, P., Marie, S., Dardalhon, V., Croft, C., . . . Di Santo, J. P. (2021). Polarized mitochondria as guardians of NK cell fitness. *Blood Adv, 5*(1), 26-38. doi:10.1182/bloodadvances.2020003458

Swann, J. B., Hayakawa, Y., Zerafa, N., Sheehan, K. C., Scott, B., Schreiber, R. D., . . . Smyth, M. J. (2007). Type I IFN contributes to NK cell homeostasis, activation, and antitumor function. *J Immunol, 178*(12), 7540-7549. doi:10.4049/jimmunol.178.12.7540

Szabo, S. J., Kim, S. T., Costa, G. L., Zhang, X., Fathman, C. G., & Glimcher, L. H. (2000). A novel transcription factor, T-bet, directs Th1 lineage commitment. *Cell, 100*(6), 655-669. doi:10.1016/s0092-8674(00)80702-3

Szanto, A., Narkar, V., Shen, Q., Uray, I. P., Davies, P. J., & Nagy, L. (2004). Retinoid X receptors: X-ploring their (patho)physiological functions. *Cell Death Differ, 11 Suppl 2*, S126-143. doi:10.1038/sj.cdd.4401533

Takeda, K., Cretney, E., Hayakawa, Y., Ota, T., Akiba, H., Ogasawara, K., . . . Smyth, M. J. (2005). TRAIL identifies immature natural killer cells in newborn mice and adult mouse liver. *Blood, 105*(5), 2082-2089. doi:10.1182/blood-2004-08-3262

Tan, M. C., Goedegebuure, P. S., Belt, B. A., Flaherty, B., Sankpal, N., Gillanders, W. E., . . . Linehan, D. C. (2009). Disruption of CCR5-dependent homing of regulatory T cells inhibits tumor growth in a murine model of pancreatic cancer. *J Immunol, 182*(3), 1746-1755. doi:10.4049/jimmunol.182.3.1746

Tang, L., Peng, H., Zhou, J., Chen, Y., Wei, H., Sun, R., . . . Tian, Z. (2016). Differential phenotypic and functional properties of liver-resident NK cells and mucosal ILC1s. *J Autoimmun, 67*, 29-35. doi:10.1016/j.jaut.2015.09.004

Taylor, P., Botto, M., & Walport, M. (1998). The complement system. *Curr Biol, 8*(8), R259-261. doi:10.1016/s0960-9822(98)70167-8

Thoma-Uszynski, S., Kiertscher, S. M., Ochoa, M. T., Bouis, D. A., Norgard, M. V., Miyake, K., . . . Modlin, R. L. (2000). Activation of toll-like receptor 2 on human dendritic cells triggers induction of IL-12, but not IL-10. *J Immunol, 165*(7), 3804-3810. doi:10.4049/jimmunol.165.7.3804

Tian, Z., Chen, Y., & Gao, B. (2013). Natural killer cells in liver disease. *Hepatology, 57*(4), 1654-1662. doi:10.1002/hep.26115

Tobin, L. M., Mavinkurve, M., Carolan, E., Kinlen, D., O'Brien, E. C., Little, M. A., . . . O'Shea, D. (2017). NK cells in childhood obesity are activated, metabolically

stressed, and functionally deficient. *JCI Insight, 2*(24). doi:10.1172/jci.insight.94939

Tosello-Trampont, A., Surette, F. A., Ewald, S. E., & Hahn, Y. S. (2017). Immunoregulatory Role of NK Cells in Tissue Inflammation and Regeneration. *Front Immunol, 8*, 301. doi:10.3389/fimmu.2017.00301

Tourniaire, F., Musinovic, H., Gouranton, E., Astier, J., Marcotorchino, J., Arreguin, A., . . . Landrier, J. F. (2015). All-trans retinoic acid induces oxidative phosphorylation and mitochondria biogenesis in adipocytes. *J Lipid Res, 56*(6), 1100-1109. doi:10.1194/jlr.M053652

Townsend, M. J., Weinmann, A. S., Matsuda, J. L., Salomon, R., Farnham, P. J., Biron, C. A., . . . Glimcher, L. H. (2004). T-bet regulates the terminal maturation and homeostasis of NK and Valpha14i NKT cells. *Immunity, 20*(4), 477-494. doi:10.1016/s1074-7613(04)00076-7

Trapani, J. A., Jans, D. A., Jans, P. J., Smyth, M. J., Browne, K. A., & Sutton, V. R. (1998). Efficient nuclear targeting of granzyme B and the nuclear consequences of apoptosis induced by granzyme B and perforin are caspase-dependent, but cell death is caspase-independent. *J Biol Chem, 273*(43), 27934-27938. doi:10.1074/jbc.273.43.27934

Trinchieri, G., Matsumoto-Kobayashi, M., Clark, S. C., Seehra, J., London, L., & Perussia, B. (1984). Response of resting human peripheral blood natural killer cells to interleukin 2. *J Exp Med, 160*(4), 1147-1169. doi:10.1084/jem.160.4.1147

van de Pavert, S. A., Ferreira, M., Domingues, R. G., Ribeiro, H., Molenaar, R., Moreira-Santos, L., . . . Veiga-Fernandes, H. (2014). Maternal retinoids control type 3 innate lymphoid cells and set the offspring immunity. *Nature, 508*(7494), 123-127. doi:10.1038/nature13158

van den Broek, M. F., Kagi, D., Zinkernagel, R. M., & Hengartner, H. (1995). Perforin dependence of natural killer cell-mediated tumor control in vivo. *Eur J Immunol, 25*(12), 3514-3516. doi:10.1002/eji.1830251246

Van, Y. H., Lee, W. H., Ortiz, S., Lee, M. H., Qin, H. J., & Liu, C. P. (2009). All-trans retinoic acid inhibits type 1 diabetes by T regulatory (Treg)-dependent suppression of interferon-gamma-producing T-cells without affecting Th17 cells. *Diabetes, 58*(1), 146-155. doi:10.2337/db08-1154

Viel, S., Marcais, A., Guimaraes, F. S., Loftus, R., Rabilloud, J., Grau, M., . . . Walzer, T. (2016). TGF-beta inhibits the activation and functions of NK cells by repressing the mTOR pathway. *Sci Signal, 9*(415), ra19. doi:10.1126/scisignal.aad1884

Vitale, M., Cantoni, C., Pietra, G., Mingari, M. C., & Moretta, L. (2014). Effect of tumor cells and tumor microenvironment on NK-cell function. *Eur J Immunol, 44*(6), 1582-1592. doi:10.1002/eji.201344272

Vitale, M., Della Chiesa, M., Carlomagno, S., Pende, D., Arico, M., Moretta, L., & Moretta, A. (2005). NK-dependent DC maturation is mediated by TNFalpha and IFNgamma released upon engagement of the NKp30 triggering receptor. *Blood, 106*(2), 566-571. doi:10.1182/blood-2004-10-4035

Vivier, E., Artis, D., Colonna, M., Diefenbach, A., Di Santo, J. P., Eberl, G., . . . Spits, H. (2018). Innate Lymphoid Cells: 10 Years On. *Cell, 174*(5), 1054-1066. doi:10.1016/j.cell.2018.07.017

Vivier, E., Morin, P., O'Brien, C., Druker, B., Schlossman, S. F., & Anderson, P. (1991). Tyrosine phosphorylation of the Fc gamma RIII(CD16): zeta complex in human natural killer cells. Induction by antibody-dependent cytotoxicity but not by

natural killing. *J Immunol, 146*(1), 206-210. Retrieved from https://www.ncbi.nlm.nih.gov/pubmed/1701792

Vivier, E., Tomasello, E., Baratin, M., Walzer, T., & Ugolini, S. (2008). Functions of natural killer cells. *Nat Immunol, 9*(5), 503-510. doi:10.1038/ni1582

Wagage, S., John, B., Krock, B. L., Hall, A. O., Randall, L. M., Karp, C. L., . . . Hunter, C. A. (2014). The aryl hydrocarbon receptor promotes IL-10 production by NK cells. *J Immunol, 192*(4), 1661-1670. doi:10.4049/jimmunol.1300497

Waggoner, S. N., Cornberg, M., Selin, L. K., & Welsh, R. M. (2011). Natural killer cells act as rheostats modulating antiviral T cells. *Nature, 481*(7381), 394-398. doi:10.1038/nature10624

Waggoner, S. N., Taniguchi, R. T., Mathew, P. A., Kumar, V., & Welsh, R. M. (2010). Absence of mouse 2B4 promotes NK cell-mediated killing of activated CD8+ T cells, leading to prolonged viral persistence and altered pathogenesis. *J Clin Invest, 120*(6), 1925-1938. doi:10.1172/JCI41264

Wagner, H., Hardt, C., Heeg, K., Pfizenmaier, K., Solbach, W., Bartlett, R., . . . Rollinghoff, M. (1980). T-T cell interactions during cytotoxic T lymphocyte (CTL) responses: T cell derived helper factor (Interleukin 2) as a probe to analyze CTL responsiveness and thymic maturation of CTL progenitors. *Immunol Rev, 51*, 215-255. doi:10.1111/j.1600-065x.1980.tb00323.x

Walzer, T., Dalod, M., Robbins, S. H., Zitvogel, L., & Vivier, E. (2005). Natural-killer cells and dendritic cells: "l'union fait la force". *Blood, 106*(7), 2252-2258. doi:10.1182/blood-2005-03-1154

Wang, G. Q., Wieckowski, E., Goldstein, L. A., Gastman, B. R., Rabinovitz, A., Gambotto, A., . . . Rabinowich, H. (2001). Resistance to granzyme B-mediated cytochrome c release in Bak-deficient cells. *J Exp Med, 194*(9), 1325-1337. doi:10.1084/jem.194.9.1325

Wang, K. S., Frank, D. A., & Ritz, J. (2000). Interleukin-2 enhances the response of natural killer cells to interleukin-12 through up-regulation of the interleukin-12 receptor and STAT4. *Blood, 95*(10), 3183-3190. Retrieved from https://www.ncbi.nlm.nih.gov/pubmed/10807786

Wang, Q., Yang, W., Uytingco, M. S., Christakos, S., & Wieder, R. (2000). 1,25-Dihydroxyvitamin D3 and all-trans-retinoic acid sensitize breast cancer cells to chemotherapy-induced cell death. *Cancer Res, 60*(7), 2040-2048. Retrieved from https://www.ncbi.nlm.nih.gov/pubmed/10766196

Wang, R., Jaw, J. J., Stutzman, N. C., Zou, Z., & Sun, P. D. (2012). Natural killer cell-produced IFN-gamma and TNF-alpha induce target cell cytolysis through up-regulation of ICAM-1. *J Leukoc Biol, 91*(2), 299-309. doi:10.1189/jlb.0611308

Wang, X., Lang, M., Zhao, T., Feng, X., Zheng, C., Huang, C., . . . Ren, H. (2017). Cancer-FOXP3 directly activated CCL5 to recruit FOXP3(+)Treg cells in pancreatic ductal adenocarcinoma. *Oncogene, 36*(21), 3048-3058. doi:10.1038/onc.2016.458

Wang, Y., Zhong, Y. J., Wang, Y. Y., Xing, J., & Wang, Z. M. (2016). All-trans retinoic acid prevents the development of type 1 diabetes by affecting the levels of interferon gamma and interleukin 4 in streptozotocin-induced murine diabetes model. *Genet Mol Res, 15*(1). doi:10.4238/gmr.15017522

Wang, Z., Cao, Y., D'Urso, C. M., & Ferrone, S. (1992). Differential susceptibility of cultured human melanoma cell lines to enhancement by retinoic acid of intercellular adhesion molecule 1 expression. *Cancer Res, 52*(17), 4766-4772. Retrieved from https://www.ncbi.nlm.nih.gov/pubmed/1355009

Wang, Z., Guan, D., Huo, J., Biswas, S. K., Huang, Y., Yang, Y., . . . Lam, K. P. (2021). IL-10 Enhances Human Natural Killer Cell Effector Functions via Metabolic

Reprogramming Regulated by mTORC1 Signaling. *Front Immunol, 12*, 619195. doi:10.3389/fimmu.2021.619195

Wansley, D. L., Yin, Y., & Prussin, C. (2013). The retinoic acid receptor-alpha modulators ATRA and Ro415253 reciprocally regulate human IL-5+ Th2 cell proliferation and cytokine expression. *Clin Mol Allergy, 11*(1), 4. doi:10.1186/1476-7961-11-4

Weidinger, G., Henning, G., ter Meulen, V., & Niewiesk, S. (2001). Inhibition of major histocompatibility complex class II-dependent antigen presentation by neutralization of gamma interferon leads to breakdown of resistance against measles virus-induced encephalitis. *J Virol, 75*(7), 3059-3065. doi:10.1128/JVI.75.7.3059-3065.2001

Wilson, J. L., Heffler, L. C., Charo, J., Scheynius, A., Bejarano, M. T., & Ljunggren, H. G. (1999). Targeting of human dendritic cells by autologous NK cells. *J Immunol, 163*(12), 6365-6370. Retrieved from https://www.ncbi.nlm.nih.gov/pubmed/10586025

Xiao, Q., He, J., Lei, A., Xu, H., Zhang, L., Zhou, P., . . . Zhou, J. (2021). PPARgamma enhances ILC2 function during allergic airway inflammation via transcription regulation of ST2. *Mucosal Immunol, 14*(2), 468-478. doi:10.1038/s41385-020-00339-6

Xiao, S., Jin, H., Korn, T., Liu, S. M., Oukka, M., Lim, B., & Kuchroo, V. K. (2008). Retinoic acid increases Foxp3+ regulatory T cells and inhibits development of Th17 cells by enhancing TGF-beta-driven Smad3 signaling and inhibiting IL-6 and IL-23 receptor expression. *J Immunol, 181*(4), 2277-2284. doi:10.4049/jimmunol.181.4.2277

Xu, H. C., Grusdat, M., Pandyra, A. A., Polz, R., Huang, J., Sharma, P., . . . Lang, P. A. (2014). Type I interferon protects antiviral CD8+ T cells from NK cell cytotoxicity. *Immunity, 40*(6), 949-960. doi:10.1016/j.immuni.2014.05.004

Xu, H. C., Huang, J., Pandyra, A. A., Lang, E., Zhuang, Y., Thons, C., . . . Lang, P. A. (2017). Lymphocytes Negatively Regulate NK Cell Activity via Qa-1b following Viral Infection. *Cell Rep, 21*(9), 2528-2540. doi:10.1016/j.celrep.2017.11.001

Yagi, R., Zhong, C., Northrup, D. L., Yu, F., Bouladoux, N., Spencer, S., . . . Zhu, J. (2014). The transcription factor GATA3 is critical for the development of all IL-7Ralpha-expressing innate lymphoid cells. *Immunity, 40*(3), 378-388. doi:10.1016/j.immuni.2014.01.012

Yanagitani, A., Yamada, S., Yasui, S., Shimomura, T., Murai, R., Murawaki, Y., . . . Shiota, G. (2004). Retinoic acid receptor alpha dominant negative form causes steatohepatitis and liver tumors in transgenic mice. *Hepatology, 40*(2), 366-375. doi:10.1002/hep.20335

Yang, X. O., Nurieva, R., Martinez, G. J., Kang, H. S., Chung, Y., Pappu, B. P., . . . Dong, C. (2008). Molecular antagonism and plasticity of regulatory and inflammatory T cell programs. *Immunity, 29*(1), 44-56. doi:10.1016/j.immuni.2008.05.007

Yao, J., Zhang, L., Zhou, J., Liu, H., & Zhang, Q. (2013). Efficient simultaneous tumor targeting delivery of all-trans retinoid acid and Paclitaxel based on hyaluronic acid-based multifunctional nanocarrier. *Mol Pharm, 10*(3), 1080-1091. doi:10.1021/mp3005808

Ye, X., Wu, Q., Liu, S., Lin, X., Zhang, B., Wu, J., . . . Su, W. (2004). Distinct role and functional mode of TR3 and RARalpha in mediating ATRA-induced signalling pathway in breast and gastric cancer cells. *Int J Biochem Cell Biol, 36*(1), 98-113. doi:10.1016/s1357-2725(03)00143-2

Yu, Y., Hagihara, M., Ando, K., Gansuvd, B., Matsuzawa, H., Tsuchiya, T., . . . Kato, S. (2001). Enhancement of human cord blood CD34+ cell-derived NK cell cytotoxicity by dendritic cells. *J Immunol, 166*(3), 1590-1600. doi:10.4049/jimmunol.166.3.1590

Zaiatz-Bittencourt, V., Finlay, D. K., & Gardiner, C. M. (2018). Canonical TGF-beta Signaling Pathway Represses Human NK Cell Metabolism. *J Immunol, 200*(12), 3934-3941. doi:10.4049/jimmunol.1701461

Zamai, L., Ahmad, M., Bennett, I. M., Azzoni, L., Alnemri, E. S., & Perussia, B. (1998). Natural killer (NK) cell-mediated cytotoxicity: differential use of TRAIL and Fas ligand by immature and mature primary human NK cells. *J Exp Med, 188*(12), 2375-2380. doi:10.1084/jem.188.12.2375

Zeng, R., Bscheider, M., Lahl, K., Lee, M., & Butcher, E. C. (2016). Generation and transcriptional programming of intestinal dendritic cells: essential role of retinoic acid. *Mucosal Immunol, 9*(1), 183-193. doi:10.1038/mi.2015.50

Zhao, J., Cheng, L., Wang, H., Yu, H., Tu, B., Fu, Q., . . . Zhang, Z. (2018). Infection and depletion of CD4+ group-1 innate lymphoid cells by HIV-1 via type-I interferon pathway. *PLoS Pathog, 14*(1), e1006819. doi:10.1371/journal.ppat.1006819

Zhou, L., Chong, M. M., & Littman, D. R. (2009). Plasticity of CD4+ T cell lineage differentiation. *Immunity, 30*(5), 646-655. doi:10.1016/j.immuni.2009.05.001

Zhou, L., Chu, C., Teng, F., Bessman, N. J., Goc, J., Santosa, E. K., . . . Sonnenberg, G. F. (2019). Innate lymphoid cells support regulatory T cells in the intestine through interleukin-2. *Nature, 568*(7752), 405-409. doi:10.1038/s41586-019-1082-x

Zhou, X., Kong, N., Wang, J., Fan, H., Zou, H., Horwitz, D., . . . Zheng, S. G. (2010). Cutting edge: all-trans retinoic acid sustains the stability and function of natural regulatory T cells in an inflammatory milieu. *J Immunol, 185*(5), 2675-2679. doi:10.4049/jimmunol.1000598

Zorn, E., Nelson, E. A., Mohseni, M., Porcheray, F., Kim, H., Litsa, D., . . . Ritz, J. (2006). IL-2 regulates FOXP3 expression in human CD4+CD25+ regulatory T cells through a STAT-dependent mechanism and induces the expansion of these cells in vivo. *Blood, 108*(5), 1571-1579. doi:10.1182/blood-2006-02-004747

Zou, Y., Chen, T., Han, M., Wang, H., Yan, W., Song, G., . . . Ning, Q. (2010). Increased killing of liver NK cells by Fas/Fas ligand and NKG2D/NKG2D ligand contributes to hepatocyte necrosis in virus-induced liver failure. *J Immunol, 184*(1), 466-475. doi:10.4049/jimmunol.0900687

ABBREVIATIONS

7AAD: 7-aminoactinomycin D

ACK: Ammonium-chloride-potassium lysis buffer

ADCC: Antibody-dependent cellular cytotoxicity

ADH: Alcohol dehydrogenase

ADP: Adenosine diphosphate

AF: Alexa flour

AHR: Aryl hydrocarbon receptor

AID: Activation-induced cytidine deaminase

AMP: Adenosine monophosphate

AntiA: Antimycin A

APC: Allophycocyanin

APC-Cy7: Allophycocyanin conjugated with cyanine7

APCs: Antigen-presenting cells

ARAT: Acyl-CoA retinol acyltransferase

ATP: Adenosine triphosphate

*at*RA: all-*trans* retinoic acid

BAT3: HLA-B associated transcript 3

BCR: B cell receptor

BM-DCs: Bone marrow derived dendritic cells

BSA: Bovine serum albumin

BUV: Brilliant Ultraviolet™

BV: Brilliant Violet™

CCl_4: Carbon tetrachloride

CCL: C-C motif chemokine ligand

CCR: C-C motif chemokine receptor

CD: Cluster of differentiation

CD200R: CD200 receptor

cDNA: complementary DNA

CILP: Common ILC progenitor

CHILP: Common helper-like ILC progenitor

CLP: Common lymphoid progenitor

CLRs: C-type lectin receptors

cNK: conventional NK cells

CRABP: Cellular retinoic acid-binding protein

CSF: Colony-stimulating factor

CT: Cycle threshold
CTLA-4: Cytotoxic T-lymphocyte-associated protein 4
CXCL10: CXC motif chemokine ligand 10
CYP26: Cytochrome P450 family 26
DAMPs: Damage-associated molecular patterns
DCs: Dendritic cells
DMEM: Dulbecco's modified Eagle Medium
DMSO: Dimethylsulphoxide
DNA: Deoxyribonucleic acid
DNAM-1: DNAX accessory molecule-1
DR: Death receptor
dsRNA: double-stranded RNA
ECAR: Extracellular acidification rate
ELISA: Enzyme-linked immunosorbent assay
Eomes: Eomesodermin
ES: Enrichment score
FABP: Fatty acid-binding protein
FACS: Fluorescence-activated cell sorting
FasL: Fas ligand
FCCP: Carbonyl cyanide-p-trifluoromethoxyphenylhydrazone
FcRIIIA (CD16A): Fc gamma receptor III a
FSC-A: Forward scatter area
FDR: False discovery rate
FITC: Fluorescein isothiocyanate
Flox: Flanked by LoxP
FoxP3: Forkhead box P3
g: relative centrifuge force ($g = 9.81\ m/s^2$)
αGalCer: alpha-Galactosylceramide
GARP: glycoprotein-A repetitions predominant
GATA3: GATA-binding protein 3
G-CSF: Granulocyte colony-stimulating factor
GM-CSF: Granulocyte-macrophage colony-stimulating factor
Gpi1: Glucose-6-phosphate isomerase 1
GSEA: Gene set enrichment analysis
H-2D: Histocompatibility 2, D region
H-2K: Histocompatibility 2, K region
H-2M: Histocompatibility 2, M region

H60: Histocompatibility 60
HA: Hemagglutinin
HCMV: Human Cytomegalovirus
HGF: Hepatocyte growth factor
HLA: Human leukocyte antigen
HN: Hemagglutinin-neuraminidase
Id2: Inhibitor of DNA-binding 2
iDCs: Immature dendritic cells
IFN: Interferon
Ig: Immunoglobulin
IκBζ: Inhibitor of nuclear factor kappa B zeta
IKK: Inhibitory-κB Kinase
IL: Interleukin
IL-2R: IL-2 receptor
IL-18Rα: IL-18 receptor alpha
ILCs: Innate lymphoid cells
intILCs: Intermediate innate lymphoid cells
IRBP: Interphotoreceptor retinoid-binding protein
IRF8: Interferon regulatory factor 8
KEGG: Kyoto encyclopedia of genes and genomes
KLRG1: Killer cell lectin-like receptor G1
Klrb1c: Killer cell lectin-like receptor subfamily B member 1C
KIR: Killer cell immunoglobulin-like receptor
KO: Knockout
LAMP1 (CD107a): Lysosomal-associated membrane protein 1
LAMP2 (CD107b): Lysosomal-associated membrane protein 2
LPS: Lipopolysaccharide
LRAT: Lecithin retinol acyltransferase
LTi: Lymphoid tissue-inducer
MAC: Membrane attack complex
MACS: Magnetic-activated cell sorting
MBL: Mannose-binding lectin
MCMV: Mouse cytomegalovirus
M-CSF: Macrophage colony-stimulating factor
MDDCs: Monocyte-derived dendritic cells
MFI: Mean florescence intensity
MHC: Major histocompatibility complex

MIC-A: MHC class I polypeptide-related sequence A
MIC-B: MHC class I polypeptide-related sequence B
MIF: Macrophage migration inhibitory factor
min: Minute(s)
mLN: Mesenteric lymph node
mNK: Mature natural killer cells
mTOR: Mammalian target of rapamycin
MULT1: Murine UL16-binding protein-like transcript
MyD88: Myeloid differentiation primary response 88
2-NBDG: 2-(N-(7-Nitrobenz-2-oxa-1,3-diazol-4-yl)Amino)-2-Deoxyglucose
NCR: Natural cytotoxicity triggering
n.d. Not detected
NES: Normalized enrichment score
NFIL3: Nuclear Factor, interleukin 3 regulated
NFκB: Nuclear factor kappa-light-chain-enhancer of activated B cells
NK cells: Natural killer cells
NKG: Natural Killer Group 2
NKP: NK lineage progenitor
NLR: NOD-like receptors
NOD: Nucleotide oligomerization domain
NOM P val: Nominal p-value
OCR: Oxygen consumption rate
Oligo: Oligomycin
OSM: Oncostatin M
OXPHOS: Oxidative phosphorylation
PAMPs: Pathogen-associated molecular patterns
PBS: Phosphate-buffered saline
PCA: Principal component analysis
PCCM: Primary cell culture media
PCNA: Proliferating cell nuclear antigen
PE: Phycoerythrin
PE-Cy7: Phycoerythrin conjugated with cyanine 7
PerCP-Cy5: Peridinin-chlorophyll protein complex conjugated with cyanine 5
PGC-1α: PPARγ-coactivator-1α
PHx: Partial hepatectomy
PMA: Phorbol 12-myristate 13-acetate
PPAR: Peroxisome proliferator-activated receptor

PPARγ cKO: $Ncr1^{iCreTg}$ $PPAR\gamma^{f/f}$ mouse

PPARγ flox: $PPAR\gamma^{f/f}$ mouse

PRRs: Pattern recognition receptors

p-value: Probability value

RALDH: Retinal dehydrogenase

RAE-1: Retinoic acid early transcript 1

RAG: Recombination-activated genes

RALDH: Retinaldehyde dehydrogenase

RANKL: Receptor activator of nuclear factor kappa-B ligand

RA: Retinoic acid

RAR: Retinoic acid receptor

RBP: Retinol-binding protein

RIG-I: Retinoic acid-inducible gene I

RIN: RNA integrity number

RLR: RIG-I-like receptors

RNA: Ribonucleic acid

ROR: RAR-related orphan receptor

ROS: Reactive oxygen species

Rot: Rotenine

Rpm: Revolutions per minute

RPMI: Roswell Park Memorial Institute

RT: Room temperature

RT-PCR: Real time polymerase chain reaction

RXR: Retinoic X receptor

SAA: Serum amyloid A

SSC-A: Side scatter area

ssRNA: single-stranded RNA

STAT: Signal transducer and activator of transcription

STRA6: Stimulated by retinoic acid 6

SEM: Standard error of the mean

TAA: Tumor associated antigens

TAM: Tumor-associated macrophages

Tbet: T-box protein expressed in T cells

TCR: T cell receptor

TGF-β: Transforming growth factor-β

T_H1 cells: Type 1 helper T cell

T_H2 cells: Type 2 helper T cell

T_H17 cells: Type 17 helper T cell

TLR: Toll-like receptors

TME: Tumor microenvironment

TMRM: Tetramethylrhodamine, methyl ester

TNF: Tumor necrosis factor

Tnfsf: TNF superfamily member

Tnfrsf: TNF receptor superfamily member

TRAIL: TNF-related apoptosis-inducing ligand

TRAIL-R: TRAIL receptor

Treg: Regulatory T cells

ULBP: UL16-binding protein

Unsti: Unstimulated

VAD: Vitamin A-deficient

VEGFA: Vascular endothelial growth factor A

WT: Wild type

XCL1: XC motif chemokine ligand 1

YAC-1: Y-1 adrenal cells

ACKNOWLEDGEMENT

On top of all, I would like to appreciate to Prof. **Adelheid Cerwenka** for providing me this great opportunity to pursue my PhD in IBC lab, surrounded by awesome people, and for supervising and supporting my project, and enabling me to broaden my research horizons.

Without Dr. **Ana Stojanovic**, I could not begin nor complete my PhD! I would like to express my gratitude for the supervision, motivation, novel ideas, and endless positive feedbacks. Although our beginning was not easy, I believe that we managed well and became good friends.

I am thankful to Dr. **Elke Burgermeister** for providing $PPAR^{fl/fl}$ mice for the project. I would like to express my appreciation to Dr. **Guoliang Cui,** as a member of my thesis advisory committee, for providing critical remarks for my project. I would like to thank Prof. **Yvonne Samstag**, as a spokesperson of Research Training Group TRAIN4CIM and a member of my thesis advisory committee, for supporting my project.

Just like a famous saying, “it takes a village to raise a child”, in my case, “it took a whole lab to complete my PhD degree”.

The first appreciation goes to our mouse team. I am grateful to **Jia-Xiang** for sharing interesting (quite often crazy) thoughts, enlightenments, as well as blunt criticism. Many thanks to **Sophia**, for saving my asses from KEIN-ENGLISCH-situations, and providing great Greek foods and of course countless hugs. I am grateful to our boat party team, **Tomáš**, and **Irene**, for the companionship, cemetery-walks-and-talks, and laughing-hard-moments. I would like to appreciate to colleagues in the other office, **Silvina**, **Francesco**, **Bianca**, and **Andreas**, and our newbie, **Sebastiano,** for creating friendly atmosphere and funny memories. I am grateful to **Petra**, for mice breeding and transportation, and to **Sina**, for assistances in all the administrative works. Many thanks to the former colleagues, **Marian**, for assisting several experiments, and **Jana**, for important tips about experiments and nice conversations. I appreciate all help and technical support from all other IBC members.

I am thankful to Research Training Group **TRAIN4CIM** for having me as a fellow and supporting my project. Special thanks go to **Aparna**, **Divya** and **Karina** for our friendship and many happy memories.

Finally yet importantly, I would like to express my deepest thankfulness to my parent, 정인훈 and 전윤숙, for the unconditional love and moral support, and to my brother, 정민권, for taking care of many things in Korea on behalf of me. Special appreciation to **Simon**, for standing by me, believing in me through all time, and supporting me during many ups and downs.